

LAMS-3034

LOS ALAMOS SCIENTIFIC LABORATORY
OF THE UNIVERSITY OF CALIFORNIA • LOS ALAMOS NEW MEXICO

BIOLOGICAL AND MEDICAL RESEARCH GROUP (H-4)
OF THE HEALTH DIVISION -- ANNUAL REPORT
JULY 1962 THROUGH JUNE 1963

DO NOT CIRCULATE

PERMANENT RETENTION

REQUIRED BY CONTRACT

FILE BARCODE



00131408

1055475

L.A.S.

LAMS-3034
UC-48, BIOLOGY AND MEDICINE
TID-4500 (26th Ed.)

LOS ALAMOS SCIENTIFIC LABORATORY
OF THE UNIVERSITY OF CALIFORNIA LOS ALAMOS NEW MEXICO

REPORT WRITTEN: July 1963

REPORT DISTRIBUTED: February 14, 1964

BIOLOGICAL AND MEDICAL RESEARCH GROUP (H-4)
OF THE HEALTH DIVISION -- ANNUAL REPORT
JULY 1962 THROUGH JUNE 1963

Group Leader, W. H. Langham
Division Leader, T. L. Shipman

Contract W-7405-ENG. 36 with the U. S. Atomic Energy Commission

All LAMS reports are informal documents, usually prepared for a special purpose and primarily prepared for use within the Laboratory rather than for general distribution. This report has not been edited, reviewed, or verified for accuracy. All LAMS reports express the views of the authors as of the time they were written and do not necessarily reflect the opinions of the Los Alamos Scientific Laboratory or the final opinion of the authors on the subject.

CONTENTS

	Page
CHAPTER 1 - INTRODUCTION	11
CHAPTER 2 - MAMMALIAN METABOLISM SECTION	21
1. Retention of Intravenously Administered Cesium ¹³² by Man	21
C. R. Richmond, J. E. London, and J. E. Furchner	
2. Lack of Effect of Exercise on the Excretion of Cesium ¹³⁷ in Mice	34
J. E. Furchner, C. R. Richmond, and G. A. Trafton	
3. Distribution of Cesium ¹³⁷ in Mice and Dogs after Chronic Exposure	41
J. E. Furchner, C. R. Richmond, and G. A. Trafton	
4. Metabolism of Manganese ⁵⁴ in Rats and Mice	49
J. E. Furchner, C. R. Richmond, and G. A. Trafton	
5. Retention of Zirconium ⁹⁵ after Oral and Intraperitoneal Administration to Mice	53
J. E. Furchner, C. R. Richmond, and G. A. Trafton	

6.	Effective Retention of Intravenously Administered Beryllium ⁷ by Rats	59
	C. R. Richmond, J. E. Furchner, and J. E. London	
7.	The Effect of Environmental Temperature on the Retention of Strontium in Mice	65
	J. E. Furchner, C. R. Richmond, and G. A. Trafton	
8.	Potassium ⁴⁰ and Cesium ¹³⁷ Levels of Beagle Hounds	73
	C. R. Richmond, J. E. Furchner, and J. E. London	
9.	Volume and Turnover of Body Water in Male <i>Macaca mulatta</i> and <i>Macaca speciosa</i> Monkeys	76
	C. R. Richmond and J. E. London	
	Mammalian Metabolism Section Publications	81
	Manuscript Submitted	82
	CHAPTER 3 - MAMMALIAN RADIOBIOLOGY SECTION	83
1.	Comparative Fundamental Physiological Parameters of <i>Macaca mulatta</i> and a New Laboratory Primate, <i>Macaca speciosa</i>	83
	J. C. Hensley and C. R. Richmond	
2.	Cellular Elements in the Peripheral Blood of <i>Macaca mulatta</i> and <i>Macaca speciosa</i> Monkeys	96
	C. R. Richmond and J. E. London	

3.	Longevity of First and Second Generation Offspring from Male Mice Exposed to Fission Neutrons and Gamma Rays	103
	J. F. Spalding and R. F. Archuleta	
4.	Acute Radiosensitivity as a Function of Age in Mice	112
	J. F. Spalding, O. S. Johnson, and R. F. Archuleta	
5.	Cold Stress as a Test for Rate of Aging in Three Lines of Mice with Different Histories of Ancestral X-Ray Exposure	116
	J. F. Spalding and T. T. Trujillo	
6.	Breeding Characteristics of Offspring from Mice with Fifteen Generations of X Irradiation to the Males	124
	J. F. Spalding and M. R. Brooks	
7.	Radiation-Induced Irreparable Biological Damage in Three Genetic Lines of Mice with Different Ancestral Histories of Radiation Exposure	129
	J. F. Spalding and R. F. Archuleta	
8.	Inability of the Mouse to Recognize Gamma Radiations. I. Variable Low Dose Rate Studies in RF Mice	133
	J. C. Hensley, J. F. Spalding, W. F. Schweitzer, and R. F. Archuleta	
	Mammalian Radiobiology Section Publications	141
	Manuscripts Submitted	142

CHAPTER 4 - LOW-LEVEL COUNTING SECTION

	143
1. Humco II: Status Report	143
P. N. Dean and E. C. Anderson	
2. Absolute Calibration of Whole-Body Gamma-Ray Spectrometer for Potassium and Cesium ¹³⁷	152
P. N. Dean and M. A. Van Dilla	
3. Evaluation of the Potassium ⁴⁰ Continuum Contribution to the Cesium ¹³⁷ Photopeak in a Sodium Iodide Crystal Spectrometer	162
E. C. Anderson, P. N. Dean, and M. A. Van Dilla	
4. Computer Programs for Analyzing Data	168
P. N. Dean	
5. Cesium ¹³⁷ Body Burdens of Control Subjects	180
E. C. Anderson and A. E. Hargett	
6. Retention of Cesium ¹³⁷ by Adults	184
M. A. Van Dilla and M. J. Fulwyler	
7. Metabolism of Radiiodine in Children and Adults Using Small (Nanocurie) Doses	187
M. A. Van Dilla and M. J. Fulwyler	
8. Effect of Ashing Temperature on Cesium and Potassium Content of Bone	201
M. A. Van Dilla, M. W. Rowe, and M. J. Fulwyler	
9. Thermoluminescent Dosimetry with Activated Lithium Fluoride	205
P. N. Dean and J. H. Larkins	

Low-Level Counting Section Publications	224
Manuscripts Submitted	225
CHAPTER 5 - CLINICAL INVESTIGATIONS SECTION	227
1. Progress in the Establishment of Karyographic Methods as a Tool in Radiopathology	227
G. L. Humason and P. C. Sanders	
2. Electronic Measurement of Cellular Volumes. IV. Determination of Scaling and Correction Factors for Conversion of Voltage to Cubic Microns	235
C. C. Lushbaugh, D. B. Hale, and N. J. Basmann	
3. Electronic Measurement of Cellular Volumes. V. Change in Red Blood Cells Resulting from Non-Physiologic pH	253
C. C. Lushbaugh, E. C. Anderson, H. I. Israel, D. B. Hale, and N. J. Basmann	
4. Electronic Measurement of Cellular Volumes. VI. Electronic Improvement of Coulter Counter Resolution	261
C. C. Lushbaugh, N. J. Basmann, and D. B. Hale	
5. Electronic Measurement of Cellular Volumes. VII. Biologic Evidence for Two Volumetrically Distinct Subpopulations of Red Blood Cells	270
C. C. Lushbaugh and D. B. Hale	

6. Electronic Measurement of Cellular Volumes.	
VIII. Volumetric Change of Circulating Erythrocytes in WW ^V Genetically Anemic Mice Implanted with w+w+ Fetal Liver	279
C. C. Lushbaugh and E. S. Russell	
Clinical Investigations Section Publications	286
Manuscripts Submitted	287
CHAPTER 6 - CELLULAR RADIOBIOLOGY SECTION	288
1. Preparation of Bacterial Deoxyribonucleic Acids	288
I. U. Boone and E. Campbell	
2. Purification and Concentration of T-4 Bacteriophage on DEAE-Cellulose Columns for DNA Isolation	296
I. U. Boone and E. Campbell	
3. Chromosome Observations in Nonirradiated Progeny from Several Lines of Irradiated RF Males	303
I. U. Boone, P. M. LaBauve, and J. F. Spalding	
4. Chromosomes in Transplanted Leukemia of AKR Mice	307
I. U. Boone and P. M. LaBauve	
Cellular Radiobiology Section Publications	312

CHAPTER 7 - MOLECULAR RADIOBIOLOGY SECTION	313
1. Nucleic Acids: A Technique for Automated Base Analysis	313
G. R. Shepherd, D. G. Ott, and P. A. Hopkins	
2. Application of Automatic Computational Techniques to the Analysis of Ultracentrifugal Sedimentation-Velocity Molecular Weight Data for Deoxyribonucleic Acid	319
G. R. Shepherd, P. N. Dean, and B. J. Noland	
3. The Representation of Oligonucleotides: A Sub-Nomenclature Problem	326
F. N. Hayes and D. G. Ott	
4. Oligonucleotide Synthesis	329
D. G. Ott, D. L. Williams, V. N. Kerr, G. T. Fritz, E. Hansbury, R. E. Hine, and F. N. Hayes	
5. Chromatography of Nucleic Acids	350
A. Murray, D. F. Petersen, T. T. Trujillo, and V. E. Mitchell	
Molecular Radiobiology Section Publications	373
Manuscripts Submitted	374

CHAPTER 1

INTRODUCTION

During this report period (FY 1963), reorientation of the biomedical research program toward molecular and cellular level studies continued at an accelerated rate. As a result, there have been a large number of changes in organization involving new hires, terminations, transfers of personnel within the group, and redefining and reallocating of responsibilities.

(a) Program Orientation

Continuing to increase emphasis on more fundamental research at the cellular and molecular levels and the termination of Dr. Lushbaugh, Section Leader of the Clinical Investigations Section, are resulting in a less diversified biomedical research program than in past years. During the next report period (FY 1964), projects involving clinical applications of radiation and radioactive isotopes will be brought to a reasonable conclusion, the section discontinued,

and the remaining personnel transferred to other sections. Some of the effort of the Low-Level Counting Section will be diverted also to other sections because of decreased interest in fallout as a result of the nuclear test ban treaty. This will result in the FY 1964 research activities being confined largely to the following program categories:

- 06-01-01 General Radiation Effects (Mammalian Radiobiology Section)
- 06-01-02 Toxicology of Radioelements (Mammalian Metabolism Section)
- 06-02-02 Radiation Genetics (Mammalian Radiobiology Section)
- 06-04 Molecular and Cellular Level Studies (Molecular and Cellular Radiobiology Sections)
- 06-06 Radiological and Health Physics and Instrumentation (Low-Level Counting Section)

The Low-Level Counting Section will continue a curtailed effort in environmental radiation studies (06-05), consisting of projects of potential interest to civil defense.

(b) Terminations

The following terminations occurred during or shortly after the end of the present report period:

Dr. C. C. Lushbaugh (Section Leader, Clinical Investigations Section).

D. B. Hale (research assistant, Clinical Investigations Section).

G. L. Humason (research assistant, Clinical Investigations Section).

M. W. Rowe (research assistant, Low-Level Counting Section).

A. E. Hargett (technician, Low-Level Counting Section).

M. Magee (technician, Molecular Radiobiology Section).

L. T. Rivera (research assistant, Cellular Radiobiology Section).

(c) Leave of Absence

Dr. Irene U. Boone (Section Leader, Cellular Radiobiology Section) was granted a year's leave of absence at the end of the report period to practice medicine in the Los Alamos Medical Center.

(d) Transfers within the Group

Dr. E. C. Anderson was transferred from the Low-Level Counting Section, of which he was the Section Leader, to the Cellular Radiobiology Section to work on the sequential biochemistry of cellular proliferation using radiotracer methodology.

T. T. Trujillo was transferred from the Mammalian Radiobiology Section to the Molecular Radiobiology Section.

O. S. Johnson was transferred from the Mammalian Metabolism Section to the Mammalian Radiobiology Section.

N. J. Basmann and V. M. Gibbs were transferred from the Clinical Investigations Section to the Cellular Radiobiology Section.

(e) Change in Administrative Responsibility

Dr. D. G. Ott was made Alternate Group Leader and assigned the specific responsibility of supervising and coordinating all fundamental research activities. This consists of those projects being pursued in the Cellular and Molecular Radiobiology Sections.

Dr. M. A. Van Dilla was made Section Leader of the Low-Level Counting Section, replacing Dr. E. C. Anderson; and Dr. D. F. Petersen was appointed Section Leader of the Cellular Radiobiology Section, replacing Dr. I. U. Boone.

(f) New Hires

During the past report period, a rather vigorous recruiting campaign was carried out to fill vacancies created by terminations and to increase the staff level in cellular and molecular radiobiology. New hires during the report period or at the beginning of FY 1964 are as follows:

Robert L. Ratliff (staff member, Molecular Radiobiology

Section), Ph.D. in Biochemistry, [REDACTED]
[REDACTED]
[REDACTED]

Donald E. Hoard (staff member, Molecular Radiobiology
Section), Ph.D. in Biochemistry, [REDACTED]
[REDACTED]
[REDACTED]
[REDACTED]

Charles T. Gregg (staff member, Molecular Radiobiology
Section), Ph.D. in Biochemistry, [REDACTED]
[REDACTED]
[REDACTED]
[REDACTED]

J. Coleman Hensley (staff member, Mammalian Radiobiology
Section), D.V.M., [REDACTED]
[REDACTED]

Mack J. Fulwyler (staff member, Low-Level Counting Sec-
tion), B.S. in Physics, [REDACTED]
[REDACTED]
[REDACTED]
[REDACTED]

Evelyn M. Campbell (research assistant, Cellular Radio-
biology Section), B.Sc., [REDACTED]
[REDACTED]
[REDACTED]

Jean S. Findlay (research assistant, Mammalian Metabolism Section), B.S., [REDACTED]

Billie J. Noland (research assistant, Molecular Radiobiology Section), B.A., [REDACTED]
[REDACTED]
[REDACTED]

Glenda L. Oakley (research assistant, Mammalian Radiobiology Section, B.S., [REDACTED]
[REDACTED]
[REDACTED]
[REDACTED]

Fannie Sapir (research assistant, Cellular Radiobiology Section), M.S., [REDACTED]
[REDACTED]

Nancy C. Brown (technician, Mammalian Radiobiology Section), [REDACTED]
[REDACTED]
[REDACTED]

Roxye L. DePriest (data analyst, Low-Level Counting Section), B.S., [REDACTED]

Valerie M. Gibbs (technician, Cellular Radiobiology Section), B.S., [REDACTED]
[REDACTED]
[REDACTED]

Leo J. Carr (electronics technician, Low-Level Counting Section), transferred from P-Division Electronics Group.

Antonio R. Vigil (electronics technician, Low-Level Counting Section), transferred from P-Division Electronics Group.

(g) New Hires (Pending Completion of Postdoctoral Fellowships or Degrees)

Robert A. Tobey (staff member, Cellular Radiobiology Section), [REDACTED] Ph.D. in Microbiology, [REDACTED]
[REDACTED]
will report for work here in January 1964.

Elva A. Hyatt (staff member, Cellular Radiobiology Section), Ph.D. in Microbiology, [REDACTED]
[REDACTED]
[REDACTED] will report for work here in April 1964.

Benjamin J. Barnhart (staff member, Cellular Radiobiology Section), Sc.D. in Biochemistry, [REDACTED]
[REDACTED]
[REDACTED]
[REDACTED]
[REDACTED]
[REDACTED] will report for work here about October 1964.

Charles H. Blomquist (staff member, Cellular Radio-
biology Section), [REDACTED] Ph.D. in Biochemistry, [REDACTED]
[REDACTED]
[REDACTED]

Arthur G. Saponara (staff member, Molecular Radio-
biology Section), [REDACTED] Ph.D. in Biochemistry, [REDACTED]
[REDACTED] all report for work here about January
1964.

(h) Organization

At the end of the present report period (first half of
FY 1964), the table of organization giving some indication
of the division of effort among the various sections is
shown on the following pages.

GROUP H-4

BIOMEDICAL RESEARCH

W. H. Langham, Ph.D., Leader
 D. G. Ott, Ph.D., Alt. Group Leader
 O. S. Johnson, B.S., Asst. Ldr. for Administration
 E. M. Sullivan, Group Secretary

MAMMALIAN METABOLISM

C. R. Richmond, Ph.D.,
 Leader

Staff Member

J. E. Furchner, Ph.D.

Research Assistants

J. S. Findlay, B.S.
 J. E. London, B.S.
 G. A. Trafton, B.S.

Technical Staff

S. Cordova
 R. Martinez

*Casual employee.

MAMMALIAN RADIOBIOLOGY

J. F. Spalding, Ph.D.,
 Leader

Staff Members

J. C. Hensley, D.V.M.
 O. S. Johnson, B.S.

Research Assistants

M. R. Brooks, B.Ch.E.
 G. L. Oakley, B.A.

Technical Staff

F. Archuleta
 R. F. Archuleta
 J. E. Atencio
 N. C. Brown
 L. Ortiz
 A. Trujillo
 D. G. Valdez
 F. Valdez
 E. A. Vigil

LOW-LEVEL COUNTING

M. A. Van Dilla, Ph.D.,
 Leader

Staff Members

P. N. Dean, M.A.
 M. J. Fulwyler, B.S.
 J. H. Larkins, B.S.
 J. D. Perrings

Technical Staff

R. L. DePriest, B.S.

Electronics Technicians

L. J. Carr
 A. R. Vigil

CELLULAR RADIOBIOLOGY

D. F. Petersen, Ph.D.,
Leader

Research Assistants

E. M. Campbell, B.S.
S. Carpenter, B.A.
S. H. Cox, B.A.
P. M. LaBauve, B.A.
P. C. Sanders, M.S.
F. Sapir, M.S.

Technical Staff

N. J. Basmann
V. M. Gibbs

Leave of Absence

I. U. Boone, M.D.

MOLECULAR RADIOBIOLOGY

F. N. Hayes, Ph.D.,
Leader

Staff Members

E. C. Anderson, Ph.D.
C. T. Gregg, Ph.D.
D. E. Hoard, Ph.D.
V. N. Kerr, M.A.
A. Murray, M.S.
R. L. Ratliff, Ph.D.
G. R. Shepherd, Ph.D.
T. T. Trujillo, B.S.
D. L. Williams, M.S.

Research Assistants

G. T. Fritz, B.S.
P. A. Goldman, B.S.
E. Hansbury, M.A.
R. E. Hine, B.S.
E. H. Lilly, B.S.
B. J. Noland, B.A.

Technical Staff

V. E. Mitchell

CHAPTER 2

MAMMALIAN METABOLISM SECTION

Retention of Intravenously Administered Cesium¹³² by Man (C. R. Richmond, J. E. London, and J. E. Furchner)

INTRODUCTION

Increasing use of short-lived Cs¹³² (6.5-day physical half-life) for calibration of whole-body counting facilities affords additional opportunities for measuring biological turnover of cesium by human subjects. The gamma-ray energy of Cs¹³² is remarkably similar to that of 28-year Cs¹³⁷ (i.e., 0.67 and 0.66 Mev, respectively), thus allowing the substitution of Cs¹³² for in vivo calibration experiments. This report presents preliminary results of the effective retention of Cs¹³² by 4 normal young adult subjects.

METHODS AND MATERIALS

The Cs¹³² was obtained from the Tokai Laboratory of the Japan Atomic Energy Research Institute. This solution was

neutralized, sterilized, and prepared for intravenous injection (1). At administration, the specific activity was approximately 0.204 mc per gram of cesium. One ml of the Cs^{132} chloride solution was administered (2) to each person between 8:00 and 9:00 a.m. The activity of the syringes was measured relative to a Cs^{137} standard before and after injection as part of the estimation of the amount of Cs^{132} injected. Table 1 gives some pertinent experimental data for each subject. All were considered to be in good health.

Prior to injection, the subjects were counted in the Los Alamos Human Counter (Humco II) to establish normal whole-body gamma-ray activities. Measurements in the sodium iodide spectrometer facility showed the presence of K^{40} and Cs^{137} only. Counting times never exceeded 500 seconds duration throughout the experiment. The raw counting data were electronically processed by an IBM 7090 computer to determine the count rates corrected for counter instability at the exact times of measurement (e.g., x is error-free in subsequent data analysis). The output of this program provides the input for the least squares curve-fit program (3). A single exponential function was used as the biological model in the analysis.

TABLE 1. DETAILS OF INDIVIDUAL EXPERIMENTS ON RETENTION OF RADIOCESIUM BY HUMAN SUBJECTS

	Subject			
	HFCs- [REDACTED]	HMCs- [REDACTED]	HMCs- [REDACTED]	HMCs- [REDACTED]
Age (years)	[REDACTED]	[REDACTED]	[REDACTED]	[REDACTED]
Weight (kg)	[REDACTED]	[REDACTED]	[REDACTED]	[REDACTED]
Form administered	Cs ¹³² Cl	Cs ¹³² Cl	Cs ¹³² Cl	Cs ¹³² Cl
Activity administered (μ c)**	0.653	0.648	0.642	0.645
Duration of experiment (days)	45	45	44	43
Number of measurements	31	32	29	15

*The code for designating cases indicates species, sex, nuclide, and case number. For example, HFCs-[REDACTED] indicates that the [REDACTED] human subject receiving radiocesium was a female. Subjects [REDACTED] and [REDACTED] were males.

** + 5 per cent error.

RESULTS AND DISCUSSION

Table 2 lists the intercept and rate parameters plus their standard deviations as calculated by the least squares curve-fit program. The small standard deviations for both parameters are indicative of the high precision of the instrumentation and the correct choice of model. One can also note in Table 2 the effect of body mass on attenuation of gamma activity arising from within the body. An inverse relation is apparent between body mass and measured count rate at time zero (a_1).

The mean effective half-life (EHL) of 6 days for Cs^{132} corresponds to a derived biological half-life (BHL) of approximately 75 days for stable cesium. It should be emphasized that a physical half-life (PHL) of 6.53 days was assumed in deriving the BHL in this study. However, if one uses 6.4 days as the PHL, the derived BHL would be about 100 days. A 6.3-day PHL corresponds to a 130-day derived BHL. Thus, one must exercise care when estimating BHL values from tracer studies done with radionuclides of short PHL. Figures 1-4 show the time course of retention for each subject. Figure 5 gives the same for all 4 subjects.

Maletskos et al. (4) report a two-exponential retention system for 5 elderly subjects given Cs^{132} intravenously. The BHL for the slow component was 80 to 90 days. Decay

TABLE 2. COMPUTER DERIVED WHOLE-BODY EFFECTIVE RETENTION PARAMETERS* FOR HUMAN SUBJECTS GIVEN Cs¹³² BY INTRAVENOUS ADMINISTRATION

Subject Code	a_1 (c · sec ⁻¹)	$k_1 + \lambda$ (days ⁻¹)	Effective** Half-Life (days)	Biological+ Half-Life (days)
HFCs- + 1.8120455E 01	6.1852959E 03 ⁺⁺ + 1.8120455E 01	1.2059031E-01 ⁺⁺ + 3.9449049E-04	5.7479744E 00	4.8001055E 01
HMCs- + 8.5926818E 00	5.6866875E 03 + 8.5926818E 00	1.1222464E-01 + 1.9032492E-04	6.1764508E 00	1.1410546E 02
HMCs- + 2.2915179E 01	5.4407803E 03 + 2.2915179E 01	1.1579220E-01 + 5.5455036E-04	5.9861544E 00	7.1887109E 01
HMCs- + 1.5190672E 01	4.9800707E 03 + 1.5190672E 01	1.1986225E-01 + 5.5219930E-04	5.7828883E 00	5.0549691E 01
Average of all 4	5.5296180E 03 + 5.6495185E 01	1.1543788E-01 + 1.4049999E-03	6.0045279E 00	7.4629473E 01

* From $R_t = a_1 e^{-(k_1 + \lambda)t}$, where a_1 and k_1 are the rate and intercept constants, respectively; t is days; e is the base of natural logarithms; and R_t is the effective retention at any time t after injection.

** 0.69315/ $k_1 + \lambda$.

+ Derived from effective half-time by assuming a physical half-life of 6.53 days for Cs¹³².

++ One standard deviation given below best value of parameter. Indicates value is 6.1852959 x 10³.

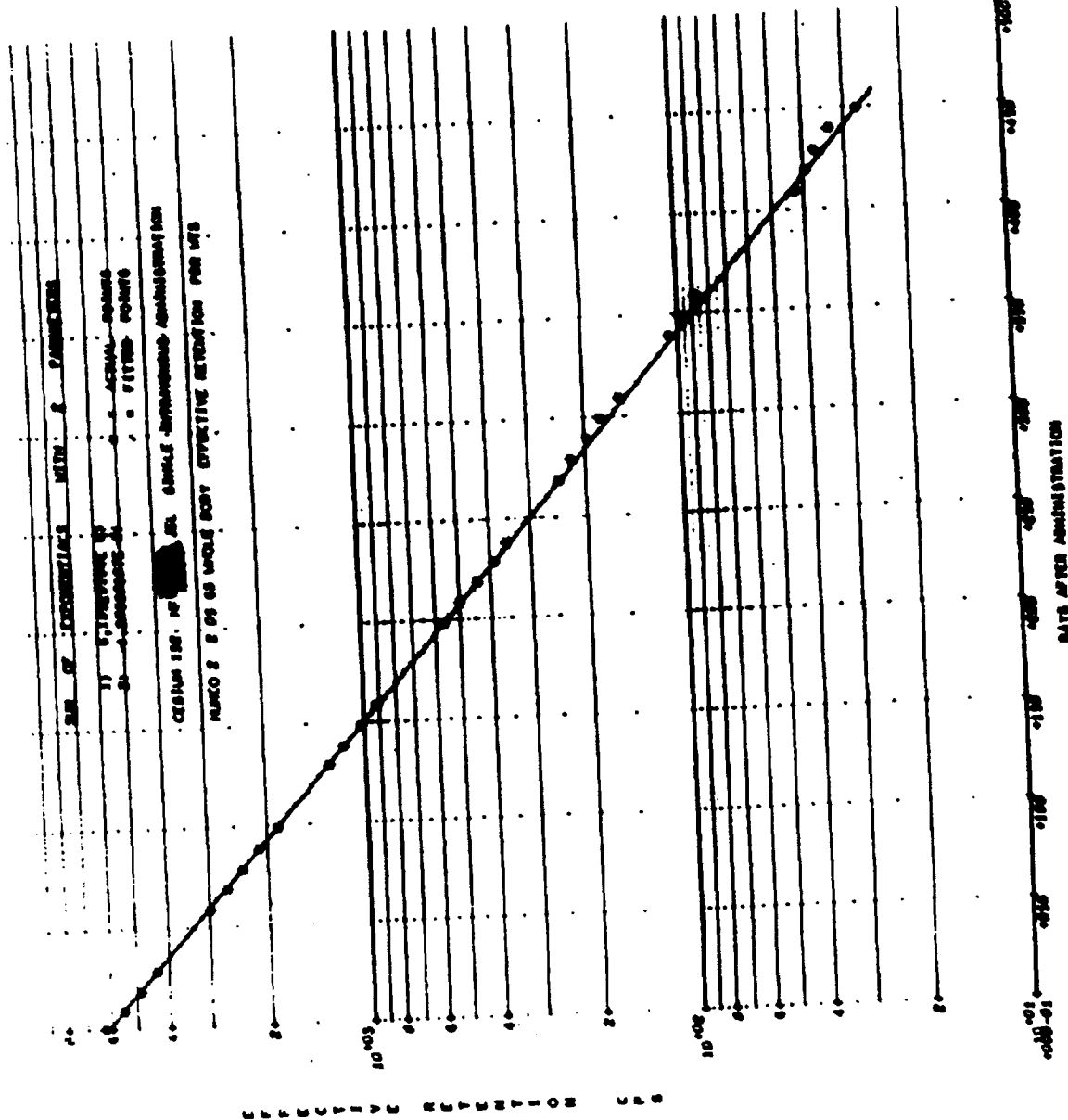


Fig. 1. Effective retention of 0.652 μCi Cs^{132} by subject HFCs-1

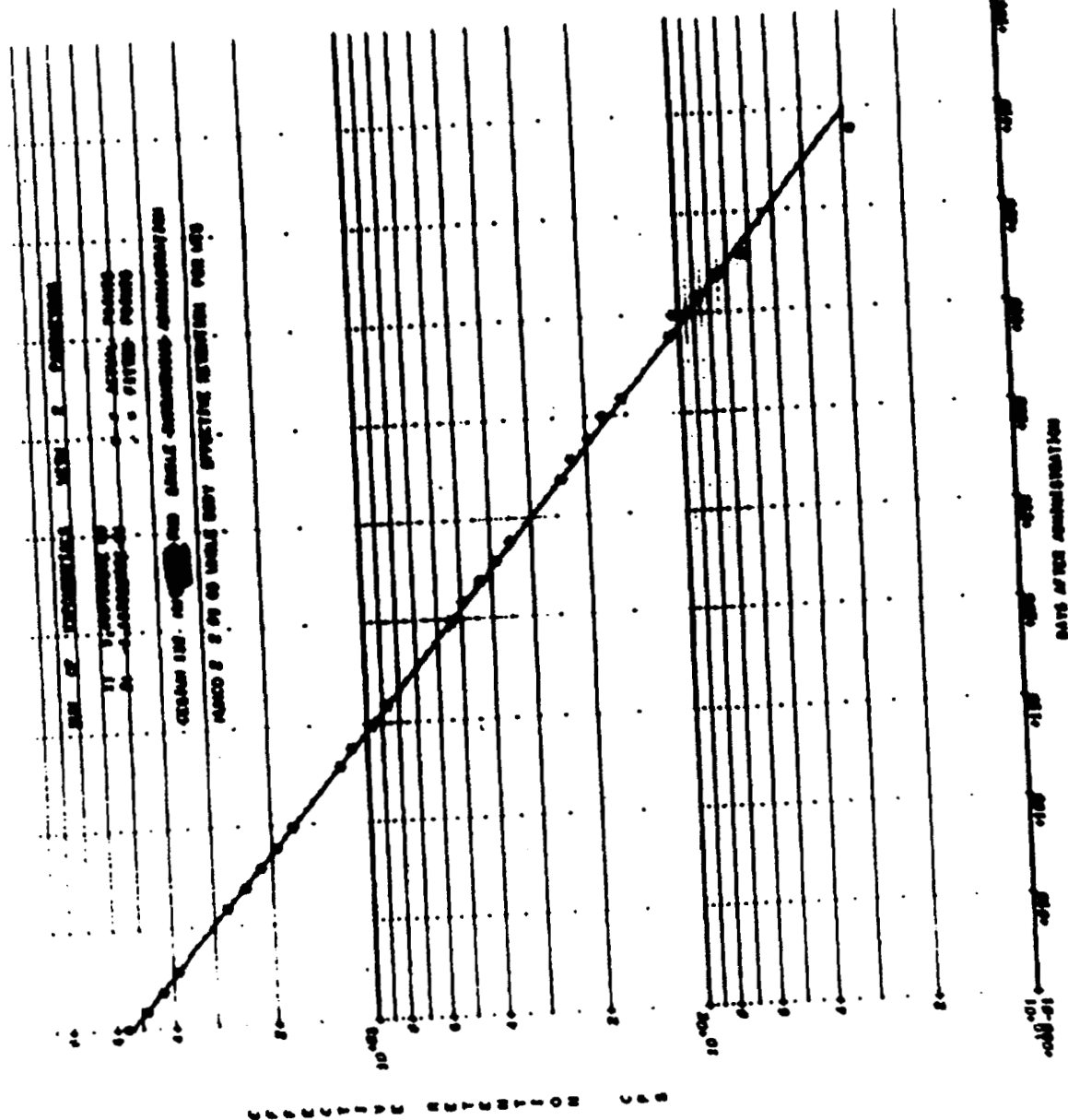


Fig. 3. Effective retention of 0.642 μ Ci Cs^{132} by subject HMCs-132



1055502

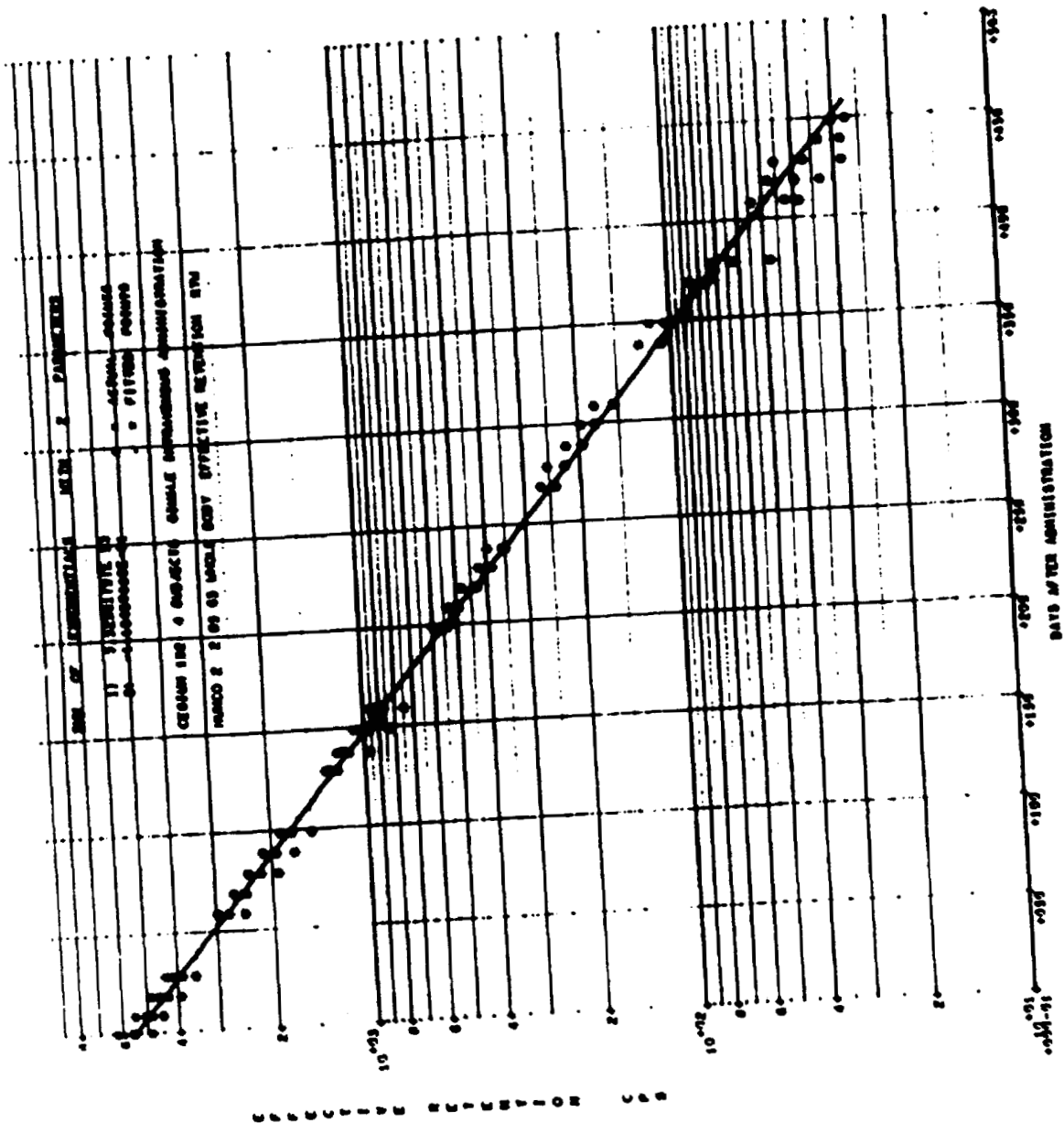


Fig. 5. Effective retention of Cs¹³² by 4 normal young adults.

1055503

corrections based on a 6.53-day PHL were used to convert the counting data to biological retention, and the latter was plotted as a function of time. The BHL derived from our Cs^{132} study is considerably shorter than BHL values obtained by us (5) and others (6-13) when Cs^{134} or Cs^{137} was used as the tracer. Liden (14) reports a BHL value of 74 days for 1 subject following intravenous administration of Cs^{134} . In general, most reported BHL values for stable cesium range between 100 and 150 days. Low specific activity is one factor which argues against the use of Cs^{132} as a tracer for stable cesium. In our studies, about 3 mg of stable cesium were administered along with the Cs^{132} to each person. The International Commission for Radiological Protection reports a value of less than 10^{-5} gram as the body content of stable cesium. Other workers (15) suggest a number closer to 1.5×10^{-3} gram. Regardless of the actual value, the administration of 3 mg stable cesium does not conform to the requirements of a true tracer study.

One would not anticipate a difference between the metabolism of Cs^{132} and Cs^{137} strictly on the basis of the masses of the radionuclides; however, this possibility cannot be completely ignored. We plan to repeat this experiment in several of the same subjects using carrier-free Cs^{137} as the tracer. Such studies can be done with high precision

when only 0.2 to 0.3 μc is administered. We should add here that the Cs^{137} body burdens of certain small population groups currently are higher than these levels as a result of nuclear weapon testing.

REFERENCES

- (1) These procedures were done by Dr. C. C. Lushbaugh of the Clinical Investigations Section of this Group.
- (2) Injections were made by Dr. C. C. Lushbaugh (see Ref. 1).
- (3) C. R. Richmond, J. E. Furchner, P. N. Dean, and P. McWilliams, Health Phys. 10, 3 (1964).
- (4) C. J. Maletskos, M. T. Clapp, M. M. Costello, and A. T. Keane, Annual Progress Report, Massachusetts Institute of Technology, Radioactivity Center (May 1962), pp. 41-45.
- (5) C. R. Richmond, J. E. Furchner, and W. H. Langham, Health Phys. 8, 201 (1962).
- (6) E. C. Anderson, R. L. Schuch, W. R. Fisher, and W. H. Langham, Science 125, 1273 (1957).
- (7) C. E. Miller and O. J. Steingraber, Semiannual Report of the Radiological Physics Division, Argonne National Laboratory Report ANL-5755 (1957), pp. 53-57.

- (8) K. T. Woodward, A. G. Schrodtt, J. E. Anderson, H. A. Claypool, and J. B. Hartgering, Division of Nuclear Medicine, Walter Reed Army Institute of Research Report DASA-1180 (1960).
- (9) C. G. Stewart, E. Vogt, A. J. W. Hitchman, and N. Jupe, Proceedings of the Second Conference on the Peaceful Uses of Atomic Energy, Geneva, 1958, P.15, p. 220, United Nations, New York (1958); see also: Progress in Nucl. Energy, Ser. VII, Med. Sci. 2, 39 (1959).
- (10) K. G. McNeill and R. M. Green, Canad. J. Phys. 37, 528 (1959).
- (11) C. E. Miller, Argonne National Laboratory Report ANL-5596 (1956).
- (12) E. Oberhausen, Proceedings of the University of New Mexico Conference on Organic Scintillation Detectors, U. S. Atomic Energy Commission Report TID-7612 (1961), pp. 286-292.
- (13) M. P. Taylor, J. Vennart, and D. M. Taylor, Physics in Med. and Biol. 7, 157 (1962).
- (14) K. Liden, Acta Radiol. 56, 237 (1961).
- (15) N. Yamagata, Nature 196, 83 (1962).

Lack of Effect of Exercise on the Excretion of Cesium¹³⁷ in Mice (J. E. Furchner, C. R. Richmond, and G. A. Trafton)

INTRODUCTION

It has been demonstrated that the excretion rate of Cs¹³⁷ in mice is inversely related to environmental temperatures (1). It is also well known that basal metabolic rates are inversely related to temperature (2,3). The present report describes an attempt to modify the excretion of Cs¹³⁷ by enforced exercise.

METHODS

Thirty RF₁ female mice 82 days old (25.1 g) were injected with ~ 0.5 µc of Cs¹³⁷Cl₂. Within 30 minutes after injection, the Cs¹³⁷ activity in each mouse was assayed in LASAC II, a 4π liquid scintillation counter, and then half were returned to cages and the other half placed in a cylindrical cage of stainless steel mesh (8 x 16 in.) that revolved at the rate of 1.7 RPM for 40 minutes every 2 hours. Both groups of animals had free access to Purina Lab Chow and water. The food consumption was measured by weighing. The animals were weighed at each assay. Urine and feces were collected and assayed periodically. The whole-body counting data were analyzed by an IBM 7090 computer programmed to perform an iterative least squares analysis.

RESULTS

The whole-body retention data for the experimental and control groups, corrected for counter fluctuation but not for decay, were described by retention functions of 3 exponential components (Table 1). Data points for each mouse were used in the least squares analysis for the best fit to all the points. Plots of the retention functions are given in Fig. 1, along with the average values (which were not used in the analysis). Derivatives of these functions are plotted as a function of time in Fig. 2. The data points in Fig. 2 represent the excretion rate per mouse per day as calculated from the assay of the excreta. Figure 3 shows the weight changes during the course of the experiment.

DISCUSSION

The data presented in Table 1 and in Figs. 1 and 2 clearly indicate no change resulted from the enforced exercise. Figure 3 indicates that control mice showed a small weight gain, after an initial loss, that was absent in the exercised animals. However, the exercised mice consumed less food (3.0 versus 3.3 g per mouse per day) than the controls. It has been pointed out that increases in metabolism due to cold increase food intake (4,5). Presumably, the enforced exercise was not vigorous enough to increase

TABLE 1. CESIUM ¹³⁷ RETENTION PARAMETERS IN NORMAL AND EXERCISED MICE

	a ₁	k ₁	a ₂	k ₂	a ₃	k ₃
Exercised	2464.0 + 418 —	1.625 + 0.272 —	2750.0 + 230 —	0.3818 + 0.0713 —	2242.0 + 307 —	0.1319 + 0.0063 —
Normal	2371.0 + 335 —	1.716 + 0.296 —	2976.0 + 262 —	0.3322 + 0.0610 —	2201.0 + 458 —	0.1288 + 0.0087 —

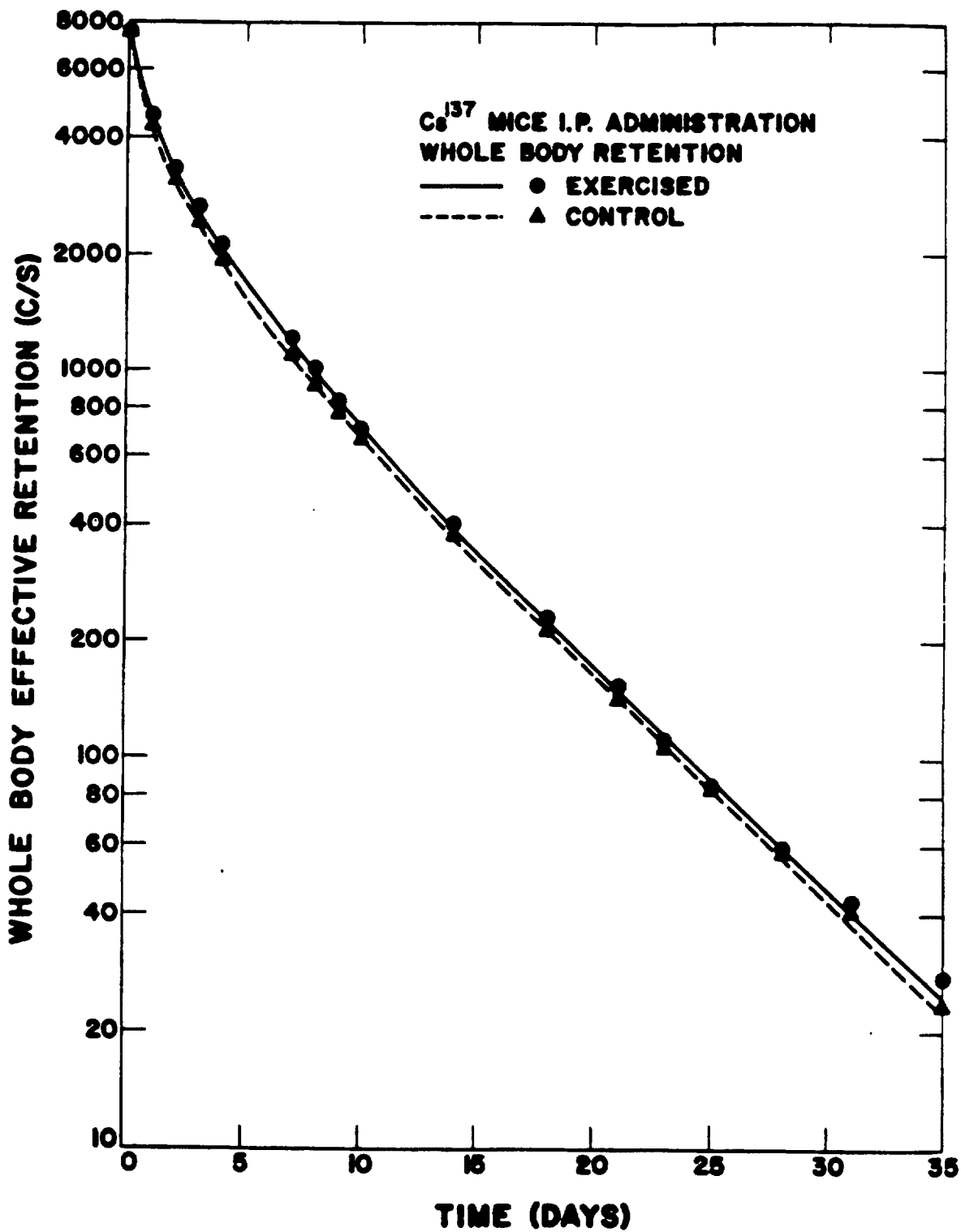


Fig. 1. Whole-body retention of Cs^{137} in normal and exercised mice.

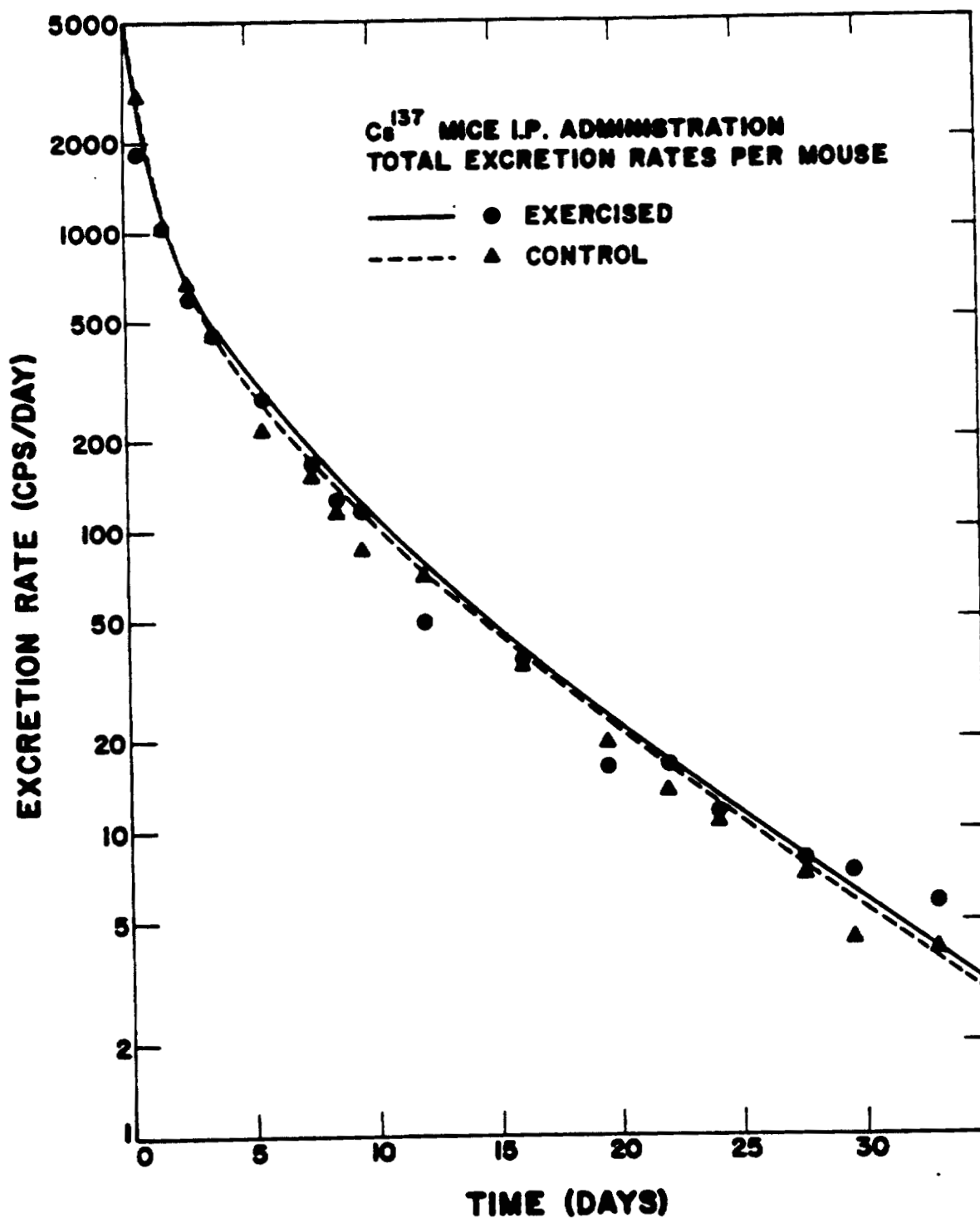


Fig. 2. Excretion of Cs^{137} from exercised and non-exercised mice.

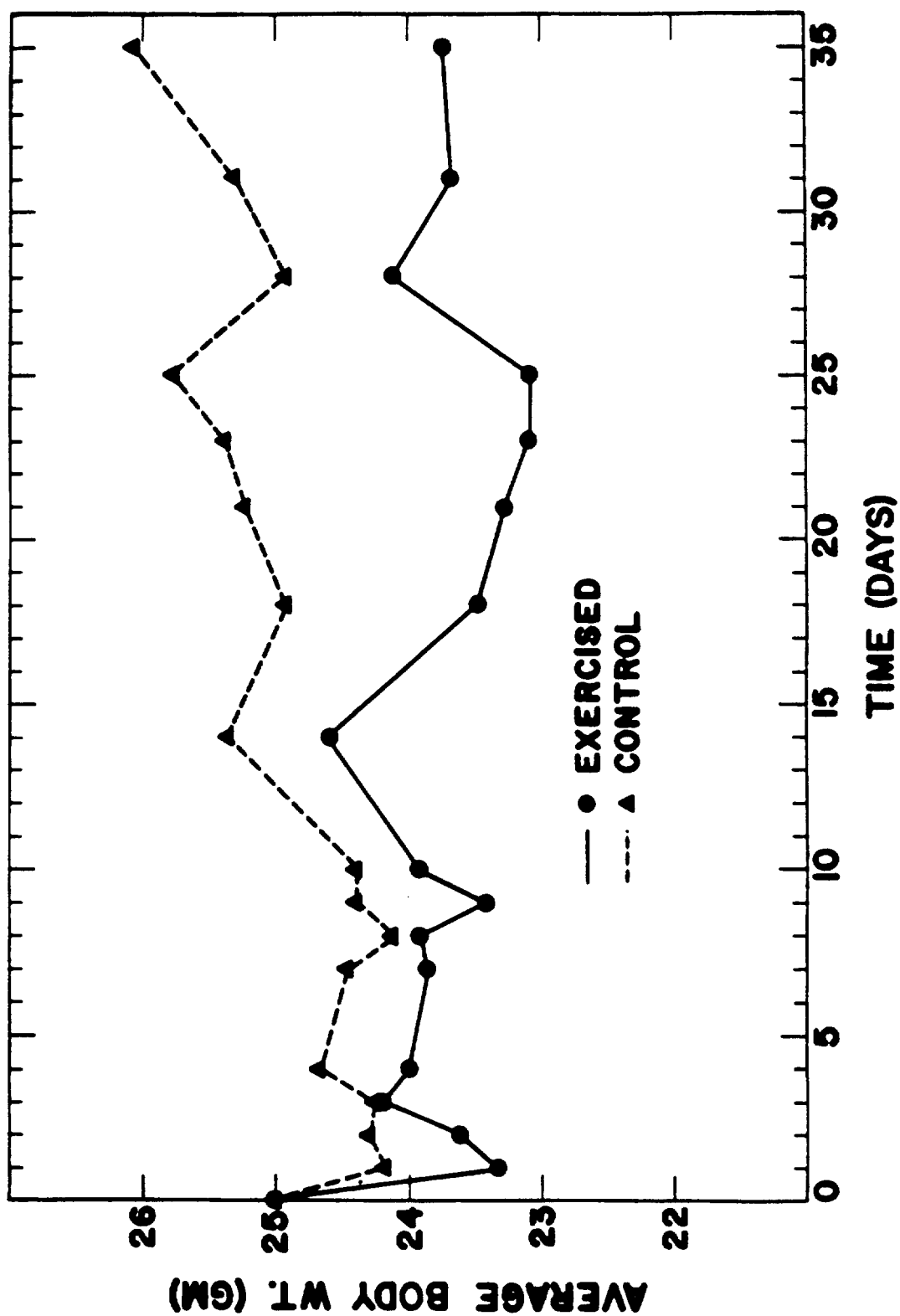


Fig. 3. Weight changes in exercised and non-exercised mice.

the metabolic rate. An increase in the RPM or in the running time, or both, may increase the metabolic rate and so affect the cesium excretion.

REFERENCES

- (1) J. E. Furchner and C. R. Richmond, J. Appl. Physiol. 18, 786 (1963).
- (2) E. F. Adolph, Am. J. Physiol. 176, 275 (1950).
- (3) S. Brody, Bioenergetics and Growth, Reinhold Publishing Corp., New York (1945).
- (4) M. J. Fregley, Am. J. Physiol. 176, 275 (1954).
- (5) J. L. Durrer and J. P. Hannon, Am. J. Physiol. 202, 375 (1962).

Distribution of Cesium¹³⁷ in Mice and Dogs after Chronic Exposure (J. E. Furchner, C. R. Richmond, and G. A. Trafton)

INTRODUCTION

There have been a number of reports pointing out bone concentrations of Cs¹³⁷ equaling or exceeding soft tissue concentrations (1,2). These reports deal with tracer amounts found in humans. Tissue distribution studies of cesium after acute exposure show that only 1 per cent is found in bone, compared to 80 per cent in muscle at 20 days (3). This report is concerned with the whole-body activity in mice and dogs during chronic exposure to Cs¹³⁷ and with the distribution in tissues after such chronic exposure.

METHODS

The drinking water of 12 RF₁ female mice was contaminated with Cs¹³⁷ at a concentration of about 0.06 µc/ml. The mice had free access to Purina Lab Chow and the contaminated drinking water. The whole-body activity, body weight, water consumption, and activity of the excreta were determined periodically over a period of 442 days. The mice were 216 days old at the beginning of the experiment (weight 29.4 g). The experiment was terminated when half the animals had died. Deaths occurred on days 221, 261, 313, 348, 359, and 402. The

survivors were killed by ether anesthesia, and the following tissues were assayed for Cs^{137} activity: pelt, gut, liver, kidneys, lungs, heart, spleen, both femurs, ovaries, uterus and adherent fat, carcass, and the remainder which consisted principally of mesentery stripped from the gut, fat, and blood.

Three male beagle hounds were fed $\sim 0.017 \mu\text{c Cs}^{137}$ on a Purina monkey pellet for a period of 674 days. At that time, the dogs were sacrificed with an intravenous overdose of sodium pentathol. The following tissues were assayed for Cs^{137} activity: pelt, gut, liver, kidneys, heart, spleen, both femurs, muscle, testes, pancreatic tissue, brain, blood, fat, and remainder.

RESULTS

The whole-body retention data for dogs and mice are shown in Fig. 1. The integral of a retention function for a single dose of Cs^{137} administered intravenously to dogs is shown as a solid line, as is the integral of the retention function for a single oral dose of Cs^{137} in mice which were the same age at t_0 as those used in the chronic study. The average distribution of Cs^{137} in mice and dogs is shown in Table 1 and in Fig. 2. In Fig. 2, the values for dogs have been "normalized" for purposes of comparison with mice

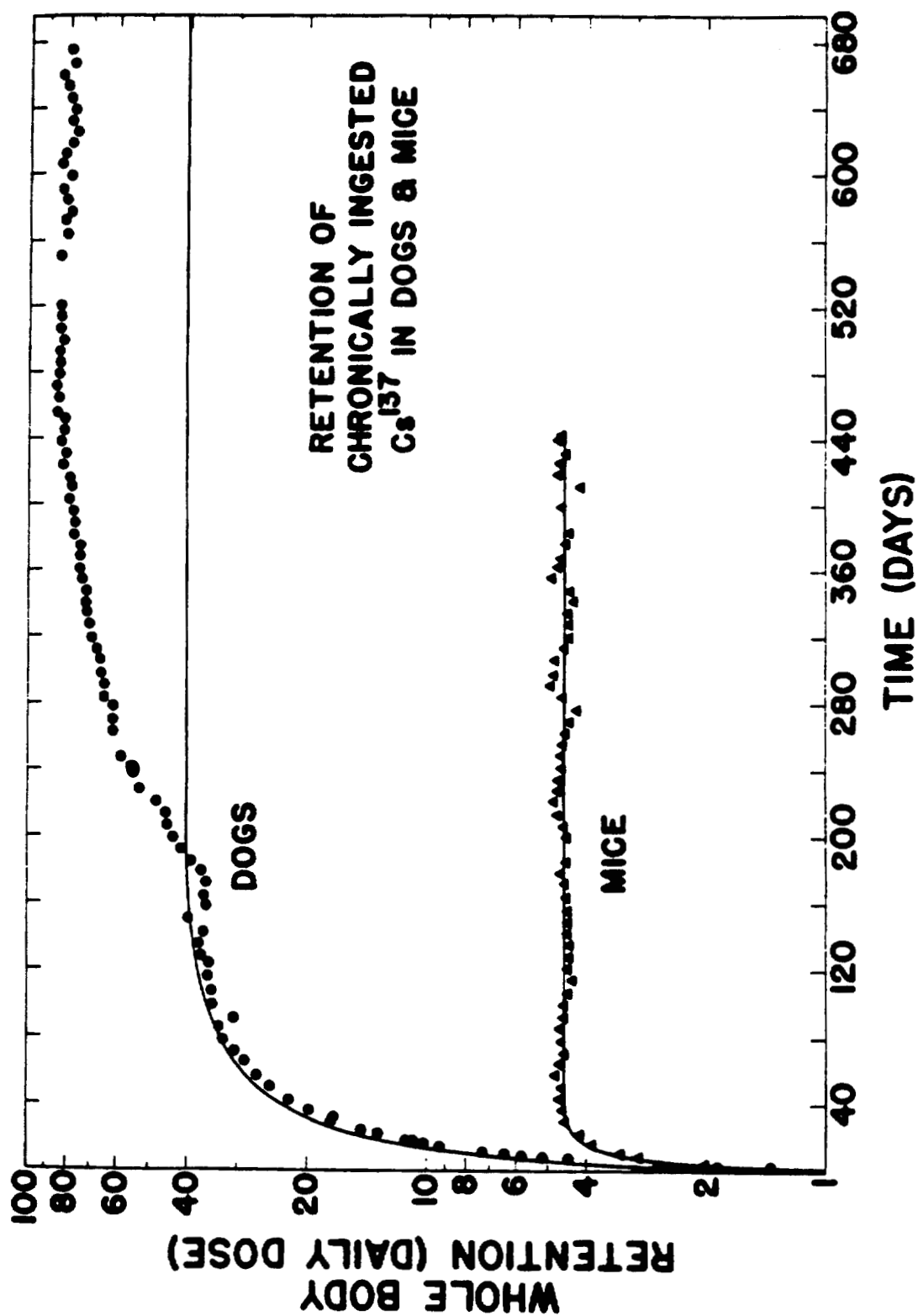


Fig. 1. Whole-body retention of chronically ingested Cs¹³⁷ in mice and dogs (plotted as multiples of the daily dose).

TABLE 1. CESIUM¹³⁷ DISTRIBUTION AFTER CHRONIC EXPOSURE

Tissue	Mice		Dogs	
	Whole-Body Burden (per cent)	Whole-Body Burden (per cent/g)	Whole-Body Burden (per cent)	Whole-Body Burden (per cent/g)
Whole-body	100.00	3.72	100.00	0.0062
Carcass	69.98	5.05	80.51	0.0078
Pelt	7.24	1.84	2.68	0.0016
Remainder	2.26	1.01	0.92	0.0008
Gut	10.69	3.58	4.76	0.0062
Liver	3.54	2.91	3.69	0.0063
Muscle	--	5.23	--	0.0129
Blood	--	--	--	0.0008
Fat	--	--	--	0.0004
Lungs	0.96	2.83	0.58	0.0043
Heart	0.89	3.49	0.77	0.0063
Femur (2)	0.63	3.60	0.99	0.0013
Brain	--	--	0.38	0.0046
Pancreas	--	--	--	0.0060
Spleen	0.67	3.66	0.20	0.0069
Gonads	1.59	1.63	0.12	0.0060
Kidneys	1.86	4.40	0.59	0.0082

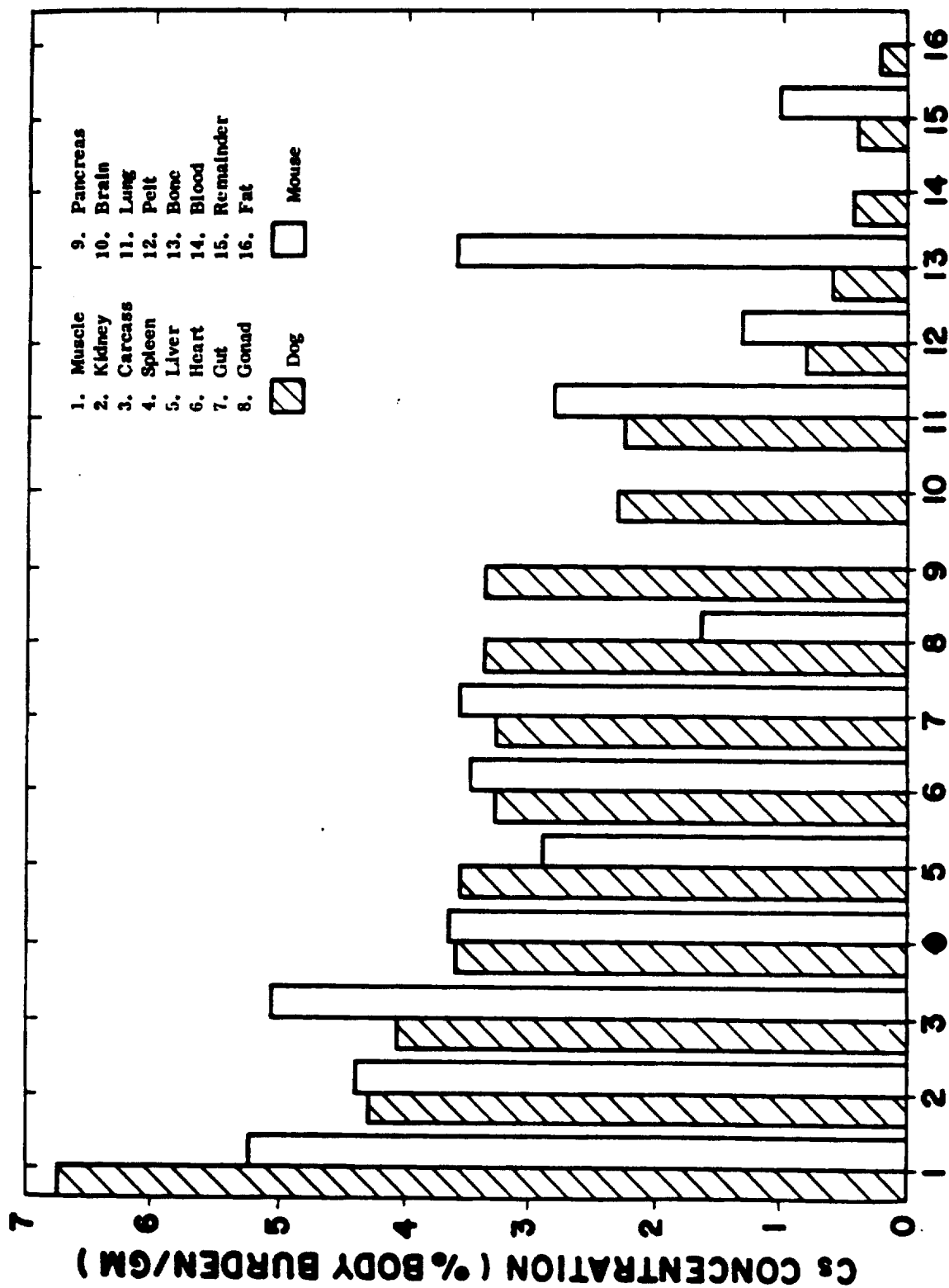


Fig. 2. Distribution of ^{137}Cs after chronic ingestion by mice and dogs (dog data "normalized" to mouse weights).

by multiplying the per cent per gram values by 590, the ratio of dog body weight to mouse body weight.

DISCUSSION

The whole-body retention of mice seems to fit the integral of the retention function satisfactorily. Some of the sharp divergences of the data points are due to deaths of individual mice. The reason for the discrepancy between the integral of the retention function for intravenously administered Cs^{137} and the chronic oral retention data for dogs is not apparent. The whole-body activity is higher by a factor of 2 than the estimate derived from the integral of the retention function. At about T_{280} , the dogs were moved from outdoor quarters during severely cold weather into heated dog runs, where they remained until they were killed. No seasonal fluctuations were apparent thereafter. It is possible that a further component may be necessary to describe whole-body retention, one that is not readily detected in an acute experiment. However, if this is the case, a deficiency in activity between T_{100} and T_{225} requires explanation. A chronic feeding experiment shows that the Cs^{137} equilibrium level in mice varies directly with temperature (4).

The tissues may be roughly divided into 3 groups (Table 1). Higher concentrations are found in the kidneys, muscle, and the

carcass which is mostly muscle. Intermediate concentrations (which are close to the whole-body concentration) are found in the gut, liver, lungs, heart, and spleen in both species. Lower concentrations are found in the pelt and remains in both species. The brain, pancreatic tissue, and gonads (testes) of the dog are in the intermediate range. The gonads (ovary and accessory sex organs) in the mouse fall in the lower concentration group, probably due to fat adherent to the uterus and Fallopian tubes. The dog femur has a low concentration comparable to that of the pelt, while the mouse femur has an intermediate concentration comparable to the heart and gut.

These groups are diagrammed in Fig. 2, where the values derived from dogs have been "normalized" for comparison. The normalization is, of course, false in the sense that organ weights are not directly proportional to body weights.

It is apparent that the bone metabolisms of the two species differ in respect to Cs^{137} . The data of Ballou and Thompson (5) show that the concentration of Cs^{137} in muscle is considerably greater than in bone in the rat. Thus, dogs and rats are similar in this respect and differ from man and mouse. At present, the authors have no explanation for these findings.

REFERENCES

- (1) R. W. Anderson and P. F. Gustafson, *Science* 137, 668 (1962).
- (2) N. Yamagata and T. Yamagata, First Annual Meeting of the Japan Radiation Research Society (September 1959).
- (3) C. R. Richmond, Los Alamos Scientific Laboratory Report LA-2207 (1958).
- (4) J. E. Furchner and C. R. Richmond, *J. Appl. Physiol.* 18, 786 (1963).
- (5) J. E. Ballou and R. C. Thompson, *Health Phys.* 1, 85 (1958).

Metabolism of Manganese⁵⁴ in Rats and Mice (J. E. Furchner, C. R. Richmond, and G. A. Trafton)

INTRODUCTION

As part of the program for measuring whole-body retention of gamma-ray-emitting isotopes with 4π scintillation counters, Mn⁵⁴ was administered to rats and mice by various routes. As long as the whole-body activities remain above the lower limit of the detection system, the studies will be continued.

RESULTS AND DISCUSSION

Figure 1 shows the variability of retention in the rat after a single oral dose. The activity (in c/sec), corrected for counter error but not for physical decay, is plotted against time. Eye-fit lines are drawn for purpose of comparison. An effective half-time of about 30 days approximately fits the latter portions of the data. At present, no explanation of why two animals retained about 30 times the amount retained by the other four animals is offered.

Figure 2 shows early retention in mice. Here again, the effective retention is plotted as a function of time. Average values for each group are plotted. It is too early to determine the significance of the difference in retention after intravenous and intraperitoneal administration. The

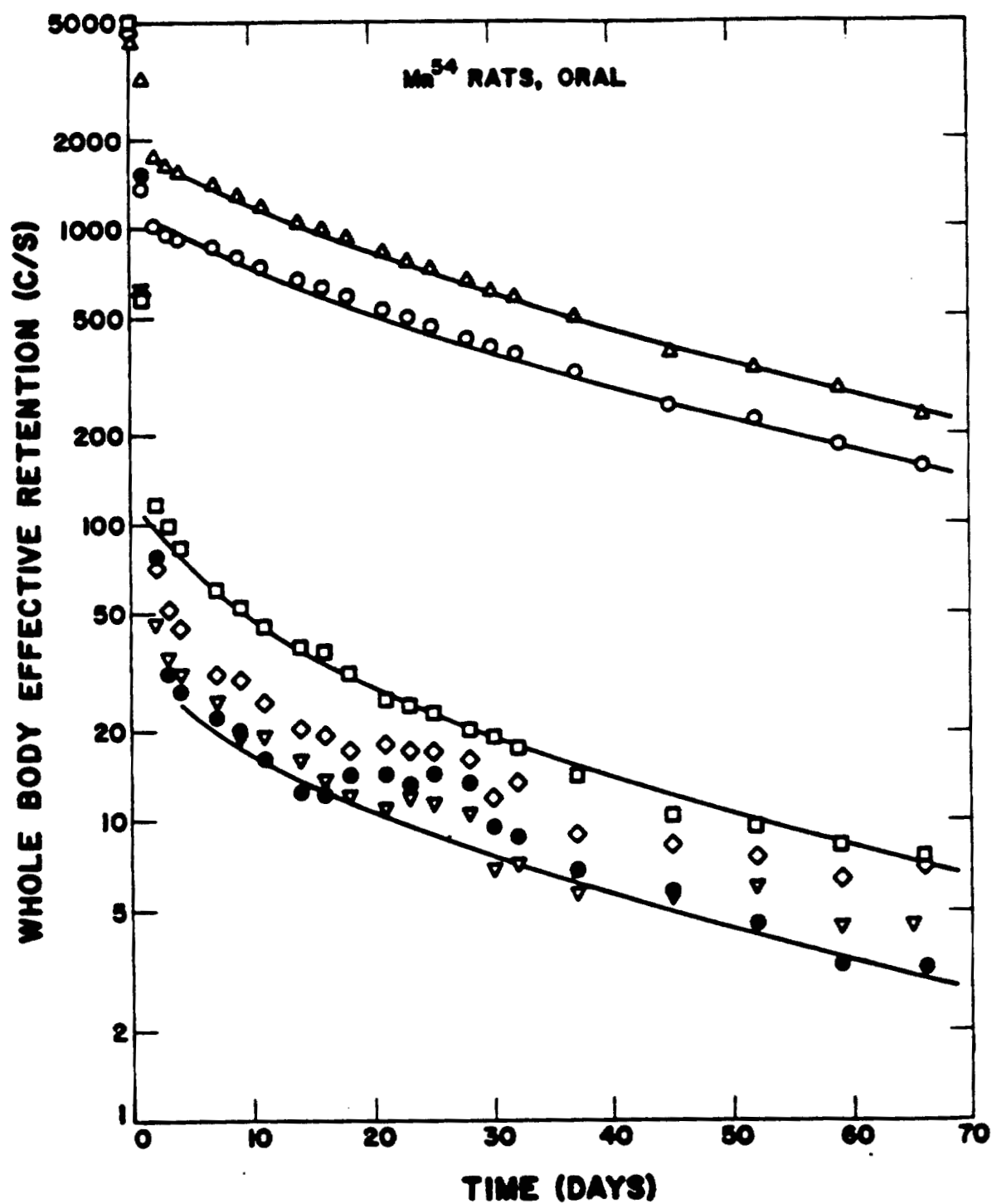


Fig. 1. Whole-body effective retention of Mn⁵⁴ in male rats after oral administration.

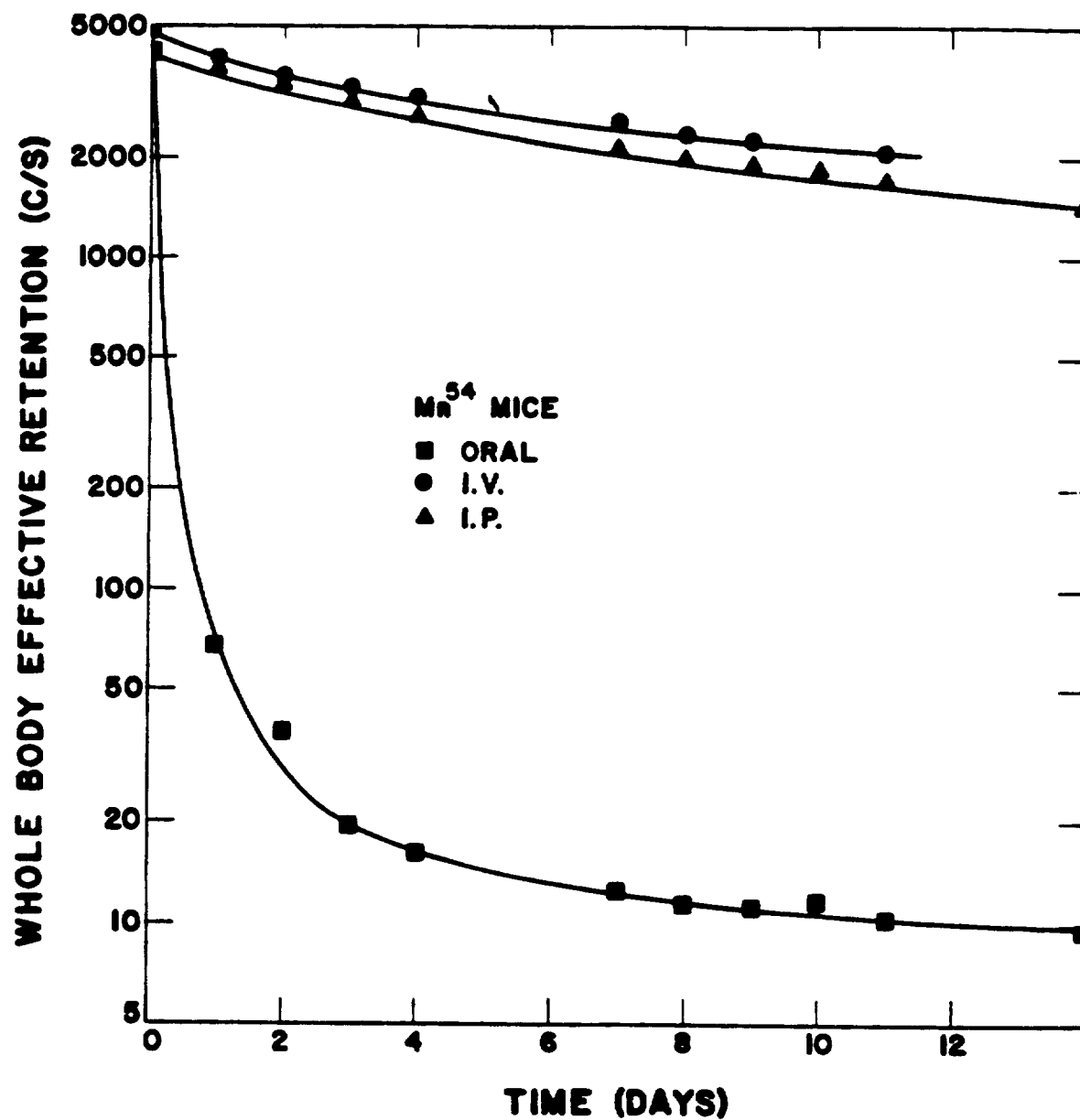


Fig. 2. Whole-body effective retention of Mn⁵⁴ by mice after oral, intraperitoneal, and intravenous administration.

mice retained about 0.5 per cent of the orally administered manganese on the third day, showing that intestinal absorption of this element is very low. The comparable figure for rats (excluding the 2 with high activity) is about 1 per cent.

Retention of manganese in monkeys and dogs will be measured, and additional rat experiments (orally administered Mn^{54}) are in progress.

Retention of Zirconium⁹⁵ after Oral and Intraperitoneal Administration to Mice (J. E. Furchner, C. R. Richmond, and G. A. Trafton)

INTRODUCTION

The increasing use of zirconium imposes interest in the retention and excretion of this element. In addition, zirconium has been examined for use as a means of displacing heavy metals deposited in bone. The present paper deals with the whole-body retention of zirconium in mice. Related studies in rats, dogs, and monkeys are in progress.

METHODS

Twelve RF₁ female mice, 54 days old (22.5 g weight), were given about 0.215 μ c of a zirconium-niobium equilibrium mixture as the citrate by gastric gavage. The mice were paired, and the activity in each pair was measured in a 4 π whole-body liquid scintillation counter for small animals. Appropriate standards were also assayed. On the first day after administration, the activity had fallen by a factor of about 100, and the activity of the group (6 pairs) was then measured in the Los Alamos Human Counter (Humco II). Measurements were continued until the 67th day after administration.

A second group of 12 mice of the same age were injected

intraperitoneally with the same amount of the zirconium-niobium mixture and assayed in the small animal counter. The animals were counted at appropriate intervals for 435 days. The whole-body counting data from this group, corrected for counter fluctuation but not for physical decay, were then analyzed by an IBM 7090 computer programmed to fit the data by an iterative least squares procedure. The data from each pair were analyzed individually, and the data from the 6 pairs were also analyzed en masse.

RESULTS

Retention functions of 3 exponential components fit the data of each pair and of the group (I. P.). Table 1 gives the parameters of the retention functions for each pair and for the group. Figure 1 shows all the data points for 1 pair of mice. At intervals, the data points for the 6 pairs are also plotted to indicate the range within the group. The smooth curve drawn through the data points is a plot of the retention function derived by the IBM 7090. In the same figure are shown the data points for whole-body retention after oral administration.

DISCUSSION

The data, as presented, represent whole-body effective

TABLE 1. EFFECTIVE RETENTION OF ZIRCONIUM⁹⁵ IN MICE AFTER ORAL AND INTRAPERITONEAL ADMINISTRATION

*	a ₁	k ₁	a ₂	k ₂	a ₃	k ₃	k _{3b}
All Mice	7534.0	1.524** 0.45	3470.0	0.09808 7.1	5320.0	0.01075 64.5	0.00009 7700.0
1st Pair	6976.0	1.494 0.46	3327.0	0.09676 7.2	5252.0	0.01078 64.2	0.00012 5800.0
2nd Pair	7518.0	1.552 0.45	3404.0	0.10027 6.9	5448.0	0.01073 64.6	0.00007 9900.0
3rd Pair	7868.0	1.241 0.56	3582.0	0.09876 7.8	5234.0	0.01070 64.8	0.00004 17,300.0
4th Pair	8317.0	1.870 0.37	3357.0	0.10499 6.6	5170.0	0.01066 65.0	0.00000 ∞
5th Pair	6793.0	1.732 0.40	3254.0	0.09805 7.1	5650.0	0.01087 63.8	0.00021 3300.0
6th Pair	7891.0	1.353 0.51	3835.0	0.09003 7.7	5188.0	0.01076 64.4	0.00010 6900.0
X	7561.0	1.540 0.45	3460.0	0.09814 7.1	5324.0	0.01075 64.5	0.00009 7700.0
Oral (all mice)	44,920.0	4.498 0.15	96.0	0.05900 11.7	104.6	0.01075 64.5	0.00009 7700.0

* From $R_t = \sum_{i=1}^3 a_i e^{-k_i t}$.

** Effective half-time in days.

1055528

LANL

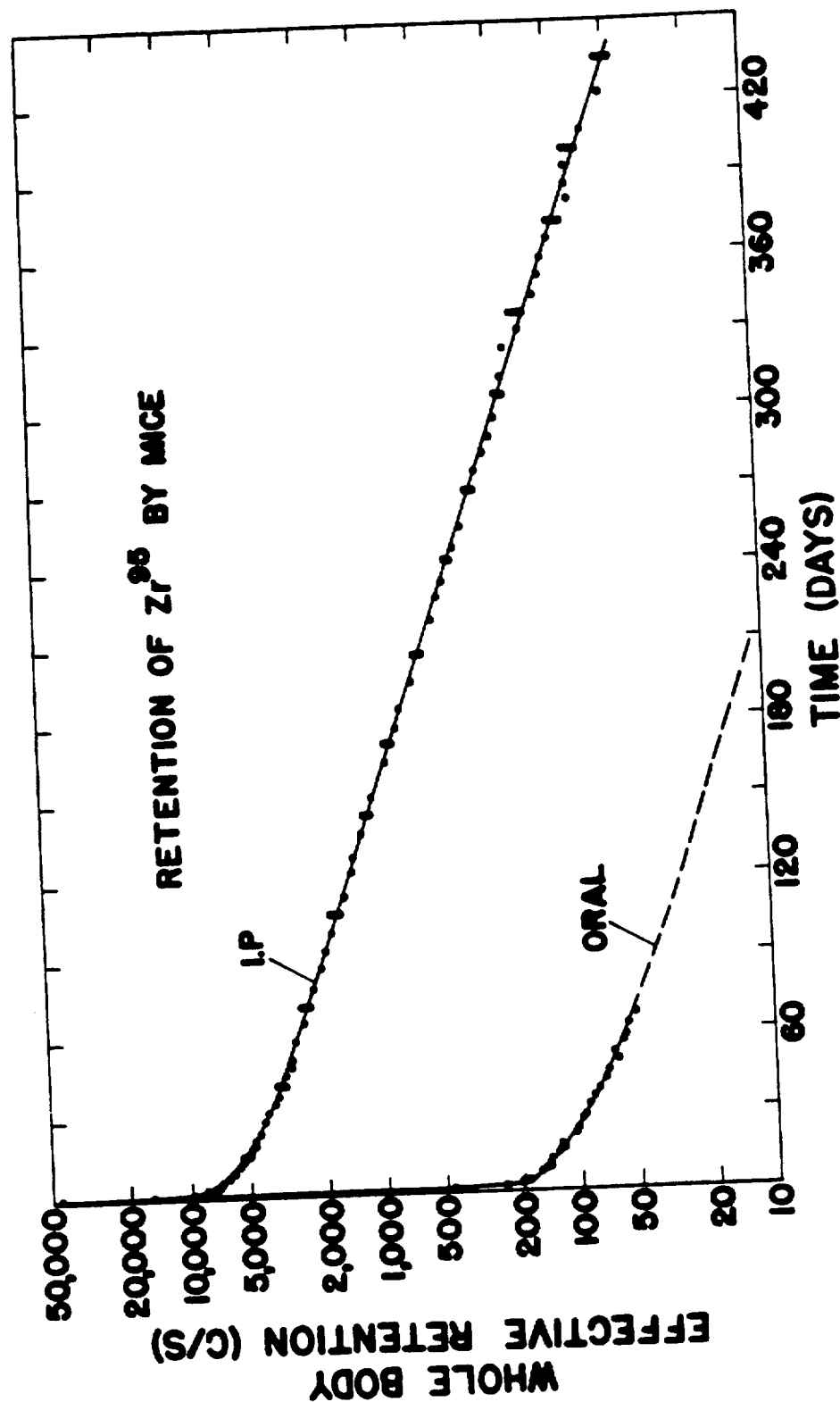


Fig. 1. Whole-body effective retention of Zr^{95} by female mice after acute, oral, and intraperitoneal administration.

1055529

retention. The retention function for the mice treated by oral administration was eye-fit with the assumption that the slope constant of the last component was the appropriate constant to use. The remaining parameters were then derived by "curve peeling." More sophisticated computer analyses will be used in a later report.

The data and parameters representing the retention after intraperitoneal administration show good agreement among the 6 pairs. The average values of these parameters agree well with the values derived from the group as a whole (lines labeled "all mice" and " \bar{X} " in Table 1). The half-times listed under k_3 approach 65 days, the physical half-time for Zr^{90} . The rate constants for effective retention (k_3) are the sum of the biological rate constant (k_{3b}) and the physical rate constant (λ_{Zr}):

$$k_3 = k_{3b} + \lambda_{Zr}.$$

The physical rate constant for Zr^{95} , with a half-time of 65 days, equals $\frac{0.693}{65} = 0.01066$. When this value is taken from k_3 , the upper values of each pair in the last column in Table 1 are the result, and the half-times derived from these rate constants range between 3000 days and infinity. For mice, the difference between 3000 days and infinity may be ignored. For longer-lived individuals, the difference

may be important if the biological retention is the parameter of interest. These data illustrate the disadvantages of studying the metabolism of nuclides having long biological half-times with isotopes having comparatively short physical half-lives.

Effective Retention of Intravenously Administered Beryllium⁷
by Rats (C. R. Richmond, J. E. Furchner, and J. E. London)

INTRODUCTION

This report summarizes our work covering the whole-body effective retention of intravenously administered carrier-free Be⁷Cl₂ by rats. This work is part of a continuing effort to establish metabolic parameters for various mammalian species with interspecific correlations as the final goal. Studies in the mouse and dog are essentially complete, as are tissue distribution studies in the rat. A complete summary should be ready for the next report.

METHODS AND MATERIALS

Six 70-day-old male Sprague-Dawley rats were used. The average body weight for the group was about 283 g. To each of 6 of the animals was given 5.5 µc of carrier-free Be⁷ contained in 0.11 ml solution as the chloride. Injection was into the lateral tail vein of the anesthetized animals. All animals were maintained in temperature controlled (75° F) rooms and allowed free access to water and Purina Lab Chow. The entire animal was measured in the Los Alamos Small Animal Counter (LASAC III) shortly after administration and at appropriate subsequent times. All counting times were of 100 seconds duration. Background and Be⁷ standards were

measured before and after the experimental animals. Effective retention parameters were then determined by computer methods. Results of urinary and fecal excretion are not reported here.

RESULTS AND DISCUSSION

Table 1 gives the effective retention parameters for each of the 6 animals and for all combined as calculated by the least squares curve-fit program. The standard deviation for each parameter is also given. Table 2 gives the effective and biological half-lives for each retention component for all the analyses. A three-component exponential model appears to fit the data quite adequately. The value of 54 days was used as the physical half-life of Be^7 in these analyses. Component 3, which tentatively may be ascribed to bone, is the component of most interest as the effective half-life is extremely close to the 54-day physical half-life. This component contributes over 95 per cent of the total area under the effective retention function when integrated from zero to infinite time. Figure 1 shows a computer derived plot of the data. Statistical weighting factors (1) were used. The analysis requires no logarithmic transformations of the observed data.

In summary, preliminary results suggest that the hard

TABLE 1. EFFECTIVE RETENTION PARAMETERS FOR MALE SPRAGUE-DAWLEY RATS GIVEN Be^{7}Cl_2
BY INTRAVENOUS ADMINISTRATION*

Rat No.	a_1	$k_1 + \lambda$	a_2	$k_2 + \lambda$	a_3	$k_3 + \lambda$
1	3.3670E 03** + 4.0562E 01 ⁺	2.7882E 00 + 1.5639E-01	8.0980E 02 + 2.7649E 01	7.9023E-02 + 5.5219E-03	4.3101E 03 + 2.7263E 01	1.3356E-02 + 5.8448E-05
2	3.9870E 03 + 5.6278E 01	3.0363E 00 + 2.2661E-01	9.9625E 02 + 3.5849E 01	1.0847E-02 + 8.0320E-03	4.7462E 03 + 2.6904E 01	1.3643E-02 + 6.3800E-05
3	3.4557E 03 + 5.0027E 01	2.8023E 00 + 1.8856E-01	8.7482E 02 + 3.6473E 01	9.5911E-02 + 8.4637E-03	4.7434E 03 + 3.6757E 01	1.3542E-02 + 9.7076E-05
4	3.7412E 03 + 4.7875E 01	3.2095E 00 + 2.4942E-01	9.5671E 02 + 3.2621E 01	9.0261E-02 + 6.4453E-03	4.8431E 03 + 3.1332E 01	1.3542E-02 + 7.0135E-05
5	3.5483E 03 + 3.8534E 01	2.5214E 00 + 1.0707E-01	9.1106E 02 + 2.4713E 01	9.2944E-02 + 5.2335E-03	4.3253E 03 + 2.0872E 01	1.3483E-02 + 4.8664E-05
6	3.7304E 03 + 5.0016E 01	4.8245E 00 + 1.2846E 00	1.0613E 03 + 3.1165E 01	9.4795E-02 + 5.8071E-03	4.3375E 03 + 2.6316E 01	1.3494E-02 + 6.1441E-05
All 6	3.6160E 03 + 1.1029E 02	3.0621E 00 + 5.0947E-01	9.1423E 02 + 7.0956E 01	9.9652E-02 + 1.6112E-02	4.5749E 03 + 5.8660E 01	1.3606E-02 + 1.3970E-04

*Animals 1 through 6 measured for 240, 204, 141, 183, 232, and 240 days, respectively.

**Indicates value is 3.3670×10^3 .

⁺Standard deviation.

TABLE 2. EFFECTIVE AND BIOLOGICAL HALF-LIVES FOR MALE SPRAGUE-DAWLEY RATS GIVEN Be^7Cl_2 BY INTRAVENOUS ADMINISTRATION

Rat No.	Effective Half-Life (days)			Biological Half-Life (days)*		
	C-1**	C-2	C-3	C-1	C-2	C-3
1	2.4860E-01 [†]	8.7715E 00	5.1897E 01	2.4975E-01	1.0473E 01	1.3323E 03
2	2.2829E-01	6.3904E 00	5.0807E 01	2.2926E-01	7.2481E 00	8.5908E 02
3	2.4735E-01	7.2270E 00	5.1187E 01	2.4849E-01	8.3436E 00	9.8247E 02
4	2.1597E-01	7.6794E 00	5.1185E 01	2.1684E-01	8.9525E 00	9.8165E 02
5	2.7490E-01	7.4577E 00	5.1410E 01	2.7631E-01	8.6527E 00	1.0718E 03
6	1.4367E-01	7.3121E 00	5.1366E 01	1.4404E-01	8.4572E 00	1.0529E 03
All 6	2.2637E-01	6.9557E 00	5.0945E 01	2.2732E-01	7.9841E 00	9.0048E 02

*Physical half-life of 54 days used to derive values from the machine calculated effective half-lives.

**Components of the retention function.

[†]Indicates value is 2.4860×10^{-1} .

tissues bind beryllium more tenaciously than do other tissues. The effective half-life for this component is approximately 51 days.

REFERENCE

- (1) C. R. Richmond, J. E. Furchner, P. N. Dean, and P. McWilliams, Health Phys.

The Effect of Environmental Temperature on the Retention of Strontium in Mice (J. E. Furchner, C. R. Richmond, and G. A. Trafton)

INTRODUCTION

It has been demonstrated that the whole-body retention and excretion of Cs^{137} are a function of the temperature at which the mice are maintained (1). The principal site of deposition for cesium in mammals is soft tissue. The effect of temperature on the whole-body retention of strontium, an element deposited principally in bone, is reported here.

METHODS

After a single intraperitoneal injection of about $0.5 \mu\text{c}$ Sr^{85} at a pH of 6.0, 30 RF_1 female mice (80 days, \bar{X} 23 g) were divided into 3 equal groups. Initial activity was determined in LASAC III, a 4π liquid scintillation counter (2). After assay, the mice were placed in cages and maintained at 34° , 22° , and 5°C ($\pm 2^\circ$). Whole-body activity was measured at convenient intervals until 172 days after injection. Weights were recorded during the experiment.

The retention data (in c/sec) were corrected for counter fluctuation (but not for physical decay) and were analyzed by an IBM 7090 computer programmed for an iterative least squares analysis (3). The parameters of the function describing

retention in each animal were determined and tested by the Duncan-Kramer test of comparison among means (4,5). The rate and intercept parameters of the functions describing retention for each group were determined by the computer, along with the standard deviation of each parameter. The values (c/sec) determined on each day of measurement were subjected to the Duncan-Kramer test.

RESULTS

Three-component exponential equations were fit to the retention data of each animal and each group of animals. In Fig. 1, where the units of the ordinate are activity (in c/sec) and those of the abscissa are time (in days), plots of the best fit retention functions for each group are drawn, along with average values and vertical bars to show the range of values. The average values were not used in the analyses of the data and are included to indicate the assay times. Overlap in the range of values for the high and low temperature groups is indicated by the solid portion of the vertical bars. The data from the animals at 22° C overlap the higher and lower values of the 5° and 34° C animals, respectively, throughout.

In Table 1, the values of the parameters describing whole-body effective retention are given with standard

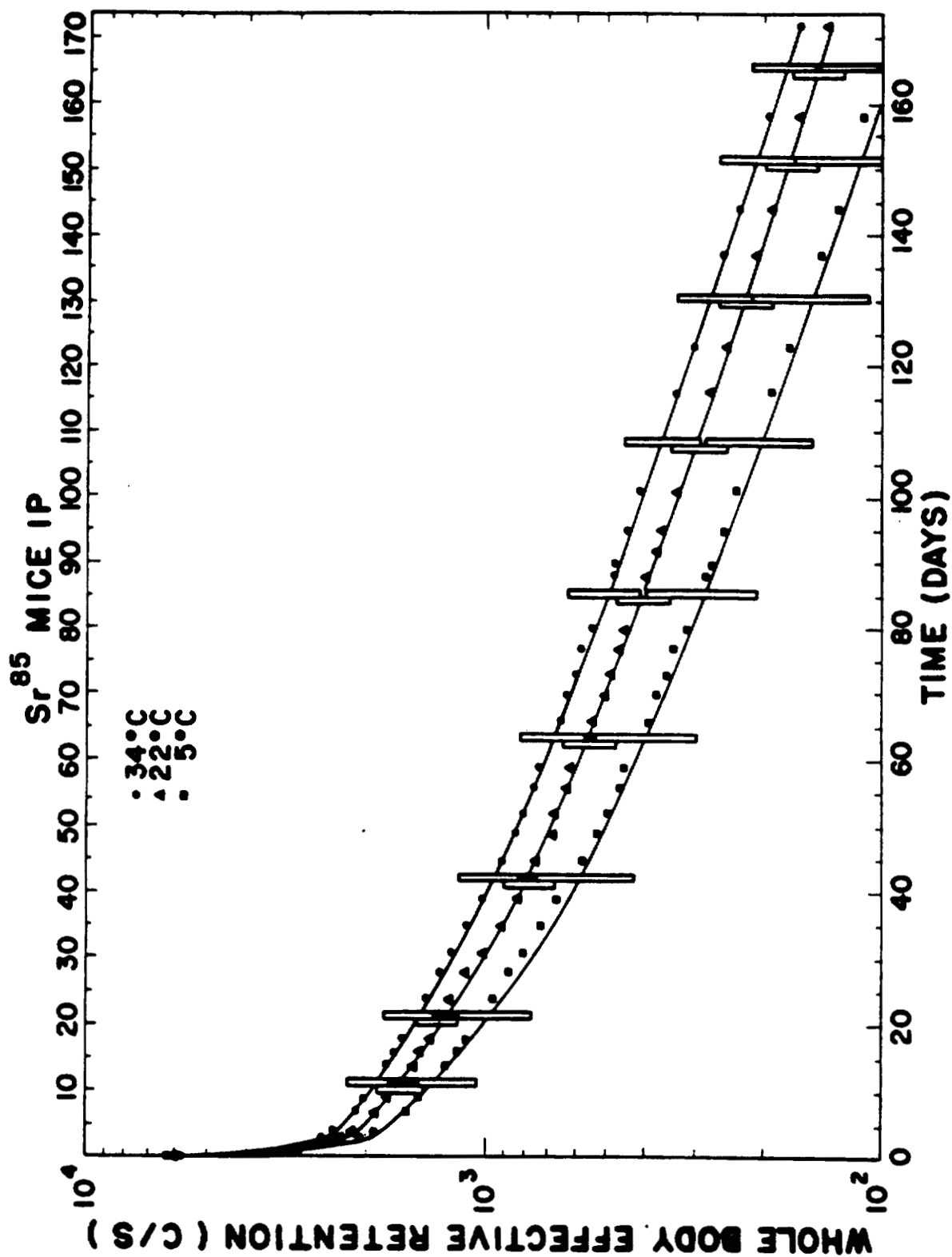


Fig. 1. Effective retention of Sr^{85} by mice at 34°, 22°, and 5° C.

TABLE 1. EFFECTIVE RETENTION OF STRONTIUM⁸⁵ IN MICE AT 34°, 22°, AND 5° C

a_1^*	k_1^*	a_2	k_2	a_3	k_3
<u>Group A (34° C)</u>					
$\frac{3114.0}{+ 107}$	$\frac{1.42}{+ 0.11}$	$\frac{1255.0}{+ 85}$	$\frac{0.0575}{+ 0.0070}$	$\frac{1445.0}{+ 98}$	$\frac{0.0127}{+ 0.0006}$
<u>Group B (22° C)</u>					
$\frac{3629.0}{+ 90}$	$\frac{1.58}{+ 0.09}$	$\frac{1248.0}{+ 64}$	$\frac{0.0588}{+ 0.0055}$	$\frac{1170.0}{+ 74}$	$\frac{0.0126}{+ 0.0005}$
<u>Group C (5° C)</u>					
$\frac{4070.0}{+ 128}$	$\frac{1.47}{+ 0.10}$	$\frac{1239.0}{+ 76}$	$\frac{0.0639}{+ 0.0074}$	$\frac{895.0}{+ 83}$	$\frac{0.0137}{+ 0.0008}$

* a_1 and k_1 are the intercept and rate constants of the retention functions. The underlined values differ from the other two corresponding values by more than 2 standard deviations.

deviations. The underlined parameters (a_1 and a_3) differ from the parameters of the other two groups by more than 2 standard deviations ($P = 0.05$). The retention parameters obtained from each mouse were averaged, and the mean values of the parameters were subjected to the Duncan-Kramer test of comparisons among means ($P = 0.01$). The results of this test agreed with results found above with the additional difference that k_3 , the rate constant of the third component for the mice maintained at 5° , differed from those of the other two groups.

A day-by-day comparison of the activity in each group was made by analysis of variance and the Duncan-Kramer test of comparisons among means. The day zero counts did not differ significantly at the 1 per cent level. The 34° and 5° C groups differed significantly at all times from day 1 to day 172; the 22° and 5° C temperature groups differed significantly from the seventh to the 172nd days, and the 22° and 34° groups differed significantly at the 1 per cent level from the ninth day to 172 days, with the exception of the 24th and 66th days, where the differences were significant at the 5 per cent level.

DISCUSSION

We are aware of no test which will test for difference

between multicomponent curves. The solutions derived by the computer program are not unique. The value given for any parameter is not independent of the values of the other parameters of the function. Therefore, the tests applied are not appropriate. The same reasoning holds true for the AOV test applied to the group values at the various assay times, because the activity in a mouse on any day is not independent of the activity at earlier times. Although the significance levels do not apply, it seems clear that the intercept parameters of the retention functions differ. Because there are no rate differences among the most rapidly moving components, it appears that more is available to be lost at this rate at lower temperatures and, because of the greater loss, less remains for loss at the slowest rate.

The differences among the measurements are small. The equilibrium level under conditions of chronic exposure to Sr^{85} ($T_{1/2} = 65$ days), estimated by the integral of the retention function, would be 30 per cent lower at 5°C than at 22°C . However, if Sr^{90} ($T_{1/2} = 28$ years) is used, the lifetime body burden in mice at 5°C (integral between 0 and 1095 days) is only half that at 22°C (Table 2). If the differences among the smallest rate constants (k_3) are real, as indicated by the Duncan-Kramer test, then the strontium in the most slowly moving pool is affected by the increased metabolic rate associated with low temperature.

TABLE 2. EFFECT OF AMBIENT TEMPERATURES ON PER CENT RETENTION OF INTRAPERITONE-ALLY ADMINISTERED STRONTIUM ⁹⁰

	a_1°	$k_1 + \lambda_{90}$	a_2	$k_2 + \lambda_{90}$	a_3	$k_3 + \lambda_{90}$	Area ^{**}
<u>Group A (34° C)</u>							
	53.6	1.41	21.6	0.0469	24.9	0.00214	10,980.00
<u>Group B (22° C)</u>							
	60.0	1.57	20.6	0.0482	19.4	0.00201	9,043.0
<u>Group C (5° C)</u>							
	65.6	1.46	20.0	0.0533	14.4	0.00309	4,985.0

$$^{\circ}a_n = \frac{a_1}{\sum_{i=1}^n a_i} \times 100, \text{ where } a_1 \text{ is the intercept constant.}$$

$$^{**}\text{Area} = \sum_{i=1}^3 \int_0^{1095} a_1 e^{-(k_1 + \lambda_{90} t)} \cdot \lambda_{90} - \text{physical decay constant}$$

for Sr ⁹⁰.

While temperature was effective in altering the amount of Sr^{85} lost at the various rates, it is not clear that relation between strontium metabolism and environmental temperature is direct as is that of O_2 consumption and environmental temperature. The data presented here suggest that short exposures (~1 week) at these temperatures would result in retention patterns similar to those presented in Fig. 1, unless the difference in the excretion rate found in the animals exposed to cold is real.

REFERENCES

- (1) J. E. Furchner and C. R. Richmond, J. Appl. Physiol. 18, 786 (1963).
- (2) R. L. Schuch, Los Alamos Scientific Laboratory Report LAMS-2455 (1960), p. 105.
- (3) R. H. Moore and R. K. Zeigler, Los Alamos Scientific Laboratory Report LA-2367 (1960).
- (4) D. B. Duncan, Biometrics 11, 1 (1955).
- (5) C. Y. Kramer, Biometrics 12, 307 (1956).

Potassium⁴⁰ and Cesium¹³⁷ Levels of Beagle Hounds (C. R. Richmond, J. E. Furchner, and J. E. London)

INTRODUCTION

Before large animals can be used in tracer studies, their natural gamma-ray activities must be accurately measured. This activity normally is comprised of K^{40} and Cs^{137} . This report summarizes our findings for 20 beagle hounds which were measured prior to low-level tracer experiments.

METHODS AND MATERIALS

Each animal was thoroughly washed and dried before being counted for 25 minutes in the Los Alamos Human Counter (Humco II). The counting time was divided into three 500-second periods, each of which was preceded and followed by a 500-second background measurement on the animal's cage. Assays were repeated on 9 of the animals roughly 1 week following the first measurement. Humco II Cs^{137} and K^{40} standards were also measured with each animal. Raw counting data were processed by a modification of a computer method programmed for the IBM 7090 by E. C. Anderson of the Low-Level Counting Section. This program will calculate the amount of potassium in the animal from the animal's K^{40} activity (assumes 3 gamma rays per second are emitted from each gram of "normal" potassium). The total Cs^{137} level,

expressed in picocuries per gram of potassium or as nanocuries of Cs^{137} , is also calculated. The original data, measured for any or all of the 6 channels, are used are pre-experimental animal backgrounds in tracer experiments.

RESULTS AND DISCUSSION

Table 1 gives the K^{40} and Cs^{137} levels for each animal. It is interesting to note that the amount of potassium per kilogram body weight is essentially the same as that for human subjects. Also, the total Cs^{137} burdens ($\text{pc Cs}^{137}/\text{g K}$) are very comparable to those for human subjects at that particular time (June-July, 1962). The replicate measurements suggest that the K^{40} determination is somewhat more reproducible than the Cs^{137} determination. This is because the precision of the Cs^{137} measurement is not as good as the 4 to 5 per cent for K^{40} . Age- or sex-dependent trends were not looked for because of the small sample size. As this type of information accumulates, however, such trends may become apparent. Also, because the genetic and environmental variation of laboratory animals is less than for human subjects, one might expect to find smaller variations in those parameters which are related to body potassium content.

TABLE 1. CESIUM¹³⁷ AND POTASSIUM LEVELS OF ADULT BEAGLE HOUNDS*

Dog No.	Weight (kg)	g K/kg	pc Cs ¹³⁷ /g K	Potassium (g)	Cesium ¹³⁷ (nc)
60	13.9	1.72	56.40	23.9	1.35
60	13.3	1.75	72.79	23.2	1.69
61	13.9	2.09	53.15	29.0	1.54
62	13.7	2.14	72.14	29.3	2.11
63	16.9	1.72	68.42	29.1	1.99
64	15.6	1.81	66.71	28.3	1.88
65	15.0	1.93	61.65	28.9	1.78
65	15.5	1.83	75.80	28.4	2.15
66	16.5	1.85	64.19	30.5	1.96
66	16.3	2.01	52.81	32.8	1.73
67	9.3	1.79	62.46	16.7	1.04
68	8.5	1.72	102.64	14.7	1.50
68	8.5	1.61	106.64	13.7	1.46
42	10.5	1.46	89.79	15.3	1.37
42	10.7	1.45	91.02	15.5	1.41
49	11.8	2.11	74.79	24.9	1.86
49	11.5	2.15	60.27	24.7	1.49
50	12.7	2.08	86.03	26.4	2.27
51	14.0	1.98	64.14	27.7	1.77
52	11.5	2.25	80.15	25.9	2.07
53	14.2	1.92	70.71	27.3	1.93
53	14.0	2.15	67.07	30.1	2.02
54	15.2	2.31	73.50	35.1	2.58
54	15.0	2.33	62.45	34.9	2.18
56	11.0	1.86	58.28	20.5	1.20
56	10.5	1.78	85.12	18.6	1.59
44	21.7	1.49	98.86	32.4	3.20
2	16.1	1.47	137.06	23.7	3.24
36	15.0	1.43	92.10	21.5	1.98

*All males except Nos. 2, 36, 42, 56, and 68.

Volume and Turnover of Body Water in Male Macaca mulatta and Macaca speciosa Monkeys (C. R. Richmond and J. E. London)

INTRODUCTION

Various metabolic, physiologic, and hematologic parameters are being determined for Macaca mulatta and Macaca speciosa monkeys. This report summarizes data on volume and turnover of body water measured by the tritiated dilution method.

METHODS AND MATERIALS

Four males of each species were used after a 3-week period of acclimation in individual metabolism cages. Based on body weight (1), gross dentition, and information from suppliers, we estimate the ages to range between 3 and 4 years. Each non-anesthetized animal was given about 1 mc of tritium water (HTO) by parenteral administration. The volume of this material was about 0.5 ml. Each syringe was weighed before and after injection to determine the exact amount administered. Animals were allowed water ad libitum during the experiment. Samples of venous blood were withdrawn from the saphenous vein on days 2, 7, 10, 14, 17, and 21 after injection. Pure water was obtained from each sample by a vacuum distillation procedure modified after Cooper et al. (2). Each sample was distilled to dryness to

avoid any possible isotopic fractionation effects. One-half ml of each HTO sample plus 0.5 ml distilled water and 15 ml scintillator solution (3) were added to a counting vial and counted in a Packard Tri-Carb counter. Adequate dilutions of the injection solution were also counted. The count rates (counts per minute per 0.5 ml body water) were fitted as a function of time (days) by an electronic computer (IBM 7090) to obtain the best fit to the data. No logarithmic transformations are made in this procedure. Figure 1 shows data for 1 animal (*Macaca mulatta*, No. 8).

Body water determinations were made according to the tritium dilution principle. However, body water samples were not obtained at some assumed time of equilibrium between the HTO and the body water. Instead, the intercept of the regression function which describes the decrease in body water HTO activity was used. Validity of this procedure has been described previously (4).

Table 1 summarizes body water, half-time, and turnover data for these animals. The agreement between the two species is quite good. No statistical tests were run because of the small number of animals. Two of the *M. speciosa* monkeys (not shown in Table 1) gave apparent body water volumes and half-times of 70 to 80 per cent of body weight and about 2 days, respectively. These animals were later found to be heavily infested with hookworms.

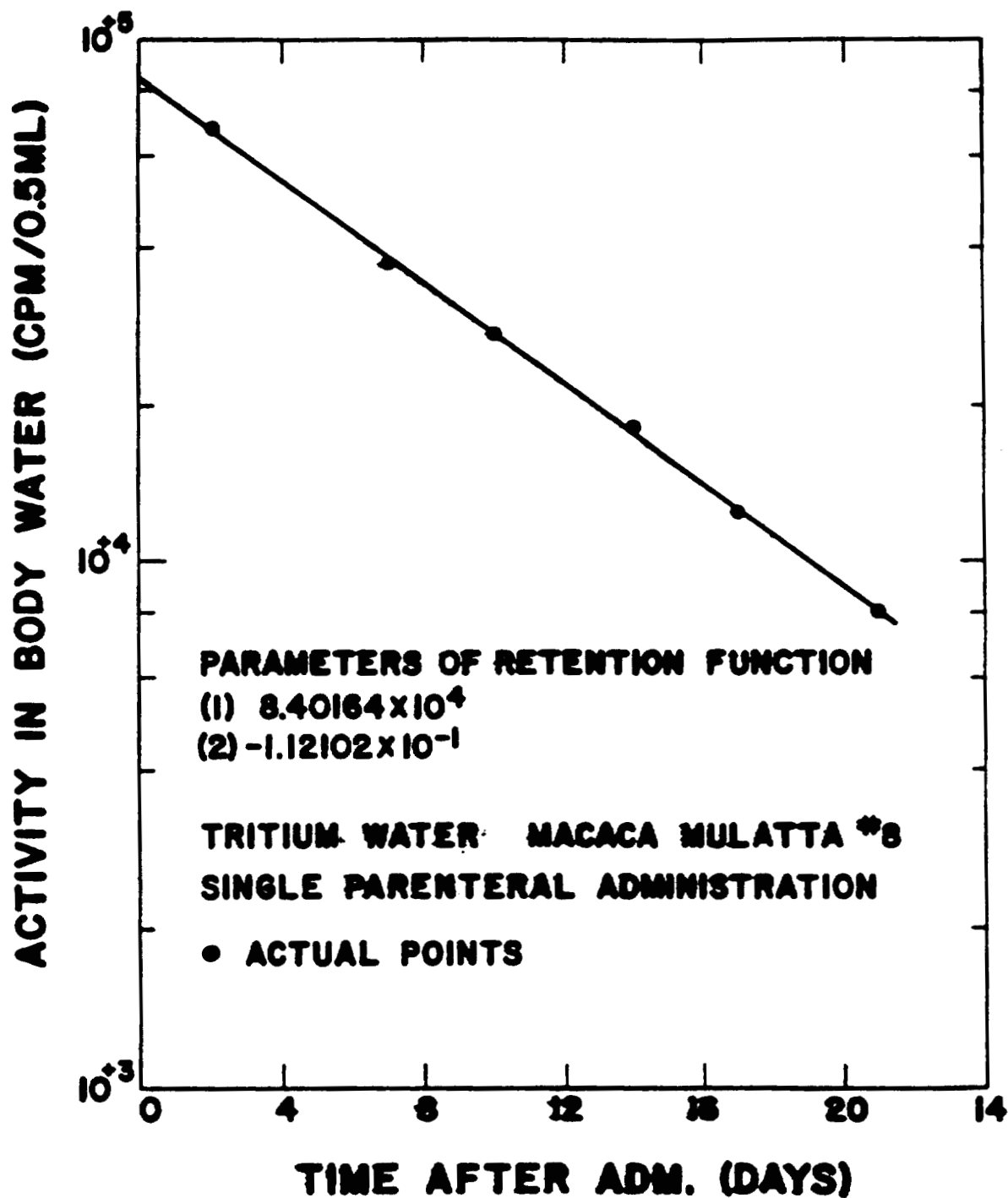


Fig. 1. Change in body HTO specific activity versus days after administration for 1 male M. mulatta monkey.

TABLE 1. VOLUME AND TURNOVER OF BODY WATER IN MALE MACACA MULATTA AND MACACA SPECIOSA MONKEYS AS MEASURED BY TRITIATED WATER

Animal No.	Body Weight (g)	Body Water (per cent of body water)	Half-Time (days)	Water Turnover* (ml/day)
<u>Macaca mulatta</u>				
1	5682	62.44	5.3	462
2	3864	62.97	4.6	364
6	4091	60.06	-	-
8	4545	69.01	6.2	352
Average 4546		63.62	5.4	393
<u>Macaca speciosa</u>				
1	4818	69.49	5.3	437
4	5795	67.19	4.9	554
Average 5307		68.34	5.1	496

*From the derivative of $V_t = V_0 e^{-kt}$, when V_0 is the volume of the exchangeable body water pool (ml), t is time zero, and k is the rate constant (fractional change per day) of the exponential function.

Respective turnover values of 393 and 496 ml per day for the *M. mulatta* and *M. speciosa* are in good agreement with values of 411 and 465 ml per day as predicted by inter-specific relations given by Richmond et al. (4).

Additional comparative studies using gamma-emitting radionuclides and whole-body counting techniques are now in progress.

REFERENCES

- (1) G. van Wagenen and H. R. Catchpole, Am. J. Phys. Anthropol. 14, 245 (1956).
- (2) J. A. D. Cooper, N. S. Radin, and C. Borden, J. Lab. Clin. Med. 52, 129 (1958).
- (3) Per liter solute composition (p-dioxane solvent);
0.375 g 2,5-diphenyloxazole, 7.5 g 2,2'-p-phenylene-bis-(5-phenyloxazole), and 125.0 g naphthalene.
- (4) C. R. Richmond, W. H. Langham, and T. T. Trujillo, J. Cell. Comp. Physiol. 59, 45 (1962).

MAMMALIAN METABOLISM SECTION

PUBLICATIONS

(1) J. E. Furchner and C. R. Richmond, Comparative Metabolism of Radionuclides in Mammals. II. Retention of Iodine¹³¹ by Four Mammalian Species, Health Phys. 9, 277 (1963).

(2) J. E. Furchner and C. R. Richmond, The Effect of Environmental Temperature on the Retention of Cesium¹³⁷ by Mice, J. Appl. Physiol. 18, 786 (1963).

(3) C. R. Richmond, J. E. Furchner, G. A. Trafton, and W. H. Langham, Comparative Metabolism of Radionuclides in Mammals. I. Uptake and Retention of Orally Administered Zinc⁶⁵ by Four Mammalian Species, Health Phys. 8, 481 (1962).

MANUSCRIPT SUBMITTED

(1) C. R. Richmond, J. E. Furchner, P. N. Dean, and P. McWilliams, Electronic Processing and Analysis of Metabolic Data, accepted for publication in Health Phys.

CHAPTER 3

MAMMALIAN RADIOBIOLOGY SECTION

Comparative Fundamental Physiological Parameters of Macaca mulatta and a New Laboratory Primate, Macaca speciosa (J. C. Hensley and C. R. Richmond)

INTRODUCTION

Four male *Macaca speciosa* monkeys were received by Group H-4 as a possible experimental primate for radiobiological studies where frequent handling is necessary. *Macaca mulatta* is recognized to be a hearty laboratory primate (1), but its inherent fierce nature frequently precludes experimental procedures where handling is required. Only experienced caretaker personnel can capably handle *M. mulatta*, and often these personnel are seriously injured in handling procedures.

The 4 *M. speciosa* in this colony have demonstrated remarkable docility. Common veterinary clinical procedures are performed with an ease equivalent to human pediatric

practices. Although references to the fact that *M. speciosa* "will not bite" are possibly inaccurate (2), extreme provocation can result in a relatively feeble attempt or success at biting.

Physiological conformation of *M. speciosa* to known values for *M. mulatta* is essential if this new species is to be routinely used in laboratory procedures.

METHODS AND RESULTS

Four male *Macaca speciosa* monkeys and 3 male and 1 female *Macaca mulatta* were subjected to physiological analysis through an E.-M. Instrument Company "Physiograph Six," a highly sensitive polygraph designed for laboratory use. The instrument sensitivity is such that common physiological parameter measurement is possible using mice.

The physiographic equipment is located within a cell-type wire-mesh shielded enclosure for the elimination of radio interference and other electrical interference with accurate measurement of desired signals.

The monkeys were placed individually in a securing device designed and fabricated at this Laboratory. Although *M. speciosa* is docile when allowed relative freedom, the restriction imposed by the securing devices caused severe alteration of parameters to be measured. *Macaca mulatta*, although fierce with freedom, frequently remains quiescent

when secured but will bite or scratch the operator at every opportunity. Therefore, 5 mg/pound body weight of "Tranvet," a commercial animal tranquilizer, was administered to preclude alteration of physiological parameters by hyperexcitability or movement.

All physiological tests on each monkey were monitored simultaneously; however, each parameter was treated both individually and collectively. Comparisons were made on established equivalents for *M. mulatta*, data acquired from *M. mulatta* in this colony, and data acquired from the *M. speciosa* mentioned above. Although neurological stereotaxic mapping and psychological studies have been made on *M. speciosa* (2), no literature is available regarding their physiology. The *M. mulatta* and *M. speciosa* used in this study were between 2-1/2 to 3-1/2 years of age.

Body Weights

Table 1 is a comparison of the parameters measured. The average body weight of the *M. mulatta* selected at random and aged from this colony as 3 years of age was 9.9 pounds. The average body weight of the 4 *M. speciosa* was determined to be 11.97 pounds. The weight ranges were wider in *M. speciosa*, however.

TABLE 1. COMPARATIVE PHYSIOLOGICAL DATA OF THE TWO SPECIES EXAMINED

Parameter Measured	Macaca speciosa		Macaca mulatta	
	Average	Range	Average	Range
Complete Cardiac (cycles/min)	243.25	228 - 260	227	194 - 264
Respiratory (cycles/min)	51.25	45 - 55	53.5	39 - 60
Galvanic Skin Response	1.4825	1.30 - 1.68	2.3125	1.90 - 2.55
Basal Resistance	X	X	X	X
Electrode Interface	$[10^3]$ ohms	$[10^3]$ ohms	$[10^3]$ ohms	$[10^3]$ ohms
Electrodermography				
Blood Pressure				
systolic	90 mm Hg	85 - 95 mm Hg	93 mm Hg	85 - 105 mm Hg
diastolic	48	35 - 60	48	40 - 45
Differential				
pulse pressure	42 mm Hg	35 - 50 mm Hg	45 mm Hg	35 - 60 mm Hg
Body Weight (pounds)	11.97	9.4 - 14.5	9.9	9.2 - 10.0

Electrocardiographs

Animals were placed in the restraining device, and the correct tranquilizer dose was administered intramuscularly in the left thigh. Electrodes necessary for all parameters were secured to record the electrocardiogram and respirogram simultaneously. EKG leads were placed at points determined by Atta and Vance (3) as best suited to record the potentials to the right ventricle, septum, and left ventricle. Potentials from the right ventricle were measured best with lead one electrode implanted beneath the skin in the fourth right intercostal space at a distance of 4 cm from the midsternal line. Septal potentials were measured best on the opposite side of the chest at a point symmetrical to lead one. Since the animals were upright rather than supine, left ventricular potentials were also monitored from lead two. Sterile needle electrodes were placed under the shaven skin at the above points. These leads were connected to a hi-gain preamplifier through a shielded input extension cable. A time constant selection of 2 seconds was made, as this constant was found to monitor the low frequency response faithfully to allow reproduction of all components of the EKG. The preamplifier was calibrated so that a 1-millivolt impulse caused a pen deflection of 1 cm. Recording paper speeds of 2.5 and 5 cm/sec were used. Auscultation revealed no

evidence of murmurs or abnormal sounds in any of the subjects tested.

Although the limited number of subjects precluded an extensive study of electrocardiography, the following table shows briefly the electrocardiographic data recorded on the subjects tested (Table 2). Recording amplitudes in *M. mulatta* were considerably higher than those of *M. speciosa*, as evidenced by greater deflections of the pen calibration.

Respirography

Respirogram recordings were obtained through the same two leads employed in the EKG study above. After calibration of the hi-gain preamplifier, a twin lead shielded input cable was connected between the hi-gain preamplifier and an impedance pneumograph transducer. The voltage impressed on the subject does not exceed 2 millivolts Rms. This does not interfere with EKG recordings due to a filter network in the coupling circuit.

Although optimum electrode placement is recommended at the fifth and sixth rib interspace, suitable recordings are traced in the fourth rib interspace in deference to suitable EKG tracings. Normal electrode impedance is 500 ohms, and light breathing patterns produce approximately a 1 per cent change per cycle, or about 5 in 500 ohms. Deflections in

TABLE 2. ELECTROCARDIOGRAPHIC ANALYSIS

Measurement	Macaca mulatta		
	Macaca speciosa	Los Alamos	Normal Ranges
Rate Average	243/min	227/min	160 - 333
P-R Interval	0.087 m/sec	0.064 m/sec	0.047 - 0.100
QRS Duration	0.041 m/sec	0.065 m/sec	0.020 - 0.036
Q-T Interval	0.116 m/sec	0.195 m/sec	0.107 - 0.200

both *M. mulatta* and *M. speciosa* respirograms did not exceed this value. Respiratory patterns in *M. mulatta* were regular and synchronous through entire tracings, indicating a regular depth and rate of breathing. Individual respiratory cycles were jerky, though synchronous (Fig. 1, tracing A). Respiratory patterns in *M. speciosa*, though highly irregular in rate, showed more organized respiratory cycles and a smoother respiratory cycle in general. The respiratory rates are detailed in Table 1. *Macaca speciosa* averaged 51.25 cycles/min, while *M. mulatta* averaged 53.5 cycles/min.

Electrosphygmography

Systolic and diastolic blood pressures and differential pulse pressures were determined with an electrosphygmograph as provided with the "Physiograph Six." The instrument is capable of recording indirect blood pressures within 5 to 10 mm Hg accuracy. The apparatus consists of a photoelectric pressure transducer, a common sphygmomanometer cuff with an attached microphone for recording Korotkoff sounds, and cuff pump connections for pressure sampling (4).

The cuff was wrapped about the right upper arm of each subject, and cuff pressure was increased to the upper limits of normal pressures expected (about 180 mm). Calibration was then completed to write out the Korotkoff sounds at a



Fig. 1. A graphic recording of the Korotkoff sounds (tracing B) and blood pressure recording of a female M. mulatta monkey. Tracing A represents a typical respiratory pattern for this monkey.

1055564

reasonable magnitude. Cuff pressure was then increased until the upper limit was once again 180 mm Hg. While recording, the pressure was slowly released to zero. The tracing (Fig. 1, tracing B) shows an increased pen deflection at the occurrence of the systolic pulse and a severe decrease in magnitude at the occurrence of the diastole. *Macaca speciosa* averaged 90 mm Hg systolic pressure and 48 mm Hg diastolic pressure, while *M. mulatta* averaged 93 mm Hg systolic and 48 mm Hg diastolic pressures. Table 1 presents the variations noted. Pulse pressure differences averaged 42 mm Hg for *M. speciosa* and 45 mm Hg for *M. mulatta* (Table 1).

Galvanic Skin Response

Since many stimuli will incite the galvanic skin response, or psychogalvanic reflex, basal skin resistance was measured to determine a basal emotional quotient for these animals. This, in effect, correlates theoretically with aggressiveness or docility of the two species of primates under investigation. Relationships are only hypothetical, as observed docility or aggressiveness cannot be measured in any other way with mathematical efficiency. Therefore, we must assume that basal skin resistance is a function of basal psychological position as sympathetic stimuli evoke levels of response, while parasympathetic stimuli inhibit or reduce levels of response (5).

Two electrodes (one a ground electrode and the other the sensing electrode) are attached to the animal. Both are plate electrodes, the former attached to the ventrum of the wrist and the latter to the dorsum of the index finger. The right forearm was used in all instances.

A constant DC current of 20 microamperes is applied to the electrodes, and the voltage across the electrodes is then amplified and recorded. With constant current applied, voltage across the electrodes is directly proportional to the electrode resistance. Any given ohmic level of resistance at the electrode interface will then be recorded as a constant amount over the basal electrode resistance, varying from 0 to 1×10^6 ohms.

After zero calibration, the galvanic skin response pre-amplifier is switched to record direct current. The basal skin resistance inherent in the animal causes a wide deflection of the recording pen. Recalibration to zero level then determines the basal interface resistance between the electrodes attached to the animal. One would note in Table 1 that calibration levels for *M. mulatta* are 64.1 per cent higher than those for *M. speciosa*, indicative of a greater response to testing procedures, though not visible grossly to the observer. Since we will assume tranquilization renders equal nonchalance to experimental procedure, we must

conclude that the aggressive nature of *M. mulatta* as opposed to *M. speciosa* is still superior, regardless of tranquilization. One may then conclude a mathematical quotient for docility or aggressiveness as observed in the normal caged animal.

DISCUSSION

A comparison of the two *Macaca* species in question seems to indicate a remarkable similarity. Differences, except galvanic skin response, are slight and would not basically alter results of experiments where *M. speciosa* is substituted for *M. mulatta*.

The *M. speciosa* used in this study were but recently acquired. After arrival, each animal was subjected to clinical examination, tuberculosis testing, treatment for intestinal parasites, and antibiotic therapy. All primates arriving at this Laboratory are subjected to rigorous testing and examination over a 60-day period. Nutritional states of the *M. speciosa* received were low and possibly beneath that of the *M. mulatta* tested, which have been in this colony for 3 years minimum under optimum environmental conditions. However, one notes that body weight ranges are considerably higher for *M. speciosa*. All animals tested were determined to be clinically sound before physiological evaluation.

Preliminary tissue culture attempts and chromosome analysis indicate a close similarity of the two species from this standpoint.

Hematological and radiometabolic studies are in progress by the Mammalian Metabolism Section.

Continued extensive metabolic and microscopic comparison are planned with possible replacement of the *M. mulatta* in this colony with the more docile and cooperative, but physiologically similar, *M. speciosa*.

REFERENCES

- (1) D. B. Lister, R. E. Benson, and R. J. Young, Ann. N. Y. Acad. Sci. 85, 738 (1960).
- (2) A. Kling and J. Orbach, Science 139(3549), 45 (1963).
- (3) A. G. Atta and P. W. Vance, Ann. N. Y. Acad. Sci. 85, 811 (1960).
- (4) L. A. Geddes, W. A. Spencer, and H. E. Hoff, Am. Heart J. 57, 361 (1959).
- (5) G. H. W. Wang, Am. J. Physiol. Med. 36, 35 (1957).

Cellular Elements in the Peripheral Blood of Macaca mulatta
and Macaca speciosa Monkeys (C. R. Richmond and J. E. London)

INTRODUCTION

Several hematological parameters were measured for Macaca mulatta and Macaca speciosa monkeys as part of a larger project to obtain comparative data for these species. This report summarizes these measurements.

METHODS AND MATERIALS

All measurements were made on fresh blood removed from the saphenous vein of the restrained non-anesthetized animals. The M. speciosa monkeys had just completed a 60-day period of quarantine since arrival at our laboratory and were in reasonably good apparent health. The M. mulatta monkeys have been maintained in our laboratory for several years and are about 3-1/2 years old based on gross dentition, estimates of the supplier, and body measurement data (1). It is assumed, on the basis of body weights and gross dentition, that the M. speciosa were approximately the same age.

Hematocrits were determined by a microhematocrit capillary tube method immediately after centrifuging the samples for 3 minutes at 12,500 rpm in an Adams microhematocrit centrifuge. Erythrocyte numbers were measured by a Coulter counter on a 1 to 10^5 dilution of whole blood adjusted to

pH 6.7. For each sample, 10^5 cells were counted so that relative cell volume could be determined as a function of channel number on an RIDL 100-channel analyzer. Differential leucocyte counts were done according to the usual clinical laboratory procedures.

RESULTS AND DISCUSSION

Table 1 gives the number of erythrocytes (10^6 per mm^3), hematocrit (ml/100 ml), and mean corpuscular volume (μ^3) for 4 female and 7 male *M. mulatta* monkeys and 4 *M. speciosa* monkeys of roughly similar weight and age. The mean hem-

TABLE 1. ERYTHROCYTE DATA FOR MACACA MULATTA AND MACACA SPECIOSA MONKEYS*

Animal No.	Sex	Erythrocytes ($10^6/\text{mm}^3$)	Hematocrit (ml/100 ml)	Mean Corpuscular Volume (μ^3)
<u>Macaca mulatta</u>				
3	F	5.86	43.2	73.7
5	F	5.82	40.3	69.2
9	F	6.96	45.4	65.2
11	F	5.24	39.1	74.6
Average		5.97	42.0	70.7
1	M	6.66	48.8	73.3
2	M	7.92	50.0	63.1
4	M	6.28	45.0	71.7
6	M	6.62	48.8	73.7
7	M	6.34	44.3	69.9
8	M	6.62	50.0	75.5
10	M	6.18	49.1	79.4
Average		6.66	48.0	72.4
<u>Macaca speciosa</u>				
1	M	6.08	42.2	69.4
2	M	5.84	42.3	72.4
3	M	5.20	40.5	77.9
4	M	6.34	43.5	68.6
Average		5.87	42.1	72.1

*Body weight 4 to 6 kg. Age estimated at 3 to 4 years, based on dentition and body weights.

The erythrocyte concentrations of *M. speciosa* were similar to those of female *M. mulatta*. All mean values in Table 1 were similar, although larger, than the 5.444×10^6 per cubic millimeter reported by Young et al. (3). A ratio of about 0.88 exists between male *M. speciosa* and male *M. mulatta* for both mean hematocrit and mean erythrocyte concentrations. This is suggested by the same mean value of about $72 \mu^3$ for the mean corpuscular volume (MCV) for males of both species. One might speculate that the *M. speciosa* had not reached the same level of acclimation as the *M. mulatta*. It does appear that these species are quite similar as to concentration of erythrocytes, hematocrit, and cell size. cursory inspection of the cell sizing data obtained from the Coulter counter shows a remarkable similarity between the erythrocyte profiles of these species.

Spector (2) gives no values for erythrocyte concentration or mean cellular volume for macaques. A MCV of 71 can be estimated from Young et al. (3). Prosser (4) suggests a value of 5×10^6 erythrocytes per cubic millimeter as a reasonable mean for "macaque erythrocytes."

Table 2 gives leucocyte values for 4 males of each species after a 21-day period in individual metabolism cages. During this time, all animals were handled and treated in essentially the same way. The higher leucocyte concentration

**TABLE 2. LEUCOCYTE CONCENTRATIONS AND DIFFERENTIAL COUNTS
FOR MALE MACACA MULATTA AND MACACA SPECIOSA MONKEYS**

Animal No.	Leucocytes (10 ³ /mm ³)	Lympho- cytes	Differential Counts (per cent)			
			Segmented Neutrophils	Mono- cytes	Eosin- ophils	Stab Cells
<u>Macaca mulatta</u>						
1	11.0	89	9	1	1	-
2	16.5	81	14	1	1	3
6	11.7	77	20	-	2	1
8	8.0	71	26	-	1	2
Mean	11.8					
<u>Macaca speciosa</u>						
1	15.2	72	21	-	7	-
2	17.2	61	35	-	4	-
3	15.5	41	59	-	-	-
4	15.5	68	24	-	8	-
Mean	15.8					

in the blood of *M. speciosa* is probably suggestive of a generally poorer state of well-being as compared with *M. mulatta*. Young et al. (3) report a mean of 14.68×10^3 leucocytes per cubic millimeter for the 5 *M. mulatta* monkeys mentioned earlier.

The relatively high percentage of neutrophils in *M. speciosa* Nos. 2 and 3 is of interest, as these animals were later found to be quite heavily infected by hookworms (*Strongyloidea*). Results of metabolic studies using tritiated water in these animals indicated abnormally large body water reservoirs and very rapid turnover rates. This was presumably caused by the heavy nematode infestation. The relatively high incidence of eosinophils in *M. speciosa* is also suggestive of parasitism.

Differential leucocyte count data did not agree with that reported by Young et al. (3). Respective percentage values for neutrophils, lymphocytes, and eosinophils were 55.8, 39.4, and 1.8. No other cell types were given. Kuskova (5) points out that the literature provides only scant and contradictory data on the composition of monkey blood. Age, sex, diurnal and seasonal factors, plus the small numbers of animals, contribute to the large variations. Recent works (6,7) give no hematological values for monkeys.

In summary, preliminary investigations on the cellular

elements in the peripheral blood show a reasonable similarity between the primate species *M. mulatta* and *M. speciosa*. Because of the general lack of information of this nature, additional data will be accrued on these species. Thyroid function and other metabolic studies should also help in comparing *M. speciosa* with *M. mulatta*.

REFERENCES

- (1) G. van Wagenen and H. R. Catchpole, *Am. J. Phys. Anthropol.* 14, 245 (1956).
- (2) W. S. Spector, ed., Handbook of Biological Data, W. B. Saunders Company, Philadelphia (1956).
- (3) R. J. Young, G. S. Melville, H. Borella, and J. E. Pickering, USAF School of Aviation Medicine, Aerospace Center (ATC), Brooks Air Force Base, Texas, Report AF-SAM-61-53 (1961).
- (4) C. L. Prosser, ed., Comparative Animal Physiology, W. B. Saunders Company, Philadelphia (1950).
- (5) M. I. Kuksova, In: Problems of Medicine and Biology in Experiments on Monkeys (I. A. Utkin, ed.), Pergamon Press, New York (1960), pp. 123-134.
- (6) O. W. Schlam, Veterinary Hematology, Lea and Febiger, Philadelphia (1961).
- (7) T. C. Ruch, Diseases of Laboratory Primates, W. B. Saunders Company, Philadelphia (1959).

Longevity of First and Second Generation Offspring from Male Mice Exposed to Fission Neutrons and Gamma Rays (J. F. Spalding and R. F. Archuleta)

INTRODUCTION

Russell (1) has reported evidence that bomb neutron exposure of male mice was instrumental in reducing not only the life expectancy of the exposed animal but also that of his offspring. This finding was of considerable importance and has been generally accepted as one of the human hazards of exposure to ionizing radiation. Because of the significance of Russell's findings, it was felt that a similar experiment designed specifically for the end point desired and done under laboratory, rather than under field, conditions was indicated. The study reported below was done to determine the effect of both neutron and gamma-ray exposures to male mice on longevity of their first and second generation offspring.

METHODS AND RESULTS

Two hundred and twenty RF male mice 8 weeks of age were used to produce the mice for the longevity study. They were randomly divided into 11 groups, 20 mice each for 10 exposure groups and 20 mice for the controls. Groups 1 through 5 were given acute doses of 32, 67, 102, 134, and 177 rads of fission

neutrons to the whole body, respectively. Groups 6 through 10 were given acute whole-body doses of Co^{60} gamma rays of 60, 120, 180, 240, and 300 rads, respectively, and Group 11 was retained as an unexposed control group.

Following neutron and gamma-ray exposures and control sham exposures, all mice from each of the 11 groups described above were placed in breeding cages with a randomized population of RF female mice 10 to 12 weeks of age with a caging ratio of 1 male to 4 females. The males remained with the females for 18 days [about one-half the duration of spermatogenesis (2)], after which time they were separated from the females. Offspring from these matings were considered to have been conceived from male germ cells irradiated in the post spermatogonial stages (sperm, spermatids, and possibly a few spermatocytes) and were identified as F_1^1 mice (first generation mice from early breedings, Fig. 1). The life span of these mice (F_1^1) and that of their offspring (second generation mice from early breedings identified as F_2^1 mice, Fig. 1) were studied.

Sixteen weeks after the males were exposed to either neutrons or gamma rays, all irradiated and control males were again placed in breeding cages with a second randomized population of RF female mice 10 to 12 weeks of age with a caging ratio of 1 male to 6 females. Offspring from these matings were, therefore, derived from irradiated spermatogonia.

LIFE SPAN STUDY OF THE F_1 AND F_2 OF $\circ \rightarrow$ MICE EXPOSED
TO FISSION NEUTRONS OR Co^{60} γ RAYS

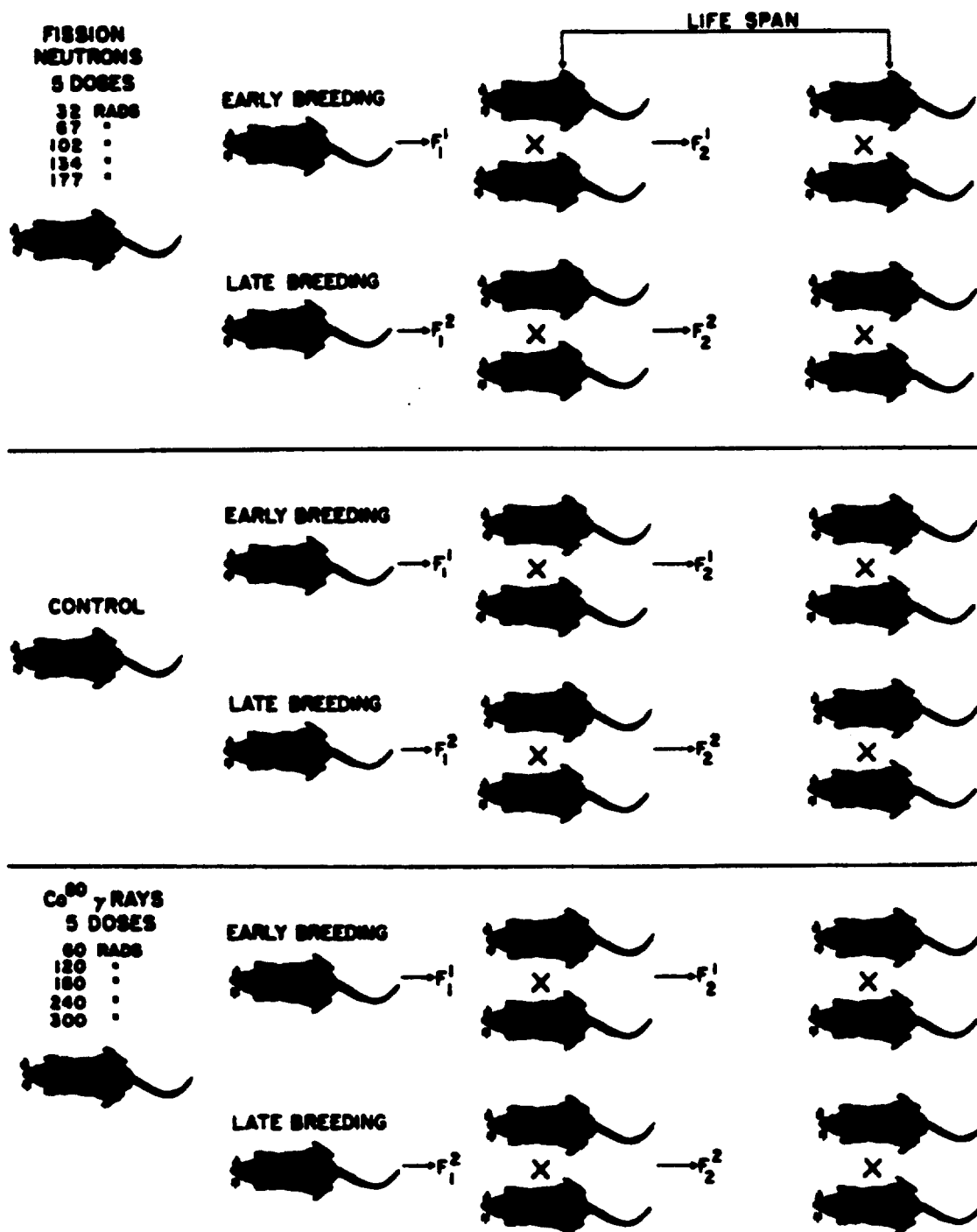


Fig. 1. Schematic of experimental design.

and were identified as F_1^2 mice (first generation mice from late breedings, Fig. 1). Longevity of these mice (F_1^2) and that of their offspring (second generation mice from late breedings identified as F_2^2 mice, Fig. 1) were studied.

The doses to the sire or grandsire, number of mice observed, and the mean lengths of life for each of the groups are tabulated in Tables 1, 2, 3, and 4. Analysis of these data failed to show any meaningful correlation between life span and dose to the sire or grandsire in either the gamma-ray or neutron exposed groups. Significant differences did appear between some doses and in some instances between sexes. However, it was not possible to fit a straight line, by the weighted least squares method, through the data in any of the four tables and to obtain a slope which would suggest that life span was affected by exposure of the sire or grandsire to ionizing radiation. In fact, the average life span for all control females was 602 days, compared to 633 days for all female offspring from irradiated sires or grandsires, and control males had an average life span of 593 days, compared to 647 for all male offspring from irradiated sires or grandsires. In both sexes, mice with irradiated parentage outlived their control counterparts. The results of this study do not support the earlier findings of Russell (1).

Changes in sex ratio have been suggested as a method of

TABLE 1. MEAN LIFE SPAN IN OFFSPRING OF MALE MICE EXPOSED TO GAMMA IRRADIATION

Total Dose to Sire (rads)	Number of Offspring		Mean Length of Life and Standard Error (days)	
	Males	Females	Males	Females
F_1^1 (Early Matings, 1 to 18 days after gamma-ray exposure)				
0	28	32	625 \pm 36	610 \pm 31
60	37	32	686 \pm 25	684 \pm 23
120	28	38	568 \pm 41	708 \pm 29
180	31	38	725 \pm 17	682 \pm 24
240	59	52	675 \pm 24	639 \pm 20
300	11	16	605 \pm 43	639 \pm 46
F_1^2 (Late Matings, 16 weeks after gamma-ray exposure)				
0	8	14	514 \pm 63	587 \pm 34
60	8	26	584 \pm 74	700 \pm 35
120	8	14	517 \pm 86	553 \pm 36
180	8	6	624 \pm 19	588 \pm 33
240	34	30	625 \pm 25	676 \pm 29
300	13	12	677 \pm 58	674 \pm 65

TABLE 2. MEAN LIFE SPAN IN GRANDOFFSPRING OF MALE MICE
EXPOSED TO GAMMA IRRADIATION

Total Dose to Grandsire (rads)	Number of Offspring		Mean Length of Life and Standard Error (days)	
	Males	Females	Males	Females
F_2^1 (Offspring of F_1^1 , Table 1)				
0	37	50	624 \pm 24	603 \pm 21
60	40	48	630 \pm 33	660 \pm 19
120	43	40	674 \pm 30	651 \pm 32
180	59	71	664 \pm 24	674 \pm 18
240	44	35	642 \pm 28	645 \pm 36
300	22	19	504 \pm 35	570 \pm 42
F_2^2 (Offspring of F_1^2 , Table 1)				
0	17	18	646 \pm 37	575 \pm 46
60	42	36	708 \pm 21	682 \pm 23
120	35	52	607 \pm 40	669 \pm 21
180	44	39	647 \pm 25	655 \pm 29
240	111	111	668 \pm 17	683 \pm 15
300	25	20	649 \pm 28	594 \pm 35

TABLE 3. MEAN LIFE SPAN IN OFFSPRING OF MALE MICE EXPOSED TO FISSION NEUTRONS

Total Dose to Sire (rads)*	Number of Offspring		Mean Length of Life and Standard Error (days)	
	Males	Females	Males	Females
F_1^1 (Early Matings, 1 to 18 days after neutron exposure)				
0	28	32	625 \pm 36	610 \pm 31
32	23	24	639 \pm 37	710 \pm 19
67	26	22	535 \pm 37	534 \pm 33
102	12	13	568 \pm 38	632 \pm 38
134	9	6	738 \pm 35	699 \pm 55
177	2	2	649 \pm 40	688 \pm 126
F_1^2 (Late Matings, 16 weeks after neutron exposure)				
0	8	14	514 \pm 63	587 \pm 34
32	12	5	563 \pm 57	613 \pm 96
67	15	12	550 \pm 58	593 \pm 54
102	20	22	629 \pm 30	719 \pm 28
134	2	12	735 \pm 87	655 \pm 49
177	None survived to weaning			

*Gamma-ray dose approximately 15 per cent of neutron dose.

TABLE 4. MEAN LIFE SPAN IN GRANDOFFSPRING OF MALE MICE
EXPOSED TO FISSION NEUTRONS

Total Dose to Grandsire (rads)*	Number of Offspring		Mean Length of Life and Standard Error (days)	
	Males	Females	Males	Females
F_2^1 (Offspring of F_1^1 , Table 3)				
0	37	50	625 \pm 24	603 \pm 21
32	38	32	643 \pm 30	658 \pm 25
67	48	57	614 \pm 26	598 \pm 21
102	12	20	643 \pm 32	507 \pm 41
134	29	34	580 \pm 47	672 \pm 29
177	None produced			
F_2^2 (Offspring of F_1^2 , Table 3)				
0	17	18	646 \pm 37	575 \pm 46
32	44	43	670 \pm 19	644 \pm 18
67	98	69	672 \pm 18	662 \pm 19
102	48	73	679 \pm 25	649 \pm 16
134	8	12	651 \pm 38	683 \pm 35
177	None produced			

* Gamma-ray dose approximately 15 per cent of neutron dose.

estimating the genetic hazards of ionizing radiations to man. According to genetic theory, F_1 offspring from irradiated sires would be predominantly males if sex-linked lethals were induced by exposure. In this study, the sex ratio of all control mice was 1.267, F_1 mice from gamma-irradiated sires had a sex ratio of 1.114, and the sex ratio of mice from neutron-irradiated sires was 0.975. These comparative sex ratios were contrary to genetic theory.

REFERENCES

- (1) W. L. Russell, Proc. Nat. Acad. Sci. 43(4), 324 (1957).
- (2) E. F. Oakberg, Am. J. Anat. 99, 507 (1956).

Acute Radiosensitivity as a Function of Age in Mice (J. F. Spalding, O. S. Johnson, and R. F. Archuleta)

INTRODUCTION

An earlier study was done (1) to determine radiation sensitivity as a function of age using the fractionated dose method, which allows for biological repair between acute exposures. It was concluded that under that type of exposure condition, radioresistance was relatively stable through the first half of adult life, at which time it deteriorated rapidly until the end of the normal life expectancy. The following is a report on acute radiosensitivity as a function of age using the LD_{50}^{30} approach.

METHODS AND RESULTS

Some 2900 RF strain virgin female mice of 14 age groups were used (Table 1). Mice in each age group were randomly divided into a minimum of 5 and a maximum of 12 acute X-ray exposure groups to bracket the LD_{50}^{30} . Acute X-ray exposures were made with a 250 KVP X-ray machine with a beryllium window tube. Exposure conditions were as follows: voltage 250 KVP; 30 ma; Thoraeus II filter; HVL 2.6 mm Cu; target-to-specimen distance 60 cm; and dose rate 50 rads/min.

Following X-ray exposure, mice were housed in standard wire-bottom cages and observed for 30 days post exposure.

TABLE 1. LD₅₀ FOR FEMALE MICE VERSUS AGE

Age (weeks)	Number of Mice	LD₅₀³⁰ (rads)	Standard Error
3.6	326	593	14.6
6.0	186	647	18.9
8.0	210	691	14.8
12.8	190	733	13.5
21.4	300	697	15.8
30.0	363	634	20.3
42.8	131	487	18.7
51.4	120	547	35.9
60.0	157	537	16.0
68.6	125	453	5.16
77.1	179	424	22.8
85.7	149	442	17.6
94.3	152	441	12.5
103.6	342	343	18.6

Deaths were recorded daily, and 30-day lethality was subjected to standard methods of probit analysis to obtain the LD_{50}^{30} for each group. The results are tabulated in Table 1 and are plotted in Fig. 1. Radioresistance increased with age, reaching maximum resistance at 13 to 17 weeks of age. Beginning at 18 to 20 weeks of age, resistance declined throughout the remainder of the life span, reaching a minimum at 104 weeks (average life span for this strain is 96 weeks).

There was no appreciable period of relative stability in radioresistance throughout the entire life span. This is not consistent with earlier studies where radioresistance was tested by the fractionated method. The difference in response to radiation exposures by these two methods suggests a constant recovery rate from sublethal X-ray exposures throughout the greater part of the life span, with a constantly changing sensitivity to lethal X-ray exposures.

Figure 1 shows increased variability of radioresistance with increased age -- a characteristic commonly associated with advancing age. It was also found that an exponential function was a better fit to the data than was a linear one. This is also characteristic of many biological parameters.

REFERENCE

- (1) J. F. Spalding and T. T. Trujillo, Radiation Res. 16, 125 (1962).

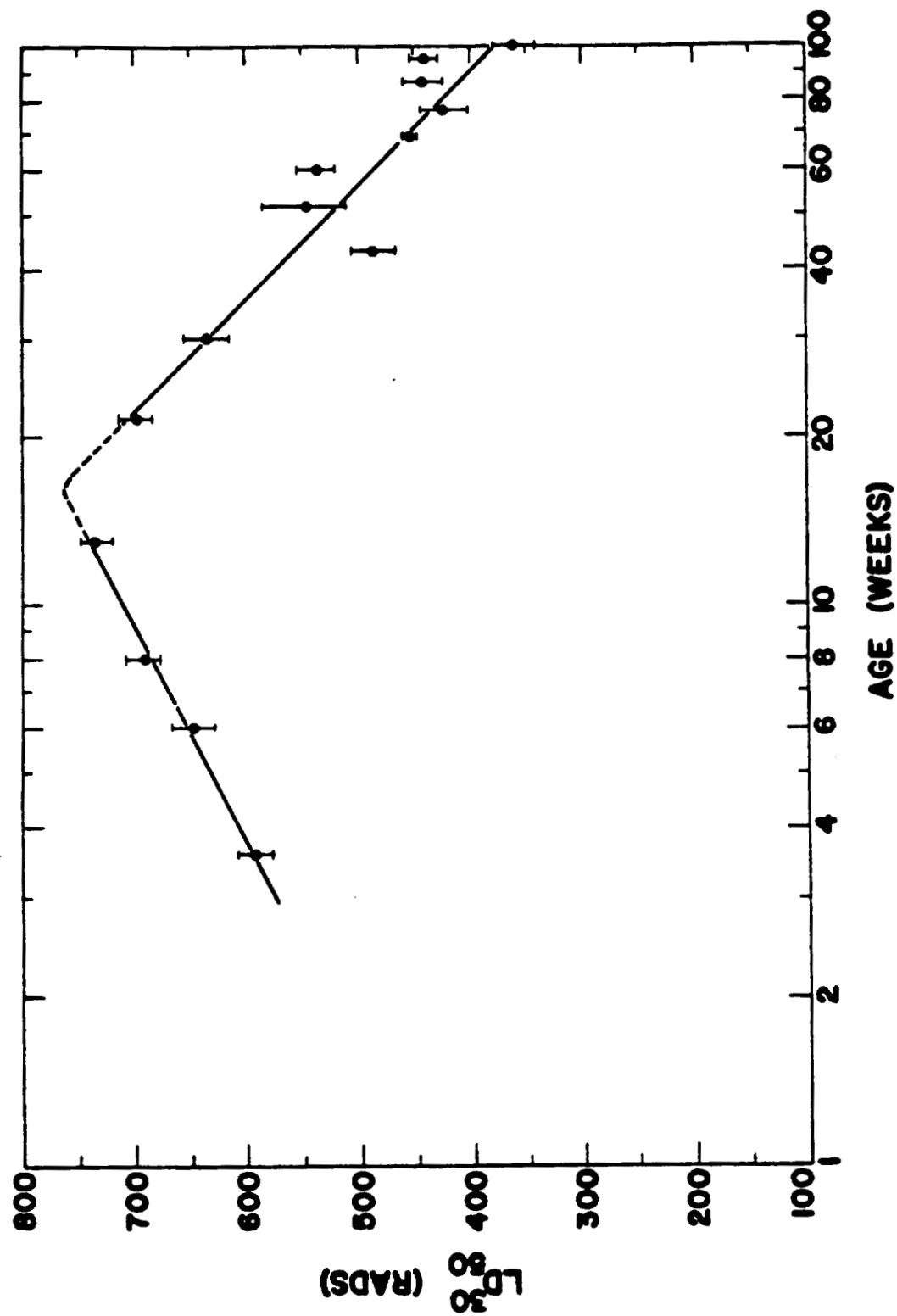


Fig. 1. LD₅₀³⁰ for RF strain female mice as a function of age.

Cold Stress as a Test for Rate of Aging in Three Lines of Mice with Different Histories of Ancestral X-Ray Exposure
(J. F. Spalding and T. T. Trujillo)

INTRODUCTION

There appear to be many similarities between aged mice and young mice with an irreparable burden of radiation injury. The Federation Proceedings on "Radiation and Ageing" (1) and one report by Upton (2) provide excellent reviews and theories on "radiation aging." It is a generally accepted fact that exposure of the total body of a mammal to ionizing radiation will reduce the life expectancy of the exposed animal (2). Trujillo (3) has shown that cold stress may be a useful tool in comparing similarities between chronologic and "radiation-accelerated" aging.

The genetic aspects of the life shortening effect on the offspring of irradiated parents are also unknown parameters of radiation injury. Russell (4) was the first to report life shortening in the offspring of male mice exposed to neutrons from an atomic detonation. Spalding et al. (5) showed a reduction in life expectancy of mice from 5 generations of X-irradiated sires. In contrast to these findings, an adjoined report shows no difference in the life span in the offspring of sires exposed to graded acute doses of neutrons or gamma rays, and offspring from both early and

late breeding were studied. It must be concluded that there is still considerable doubt as to whether or not the genetic mechanism which regulates life span is affected by exposure to ionizing radiation. However, since there is some evidence (4,5) that a premature aging factor may be inherited from sires exposed to ionizing radiation, and since resistance to cold stress appears to vary with age (3), it was felt that cold stress might be a useful test to determine the rate of aging of mice with a history of irradiated sires as compared to that of control mice. The study reported here is an attempt to test this thesis.

METHODS AND RESULTS

Virgin female RFM strain mice from the following three basic lines were used: irradiated line (granddaughters of the 15th generation of sires given 200 rads of X rays at weaning for 15 consecutive generations); irradiated sub-line (granddaughters of the 15th generation of sires given 200 rads of X rays at weaning for only the first 10 consecutive generations); and granddaughters of the 15th generation of control mice with no history of X irradiation. All three lines originated from one mating, and brother-sister matings were used in each of the three lines.

Exposure conditions for irradiated males in the

irradiated line and the irradiated sub-line were as follows: 250 KVP with a beryllium window tube; 30 ma filament current; Thoraeus II filter; 20 mm Cu HVL; 60 cm target-to-specimen distance; and 50 rads/min dose rate. Victoreen 100-r chambers were used. Dose measurements were made at the midline of Lucite mouse phantoms in Lucite chambers geometrically designed to give uniform doses at any chamber position. Victoreen readings were corrected for barometric pressure and temperature and converted to tissue dose by the factor $1 \text{ r} = 0.96 \text{ rad}$.

Five age groups (age range between 6 weeks and 12 months, Table 1) from each of the 3 lines described above were randomly caged in individual compartments, supplied with food and water ad libitum, and placed in a cold environment at a temperature of 6 to 7° C for 14 days. After the 14-day period of cold stress, the mice were maintained at room temperature for 10 days. Records of survival during the 14-day stress and 10-day post stress periods were made and compared for each age group within each of the 3 lines.

The results of this preliminary study are shown in Tables 1, 2, and 3 and in Fig. 1. The 3 lines of mice studied showed a considerable amount of variability of response to cold stress throughout the age interval studied. However, as shown in Fig. 1, there was a definite trend toward decreased resistance to cold with increased age. When a best fit slope was fitted

TABLE 1. SURVIVAL OF FIVE AGE GROUPS OF IRRADIATED LINE*
MICE FROM COLD STRESS**

Age (months)	Number of Mice	Survival	
		Number	Per Cent
1.39	92	84	91.3
3.01	52	52	100.0
6.65	109	98	90.6
8.38	100	49	49.0
12.66	129	82	63.6

*Seventeenth generation mice in which each of the first 15 generations of males was exposed to 200 rads of X rays at 24 to 28 days of age.

**Expression of best fit: $Y = 100 + -3.37 X$.

**TABLE 2. SURVIVAL OF FIVE AGE GROUPS OF IRRADIATED SUB-LINE*
MICE FROM COLD STRESS****

Age (months)	Number of Mice	Survival	
		Number	Per Cent
2.23	94	86	91.4
3.21	52	51	98.0
6.61	85	67	78.8
8.38	102	52	51.0
12.75	119	87	73.1

*Seventeenth generation mice in which each of the first 10 generations of males was exposed to 200 rads of X rays at 24 to 28 days of age.

**Expression of best fit: $Y = 100 + -3.5 X$.

**TABLE 3. SURVIVAL OF FIVE AGE GROUPS OF CONTROL LINE* MICE
FROM COLD STRESS****

Age (months)	Number of Mice	Survival	
		Number	Per Cent
2.18	92	87	94.5
3.04	52	50	96.1
6.65	96	87	90.6
8.59	98	60	61.2
12.46	92	67	72.8

*Seventeenth generation mice with no history of X-ray exposure to the line.

**Expression of best fit: $Y = 100 + -2.64 X$.

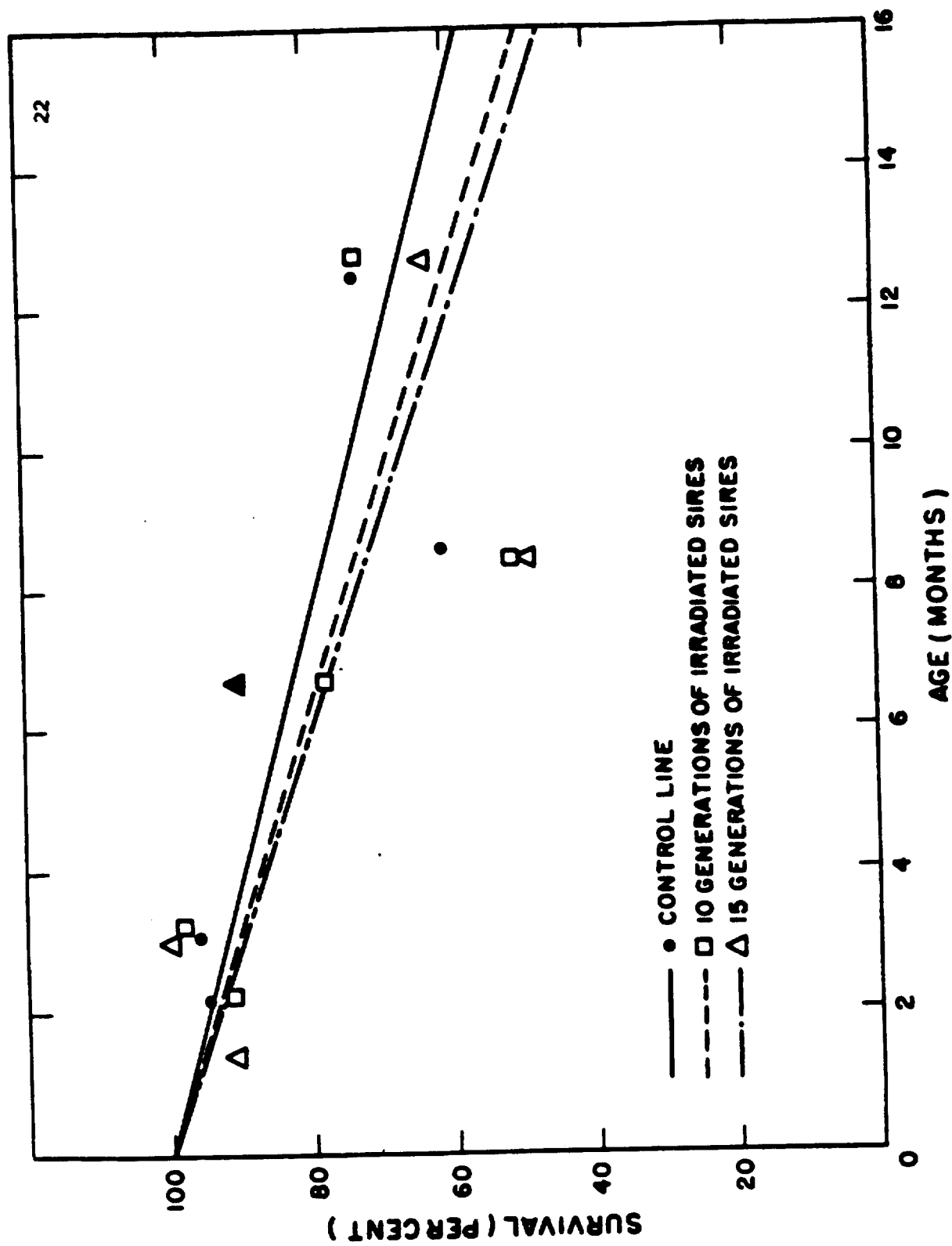


Fig. 1. Least squares fit of survival data of cold stress versus aging rate.

to the data in Tables 1, 2, and 3, with the intercept fixed at 100 per cent, the slopes were shown to increase in accordance with the number of generations of X irradiation (Fig. 1). This observation suggests that (using cold stress as the test system) mice from 10 generations of irradiated sires aged more rapidly than did control mice and that mice with 15 generations of irradiated sires aged more rapidly than did mice with 10 generations of irradiated sires. In the mouse, the optimum age range for studying aging by the cold stress method is 12 to 22 months. Unfortunately, our environmental room was unavailable for the studies after completion of the 12-month age group study. These preliminary results point to the possibility of cold stress as a test of rate of aging, but more complete studies await the availability of an environmental chamber.

REFERENCES

- (1) P. Handler, ed., Radiation and Ageing, Fed. Proc. 20(2), Part 2, Suppl. 8 (1961).
- (2) A. C. Upton, Gerontologia 4, 162 (1960).
- (3) T. T. Trujillo, J. F. Spalding, and W. H. Langham, Radiation Res. 16, 144 (1962).
- (4) W. L. Russell, Proc. Nat. Acad. Sci. 43, 324 (1957).
- (5) J. F. Spalding and V. G. Strang, Radiation Res. 16, 159 (1962).

Breeding Characteristics of Offspring from Mice with Fifteen
Generations of X Irradiation to the Males (J. F. Spalding
and M. R. Brooks)

INTRODUCTION

This is a continuing study in which the breeding efficiency of mice from X-irradiated sires is studied at 5-generation intervals. When this study was started, little or no information was available on the genetic consequence of X irradiation to consecutive generations of mammals. This program was designed to study the breeding characteristics and nonspecific genetic effects of X irradiation to the sires in a continuing population of mice.

METHODS AND RESULTS

Breeding characteristics were studied on 3 basic lines: (a) control line, 16th generation mice with no history of ionizing radiation above background; (b) irradiated line, offspring of 15 generations of X irradiation to the males; and (c) irradiated sub-line, 16th generation mice in which only the first 10 generations of males were given exposures of X rays. The origin of the mice studied is illustrated in Fig. 1.

One hundred sib pairs of mice from each of the 3 basic lines were mated at weaning and were allowed to mate ad libitum

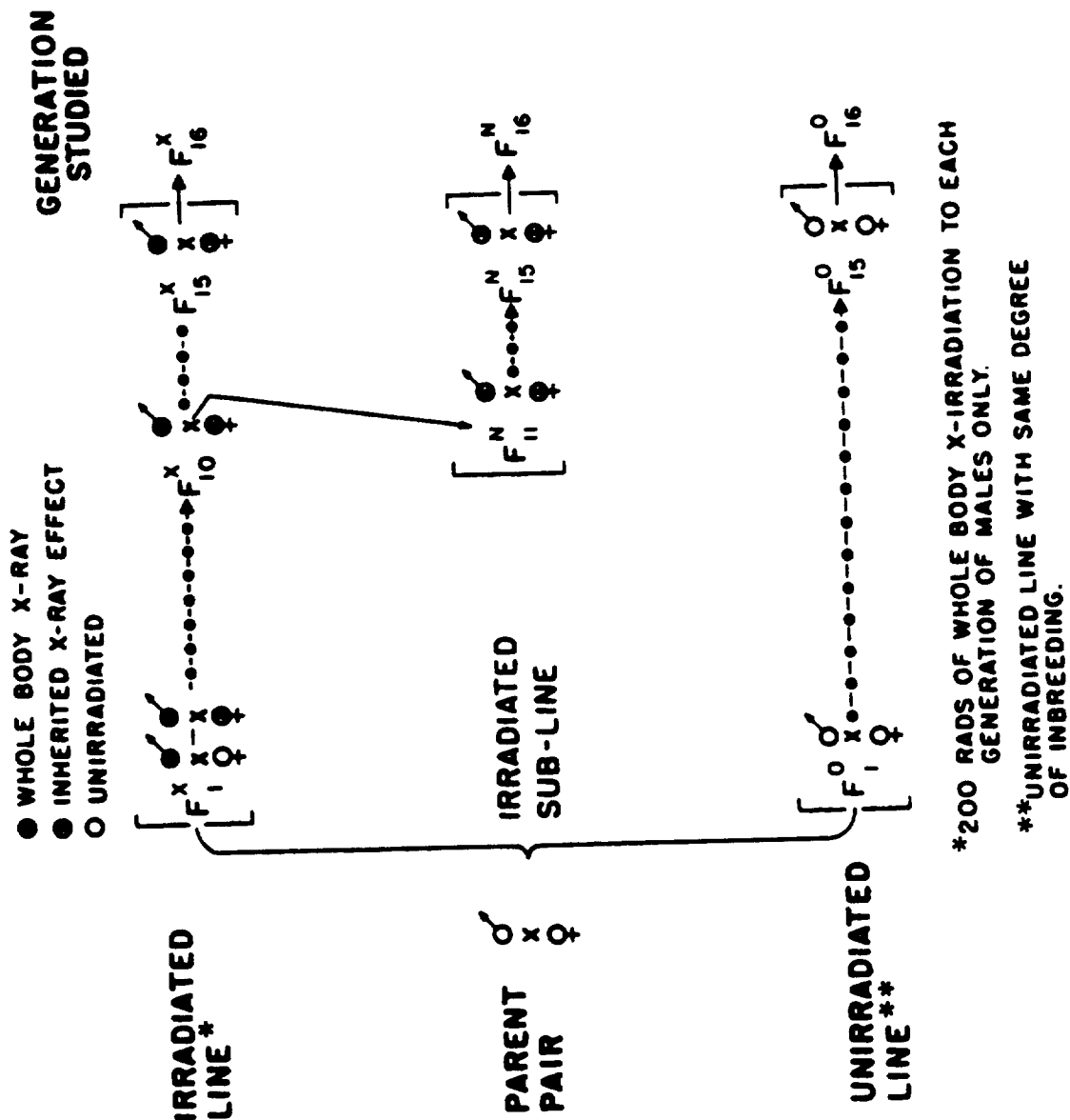


Fig. 1. Experimental design showing irradiation history of 3 basic lines of mice studied.

for their entire life span. A record of the reproductive proficiency of each line was maintained for line comparisons. The comparative productivity of each of the 3 basic lines is tabulated in Tables 1 and 2.

Notable differences appear among the 3 lines for several characteristics. Litter size was largest in the control line, smallest in the irradiated line, and intermediate in the irradiated sub-line. It was interesting to note that litter size could be rated according to the number of generations exposed to X irradiation, with the control line receiving the highest rating. On the contrary, however, age at last litter, reproductive life, and number of conceptions are rated in the reverse order with the irradiated line being rated first. There appears to be an attempt by Nature to compensate for genetic damage causing reduced litter size by prolonging the reproductive period of the female. The success of this compensatory effect is reflected in the total number of mice weaned (Table 2). Both irradiated lines outranked the control line in number of mice weaned.

Such characteristics as litter size (Table 1), number of litters cannibalized, and number of mice born dead (Table 2) reflect the radiation-induced genetic decrement to the reproductive efficiency of the irradiated line and irradiated sub-line. However, the extended reproductive life of these 2 lines suggests a natural compensation.

TABLE 1. GROUP AVERAGES

Characteristic	Control Line (sibs)	Irradiated Line (sibs)	Irradiated Sub-Line (sibs)
Age at First Litter (days)	71.7	72.2	78.2
Age at Last Litter (days)	264.2	333.1	300.7
Reproductive Life (days)	193.5	261.9	223.5
Conceptions (number)	5.99	7.69	7.23
Litter Size			
At Birth	5.39	3.91	4.42
At Weaning	4.13	3.34	3.86
Weaning Weight (grams)			
Per Individual	10.4	10.5	10.8
Per Litter	42.7	35.1	41.9

TABLE 2. GROUP TOTALS AND SEX RATIOS

Characteristic	Control Line (sibs)	Irradiated Line (sibs)	Irradiated Sub-Line (sibs)
Total Number of Mice Born (per group)	3,216	2,888	3,042
Sex Ratio (male/female)	1.09	1.15	1.11
Total Number of Mice Weaned (per group)	2,410	2,486	2,673
Number of Litters Cannibalized before Weaning	179	335	229
Number of Mice Born Dead	40	316	96
Number of Pairs Producing			
Average Litter Size of			
3 or Less	6	27	14
2 or Less Litters	9	8	10
No Litters	0	3	3

Radiation-Induced Irreparable Biological Damage in Three
Genetic Lines of Mice with Different Ancestral Histories of
Radiation Exposure (J. F. Spalding and R. F. Archuleta)

INTRODUCTION

Earlier studies (1,2) have shown that mice from a genetic line in which the males received X-ray exposure each of several consecutive generations were less tolerant of protracted low-intensity gamma rays and fractionated X rays than were mice from the same origin but with no ancestral X-ray exposure. The difference in radiosensitivity between the two lines may be attributed to a number of factors. However, in the broadest sense, radioresistance or radiosensitivity is determined by the amount of irreparable injury induced and the repair rate of the reparable portion of radiation injury. The following study is an attempt to determine which of the above factors are primarily responsible for the difference in radiosensitivity of the two lines.

METHODS AND RESULTS

Approximately 50 virgin female mice (7 ± 0.5 months of age) from each of the 3 basic genetic lines described in the preceding report were used (3), and the mice used in this study were seventeenth generation mice or litters from the

previous study. Fifty mice from each of the 3 lines were exposed to gamma irradiation at a dose rate of 1.69 rads/hr until an accumulated dose of 1500 rads was achieved. Following this conditioning exposure, the mice were allowed 90 days to recuperate from the reparable damage induced by exposure to ionizing radiation. On day 31 of the recovery period, all mice in each group were placed in individual compartments and exposed to low temperature stress (6 to 7° C) for 14 consecutive days. The number of mice in each group surviving this 14-day cold stress and a 10-day post stress period was recorded for purposes of comparison. Table 1 shows the results of this study. Survival from cold stress was substantially lower in the irradiated line and irradiated sub-line than in control line mice. The decreased resistance to cold stress in the irradiated lines over that of the control line may be due to the amount of irreparable damage induced by 1500 rads of gamma-ray exposure. In other words, irreparable damage in the irradiated lines might have been 10 to 15 per cent of the total accumulated dose, while in the control line it was only 5 per cent. However, since control line mice were much more resistant to cold stress than mice of this chronological age with a 1500-rad gamma-ray exposure would be expected to be (4), these findings are inconclusive and suggest further studies.

TABLE 1. ABILITY OF THREE GENETIC LINES OF MICE TO TOLERATE
COLD STRESS FOLLOWING PROTRACTED GAMMA-RAY STRESS*

Conditioning Dose (rads gamma)	Age (months)	Number of Mice	Survival	
			Number	Per Cent
<u>Group I (Irradiated Line)</u>				
1500	7 \pm 0.5	48	35	72.9
<u>Group II (Irradiated Sub-Line)</u>				
1500	7 \pm 0.5	50	37	74.0
<u>Group III (Control Line)</u>				
1500	7 \pm 0.5	49	48	97.9

*A 90-day interval was allowed between gamma conditioning dose and cold stress.

REFERENCES

- (1) J. F. Spalding and V. G. Strang, Radiation Res. 15, 329 (1961).
- (2) J. F. Spalding, V. G. Strang, and W. L. LeStourgeon, Radiation Res. 18, 479 (1963).
- (3) J. F. Spalding and M. R. Brooks, Breeding Characteristics of Offspring from Mice with Fifteen Generations of X Irradiation to the Males, this report, p. 124.
- (4) J. F. Spalding and T. T. Trujillo, Cold Stress as a Test for Rate of Aging in Three Lines of Mice with Different Histories of Ancestral X-Ray Exposure, this report, p. 116.

Inability of the Mouse to Recognize Gamma Radiations. I.
Variable Low Dose Rate Studies in RF Mice (J. C. Hensley,
J. F. Spalding, W. F. Schweitzer,* and R. F. Archuleta)

INTRODUCTION

The recognition of ionizing radiations by mammalian subjects has been reported by Andrews and Peterson (1). These authors concluded that no recognition of X irradiation is observed by mice when exposed to 10 r/min or less during acute exposures, with questionable avoidance noted as rates approached 50 r/min, and definite avoidance response as rates increased. Their conclusions were based on visual observation. Others have made visual observations of behavioral disturbance reactions in radiation fields (2).

No application of accurate dosimetry to a study of the recognition of radiations by individual subjects has been reported. The dose rates used in this study are below those of previous recognition studies to eliminate interference of radioneurological disorder with selection of position in a radiation field.

METHODS AND RESULTS

Thirty RF mice were selected randomly from a group of 3- to 4-month-old mice. Observation of mice this age indicates maximal curiosity and activity.

*From LASL Group H-8.

Individual AgPO_3 glass rods were implanted aseptically subcutaneously at the abdominal midline (1 cm posterior of the xiphoid in each mouse). Identical AgPO_3 rods were positioned as stationary dosimeters. Rods implanted were 6 mm in length and 1 mm in diameter -- a convenient size for implantation. Tolerance of these rods to tissue fluids and excellent stability are recognized.

The range of dosimetry possible with these rods was from 10 to 10^5 r gamma. Exposure of significance causes formation of stable fluorescent loci within the rods which, when excited by near ultraviolet light, produce illuminescence of a wave length of 6400 Å. Fluorescence is relative to the total dose absorbed. A Turner Fluorimeter was used for analysis. A 3-curie Co^{60} source was used for exposures (Fig. 1). The mice were positioned 10 per cage in the cage-run assembly shown in Fig. 1. Food, water, and bedding were supplied at these cage positions. Light sources were equidistant from each cage position and of equal intensity. Ambient temperatures were essentially equal at all points. The entire assembly was positioned 18 in. above the floor and was leveled. It was assumed that environmental clues as to direction from the source were absent.

The position of the mice was noted at the same time each day. Thirty-two observations were made where 90 per cent of

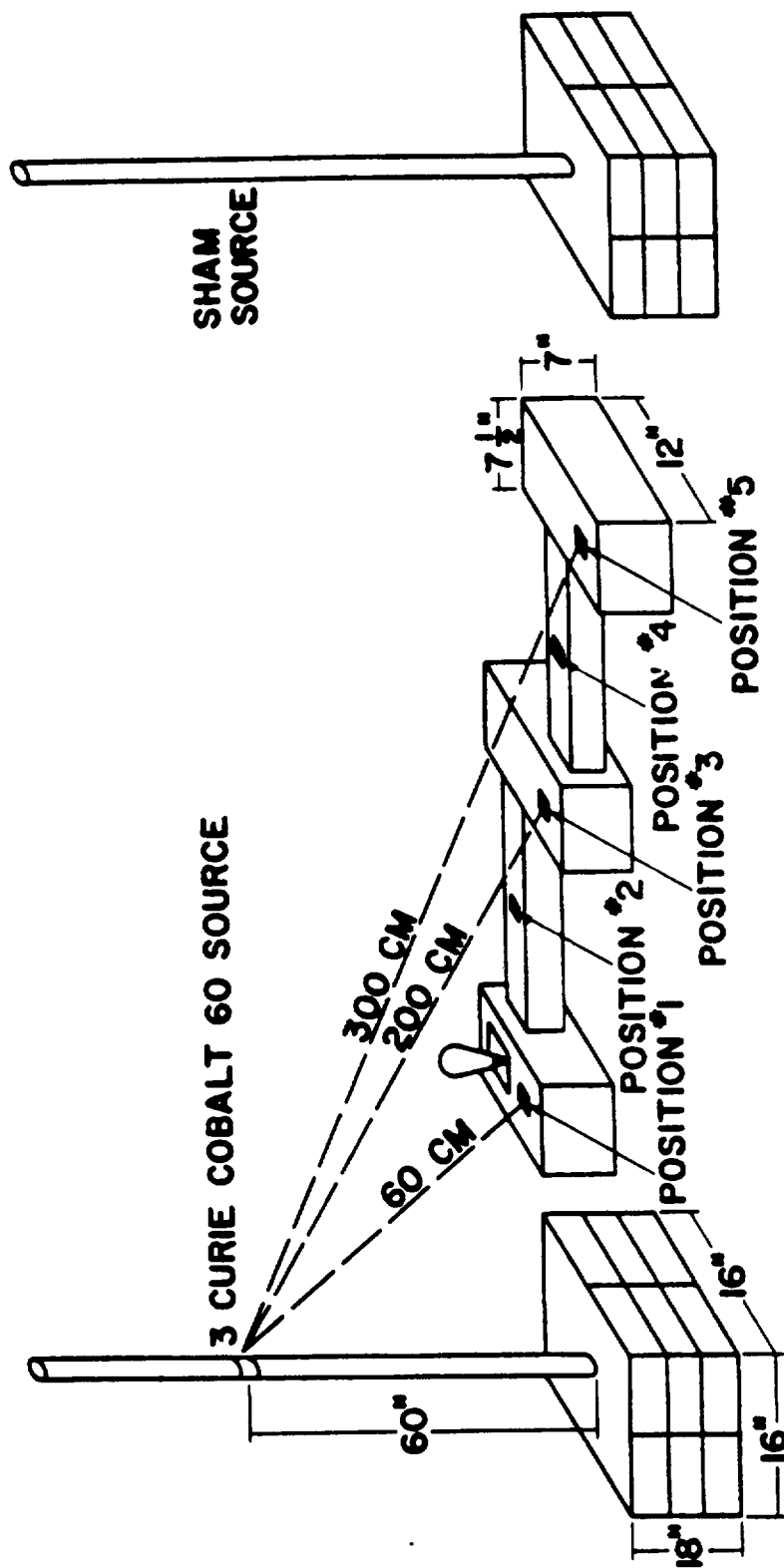


Fig. 1. Arrangement of exposure points for radiation recognition. Mice were allowed unrestricted access to all 3 cages, each of which provided food, water, and bedding. AgPO_3 glass rod dosimeters were positioned at points indicated.

the subjects were at a specific position in the cage-run assembly. The dose rate at each position was also monitored by AgPO_3 glass rods (Fig. 1). The total dose to each position is indicated in Fig. 2. Cage positions I, II, and III received total accumulated doses of 5702.76, 2105.32, and 900.0 r, respectively. Dosimeter positions I through V indicated dose rates ranging from 7.57 to 1.20 r/hr (Fig. 1) during the 752-hour period.

The average accumulated dose received by implanted dosimeters was 2628×10^3 rads, within the range of 2.3×10^3 to 2.8×10^3 rads. Figure 3 indicates the percentage of animals receiving total absorbed doses indicated in the range categories of 0.05 MAD variance. Note that distribution of dose accumulation was decidedly toward the higher dose ranges, indicating a tendency to spend a proportionately greater percentage of time during irradiation in the vicinity of the Co^{60} source.

Figure 2 indicates the observed position of the mice. Had the subjects actually spent time as observed in the vicinity of the source, the average actual dose would have been 0.68 rad/mouse more than that derived from implanted dosimeters, indicating that actual time spent in the vicinity of the source was greater than noted.

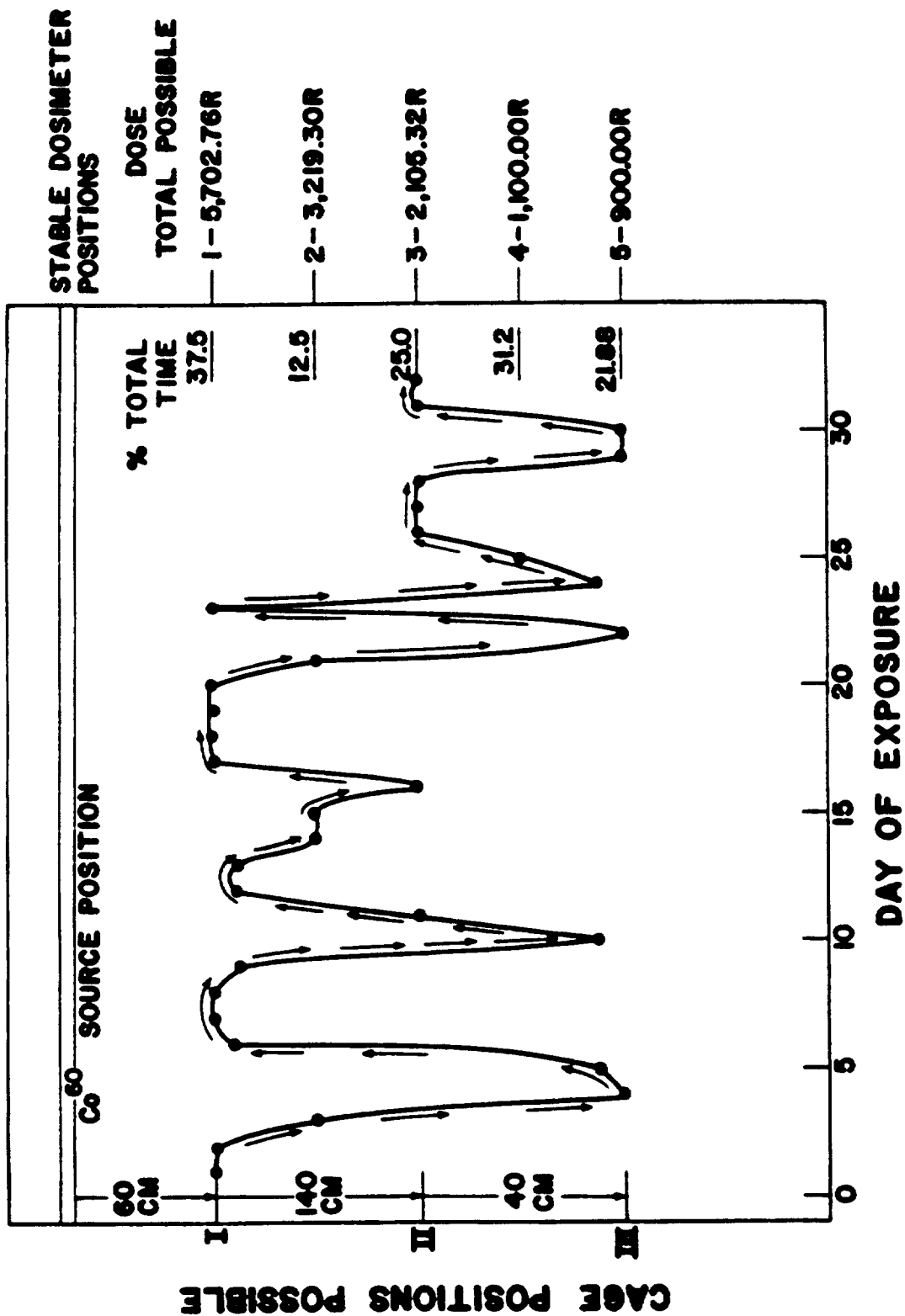


Fig. 2. Observed position tendency of mice in cage-run assembly in relation to the Co60 source (right column, total possible dose for 1000-hour period at each stationary dosimeter locus).

1055610

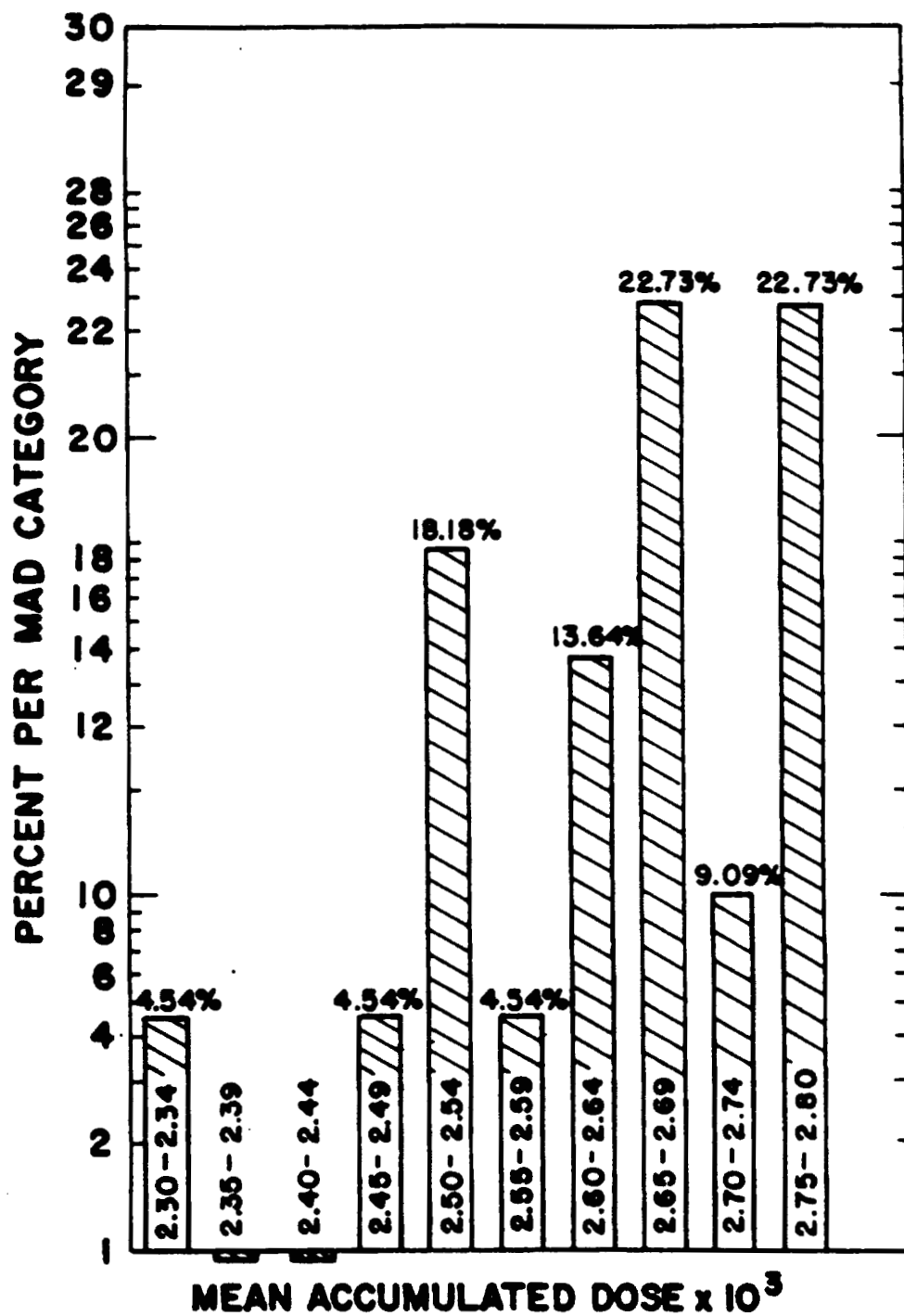


Fig. 3. Categorical breakdown at 50 r of total doses received by mice, representing the per cent mice receiving total doses of a given MAD range.

DISCUSSION

Since there were no environmental clues to location of the source in relation to the cage-run assembly, one must conclude that low dose rate gamma radiations, regardless of accumulated dose totals, do not evoke a recognition response in mice. Since dose rates were sufficiently low to avoid neurological disorder from exposure, and since actual exposure was determined by individual dosimeters carried by the mice, no alteration of recognition evaluation was observed visually and no "exposure confusion" was manifested.

The average mouse dose rates, compared to those of stationary dosimeters, contrarily indicated a tendency to equilibrium between possible dose rate points, with a positive tendency toward positions closer to the source.

More extensive studies are planned involving extremes in dose rates and total possible dose for determination of recognition possible within exposure fields where inability to recognize high dose rates will result in early mortality.

REFERENCES

- (1) H. L. Andrews and D. C. Peterson, Radiation Res. 17, 514 (1962).
- (2) H. F. Harlow, In: International Symposium on the Response of the Nervous System to Ionizing Radiation, Academic Press, New York (1962), pp. 627-644.

MAMMALIAN RADIOBIOLOGY SECTION

PUBLICATIONS

(1) J. F. Spalding, V. G. Strang, and W. L. LeSturgeon, Characteristics of Offspring from Ten Generations of X-Irradiated Male Mice, Genetics 48, 341 (1963).

(2) J. F. Spalding, V. G. Strang, and W. L. LeSturgeon, The Effect of Ancestral Irradiation Exposure on Radioresistance in Their Descendants, Radiation Res. 18, 479 (1963).

(3) J. F. Spalding, Biological Recovery from Radiation Injury, In: Encyclopedia of X-Rays and Gamma Rays (G. L. Clark, ed.), Reinhold Publishing Corporation, New York (1963), pp. 929-931.

MANUSCRIPTS SUBMITTED

(1) J. F. Spalding, Longevity of First and Second Generation Offspring from Male Mice Exposed to Fission Neutrons and Gamma Rays, to be published in Proceedings of the International Symposium on the Effects of Ionizing Radiation on the Reproductive System, Fort Collins, Colo. (September 17-19, 1962).

(2) J. F. Spalding, M. R. Brooks, and R. F. Archuleta, Genetic Effects of X Irradiation of 10, 15, and 20 Generations of Male Mice, submitted to Health Physics.

(3) J. F. Spalding and J. A. Sayeg, Dose Rate Effects on Lethality of Mice Exposed to Fission Neutrons, to be published in the Proceedings of the IAEA Symposium on the Biological Effects of Neutron Irradiation, Brookhaven National Laboratory (October 7-11, 1963).

CHAPTER 4

LOW-LEVEL COUNTING SECTION

Humco II: Status Report (P. N. Dean and E. C. Anderson)

Humco II has now been fully calibrated for measuring Cs^{137} and potassium. The Cs^{137} calibration was initially done using water phantoms. When Cs^{132} became available, it was used with human subjects. Cesium¹³² is very useful for this purpose in that it has a 6.2-day half-life and a gamma-ray energy of 0.667 Mev (0.662 for Cs^{137}). The potassium calibration was done using K^{42} with a half-life of 12.5 hours and a gamma energy of 1.53 Mev (1.46 for K^{40}). The two calibration curves are shown in Figs. 1 and 2.

Humco I was removed in the fall of 1962. This allowed the construction of a well such that there is now a single room containing all equipment associated with Humco II and used exclusively for whole-body counting. Figures 3 and 4 show the present arrangement of the room and equipment.

In January 1963, a failure of the high voltage supply

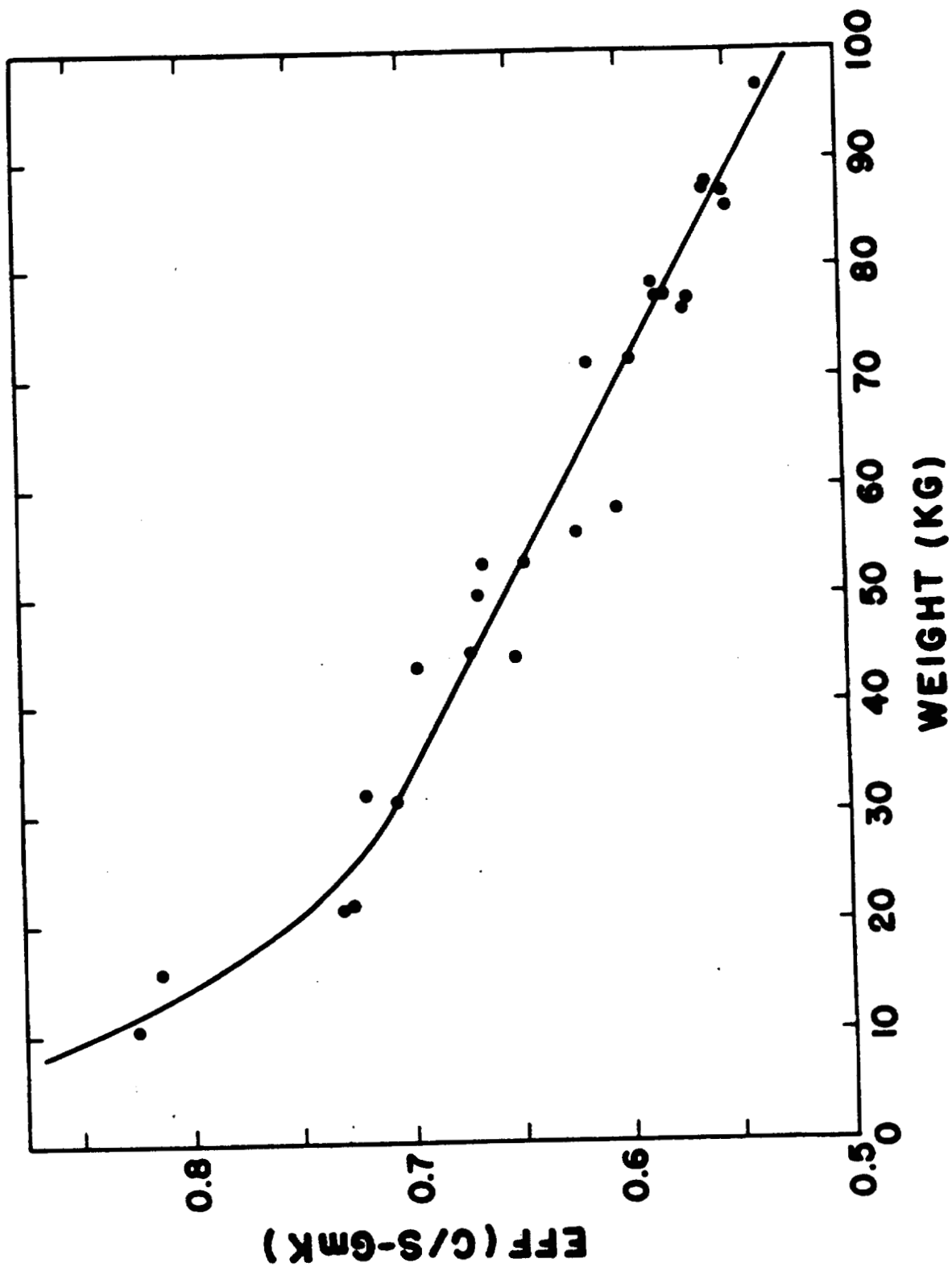


Fig. 1. Potassium counting efficiency versus weight in channel 5.

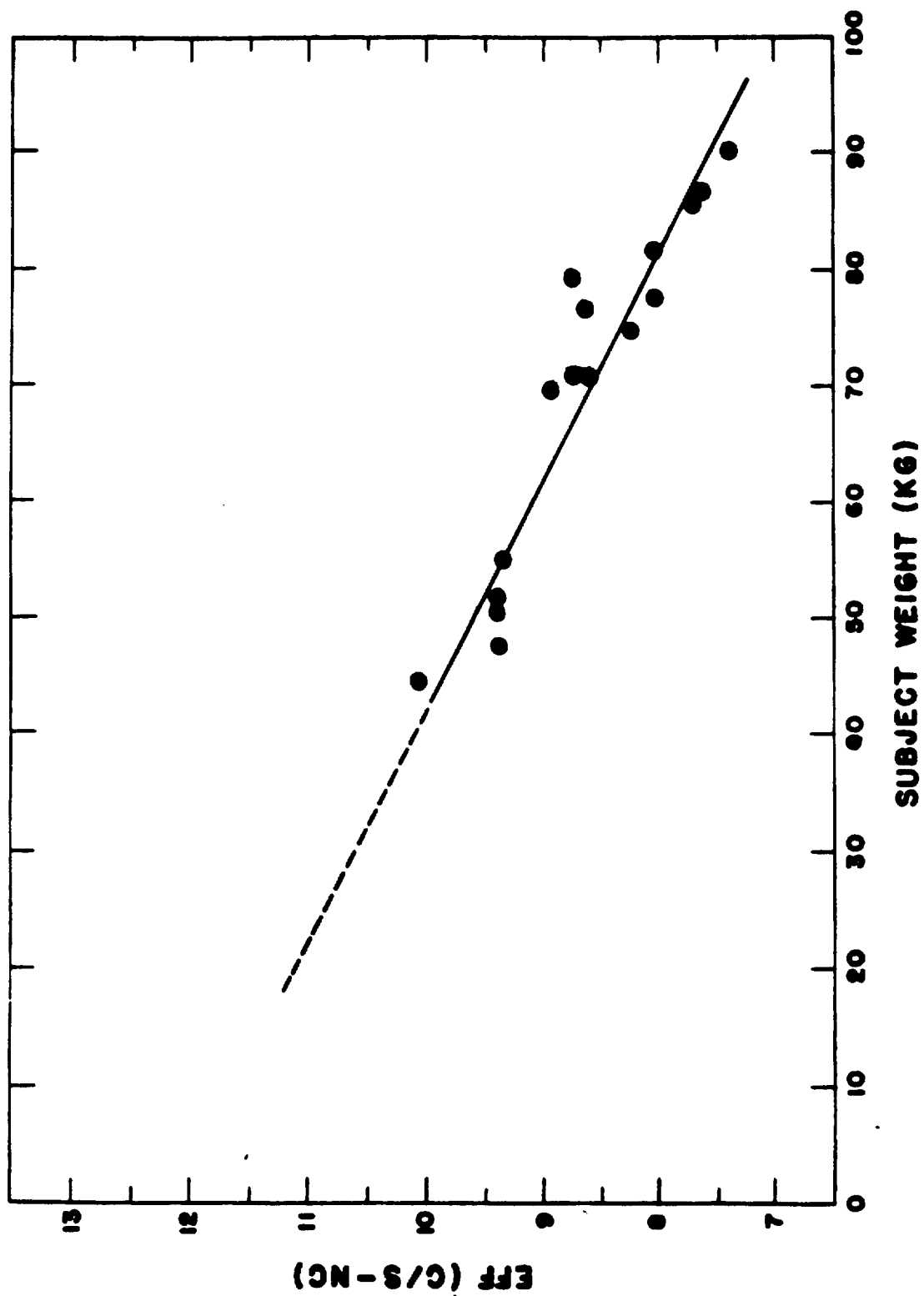


Fig. 2. Cesium counting efficiency versus weight in channel 3.

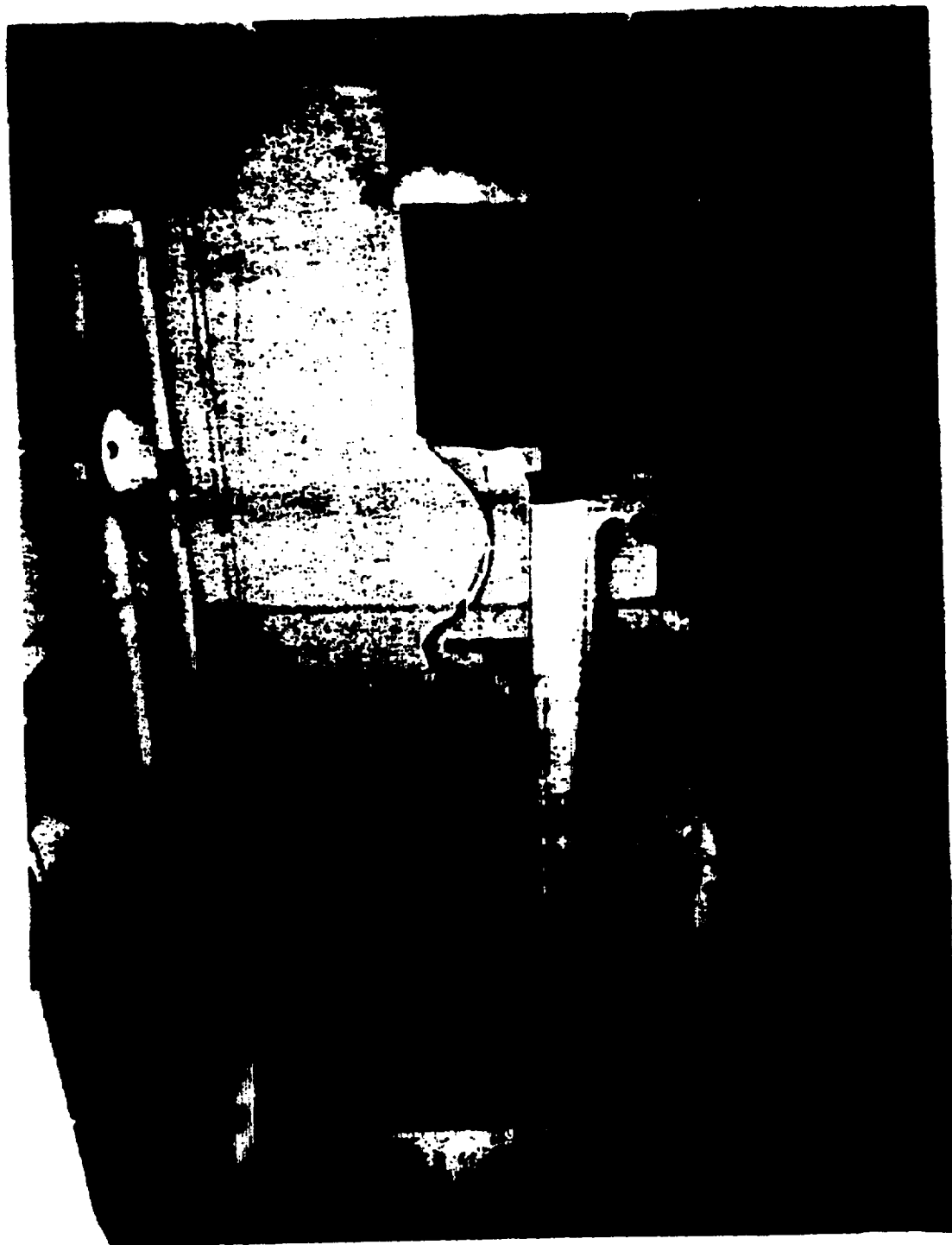


Fig. 3. Over-all view of Humco II whole-body counting facility.



Fig. 4. Humco II instrumentation console.

introduced an instability into the counter. It is believed that this was due to an excessive voltage being applied to the photomultiplier tubes by the high voltage supply, as it broke down. Since this condition could permanently damage the photomultipliers, steps have been taken to prevent its recurrence. An electronic device has been constructed such that if the high voltage ever changes (either plus or minus) by more than a predetermined amount, the high voltage supply will be turned off. Under present operating conditions, the monitor is set to trigger on a change in high voltage of ± 1 per cent.

A slight decrease in signal output of the photomultiplier-scintillator combination led to the flushing of the scintillator solution with argon. It is believed that since the tank has a small diameter vent pipe to the atmosphere, oxygen had entered the solution, thus causing a decrease in pulse height from the scintillator. The counter had operated for 9 months without argon flushing. To prevent a recurrence of this problem, it has been decided that 60 cubic feet of argon will be bubbled through the scintillator once every 2 months at the rate of 4 cubic feet per hour.

During the time from April 1962 to June 1963, a total of 345 measurements were made of the gamma activity (both K^{40} and Cs^{137}) of human subjects using Humco II. This was a

random population sample consisting of visitors to the Health Research Laboratory and residents of Los Alamos. A determination of potassium concentration versus age was made on these subjects. Two previous studies of potassium concentration versus age were made using Humco I and have been reported (1, 2). The present study was made to determine whether data from Humco II would agree with that from Humco I. Figure 5 shows the results from all three studies. The plotted points are from the Humco II study with an error of 1 standard deviation of the mean ($\sigma_1 \sqrt{n}$, where σ_1 is calculated from the observed scatter of the data, and n is the number of determinations). The somewhat larger scatter of the points is due to the small sample size, the variation in a group of given age and sex corresponding to an average σ_1 of 12 per cent -- similar to that previously observed.

The results for adult females agree within experimental error with the previous curves. For adult males, there is a tendency for the present data to lie several per cent above the previous. The male peak at age 16 is about as in the 1959-1960 data. The peak at age 8 appears to be confirmed, although the statistics are marginal. The primary value of these data is to provide an independent operational confirmation of the agreement of the average potassium calibrations of Humco I and Humco II.

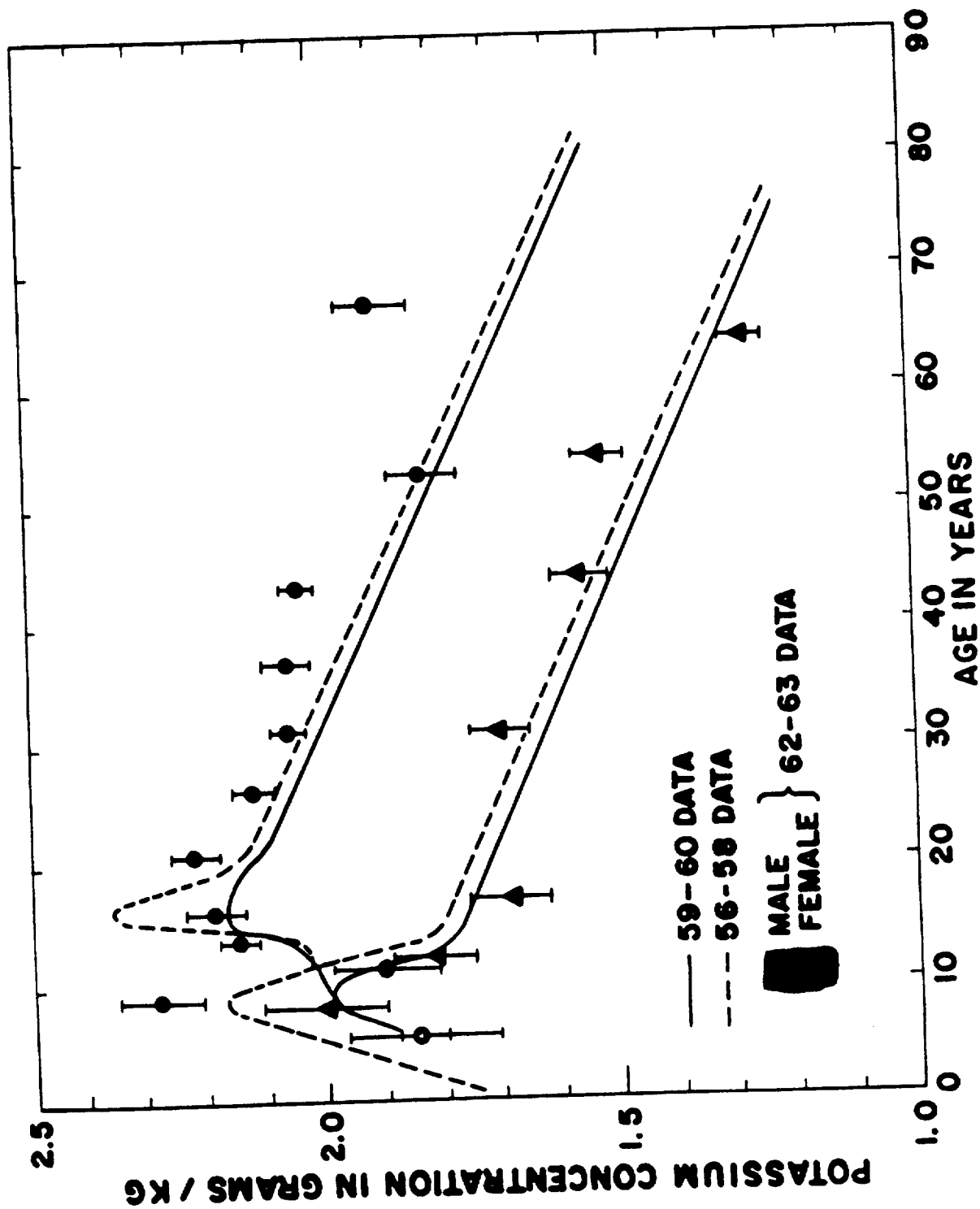


Fig. 5. Variation of human body potassium concentration with age and sex.

REFERENCES

- (1) E. C. Anderson and W. H. Langham, *Science* 130, 3377 (1959).
- (2) E. C. Anderson and B. E. Clinton, *Los Alamos Scientific Laboratory Report LAMS-2526* (1961), pp. 121-128.

Absolute Calibration of Whole-Body Gamma-Ray Spectrometer
for Potassium and Cesium¹³⁷ (P. N. Dean and M. A. Van Dilla)

INTRODUCTION

Past work with the human gamma-ray spectrometer at this Laboratory did not require absolute calibration for potassium and Cs¹³⁷. When Humco II was put into operation, however, careful absolute calibration was necessary, and we took advantage of this opportunity to calibrate the spectrometer also. The spectrometer facility consists of a 9-3/8 x 6-in. NaI crystal in a movable overhead mount in a steel room made of 7-in. thick steel (naval armor plate). The subject reclines in a tilting chair made from a standard commercial lawn chair following the Argonne design (Fig. 1). Potassium⁴² and Cs¹³² were used in the calibration; the results for a wide range of subject weights for both counters are given below.

METHODS

The K⁴² calibration technique has been described elsewhere (1). Cesium¹³², obtained from the Japan Atomic Energy Research Institute, was used because it has a short half-life (6.53 days) and emits a gamma ray of energy 0.667 Mev (0.662 for Cs¹³⁷). The Cs¹³² decay scheme has been reported in detail (2). The isotope was administered intravenously. The syringes were counted both before and after injection and



Fig. 1. The Los Alamos whole-body spectrometer.

1055626

compared to a Cs^{137} standard, which yielded the equivalent microcuries of Cs^{137} given to the subjects. The first calibration experiment used 4 male subjects in the age range of 28 to 42 years and weight range of 70 to 81 kg. These subjects were counted at 2, 3, and 4 hours to determine the mixing time for the isotope. All succeeding subjects were then counted after a time interval such that the count rate from the Cs^{137} was not changing with time. An additional 8 male subjects and 8 female subjects were used in the age range of 23 to 52 years and weight range of 44 to 89 kg.

RESULTS

Figure 2 shows the counting efficiency of the human spectrometer for potassium as a function of subject weight. The plotted points are counts per minute per gram of potassium versus body weight. Only the K^{40} full energy peak is used. The solid line is a least squares computer fit to the data points. The standard deviation of an individual point is ± 5.1 per cent, so that the uncertainty in a given potassium determination would be 5.1 per cent plus effect of counting statistics and any other possible errors. Actually, counting statistics do not introduce the major error for adults. Thus, for a [REDACTED] male (serial number [REDACTED]), the standard deviation was 2.2 per cent for a 50-minute count of subject

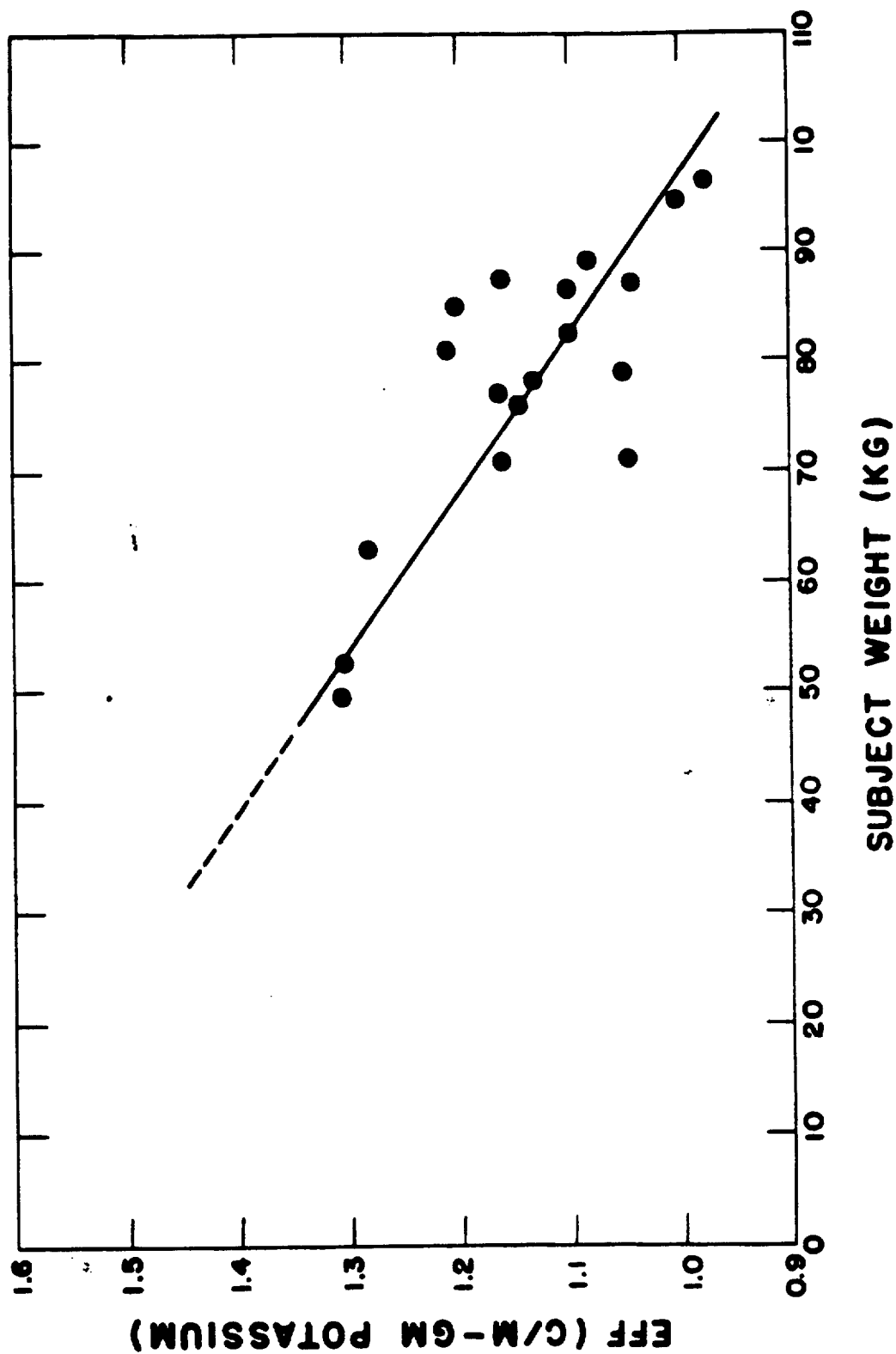


Fig. 2. Potassium counting efficiency (in c/min per g K) versus weight (in kg).

and background and 4.9 per cent for a 10-minute count. The effect of subject weight is appreciable, being 35 per cent over the weight range of 50 to 100 kg.

Figure 3 shows the results of the Cs^{132} calibration experiment. The plotted points are counts per minute per nanocurie of Cs^{137} versus body weight. Conversion of data in terms of Cs^{137} was made with a Cs^{137} standard (Group J-11 vial 1a) supplied by the Radiochemistry Group of LASL. Only the full energy peak above the continuum was used in computing count rate. The solid line is a least squares computer fit to the data points. The standard deviation of a single measurement is ± 3.6 per cent, so that the uncertainty in a given Cs^{137} determination would be this number plus the effect of counting statistics and any other errors. For the same subject mentioned above with a Cs^{137} content of about 17 nanocuries, the error due to counting statistics and estimation of the continuum was 6.4 per cent for a 50-minute period. The effect of weight on counting efficiency is considerably less than for potassium, being 11 per cent over the weight range of 50 to 100 kg. Thus, the major error for subjects with fallout Cs^{137} in the 5- to 10-nanocurie range is due to counting statistics, weight effects being less important.

In comparing the two calibration results for the human

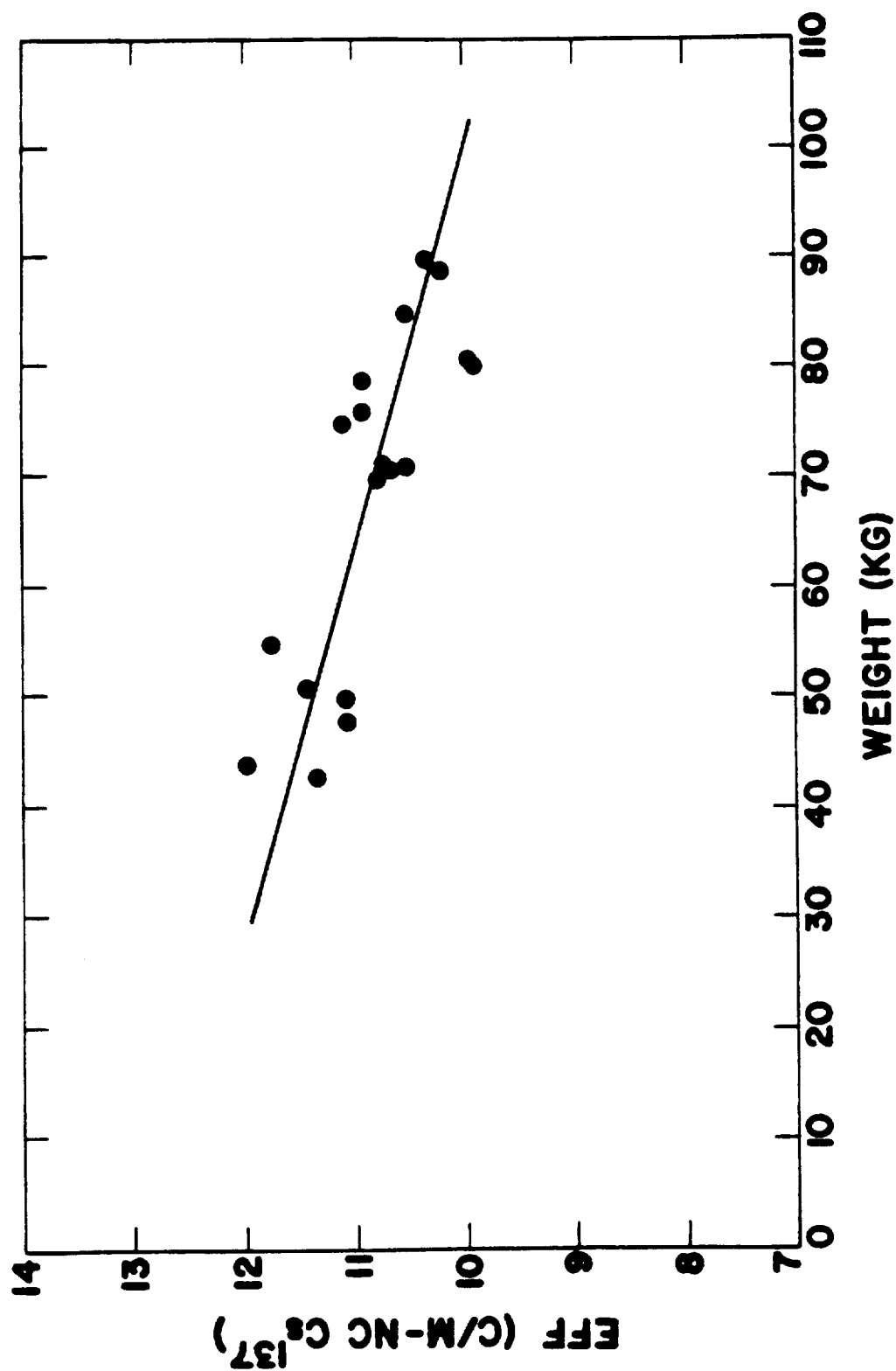


Fig. 3. Cesium¹³⁷ counting efficiency (in c/min per nanocurie Cs¹³⁷) versus weight (in kg).

spectrometer, the greater importance of counting statistics in estimation of fallout Cs^{137} was expected, but the smaller weight dependence for this isotope was a surprise. No explanation for this is apparent.

It is interesting to compare the calibration results for the spectrometer and Humco II. One would expect the latter to be less responsive to the weight and size of a subject because it is essentially a 4 π counter, but how much less is hard to estimate a priori. The results for the two counters are summarized in Table 1. Note that for the case of potassium, the uncertainty due to weight for Humco II is lower by a factor of 2.5, which is a significant advantage. It is curious that the weight correction varies with weight in a similar fashion for the two counters, suggesting that geometry effects are similar and the variation is due to self-absorption by the subject. For the case of Cs^{137} , the uncertainty due to weight for Humco II is lower by a factor of 1.2. This difference was expected but in this case is not a very significant advantage.

Finally, one may ask how potassium results on the same series of normal subjects measured in both counters compare. Such data are presented in Table 2 and show that one gets the same answer on the average, but that measurements on an individual may differ by 10 to 15 per cent. The standard deviation for this set of subjects is 4.8 per cent.

TABLE 1. CALIBRATION OF HUMCO II AND HUMAN SPECTROMETER AT LASL

	Humco II	Spectrometer
<u>Potassium</u>		
c/min per g K (70-kg man)	35.1	1.19
c/min Background	21,240	210
Standard Deviation (weight)	$\pm 2.1 \%$	$\pm 5.1 \%$
Weight correction (50-100 kg)	1.27	1.35
<u>Cesium¹³⁷</u>		
c/min per nanocurie Cs ¹³⁷ (70-kg man)	514	10.8
c/min Background	33,480	269
Standard Deviation (weight)	$\pm 2.9 \%$	$\pm 3.6 \%$
Weight Correction (50-100 kg)	1.36	1.11

TABLE 2. POTASSIUM ASSAY ON SAME SUBJECTS WITH HUMCO II AND
SPECTROMETER

Subject	Weight (kg)	g K (Humco II)
		g K (Spectrometer)
		1.02
		0.997
		0.964
		1.01
		1.13
		0.995
		0.979
		0.994
		1.06
		1.00
		0.903
		0.978
		1.03
		0.927
		0.974
		1.03
Average		0.999
Standard Deviation		4.8 %

REFERENCES

- (1) P. N. Dean, Experimental Technique for High Precision Calibration of Whole Body Counters, presented at the Second Symposium on Radioactivity in Man, Northwestern University Medical School (September 1962); to be published in proceedings.
- (2) R. L. Robinson, N. R. Johnson, and E. Eichler, Phys. Rev. 128(1), 252 (1962).

Evaluation of the Potassium⁴⁰ Continuum Contribution to the
Cesium¹³⁷ Photopeak in a Sodium Iodide Crystal Spectrometer
(E. C. Anderson, P. N. Dean, and M. A. Van Dilla)

INTRODUCTION

In making a quantitative calculation of the Cs¹³⁷ body burden of a subject from the measured gamma-ray spectrum, it is necessary to correct for the counting rate from the scattered gamma rays of K⁴⁰. This correction can be evaluated from the shape of the K⁴⁰ spectrum and the potassium content, if the latter is known. Dr. C. E. Miller of the Argonne National Laboratory has pointed out (1) that while the ratio of the potassium photopeak to the potassium continuum varies with subject weight, the shape of the continuum itself is nearly independent of weight. He has proposed, therefore, that one can determine the potassium correction in the absence of K⁴² determinations of spectral shape by making use of the constancy of the ratio of the potassium count in the energy band 525 to 725 kev (spanning the Cs¹³⁷ photopeak) to that in the energy band 775 to 1275 kev, the latter being a region of the potassium continuum lying above the Cs¹³⁷ photopeak and below the K⁴⁰ photopeak. He reports a value of 0.52 for this ratio for several subjects. Dr. C. J. Maletskos of the Massachusetts Institute of Technology (2) has also studied this method and has found a ratio of 0.49 and 0.53 for

2 subjects -- in good agreement with Miller's value. Having recently completed a K^{42} calibration of our 9 x 6-in. crystal spectrometer, we had the opportunity to check this ratio as a function of weight for 27 subjects.

METHODS AND RESULTS





A group of 22 male and 5 female subjects were given K^{42} intravenously as part of a calibration program to determine the absolute efficiencies of the LASL low-level gamma counters (3). Gamma-ray spectra were measured before and after administration of the tracer, and net spectra due to K^{42} alone were calculated at 5 hours, at which time no further changes due to mixing within the body could be detected. The ratio of counting rate in the Cs^{137} channel (525 to 725 kev) to that in the higher energy potassium continuum (775 to 1275 kev) was calculated, and the results are shown in Table 1 and in Fig. 1. The average values, 0.536 for men and 0.483 for women, are close to the previously reported values.

A least squares linear regression line was fitted to the data with the result that,

$$R = (0.447 \pm 0.026) + (0.00112 \pm 0.00036) W,$$

where R is the ratio, and W is the subject's weight (in kg).

TABLE 1. POTASSIUM⁴² RATIO $\left(\frac{525 - 752 \text{ kev}}{775 - 1275 \text{ kev}} \right)$

Subject	Weight (kg)	Ratio
<u>MALES:</u>		
		0.528
		0.483
		0.532
		0.530
		0.510
		0.562
		0.514
		0.579
		0.505
		0.481
		0.514
		0.533
		0.523
		0.554
		0.562
		0.552
		0.556
		0.488
		0.562
		0.584
		0.514
		0.594
Average		0.536
<u>FEMALES:</u>		
		0.461
		0.519
		0.456
		0.519
		0.513
Average		0.483

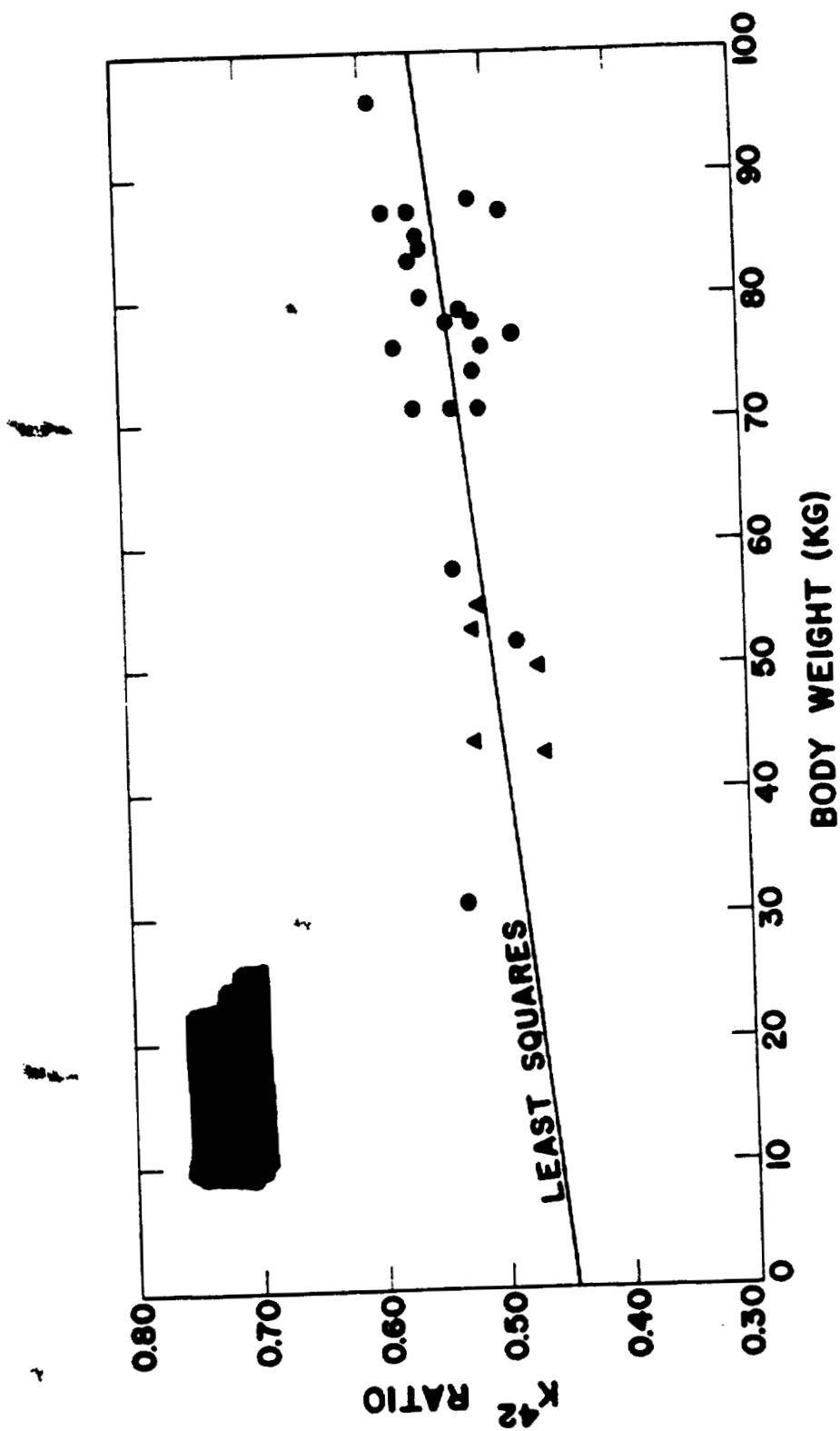


Fig. 1. Ratio of K^{42} counting rates in two energy bands (525 to 725 keV and 775 to 1275 keV) as a function of the subject's weight.

The standard deviation of the individual points about the computed line is 0.031, or 5.9 per cent of the mean value of R (0.526). If no dependence on weight is assumed, the standard deviation about the average value of R is 6.8 per cent. It is apparent that the weight dependence is indeed small, the standard deviation being reduced by only 13 per cent when correction for weight is made. However, the random variance is rather large.

DISCUSSION

The utility of this method depends on the magnitude of the Cs^{137} error introduced by the uncertainty of the ratio. The counting efficiency of K^{40} in the 525- to 725-Mev band is 1.24 c/min per gram for a 70-kg subject with our crystal. With a body content of 140 g (average adult male), this corresponds to 174 c/min. If this quantity were predicted by using the ratio R, the 6 per cent uncertainty in the latter would produce a ± 10 c/min error in the former. The Cs^{137} efficiency in this energy band is 13.3 c/min per nanocurie; therefore, this error corresponds to an 0.8 nanocurie error (10) in the Cs^{137} burden. If the body burden were 7 nanocuries (about the present average), this error is 11 per cent.

Since the standard deviation of the frequency distribution of Cs^{137} in the population is about 30 per cent (4),

an error of 11 per cent on individual subjects is negligible in studies in which large numbers of persons are measured to determine the population average. Also for repeated measurements of the same individuals to determine temporal changes, R will presumably not change and a consistent error will not affect the evaluation of the relative changes with time. It would seem, therefore, that this method of correction for potassium would be useful in those cases in which complete computer analyses of the spectra are not possible.

REFERENCES

- (1) C. E. Miller, Argonne National Laboratory, private communication.
- (2) C. J. Maletskos, Massachusetts Institute of Technology, private communication.
- (3) P. N. Dean, Experimental Technique for High Precision Calibration of Whole-Body Counters: Application to a 4 π Liquid Scintillator and a Large Sodium Iodide (Tl) Crystal Spectrometer, presented at the Northwestern University Medical School, Second Symposium on the Radioactivity of Man, Chicago, Illinois (September 5-7, 1962).
- (4) E. C. Anderson and W. H. Langham, Cesium¹³⁷ Levels in United States Powdered Milk and in the Population: Summary Report, in manuscript (1963).

Computer Programs for Analyzing Data (P. N. Dean)

INTRODUCTION

Several computer programs have been written to aid in analyzing data. This was done in an effort to make data analysis faster, more accurate, and more economical. All programs were written in FORTRAN II for use with the IBM 7090 of the Los Alamos Scientific Laboratory's Computing Center. The Center operates the computers under what is called the Monitor System. One merely delivers his program and data cards to the Center, which then runs batches of problems on the computer several times during the day. Under this system, the time delay between delivering a problem to the Computing Center and receiving the output (printed sheets, film, cards) is about 2 to 3 hours.

METHODS AND RESULTS

Program Number 1 (HAV-8)

This program is the eighth version of the Humco Average program. This version was written to investigate optimum counting times for maximum statistical accuracy using Humco II. The program uses the standard Humco II data card with 6 counting channels. To generate the test data, the counter is operated continuously, punching a data card at

predetermined intervals of 10 to 500 seconds. The program reads in all data cards and divides them into groups of arbitrary size (for example, 4). It averages these 4 cards for each channel and gives the average count rate in each channel with the observed standard deviation from the group mean. It then separates the averages into sets of 4 and averages them, effectively multiplying the counting time by a factor of 4. It continues this operation until fewer than 4 averages remain. An example is shown in Table 1, which shows the analysis of the background stability of Humco II. This problem arose in attempting to determine the optimum counting time to obtain the maximum precision in repeated measurements of the total potassium in an individual. The analysis shows that the precision of a single determination is limited to about 0.7 per cent by background fluctuations with the optimum counting time of 30 minutes.

Program Number 2 (SUM-1 and SUM-2)

These two programs are the same except for input card format. One is written for Humco II data cards, and one is written for LASAC III data cards. These programs are simply data manipulating programs, designed to give the experimenter a preliminary look at his data in a convenient form before any attempt at data analysis with other programs. They read

TABLE 1. LIMITATION OF POTASSIUM PRECISION BY BACKGROUND INSTABILITY ON HUMCO II

Serial No.	Number of Determinations	Duration of Test	Number of Averages	Time	Standard Deviation σ_1 as Per Cent of Background		σ_1 Adult Potassium (per cent)
					Statistical	Observed	
[REDACTED]	2836	16 days	709	8 min	0.26	0.24	1.0
				33 min	0.13	0.15	0.63
				2.2 hr	0.065	0.21	0.90
				8.8 hr	0.032	0.25	1.0
[REDACTED]	480	13 hr	120	1.7 min	0.52	0.49	2.1
				7 min	0.26	0.25	1.1
				27 min	0.13	0.16	0.7
[REDACTED]	484	13 hr	121	1.7 min	0.53	0.49	2.1
				7 min	0.27	0.27	1.1
				27 min	0.13	0.27	1.0

in the data cards, subtract backgrounds from subject and standard data cards, and list the results in a table with headings. An example is shown in Table 2. The program can also be instructed to sum any combination of the data channels and to print this result also.

Program Number 3 (PBR-2 and PBR-3)

As with the SUM programs, these differ only in the input data card format. These programs compute per cent biological retention as well as effective retention. They subtract backgrounds from standard and subject data cards, correct subject count rates for changes in counter efficiency by comparing the standard count rates on the initial day of the experiment with count rates on any successive day corrected for decay (ratio), and compute per cent biological retention (PBR),

$$PBR = \frac{(S/A)_o}{(S/A)_n},$$

where S is the subject's count rate, A is the standard count rate, o is the initial day of the experiment, and n is any day after beginning the experiment. An example of the output of this program is shown in Table 3.

TABLE 2. OUTPUT LISTING OF PROGRAM SUM-2 APPLIED TO DATA FROM A SMALL ANIMAL COUNTER

CL	ISER	Z	AN	TIME	ISO. ID	ZERO DATE	WGT	CT	RT	TI ID	CH1	CH2	CH3	CH4	SUM	COUNT DATE
29	1169	55	0	1018	5100	22563	0	100	5	0	45.52	11.92	6.93	8.96	11.92	4/ 3/63
28	1168	55	0	1016	5100	22563	0	100	5	0	7211.60	2224.79	421.51	19.34	2224.79	4/ 3/63
20	1162	55	1	1003	5100	22563	429	100	5	0	1555.95	642.95	107.33	3.04	642.95	4/ 3/63
20	1163	55	2	1005	5100	22563	396	100	5	0	1366.33	627.19	109.76	3.21	627.19	4/ 3/63
20	1164	55	3	1009	5100	22563	360	100	5	0	1304.70	574.20	98.76	3.19	574.20	4/ 3/63
20	1165	55	4	1010	5100	22563	390	100	5	0	1403.17	584.21	93.35	2.98	584.21	4/ 3/63
20	1166	55	5	1012	5100	22563	410	100	5	0	1244.94	580.85	101.08	3.04	580.85	4/ 3/63
20	1167	55	6	1014	5100	22563	370	100	5	0	1289.42	589.92	95.88	3.02	589.92	4/ 3/63

CL - class number; 29 - background; 28 - standard; and 20 - subject.

ISER - serial number of count.

Z - atomic number of tracer.

AN - animal number.

TIME - time of count.

ISO ID - isotope identification.

ZERO DATE - date of administration of tracer.

WGT - weight of animal in grams.

CT - counting time in seconds.

RT - route of administration.

TI ID - tissue identification.

CH1 - CH4 - net counts accumulated.

SUM - summation of preselected channels.

COUNT DATE - date of count.

TABLE 3. OUTPUT LISTING OF PROGRAM PBR-2 APPLIED TO DATA FROM SMALL ANIMAL COUNTER

DATE OF COUNT 3/20/63									
ISOTOPE CODE	COUNT RATE	RATIO TO INI. DAY	ROUTE OF ADM.	TISSUE TYPE	ATOMIC NUMBER	INITIAL DATE 2/25/63			
15	5021.30	1.131	5	0	55	1000			
CL	SERIAL NUMBER	ANIMAL NUMBER	WEIGHT (GM)	TIME OF COUNT	ELAPSED TIME (DAYS)	PER CENT BIOL. RET.	SUBJECT CT. RATE	COUNT TIME (SEC)	
20	935	1	365	1042	23.0	21.445728	1188.93	100	
20	936	2	380	1044	23.0	18.936160	991.30	100	
20	937	3	373	1046	23.0	21.209635	1149.70	100	
20	938	4	368	1048	23.0	23.578080	1353.24	100	
20	939	5	375	1049	23.0	19.631703	1165.97	100	
20	940	6	390	1051	23.0	21.591542	1258.73	100	
0	0	0	0	0	0.	21.065475	1184.65	0	

Program Number 4 (RTW-2)

This is a program similar to the PBR programs and computes retention, elapsed time, and a weighting factor based on counting statistics. It is, however, written for use in multiple tracer studies (in this case, 2). Also, it does not compute per cent biological retention, only effective retention. An example of a multiple tracer experiment using Zr^{95} and Zn^{65} is shown in Table 4.

Program Number 5 (MWt-1)

This is a program written to compute the molecular weight of the DNA molecule using data from the analytical ultracentrifuge. The method of computation is discussed thoroughly in another part of this report.

Program Number 6 (IQ-2)

This program is written to compute isotope quantity. It is a quantitative program written to be used in resolving complex gamma spectra as measured with a multichannel pulse height analyzer. It works as follows. A "library" containing accurate spectra of each component of the sample is required. A series of "i" equations is then generated:

$$Y_i = \sum_j a_j E_{ij},$$

TABLE 4. OUTPUT LISTING FROM PROGRAM RTW-2 APPLIED TO DATA FROM SMALL ANIMAL COUNTER

DAY OF COUNT 5/29/63					INITIAL DATE 5/14/63		
ISOTOPE CODE	COUNT RATE	RATIO TO INI. DAY	ROUTE OF ADM.	TISSUE TYPE	CHANNELS SUMMED		
SR-85	3561.83	0.988	5	0	12		
ZN-65	3936.91	0.987					
SERIAL NUMBER	ANIMAL NUMBER	WEIGHT (GM)	TIME OF COUNT	ELAPSED TIME (DAYS)	SR-85 CORRECTED RATE (CPS)	ZN-65 CORRECTED RATE (CPS)	COUNT TIME (SEC)
20 1926	1	384	849	14.9	1417.9	1407.8	100
20 1927	2	347	851	14.9	1746.0	1676.3	100
20 1928	3	360	853	14.9	1401.2	1532.7	100
20 1929	4	378	855	14.9	1563.1	1572.0	100
20 1930	5	365	857	14.9	1636.3	1779.3	100
20 1931	6	413	859	14.9	1760.0	1690.0	100
0 0 0	0	0	0	0.	1587.4	1609.7	0

where Y_i is the count rate in channel i , a_j is the fraction of isotope j present in the sample, and E_{ij} is the count rate in channel i from a known amount of isotope j .

The program solves for the a_j using the least squares technique. An example of the output listing of the program is shown in Table 5. Also available in a printed form are the input data, consisting of library spectra and sample spectrum, the computed spectrum, and the residual spectrum. The output data are also available plotted on 35-mm film. Figure 1 shows an actual plot by the computer of the sample spectrum as measured and as computed. Figure 2 shows the residual spectrum, which should show an average of zero and no pronounced peaks to indicate an accurate analysis.

An additional program is now being written which will be used to analyze complex gamma-ray spectra when the components of the spectra are not known.

TABLE 5. OUTPUT LISTING OF PROGRAM IQ-2 APPLIED TO DATA FROM MULTICHANNEL PULSE HEIGHT ANALYZER

FIRST CHANNEL USED = 21
 LAST CHANNEL USED = 100
 TOTAL CHANNELS = 80
 WEIGHTING FACTOR USED = 1/Y

WEIGHTED VARIANCE = 3.5985523E CO
 UNWEIGHTED SUM OF SQUARES OF THE DEVIATIONS = 2.2787844E 06

THE FOLLOWING BACKGROUND WAS SUBTRACTED FROM THE LIBRARY.
 OVERNIGHT BKGC. 1 GAL. WATER 21NOV63 2.00MEV 100CH 1844457

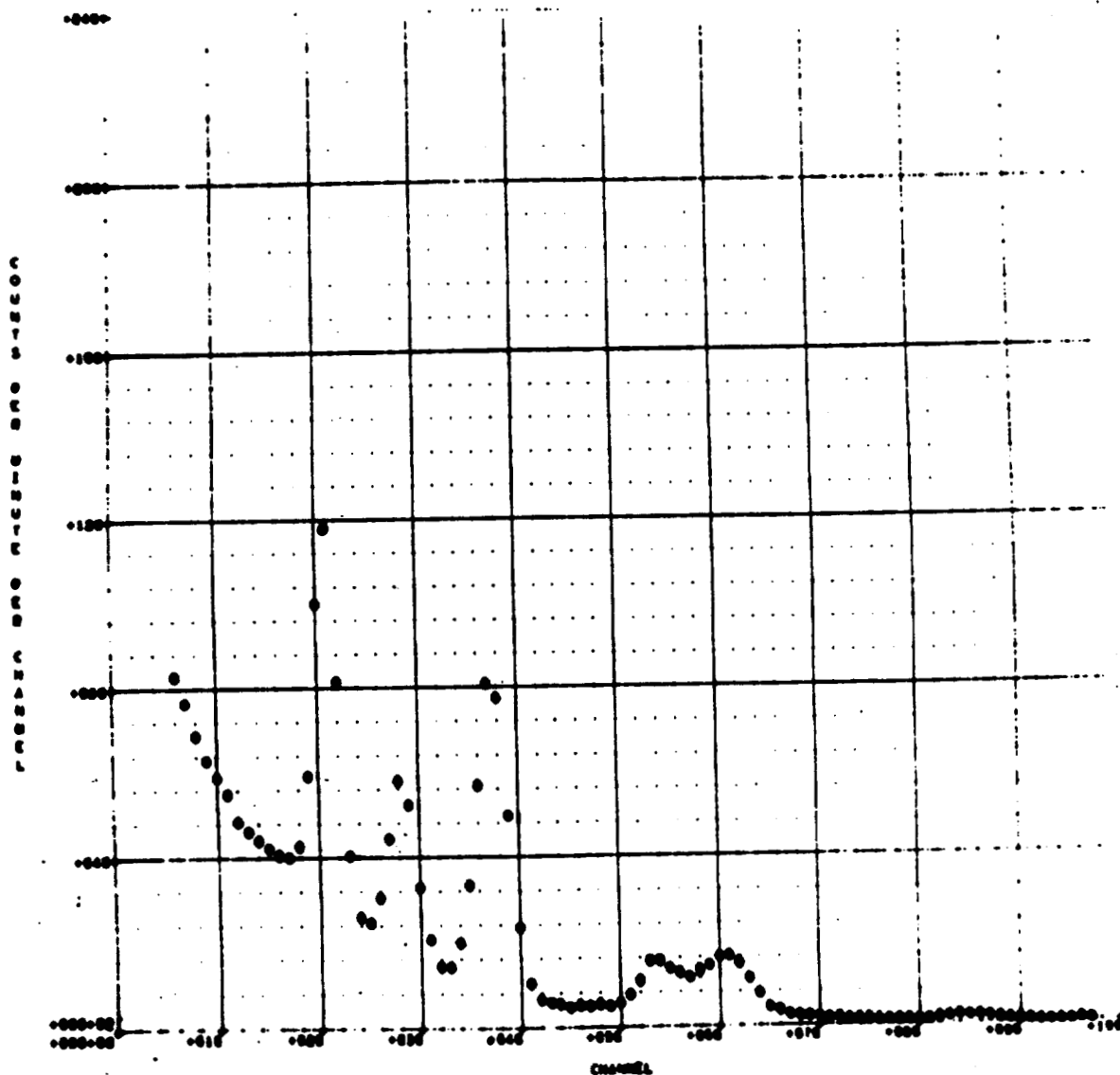
THE LIBRARY CONSISTS OF THE FOLLOWING ISOTOPES.

			COUNT TIME	ACC-1 TOTAL	SUM OF 100 CH
KCL	100GMC IN 1 GALLON WATER	2.00MEV 100CH	60.00	-0.	60050.
CS-137	C.10 UC IN 1 GALLON WATER	2.00MEV 100CH	4.00	-0.	53764.
I-131	C.12 UC IN 1 GALLON WATER	2.00MEV 100CH	4.00	-0.	56306.
	OVERNIGHT BKGC. 1 GAL. WATER 16MAY63 2.00MEV 100CH	1844419	1000.00	-0.	596662.

SAMPLE

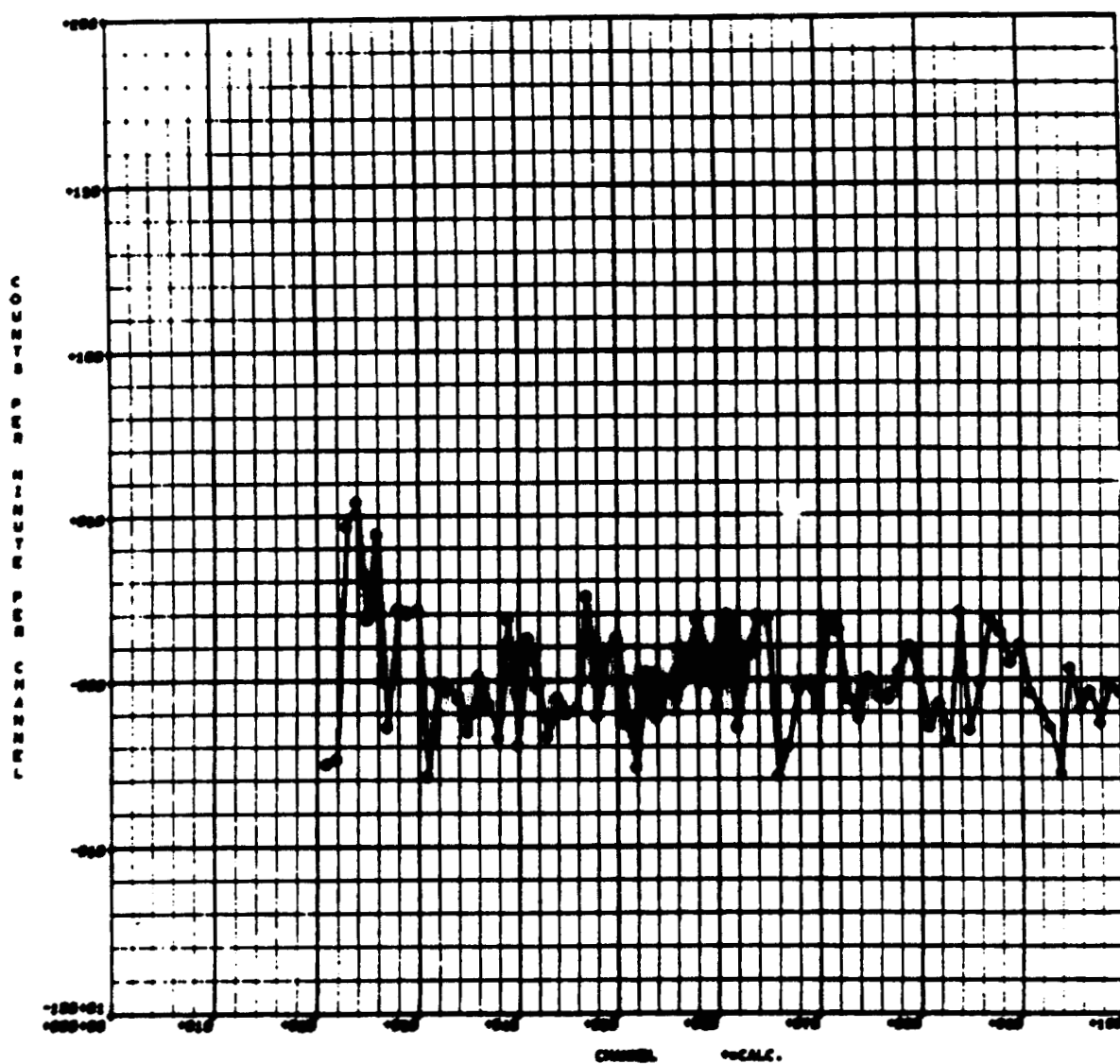
MILK PURCH. 22MAY63 COUNTED 23MAY63 2.00MEV 100CH 1844526 900.00 -0. 609094.

ISOTOPE	FRAC. OF LIB. SPECTRUM PRES.	STANDARD DEVIATION
KCL	2.1507E 00	3.3826E-C1
CS-137	4.5137E-C1	2.5245E-C2
I-131	5.9361E-02	1.9187E-C2
	8.9064E-01	1.3406E-C2



10-2 EXP. EQUAL PARTS CO-60, Na-22, Mn-54, Cs-137, Sr-90

Fig. 1. Computed and input spectra from an analysis of a mixture of Co^{60} , Na^{22} , Mn^{54} , Cs^{137} , and Sr^{85} (O = input data, and + = calculated spectrum).



MILK PUNCH. 10APR63 COUNTED 10APR63 2.00EV 100CH 1000000

Fig. 2. Residual spectrum from an analysis of a milk sample for Cs^{137} , K^{40} , and I^{131} .

Cesium¹³⁷ Body Burdens of Control Subjects (E. C. Anderson
and A. E. Hargett)

INTRODUCTION

Measurements on a group of control subjects previously reported (1) have been continued into 1963 and show a second sharp rise in the Cs¹³⁷ levels beginning in November 1962.

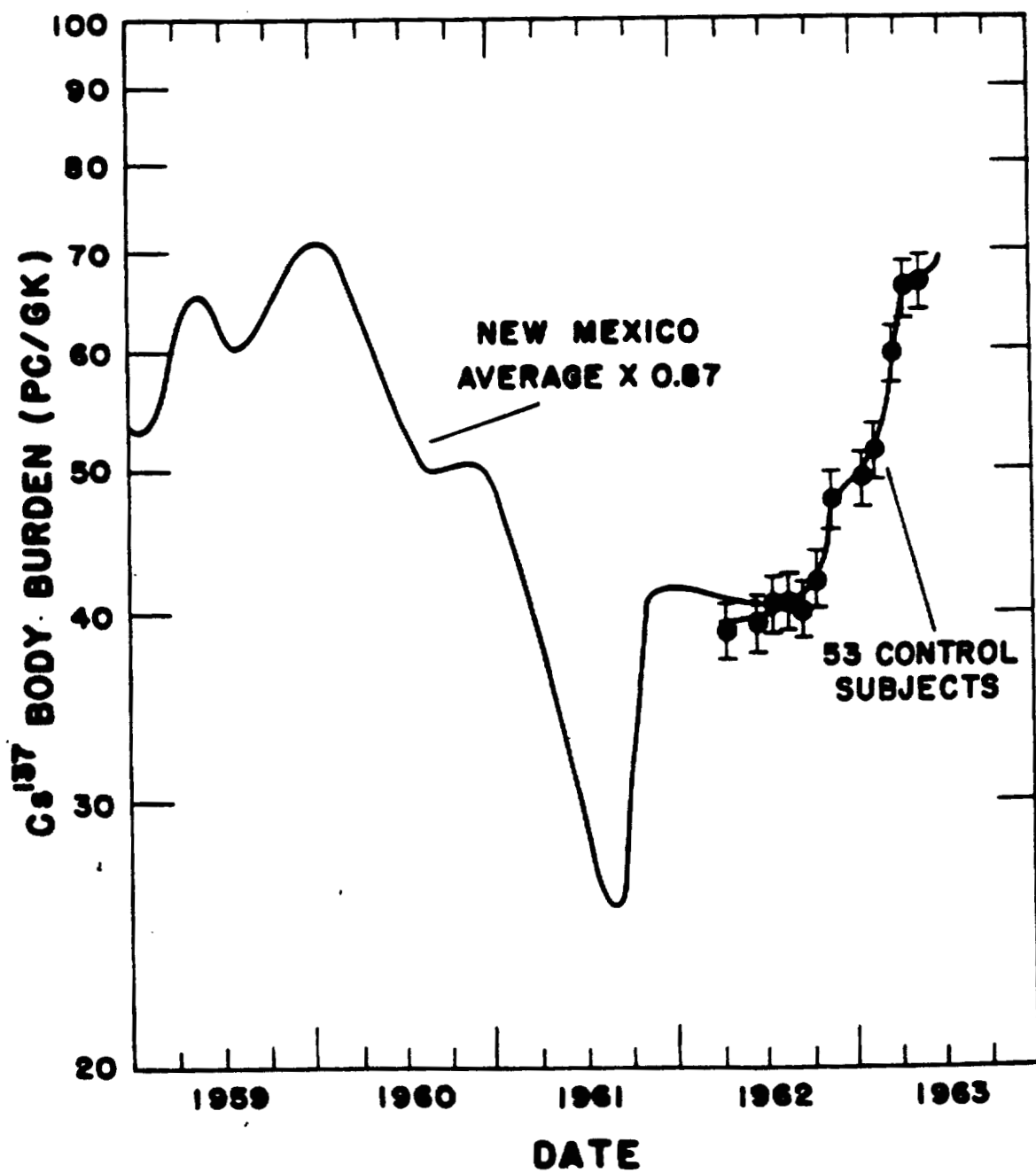
METHODS AND RESULTS

Monthly averages for two control groups are given in Table 1 for the period January 1962 through March 1963. The monthly controls are a group of 59 subjects measured once a month; on the average, 53 of these subjects are available in a given month. The other group consists of 12 subjects measured weekly. Entries marked with an asterisk are measurements made with Humco I (January through May 1962); the remainder are Humco II measurements (April 1962 through May 1963). The calibration of the new counter is 0.87 that of the original and is believed to be more reliable since it is based on more extensive in vivo calibrations. In Fig. 1, the new data on monthly controls are compared with previous results (1), which are multiplied by 0.87 to normalize them to the new calibration.

TABLE 1. CESIUM¹³⁷ BURDENS OF NEW MEXICO SUBJECTS

Month	Monthly Controls		Weekly Controls	
	Number of Subjects	Average Cs ¹³⁷ (pc/g K)	Number of Measurements	Average Cs ¹³⁷ (pc/g K)
<u>1962</u>				
January	56	47.7 \pm 1.4*	32	47.1 \pm 1.7*
February	55	44.9 \pm 1.8*	21	41.4 \pm 1.6*
March	55	42.6 \pm 1.5*	23	41.3 \pm 2.1*
April	58	46.5 \pm 1.6*	18	39.3 \pm 1.6*
	46	38.8 \pm 1.5	6	39.6 \pm 2.4
May	58	45.5 \pm 1.3*	28	45.3 \pm 1.2*
			10	41.0 \pm 2.1
June	56	39.2 \pm 1.0	45	39.7 \pm 1.1
July	54	40.6 \pm 1.2	83	40.4 \pm 0.8
August	52	40.5 \pm 1.4	61	36.6 \pm 0.8
September	59	40.0 \pm 1.0	19	38.5 \pm 1.4
October	57	42.2 \pm 1.2	19	43.4 \pm 2.7
November	49	47.4 \pm 1.8	14	54.3 \pm 5.3
<u>1963</u>				
January	57	49.1 \pm 1.5	28	52.7 \pm 2.1
February	51	51.2 \pm 1.7	22	53.4 \pm 2.5
March	52	59.8 \pm 2.4	22	61.0 \pm 3.2
April	47	65.7 \pm 2.6	26	64.0 \pm 2.7
May	45	66.3 \pm 2.7	32	63.8 \pm 2.2

* Humco I data; remainder are Humco II measurements.



DISCUSSION

In 1962 as in 1961, there was a sharp increase of Cs¹³⁷ beginning in the fall of the year. However, in 1963 the rise continued and by April the levels approached the highest values previously observed at the beginning of 1960. There was little or no increase in May.

REFERENCE

- (1) E. C. Anderson and A. E. Hargett, Los Alamos Scientific Laboratory Report LAMS-2780 (1962), pp. 139-143.

Retention of Cesium¹³⁷ by Adults (M. A. Van Dilla and M. J. Fulwyler)

INTRODUCTION

In October 1962, an accident at The Lovelace Foundation resulted in a Cs¹³⁷ inhalation exposure to several laboratory workers. Maximum body burdens of a few tenths of a micro-curie were incurred; therefore, no health hazard was involved. However, it seemed useful to follow the retention of Cs¹³⁷ in these subjects, since data on humans are scarce, especially via the inhalation route. When possible, the subjects were measured in both Humco II and the human spectrometer to aid the intercalibration of these two quite different instruments.

METHODS AND RESULTS

The subjects were measured for 5 to 10 minutes in the spectrometer and for 3-1/3 minutes in Humco II. The results are summarized in Fig. 1 for 3 subjects with the highest Cs¹³⁷ burdens and who were available for counting in the months following exposure. Note that initially there was a rise in body burden, presumably due to incomplete cleanup of the area after the accident and re-exposure to Cs¹³⁷. However, subsequently the body burden fell, both counters giving very similar results. The indication at the present writing is

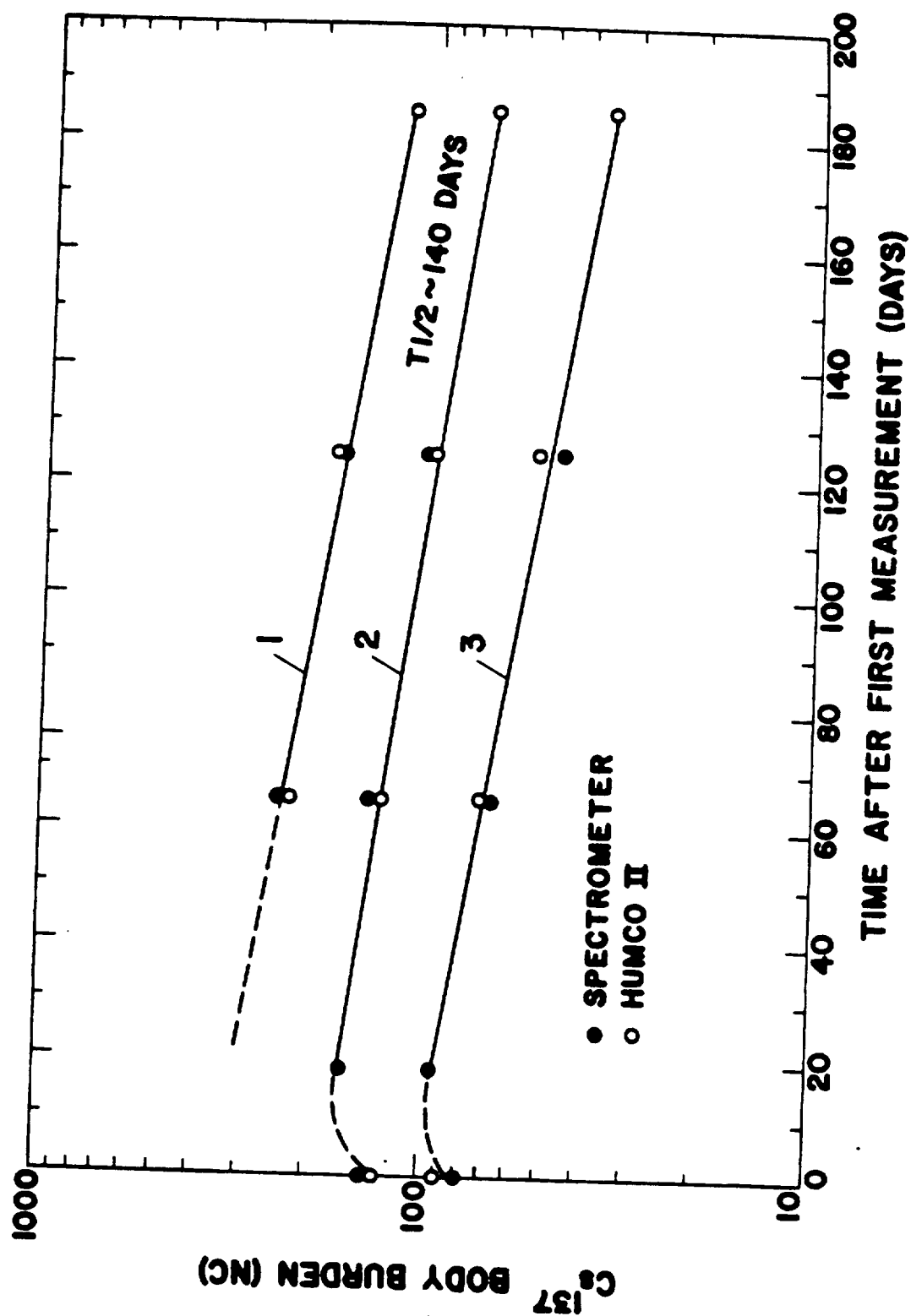


Fig. 1. Retention of Cs^{137} by 3 laboratory workers after inhalation exposure.

that the material is being released from the body exponentially with a biological half-life of about 140 days, in agreement with earlier work of Richmond (1).

REFERENCE

- (1) C. R. Richmond, J. E. Furchner, and W. H. Langham,
Health Phys. 8, 201 (1962).

Metabolism of Radioiodine in Children and Adults Using Small (Nanocurie) Doses (M. A. Van Dilla and M. J. Fulwyler)

INTRODUCTION

To estimate properly the dose to the human thyroid resulting from ingestion of radioiodine, it is necessary to know the retention of iodine by the thyroid as a function of time. In the case of children, there is a scarcity of such data. Recently it has been shown possible to measure much less than 1 nanocurie of fallout I^{131} in people (1,2). These facts have prompted the present experiments to accumulate radioiodine metabolism data for children using doses in the 10-nanocurie range.

One of the problems encountered in measuring thyroid radioiodine is the uncertainty of thyroid depth in neck tissue. This uncertainty can lead to error due to unknown attenuation of radiation by overlying tissue and unknown thyroid-to-detector geometry. Work at very low levels requires the detector close to the thyroid, increasing geometry error. We have attempted to correct for these errors using a double-tracer method (I^{125} and I^{131}) described below. Preliminary results on adults and children are given; so far, no differences in uptake or biological half-life have been observed.

METHODS

The method uses a mixture of two iodine isotopes: I^{125} (60-day half-life, 27-kev X rays) and I^{131} (8-day half-life, 364-kev gamma rays). This mixture constitutes a tracer with two abundant photon yields (27 and 364 kev) widely separated in energy. Because of this energy separation, these photons have very different attenuation (i.e., half-thicknesses of 2.2 and 6.3 cm of water, respectively); the relative attenuation gives a measure of thyroid depth. To establish this relationship, a polystyrene neck mockup similar to the Oak Ridge Institute of Nuclear Studies standard (3) and shown in Fig. 1 was constructed. Overlying tissue was simulated by layers of lean beefsteak pressed to uniform thickness and frozen to the contour of the neck mockup. These uniform "tissue" layers were added to obtain a relationship between X/γ^* and thickness of overlying tissue, and the corresponding correction factor. The results are given in Figs. 2 and 3, from which can be determined both depth and the factor needed to correct the observed count rate to zero overlying tissue.

*More precisely, the ratio of photopeak areas for a source containing equal activities of I^{125} and I^{131} . If unequal activities are employed in a given experiment, correct the observed X-ray photopeak area by the factor $1 - (k - 1)(0.0350)$, where k = the ratio of I^{131} activity to I^{125} activity administered.

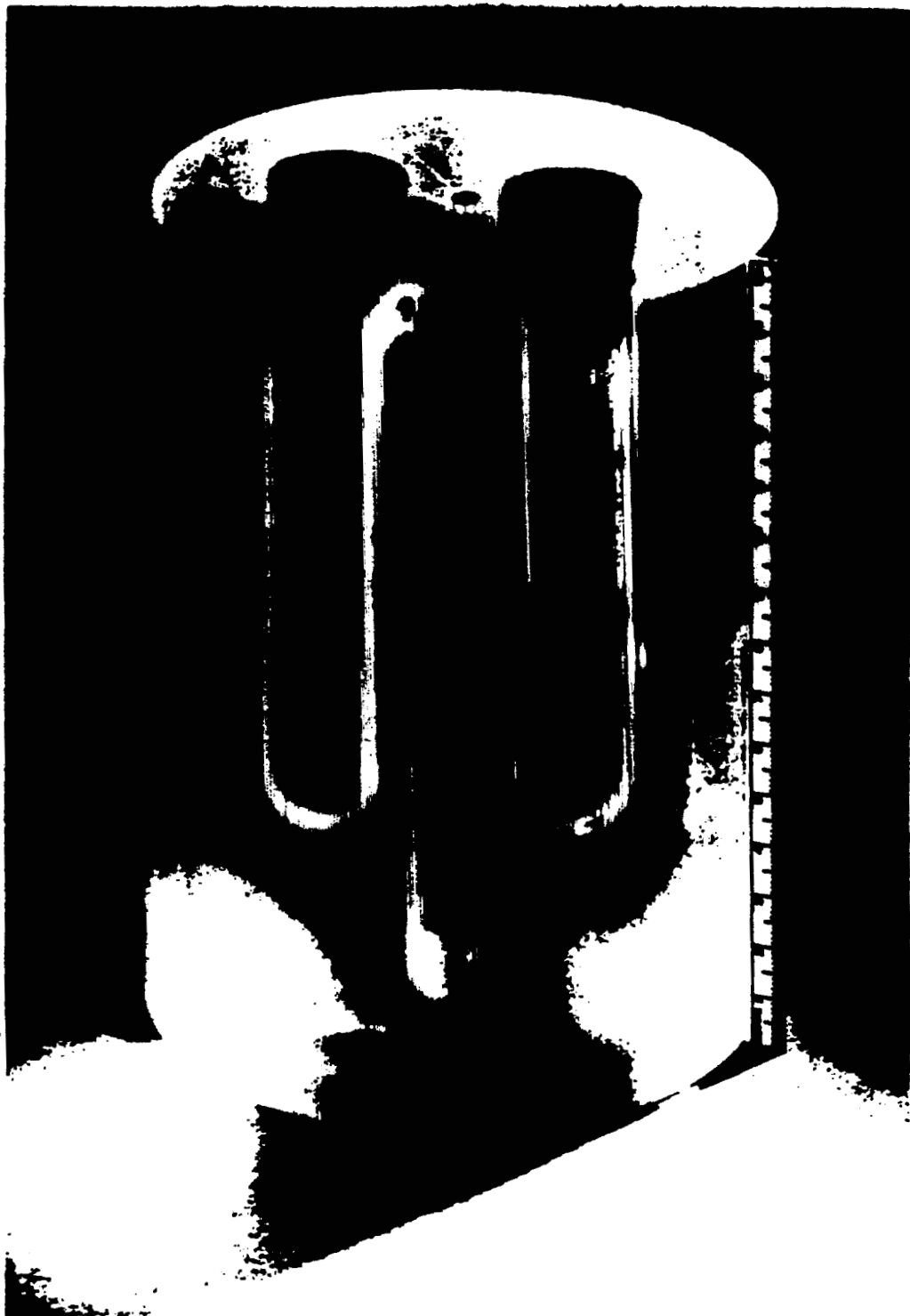


Fig. 1. Polystyrene neck mockup.

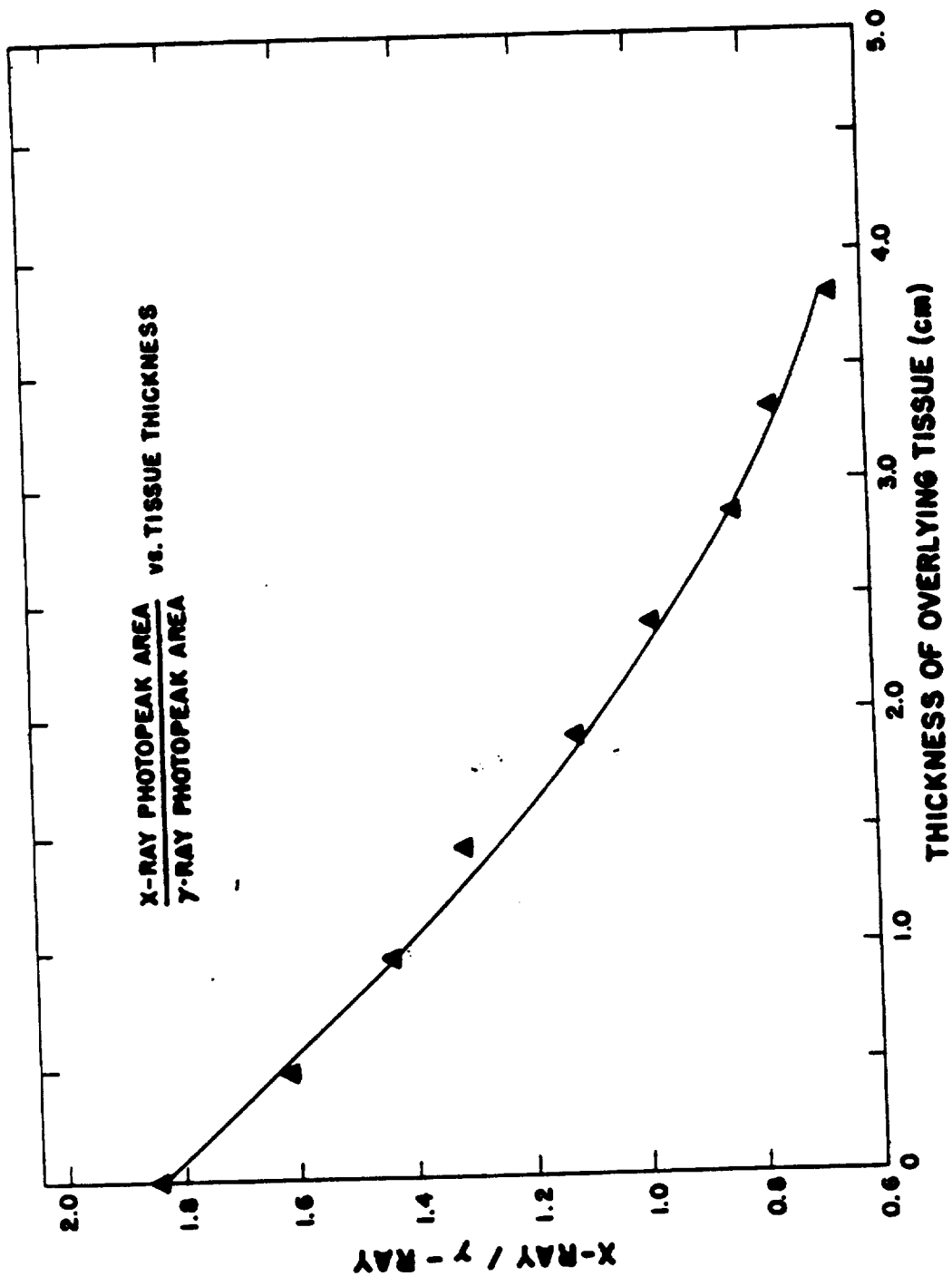


Fig. 2. Relationship of $\frac{\text{X-ray photopeak area}}{\gamma\text{-ray photopeak area}}$ to thyroid depth in neck tissue for equal activities of I^{125} and I^{131} .

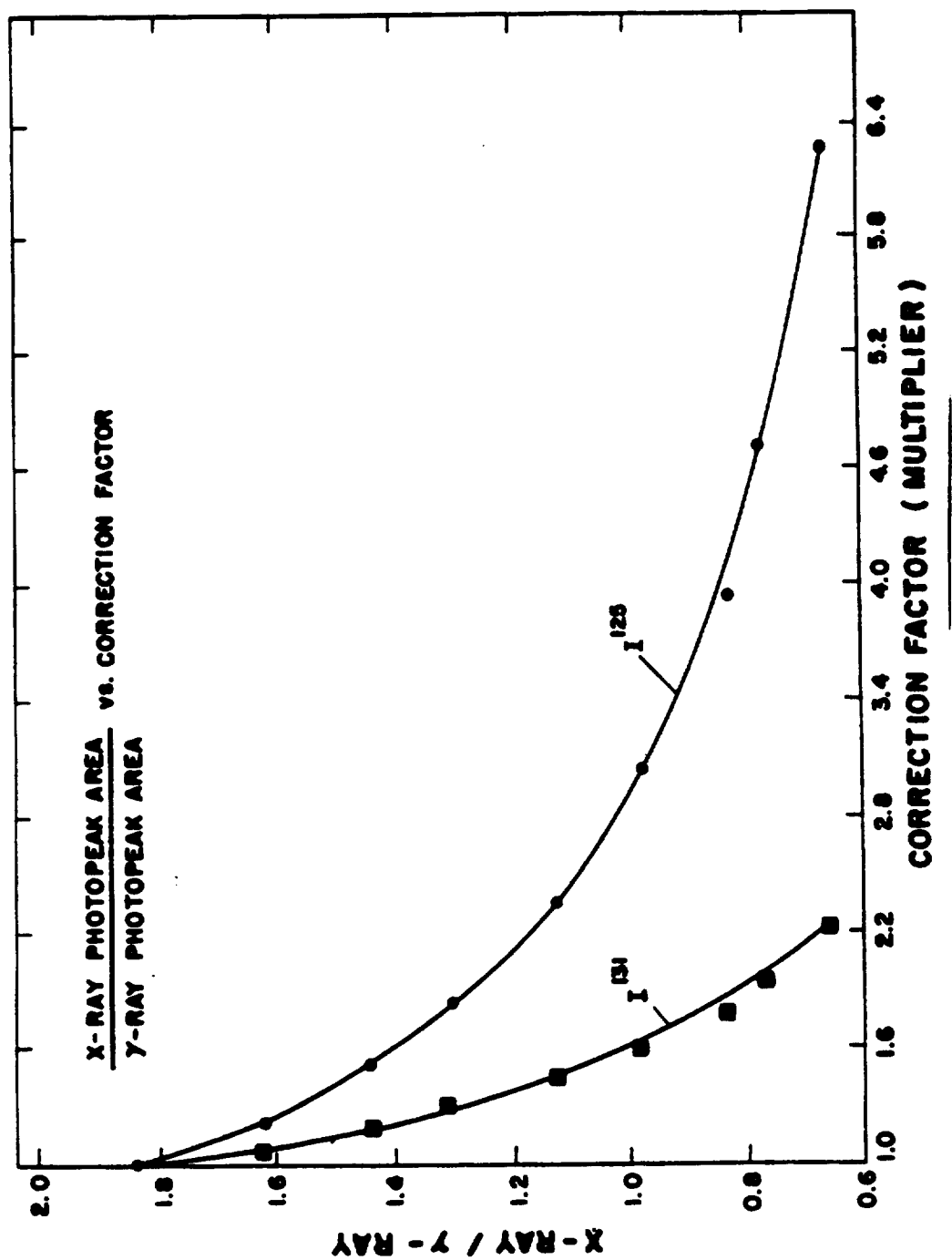


Fig. 3. Relationship of $\frac{\text{X-ray photopeak area}}{\gamma\text{-ray photopeak area}}$ to correction factor for equal activities of I^{125} and I^{131} .

The detector chosen was an 8 x 4-in. NaI crystal (with a 0.005-in. entry window to minimize attenuation of the soft X rays) mounted in a steel room as a whole-body spectrometer. To account for room and subject (non-thyroid) background, a thyroid eclipsing lead shield, as described by Brucer (3), is used. The shield is placed between the crystal and the subject's neck, eclipsing the thyroid area from view of the crystal (Fig. 4). The dimensions are 4 x 4 x 1/2 in. for adults and 3 x 3 x 1/2 in. for children.

The subject reclines in a tilting chair so that the head is tipped back fully exposing the thyroid area. During the thyroid count, neck-to-crystal distance is maintained constant by a Lucite spacer rod 3-1/4 in. long fixed to the center of the crystal (Fig. 5). The crystal is positioned so that the spacer rod lightly touches the subject's neck. Counting children in the age group of 4 to 9 years is complicated by the need to keep them still during the 15-minute count. To attract and to hold their attention, a small Sony television set is mounted above the crystal in such a way that good viewing requires that the head be kept in the desired position (Fig. 6). This has proven very successful, although occasionally it is difficult to remove the child during a particularly fascinating cartoon. With this arrangement, considerably longer counting times appear to



Fig. 4. Subject in tilting chair during background count (with lead shield).



Fig. 5. Subject in tilting chair during thyroid count (no lead shield).

1055667



Fig. 6. Subject in tilting chair viewing television.

be entirely feasible. During the measurement, an adult remains in the steel room shielded from the crystal by a steel partition. With the aid of a mirror, he is able to see the Lucite spacer rod lightly touching the child's neck. If the child moves, a reminder to sit still and to watch the T. V. is usually adequate.

EXPERIMENTAL RESULTS

An experiment on a group of 6 normal adults preceded the experiment on children. The I^{131} dose administered was 17.3 nanocuries. Difficulties were encountered with the carrier-free I^{125} solution and hence this dose is not certain; 6.2 nanocuries is the best estimate. Unfortunately, this makes the X/ γ ratios of little value, and an uptake correction cannot be derived from the data. However, the biological half-lives determined from the two isotopes are valid and should agree. This was found to be the case. The results are summarized in Table 1. It is to be noted that these subjects all have similar (except [redacted] and normal uptakes, while the biological half-times vary considerably. According to Lushbaugh et al. (4), the normal biological half-time is about 90 days, so that the values for subjects [redacted] and [redacted] are larger than normal, while the value for subject [redacted] is quite small. It is interesting that subject [redacted] has a

TABLE 1. RADIOIODINE METABOLISM IN SIX ADULTS

Sub- ject	Age (yrs)	Sex	Weight (kg)	Height (cm)	Uptake at 7 Days* (per cent)	T _{Bio} (days)	T _{Eff} (days)
		M			29	107	7.51
		M			23	∞	8.07
		M			23	> 200	7.76
		M			22	75	7.30
		M			26	98	7.46
		M			15	27	6.22

* Assumes 1.5 cm overlying tissue.

history of low EMR, which is consistent with his relatively low uptake and short biological half-time.

Having obtained reasonable results with adults, only the quantitative difficulty with the I^{125} stood in the way of extending the experiments to children. This problem was solved by adding 0.5 μ g NaI carrier to each dose and then measuring the dose actually ingested by each child. Eight children, ranging in age from 4 to 10 years, each received a nominal 11 nanocuries I^{125} and 15 nanocuries I^{131} oral dose, and 15-minute measurements (10 minutes with no shield and 5 minutes with lead shield) began the following day. It is planned to count 3 times weekly for 6 weeks, and then at less frequent intervals until the I^{125} peak dies away. At the present writing (June 6, 1963), we have about 2 weeks of data processed and summarized in Table 2. Note that uptakes are very similar to those for the adults. Thickness of overlying tissue is small in all cases, resulting in similar correction factors. Indications are that biological half-lives will be long compared to the 8-day physical half-life, and perhaps similar to adults. Thus far, no differences in radioiodine metabolism have been observed between children and adults.

TABLE 2. RADIOIODINE METABOLISM IN EIGHT CHILDREN

Sub- ject	Age (yrs)	Sex	Weight (kg)	Height (cm)	Overlying Tissue Thickness (cm)	Correc- tion Factor	Uptake at 7 Days (per cent)
[REDACTED]	[REDACTED]	F	[REDACTED]	[REDACTED]	0.45	0.92	22
[REDACTED]	[REDACTED]	M	[REDACTED]	[REDACTED]	0.50	0.91	23
[REDACTED]	[REDACTED]	F	[REDACTED]	[REDACTED]	0.82	0.86	27
[REDACTED]	[REDACTED]	F	[REDACTED]	[REDACTED]	0.73	0.88	21
[REDACTED]	[REDACTED]	M	[REDACTED]	[REDACTED]	0.90	0.85	18
[REDACTED]	[REDACTED]	F	[REDACTED]	[REDACTED]	0.75	0.87	19
[REDACTED]	[REDACTED]	M	[REDACTED]	[REDACTED]	0.80	0.86	9.5
[REDACTED]	[REDACTED]	M	[REDACTED]	[REDACTED]	0.53	0.91	11

REFERENCES

- (1) H. E. Palmer and F. Swanberg, Jr., Hanford Atomic Laboratory Report HW-SA-2612 (1962).
- (2) M. Eisenbud, Y. Mochizuki, A. S. Goldin, and G. R. Laurer, Science 136(3514), 370 (1962).
- (3) M. Brucer, Oak Ridge Institute of Nuclear Studies Report ORINS-19 (June 1959).
- (4) C. C. Lushbaugh, D. B. Hale, and C. R. Richmond, Los Alamos Scientific Laboratory Report LAMS-2526 (1960), p. 364.

Effect of Ashing Temperature on Cesium and Potassium Content
of Bone (M. A. Van Dilla, M. W. Rowe, and M. J. Fulwyler)

INTRODUCTION

In the summer of 1961, several hundred human bone ash samples were sent to this Laboratory by J. L. Kulp of the Lamont Geological Observatory, Columbia University. Each sample represented the total skeleton of cadavers obtained in 1953-1959 in the New York City area. A fraction of each sample was measured for Sr^{90} as part of a world-wide program on the distribution of Sr^{90} from fallout. Some were also analyzed for radium. Since Dr. Kulp's group had dropped out of this program and the samples were of considerable potential value for measurement of natural and fallout radioactivity and trace elements, they were transferred to this Laboratory. According to Dr. Kulp, ashing took place at 600 to 900° C, with no record for the individual samples; care was taken to avoid any contamination, and soft tissue was removed prior to the skeletal ashing process.

METHODS

Several of the samples were assayed for potassium and Cs^{137} using a 7-1/2 x 4-in. NaI gamma-ray spectrometer. The potassium results were of the right order of magnitude for bone, but the Cs^{137} results seemed much lower than expected.

We suspected that the ashing temperatures might be driving off appreciable Cs^{137} and perhaps potassium too. Luckily, several long bones (2 femurs, 2 fibulas, and 2 tibias) from a beagle fed Cs^{137} chronically were available. These bones were chilled in liquid nitrogen, shattered into small fragments, mixed, and divided into 4 equal fractions. Each was assayed for Cs^{137} content, and then successive samples were ashed overnight in a muffle furnace at 600, 700, 800, and 900° C and finally remeasured. The results are shown in Fig. 1 and make clear that muffling must be done at lower temperatures than were used on the human skeletal samples to avoid loss of Cs^{137} .

It was not possible to detect natural potassium in these small bone samples; therefore, a much larger sample of locally purchased beef bone was measured. The gamma-ray spectrum showed the presence of 12.8-day $\text{Ba}^{140}/\text{La}^{140}$ from fallout; this was fortunate, since it eliminated the need for mockups to calibrate the K^{40} . That is, both barium and lanthanum are refractory (melting points 725 and 826° C, respectively, which are similar to the melting points of calcium and strontium) and so will be unaffected by the ashing procedure. Thus, the ratio of the 1.46-keV K^{40} gamma-ray peak to the 1.60-MeV La^{140} peak before and after ashing (corrected for radioactive decay) is the fraction of

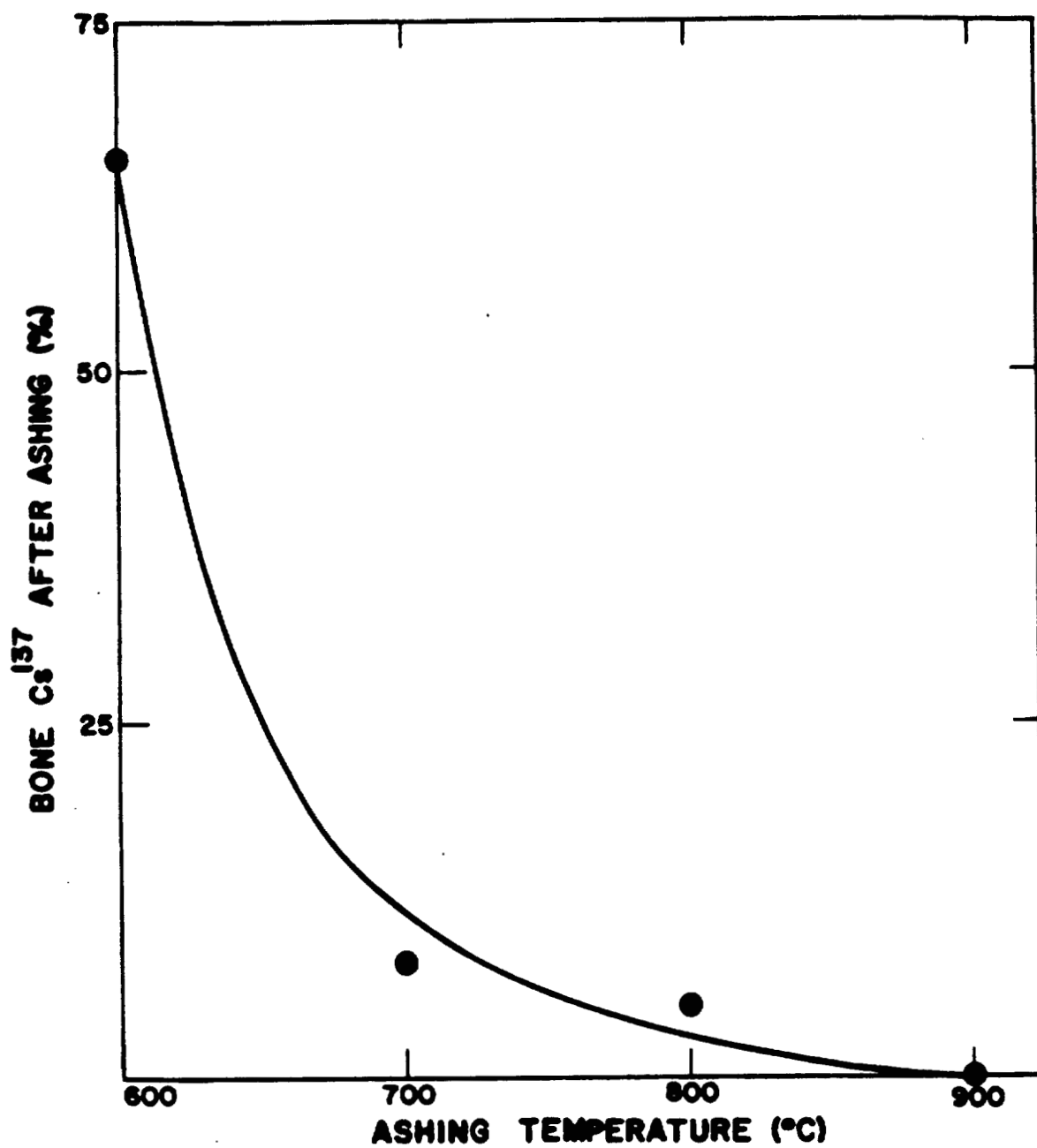


Fig. 1. Cesium¹³⁷ remaining in dog bone after ashing at 600 to 900° C.

potassium still in the sample after ashing. It was found that about 70 per cent of the potassium remained after overnight muffling at 600° C. At 900° C, only 56 per cent was left in the sample.* Thus, it is concluded that the Lamont human skeletal ash samples are of no value for determining the fallout Cs^{137} or natural potassium content of the human skeleton; however, natural radium and thorium contents will be unaffected by the relatively high muffling temperatures used and these data would be valuable. Some radium measurements on these samples have already been made by Kulp's group using the radon emanation method, but no thorium measurements whatsoever have been made. We plan to make such measurements using a gamma-ray coincidence spectrometer.

*This measurement was made a few months later, when there was too little $\text{Ba}^{140}/\text{La}^{140}$ to be useful. A more complicated mockup procedure was used.

Thermoluminescent Dosimetry with Activated Lithium Fluoride
(P. N. Dean and J. H. Larkins)

INTRODUCTION

In October 1962, work was begun on the development of a thermoluminescent dosimeter. Two types of this material have been studied: Al_2O_3 and LiF . The material selected for our application was LiF powder, primarily because of its tissue-equivalence and ease in handling. A device has been constructed to heat the powder and to measure the amount of emitted light. The normal operating range of the instrument is 100 mrad to 50 rads. It can be extended at the upper end to 20,000 rads with minor changes. Dosimeter size is normally 100 mg of powder, contained in polyethylene tubing (1/16 in. in diameter by 1-1/2 in. in length).

METHODS AND RESULTS

The use of thermoluminescent materials to measure absorbed dose of ionizing radiations has been fairly extensively covered in the literature (1-6). Thermoluminescence is the emission of light by a substance upon being heated after previously being exposed to ionizing radiation. The amount of light emitted depends on the type of material used and the total amount of energy absorbed from the ionizing radiation. For a particular material, the amount of light emitted

is proportional to the rad dose absorbed. There are two methods of determining the dose absorbed by the powder. When the irradiated powder is heated, the light intensity is a function of temperature. A plot of intensity versus temperature, called the "glow curve," is shown in Fig. 1 for $\text{CaF}_2:3.0\% \text{ Mn}$ (5). Either the peak height (maximum intensity) or the total area under the curve (total light emitted) can be used as a measure of dose. As to be expected, the total light emitted is the more accurate indication of dose. The peak method depends too strongly on reproducible heating cycles.

Two types of thermoluminescent materials have been used here: Al_2O_3 and LiF . The Al_2O_3 , obtained from Controls for Radiation, Inc., was used first primarily to study the techniques involved in heating the powder and measuring the amount of emitted light. It was never seriously considered as the operating dosimeter because of its rather large energy-dependence and a number of low energy traps. The low energy traps result in a loss of stored energy at room temperature and slightly higher. The ideal material would have deep, stable traps. Figure 2 shows the "glow curve" from natural Al_2O_3 .

The material selected for routine use at this Laboratory was activated powdered LiF crystals obtained from

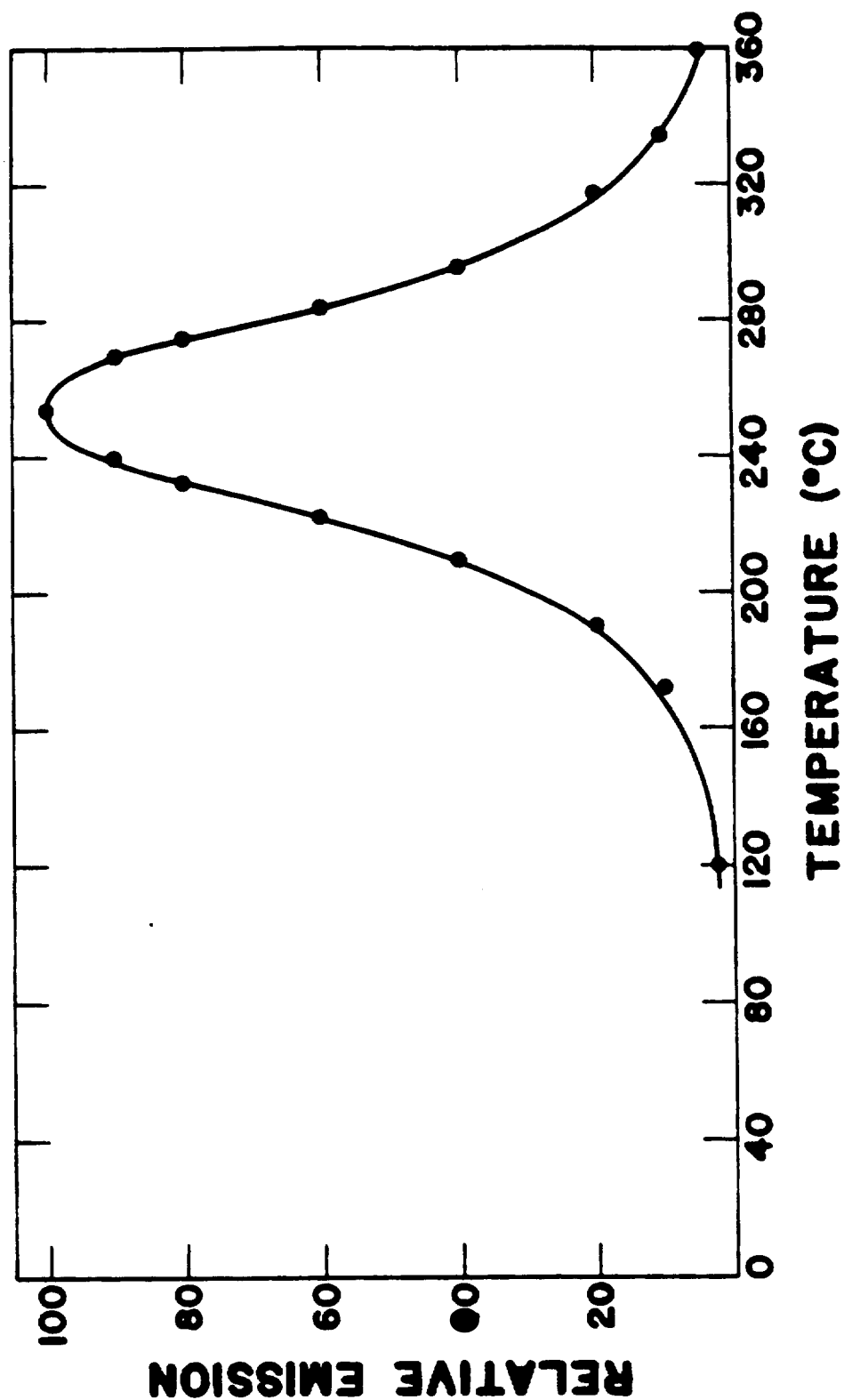


Fig. 1. Thermoluminescence of synthetic $\text{CaF}_2:7.0\% \text{ Mn}$ [after Ginther and Kirk (5)].

1055680

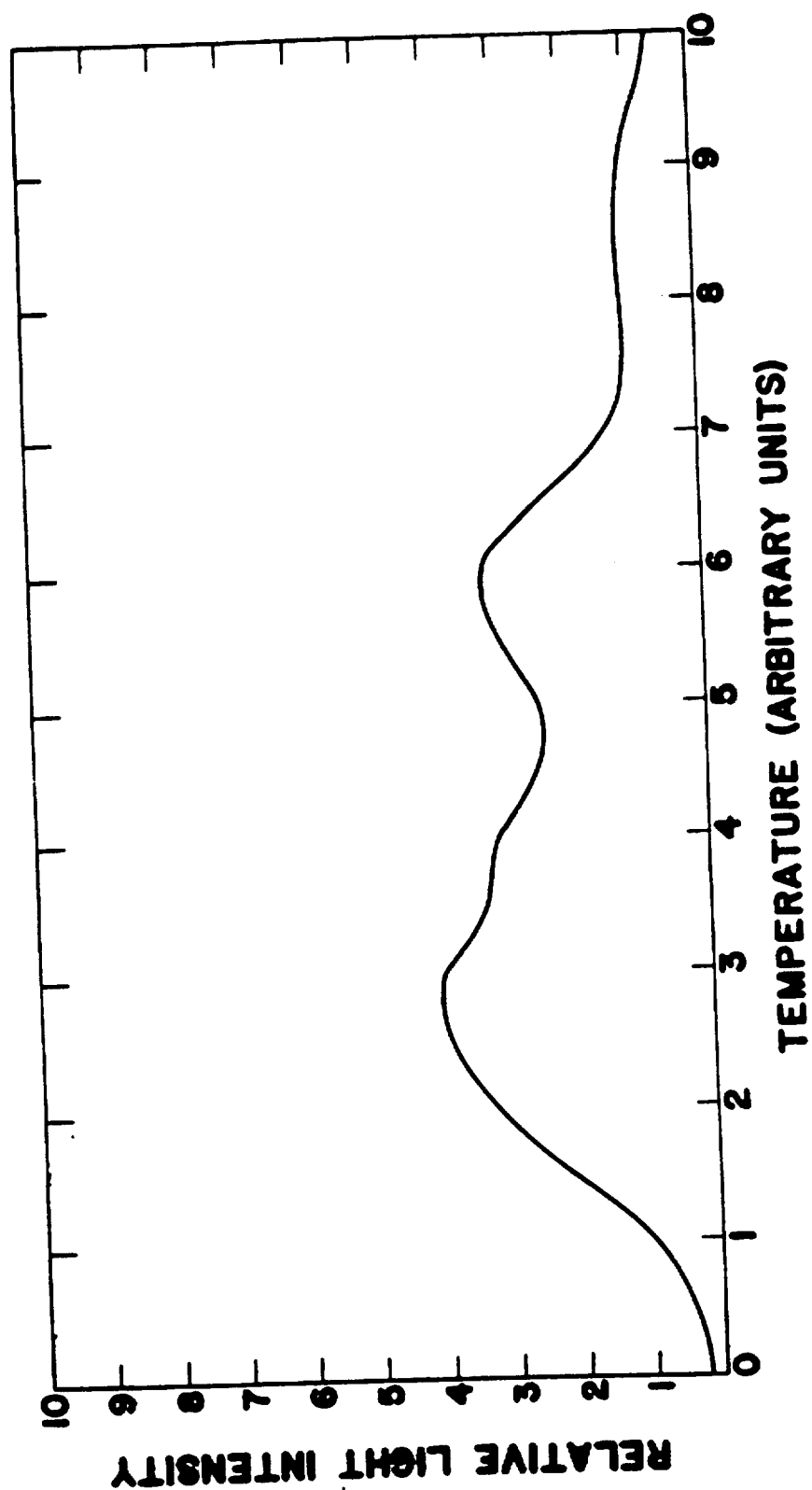


Fig. 2. Thermoluminescence of natural Al_2O_3 .

the Harshaw Chemical Company. There are two important reasons for the selection of LiF. First, the LiF powder can be heated in air without changing its thermoluminescent properties. Consequently, it can be re-used. Since the powder can be used in air, it can be put into any desired container for exposure. Second, it is near tissue-equivalence, making it very useful in depth-dose studies. Its response is essentially independent of energy down to about 100 kev. At 40 kev, its response is 40 per cent above the value at higher energies. It has been reported recently that a shield of stainless steel containing 70 per cent holes will make the dosimeter response independent of energy down to 30 kev.

The reader presently in use is the third one built (Fig. 3). It consists basically of a stainless steel planchet for heating the powder and a photomultiplier for measuring the amount of emitted light. Figure 4 is a cross section of the reader. The reading procedure is as follows. The exposed powder is weighed and then placed in a stainless steel planchet. The temperature of the planchet is raised rapidly to about 200° C by flowing 160 amperes of current through it for 6 seconds. The temperature reached at this time is then maintained by reducing the current to 40 amperes for a total readout time of 30 seconds. This heating cycle has been found to release about 99 per cent of the stored energy with one heating. Figure 5a shows the light emitted by the planchet

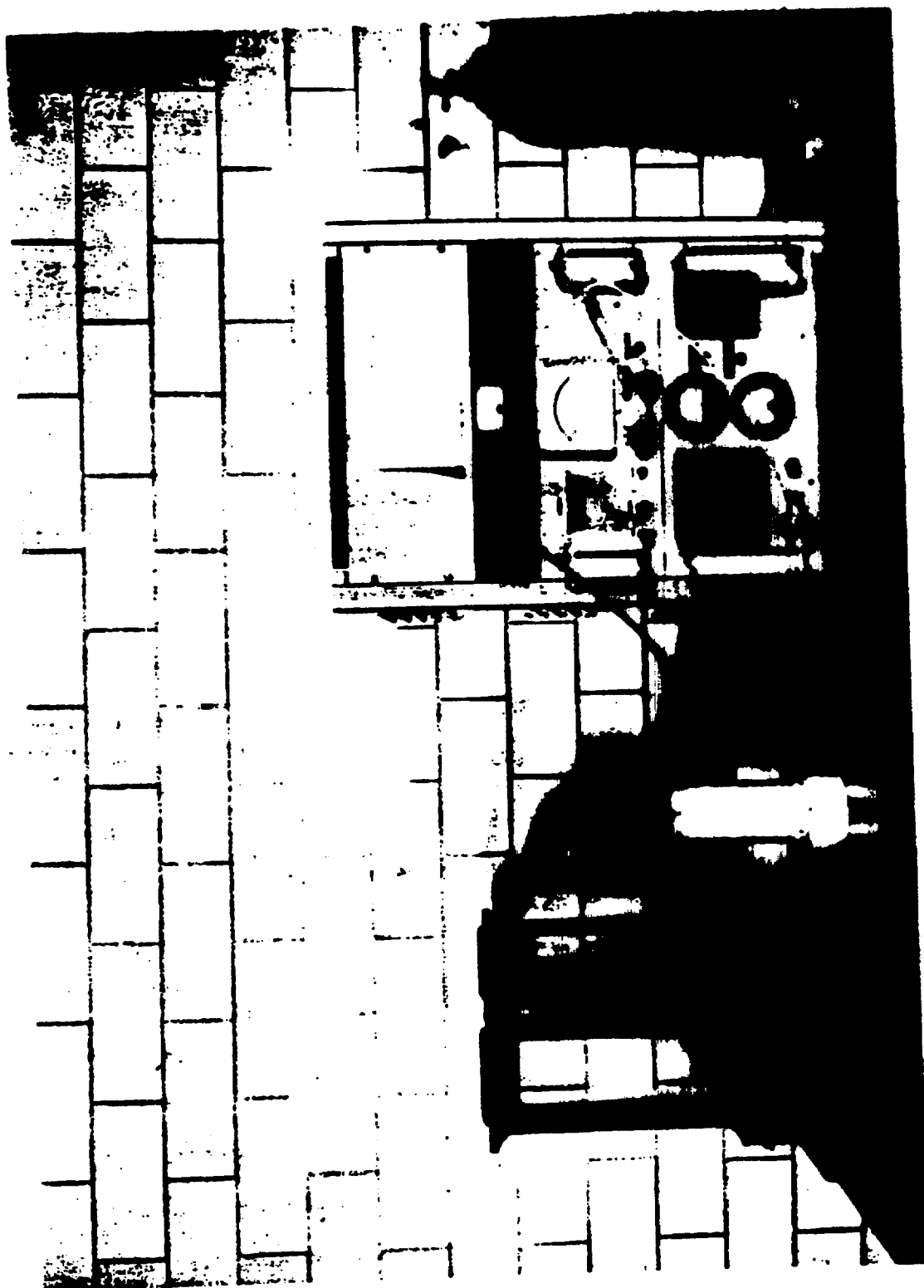


Fig. 3. Thermoluminescence reader.

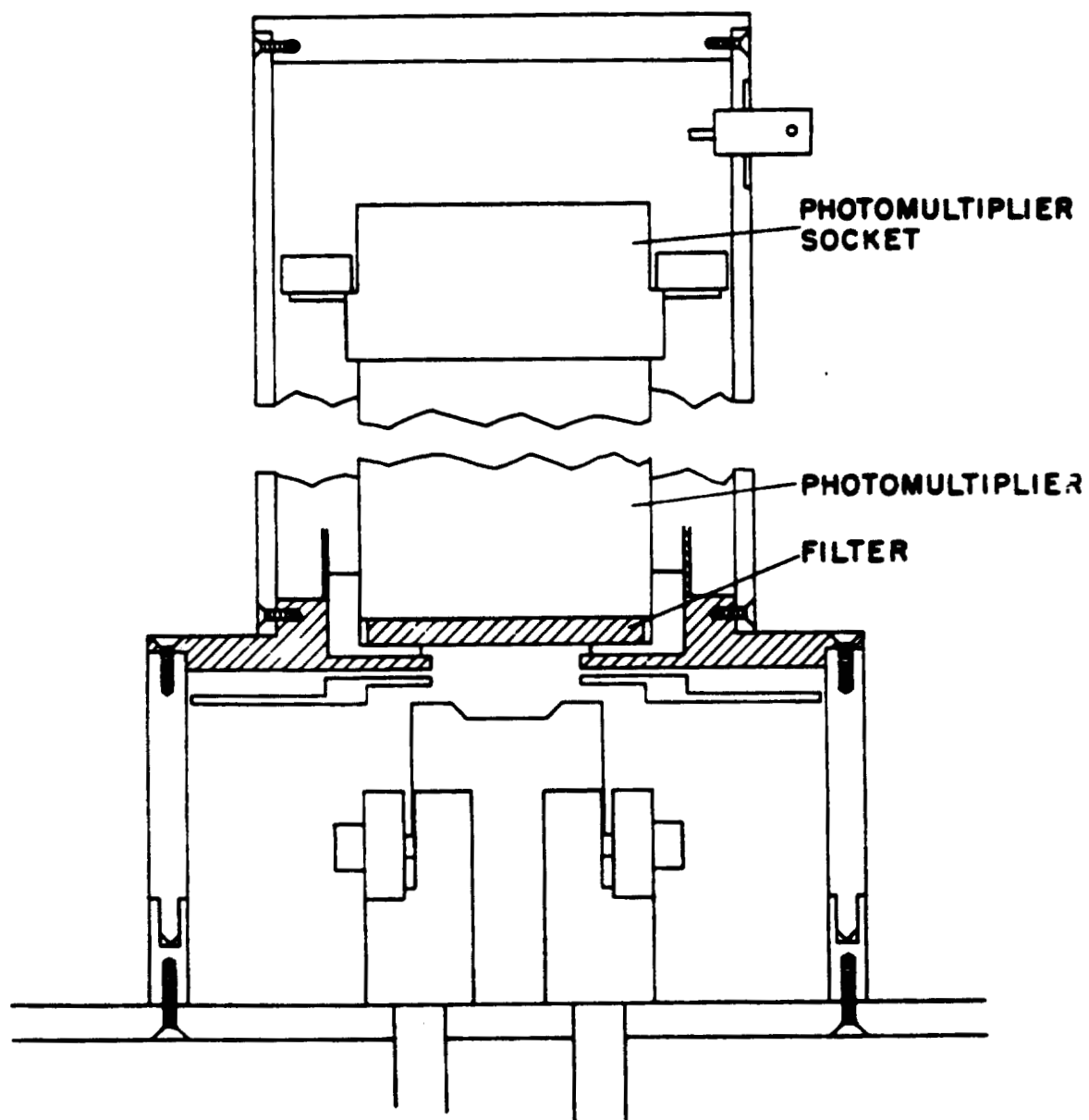


Fig. 4. Cross sectional view of thermoluminescence reader.

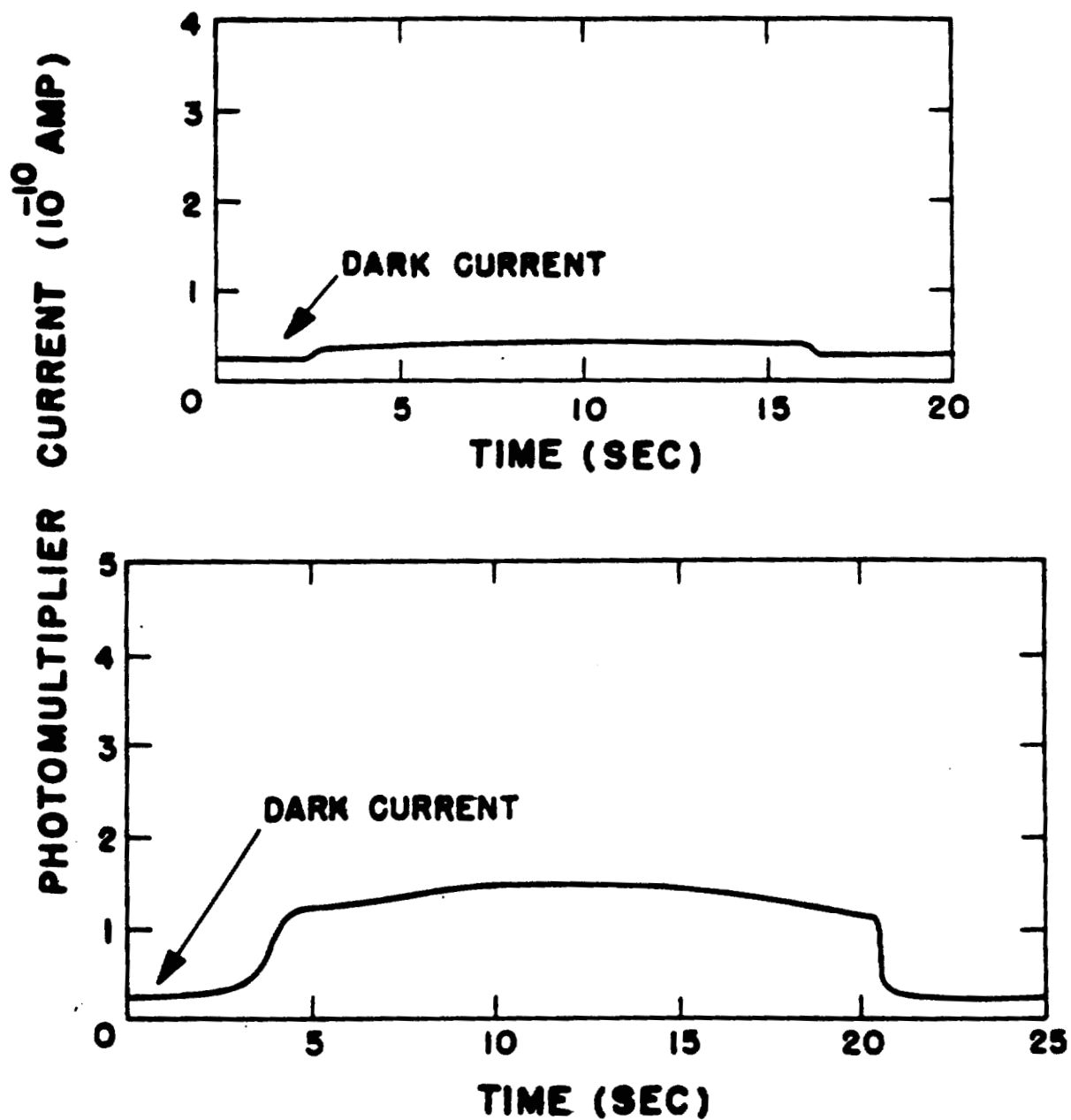


Fig. 5. (a) Light emitted by stainless steel planchet upon being heated plus dark current of photomultiplier. (b) Light emitted by unexposed LiF powder upon being heated plus dark current of photomultiplier.

alone when it is heated (black body or thermal radiation). This is one part of the "background" of a reading. These graphs are obtained by recording the photomultiplier current during the heating cycle. Thus, the abscissa is in time units and does not correspond to temperature of the powder. The powder reaches maximum temperature in slightly more than 6 seconds. The dark current of the photomultiplier is indicated on the graph. Figure 5b shows the light emitted by unexposed LiF powder upon being heated with our standard heating cycle. As for Fig. 5a, this light is due to thermal radiation from the powder. A filter has been placed between the powder and the photomultiplier to reduce the amount of this light that is seen by the photomultiplier. The amount that does get through is equivalent to about 50 mrad dose. These two graphs also show why we selected the above described heating cycle. At the end of the heating cycle, the intensity of light emitted is essentially constant. Thus, small errors in timing cause only negligible errors in amount of light released. For a 10-rad sample, an error of 1 second in the timing cycle would cause an error in the reading of the dose of less than 0.2 per cent. Some readers are designed with a constant heating rate such that the temperature is steadily increasing. In this case, the light intensity is constantly changing with time and the control

of the timing cycle and the heating currents is much more critical.

The energy stored in LiF due to exposure to ionizing radiation exhibits a phenomenon known as "fading." This means that some of the energy is released at room temperature. This is generally an effect with a long time constant. It is due to the presence of an intermediate depth trap in the LiF. Figure 6a shows the thermoluminescence of a LiF sample exposed to 250 KVP X rays and read 1 hour later. The peak indicated is due to the intermediate trap. It is released at a somewhat lower temperature (100°C) than the deep trap (250°C). Figure 6b (at 24 hours after exposure) shows the disappearance of the peak. Figure 7a shows a study of this effect. To remove the fading so that corrections would not have to be applied to a reading depending on how long after exposure a sample was read, the powder was first heated to 110°C . Figure 7b shows the results. The sample was baked at 110°C for 7 minutes, 1-1/2 hours after being exposed to 10 rads of X rays. The fading effect has been essentially removed. This causes a decrease in total light emitted by the sample of about 5 per cent, which is completely acceptable.

A limited investigation was made to determine the minimum dose that could be reliably detected. Due to the rather large integrated "background" current from thermal radiation

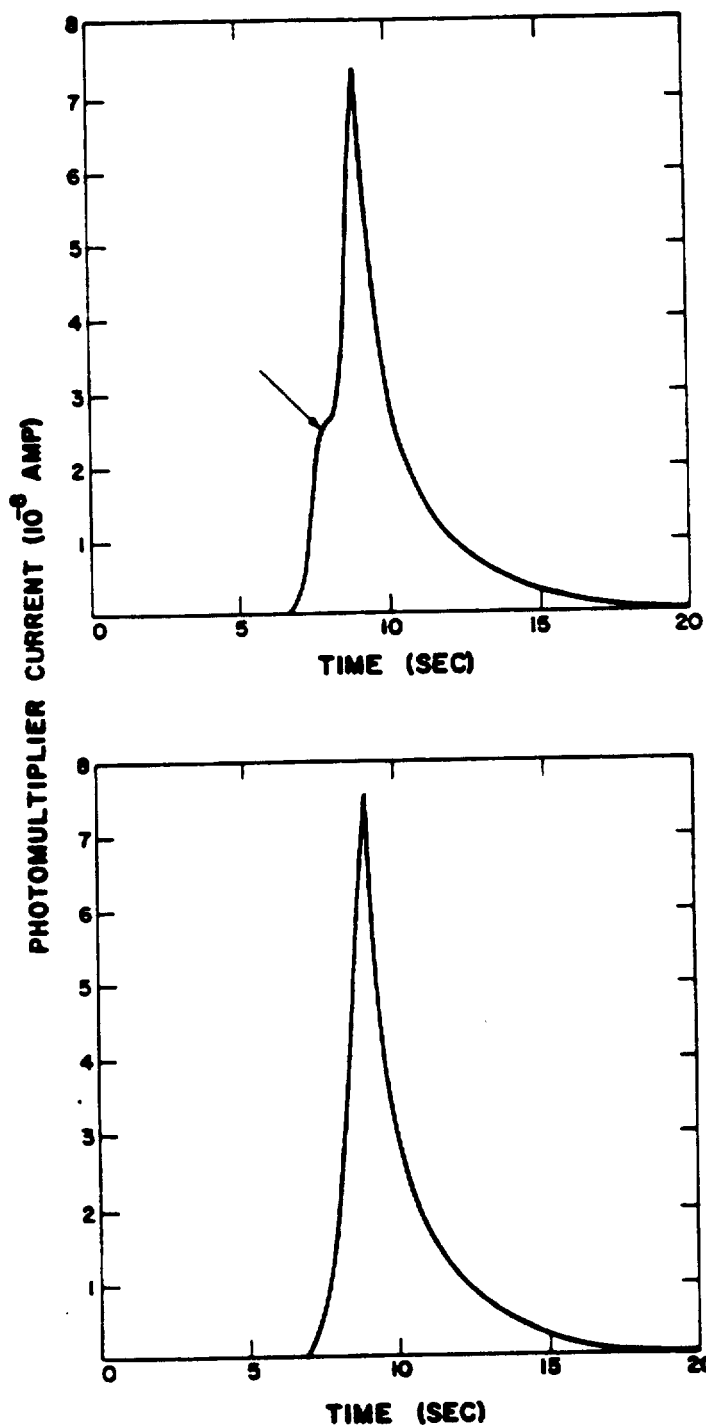


Fig. 6. (a) Thermoluminescence of LiF read 1 hour after exposure to 10 rads of X rays. (b) Thermoluminescence of LiF read 24 hours after exposure to 10 rads of X rays.

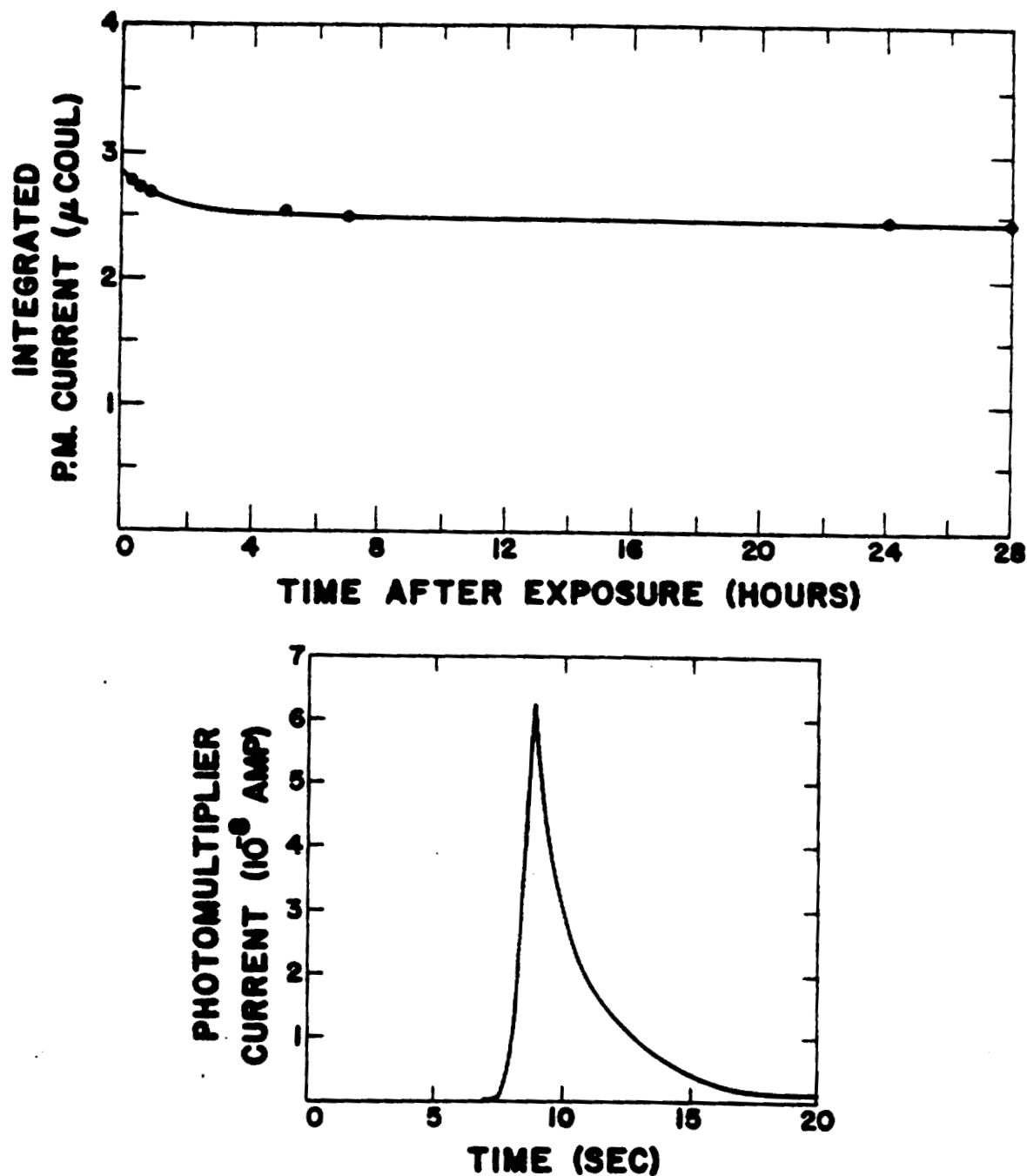


Fig. 7. (a) Light emitted by LiF, as measured by a photomultiplier, exposed to 10 rads of X rays versus time of reading after exposure. (b) Thermoluminescence of LiF heated to 110° C for 7 minutes, 1-1/2 hours after exposure to 10 rads of X rays.

of the powder, low doses have to be read by using the recorder. Figure 8a shows the technique. The dashed curve is from powder that has been baked at 300° C for 1 hour to remove all energy stored in the powder. The solid line is the photomultiplier current profile from a sample that was exposed to 20 mrads of 250 KVP X rays. With this powder, the 20-mrad dose roughly doubles the integrated current. Based on fluctuations in the background of the powder due to uneven spreading of the powder in the planchet (3 per cent effect) and differences in resistivity of the planchets, it is felt that the lower limit of usefulness of this device is 10 mrads. The accuracy of a measurement of 10 mrads is roughly \pm 50 per cent. By paying careful attention to selection of planchets and handling of the powder, this accuracy can be improved.

An additional difficulty in measuring low doses was discovered. Lithium fluoride was found to be sensitive to light (incandescent, fluorescent, and especially ultraviolet). Figure 8b shows the effect of exposing a sample of 100 mg of LiF to normal room light for 30 minutes. The dashed line is from a sample that was baked at 300° C and then read without being exposed to light. The curves are plotted on an expanded scale, the difference being equivalent to about 25 mrads. Consequently, to measure doses less than 50 mrads, the powder should be baked at 300° C and immediately

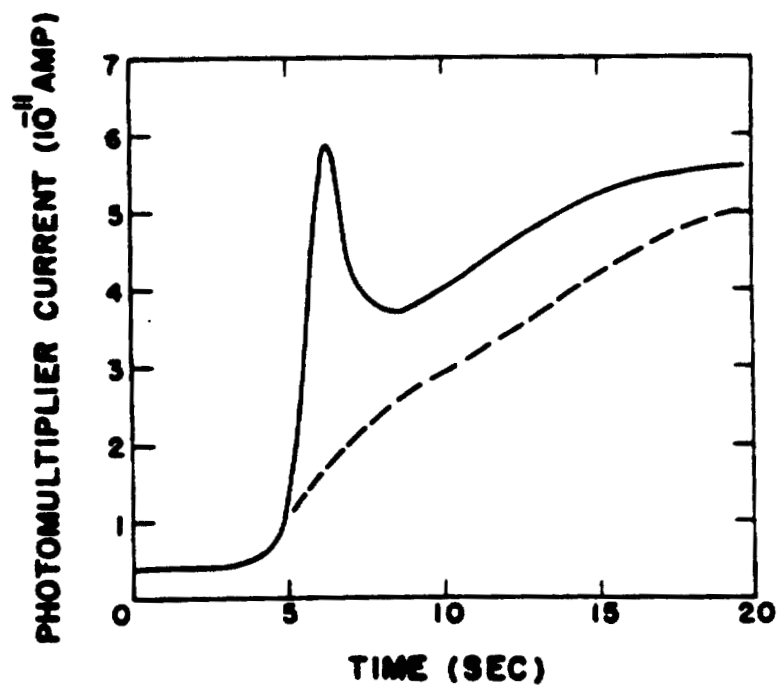
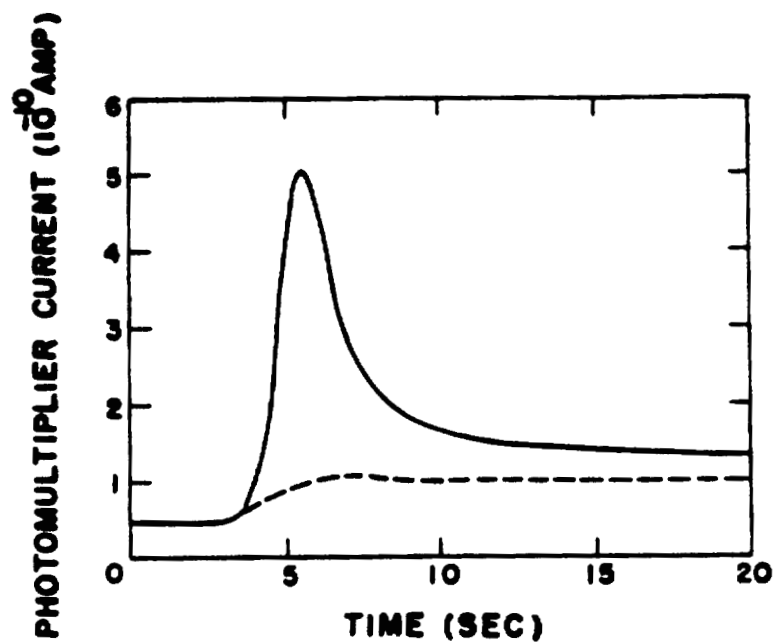


Fig. 8. (a) Thermoluminescence of 100 mg of LiF powder exposed to 20 mrads of X rays. (b) Thermoluminescence of 100 mg of LiF exposed to bright light for 30 minutes.

placed in light-tight containers for exposure (e.g., black polyethylene tubing).

The normal operating range of the present instrument is 100 mrad to 50 rads, using 100-mg samples. This is with 750 volts on the photomultiplier. The range can be extended upward in two ways. One is to reduce the size of the sample. The minimum size is limited only by accuracy of weighing and losses in handling the powder. This is generally about 10 mg, extending the range to 500 rads. Another way to extend the range is to reduce the voltage on the photomultiplier and consequently its sensitivity. Table 1 shows the effect of reducing the voltage, extending the range at 500 volts to 2000 rads.

Constancy of calibration of the detector is checked in the following manner. A plutonium source was mixed with ZnS and encapsulated into a disc 1 in. in diameter. The source gives 26,000 c/min. The disc is placed on the planchet holder and the photomultiplier put into position. After waiting 5 minutes for fluorescence of the ZnS from room light to die out, the current from the photomultiplier due to radiation-induced fluorescence of the ZnS by the plutonium is measured. This is constant with time and allows for correction of drifts in absolute sensitivity of the detector.

The response of the LiF detector was checked against Victoreen ionization chambers. A set of 24 100-mg samples

TABLE 1. SENSITIVITY OF READER VERSUS PHOTOMULTIPLIER HIGH VOLTAGE

High Voltage (volts)	Sensitivity (rads/μcoul-mg)
750	0.0476
700	0.0857
650	0.164
600	0.339
550	0.715
500	1.64

was exposed to the 100-curie Co^{60} source at the Biomedical Research Group's radiation exposure facility (TA-51). They were placed at 8 positions 20 to 500 cm from the source, with a dose rate range of 0.08 to 54 r/min. Figure 9 shows the dose rate (in r/min) versus distance from the source (in cm). The agreement between the ionization chambers and the LiF is quite good. The curve deviates from $1/r^2$ dependence at distances beyond 400 cm because of the presence of a wall at 600 cm which causes considerable backscatter of the gamma radiation.

DISCUSSION

Thermoluminescent dosimetry with LiF is a very promising technique for use in radiobiology and in health physics applications. The reader described in this report was designed to have a useful operating range of 100 mrad to 2000 rads. The dosimeter is essentially energy-independent and has a proportional response to ionizing radiation. Enclosed in polyethylene tubing and being itself tissue-equivalent, the dosimeter would appear to be ideal for depth-dose studies and as a personal dosimeter for animals in group studies. Its size is small and any shape is possible. There are no electrical leads to bring out. There is no perturbation of the radiation field due to other parts of the dosimeter, as in the case of the condenser ion chamber.

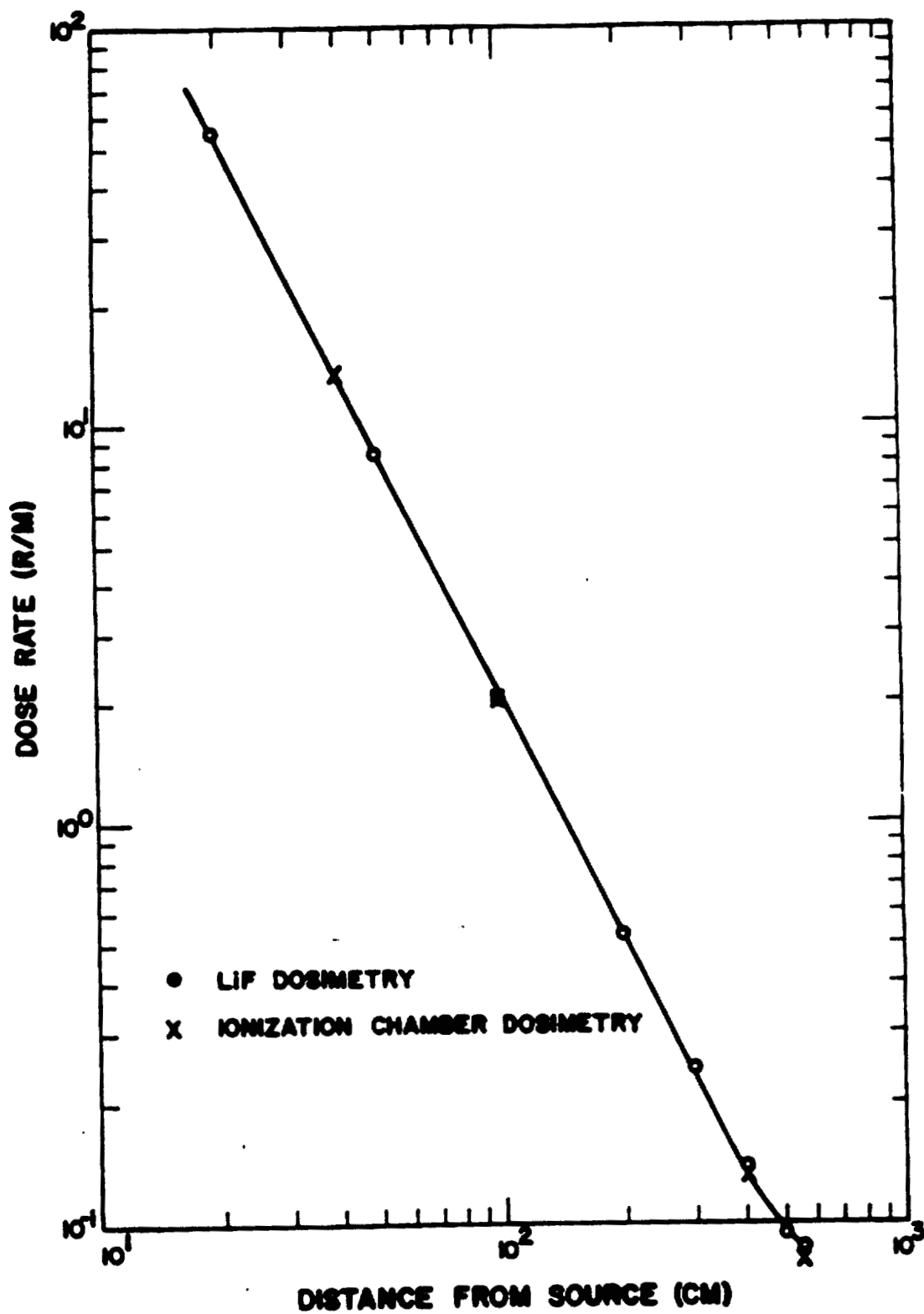


Fig. 9. Dose rate versus distance for 100-curie Co^{60} source at TA-51.

REFERENCES

- (1) F. Daniels, C. A. Boyd, and D. F. Saunders, *Science* 117, 343 (1953).
- (2) F. T. Morehead and F. Daniels, *J. Chem. Phys.* 27, 1318 (1957).
- (3) J. H. Schulman, F. H. Attix, E. J. West, and R. J. Ginther, *Rev. Sci. Instr.* 31, 1263 (1960).
- (4) J. R. Cameron, F. Daniels, N. Johnson, and G. Kenney, *Science* 134, 333 (1962).
- (5) R. J. Ginther and R. D. Kirk, Report of Naval Research Laboratory Progress (September 12-20, 1956).
- (6) F. Daniels and W. P. Rieman, Chemical Procurement Agency Final Report No. 4-12-80-001 (1954).

LOW-LEVEL COUNTING SECTION

PUBLICATIONS

(1) E. C. Anderson, Extraction of Fission Products from Rover Fuel Elements, Los Alamos Scientific Laboratory Report LAMS-2783 (January 4, 1963).

(2) W. H. Langham, Some Radiobiological Aspects of Early Manned Space Flight, Proceedings of the Lunar and Planetary Exploration Colloquium, Vol. III(2), 117 (1963).

(3) W. H. Langham, J. N. P. Lawrence, J. McClelland, and L. H. Hempelmann, The Los Alamos Scientific Laboratory's Experience with Plutonium in Man, Health Phys. 8, 753 (1962).

(4) M. W. Rowe, Quantitative Measurement of Gamma-Ray-Emitting Radionuclides in Meteorites, Los Alamos Scientific Laboratory Report LA-2765 (January 31, 1963).

MANUSCRIPTS SUBMITTED

(1) E. C. Anderson, Three-Component Body Composition Analysis Based on Potassium and Water Determinations, submitted to Ann. N. Y. Acad. Sci.

(2) E. C. Anderson, Determination of Body Potassium by 4 π Gamma Counting, to be published in the Proceedings of the Second Symposium on Radioactivity in Man, Northwestern University Medical School, Chicago, Ill. (September 5-7, 1962).

(3) P. N. Dean, Computer Techniques in Gamma Spectrometry, to be published in the Proceedings of the International Symposium on Natural Radiation Environment, Rice University, Houston, Texas (April 11-13, 1963).

(4) P. N. Dean, Experimental Technique for High Precision Calibration of Whole-Body Counters: Application to a 4 π Liquid Scintillator and a Large Sodium Iodide (Tl) Crystal Spectrometer, to be published in the Proceedings of the Second Symposium on Radioactivity in Man, Northwestern University Medical School, Chicago, Ill. (September 5-7, 1962).

(5) M. W. Rowe, M. A. Van Dilla, and E. C. Anderson,
On the Radioactivity of Stone Meteorites, submitted to
Geochim. Cosmochim. Acta.

(6) M. A. Van Dilla and M. J. Fulwyler, Thyroid Metab-
olism in Children and Adults Using Very Small (Nanocurie)
Doses of Iodine¹²⁵ and Iodine¹³¹, to be published in the
Proceedings of the Hanford Symposium on the Biology of
Radioiodine, Richland, Washington (June 17-19, 1963), Health
Phys.

CHAPTER 5

CLINICAL INVESTIGATIONS SECTION

Progress in the Establishment of Karyographic Methods as a Tool in Radiopathology (G. L. Humason and P. C. Sanders)

INTRODUCTION

Although it has been well established by Bender et al. (1-5) and by the British with irradiated spondylitis cases (6-8) that ionizing radiation produces chromosomal alterations in man and animals, information is lacking concerning (a) the minimum amount of radiation exposure required to produce such damage permanently; (b) the ability of man and other primates to free themselves of such genetic damage; (c) the prognostic significance of such demonstrable changes; and (d) the plausibility of using cytogenetic changes as an index of radiation exposure, and of alpha and proton radiation in particular.

METHODS

With these objectives in mind, a reliable and simple method for obtaining many metaphases for cytogenetic analysis and statistical correlation with radiation dosages was developed (9) through modifications of techniques of Moorhead et al. (10). This method worked well with the peripheral blood of man, dog, rat, and chicken, but did not produce particularly rich cultures of peripheral blood cells from the Macaca. This difficulty seemed overcome best by the addition of NCTC 109 to F-10 medium (6). Adequate cultures of monkey blood rich in metaphases were recently obtained using as a culture medium 70 per cent NCTC 109, 10 per cent F-10 medium, 15 per cent fetal bovine serum, and 5 per cent human cord serum. Phytohemagglutinin (0.1 ml) was added to each 5.0 ml of this mixture. The following technique, a further modification of the method of Humason and Sanders (9) was found to increase the yield of cells for cytogenetic analysis.

1. Spin 8 to 10 ml of venous blood 15 minutes at 900 RPM. Draw off all plasma (8 to 10 ml of blood yields about 2 to 3 ml plasma); the inclusion of some red cells presents no difficulty in culturing. Plant in culture medium 10 to 15 drops of plasma to 5.0 ml of medium. Incubate at 37° C for 72 hours.

2. Add colchicine (step 4).^{*} Incubate 24 hours.
3. Spin down cells and wash with saline D (step 5).
4. Treat with warm water (step 6) and incubate in hypotonic condition at 37° C for 1-1/2 hours. Resuspend cells once during this period.

5. Fix (step 8).

Because it is more difficult to spread monkey than human metaphases, a method had to be devised to improve the spreading obtained in the Humason and Sanders method in steps 9 and 10. The following method has proved successful.

6. After acetic acid-alcohol fixation, spin down. Discard supernatant. Add 45 per cent acetic acid (aqueous) to the cells, approximately 3 to 4 ml of fixative to 0.1 ml of cells for 15 to 30 minutes.

7. Spin down. Discard supernatant and add enough fresh 45 per cent acetic acid to total approximately 3 times the original volume of button of packed cells. Then with Pasteur pipette, thoroughly resuspend cells so that all clumps, if any, are broken. With the pipette, place 3 or 4 separate drops of suspension on clean dry slides, cover with Petri dish, and allow to air-dry. After standing about 15 minutes, stir drops carefully with a clean dissecting needle to help

^{*}Step numbers as given in Ref. 9.

distribute the cells in the drops and to reduce their concentration at the periphery.

After 10 to 15 minutes of air-drying, flame-drying can be tried on some of the slides. Tip the slide to allow drops to spread and flame-dry as in step 10. This sometimes helps to break up reluctant metaphases.

8. Stain according to the method of Puck (11).

RESULTS

Chromosome analyses have been made using these methods on 15 *Macaca mulatta* and 11 *M. speciosa*. Well-spread metaphases were selected for photography, and two prints were made. One photograph was used for determining arm length measurements using double sticky tape (Scotch brand) and surgical silk according to the technique of Puck (11). The other photograph was used to cut out individual chromosomes for the orderly arrangement as an adjunct to classification. The chromosomes were paired and the karyotypes completed from the resulting arm lengths and their ratios, along with visual matching. Patau's method (12) for plotting a karyogram by using the short arm as the ordinate and the long arm as the abscissa (Fig. 1) was found to be of considerable assistance in matching members of similar appearing pairs of chromosomes. The complements of the two species (*M. mulatta* and *M. speciosa*)

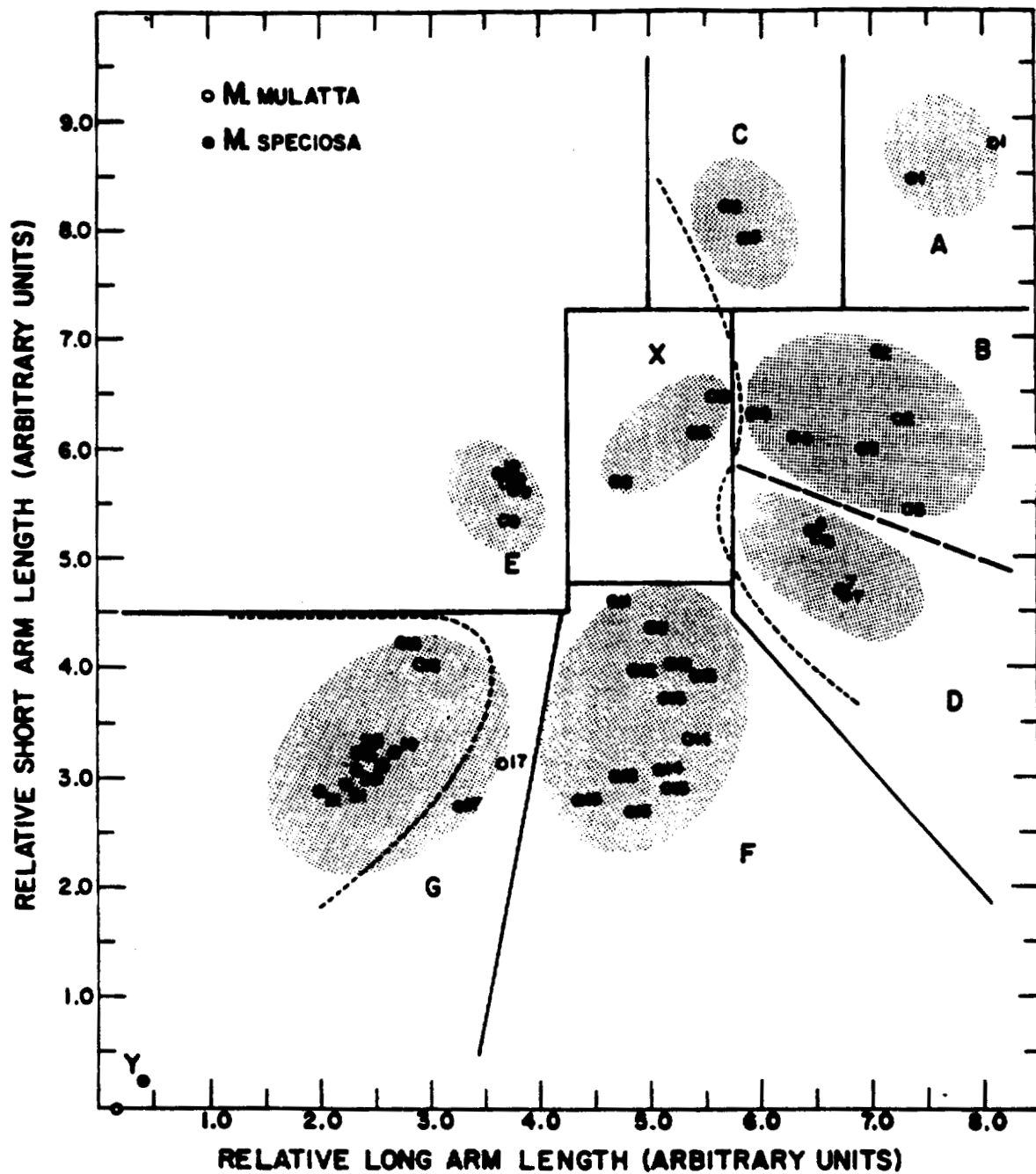


Fig. 1. Graph showing Patau's method of grouping chromosome pairs applied to an analysis of Macaca blood.

were found to be identical, agreeing well with those previously determined by Rothfels and Siminovitch (13) for *M. mulatta*, as shown in Table 1.

These technical studies of the cytogenetic characteristics of normal primate blood were paralleled with karyographic analyses of the cultured peripheral blood and skin of 4 normal persons and 4 persons known to have been exposed previously to inadvertent whole-body irradiation. These studies, some of which are still in progress, were done in order to characterize the nature and frequency of radiation-induced alterations of human chromosomes under these tissue cultural and technological conditions. In the next phase of this investigation, the blood of monkeys exposed to accurately determined amounts of various ionizing radiations will be studied at intervals and compared with the incidence of persistent alterations in the chromosomal cytology found in the blood of irradiated persons.

REFERENCES

- (1) M. A. Bender, *Science* 126(8), 974 (1957).
- (2) M. A. Bender and S. Wolff, *Am. Naturalist* 45, 39 (1961).
- (3) M. A. Bender, X-Ray-Induced Chromosome Aberrations in Mammalian Cells in vitro and in vivo. Immediate and Low Level Effects of Ionizing Radiations (A. A. Buzzati-Traverso, ed.), Taylor and Francis, Ltd., London (1960), pp. 103-118.

**TABLE 1. TYPICAL CYTOGENETIC ANALYSIS OF PERIPHERAL BLOOD
CELLS OF MACACA SPECIOSA**

Group*	Chromosome Number	Average Arm Ratio (l/s)	Per Cent of Total Complement Length
A	1	1.51	8.43
B	2	1.96	7.67
	3	2.05	7.18
	4	1.92	6.01
C	5	1.33	6.39
D	6	2.41	5.70
	7	2.63	5.53
X	8	1.72	4.96
E	9	1.20	4.27
	10	1.05	4.23
F	11	1.99	4.50
	12	2.49	4.56
	13	2.53	4.87
	14	3.04	4.13
G	15	3.81	4.27
	16	3.49	3.59
H	17	2.31	2.78
I	18	1.31	3.69
	19	1.47	2.56
	20	1.33	2.49
	21	1.31	2.13
Y	8 _y *	--	--

*Reference 13.

- (4) M. A. Bender and P. C. Gooch, Types and Rates of X-Ray-Induced Chromosome Aberrations in Human Blood Irradiated in vitro, Biology Division, Oak Ridge National Laboratory Report (1961), 25 p.
- (5) M. A. Bender and P. C. Gooch, Persistent Chromosome Aberrations in Irradiated Humans, Biology Division, Oak Ridge National Laboratory Report (1961), 20 p.
- (6) I. Tough, K. E. Buckton, A. G. Baillie, and W. M. Court-Brown, Lancet II, 849 (1960).
- (7) E. Boyd, W. W. Buchanan, and B. Lennox, Lancet I, 977 (1961).
- (8) J. S. S. Stewart and A. R. Sanderson, Lancet I, 978 (1961).
- (9) G. L. Humason and P. C. Sanders, Stain Techn. 38, 338 (1963).
- (10) P. S. Moorhead, W. J. Mellman, D. M. Batipps, and D. A. Hungerford, Exp. Cell Res. 20, 613 (1960).
- (11) T. T. Puck, ed., Quantitative Mammalian Cell Culture, A Summary of Methods Used in the Department of Biophysics, University of Colorado Medical Center, 2nd ed.
- (12) K. Patau, Am. J. Human Genetics 12, 250 (1960).
- (13) K. H. Rothfels and L. Siminovitch, Chromosoma 9, 163 (1958).

Electronic Measurement of Cellular Volumes. IV. Determination of Scaling and Correction Factors for Conversion of Voltage to Cubic Microns (C. C. Lushbaugh, D. B. Hale, and N. J. Basmann)

INTRODUCTION

Electronic measurement of cellular volumes has numerous potential applications in experimental and clinical hematology (1-4). The usefulness of these applications is presently limited by difficulties involved in accurate calibration of the electronic apparatus and in the mathematical interpretations of the results. The translation of frequency distribution profiles of pulse height voltages into populations of erythrocytes of varying volumes presents semantic difficulties to hematologic microscopists. A particle volume analyzer system assembled around an electronic particle counter* was recently described which seemed to resolve many of these difficulties and to produce hematologically useful results (1,2). Since then, this apparatus has been improved by several commercially available electronic units. In addition, a more accurate system of calibration has been developed which allows correction for changes not only in aperture currents as

*Coulter Electronics, Miami, Florida.

previously described (1) but also for changes in aperture diameter, amplifier gains, and pH of the conducting solution used to suspend the cells. These determinations and the resulting scaling factors show that a much wider range of particles or cells can be sized with this device than previously envisioned. They also reveal that such an analyzer system and its set of apertures must be individually calibrated if actual, rather than relative, erythrocyte volumes are desired. The present paper reports a method for the comprehensive calibration of such equipment and the development of the various necessary scaling factors which are needed to convert pulse height voltages into cubic microns so that measurement and distribution of cellular volumes varying in size from bacteria to the largest HeLa cells can be determined.

DESCRIPTION OF THE APPARATUS

The particle volume analyzer system is composed of 9 pieces of equipment, as shown in Fig. 1. These are inter-related electronically as previously diagrammed (1). The basic units (Fig. 1, C and E) are the aperture tube and mercury manometer chassis (C), where the pulses are generated as the particles pass through the aperture (ApD) in the aperture tube and are enumerated in the particle counter (E).

This particle counter (Coulter Model A) was modified so that the internal coarse control for amplifying pulses after they were formed could be changed at will by turning an external dial knob (g) through 6 positions. The internal fine gain control was left fixed at 2.3 on its dial, since with this setting changes in the coarse gain (g) were constant. The Coulter threshold knob (t) was kept at 10 in order to delete counts due to small debris during the RBC counts used with Hmct to determine MCV. Since the pulses from the Coulter apparatus were obtained for pulse height analysis from the cathode follower circuit (1), the position of the Coulter threshold setting (t) does not limit the size of the pulses (PHv) going to the pulse height analyzer unit (A). Dial a of the Coulter counter enables the choice of 8 different currents (ApC) through the sizing aperture (ApD). The 400-channel analyzer (A) is divisible into four 100-channel units with separate memories so that 4 analyses can be made sequentially before printing out results. Correction for analyzer dead time is made automatically so that variable concentrations of particles are counted with constant statistical errors. As this unit sorts and stores with voltage of a pulse, this event is recorded on a cathode display of the contents of the 100 channels and a "count" is subtracted by the store pulse scaler unit (I). This unit (I) counts down

Fig. 1. The pulse height-particle volume analyzer and its component parts: (A) 400-channel pulse height analyzer;* (B) X-Y plotter or automatic grapher;** (C) aperture tube-manometer chassis;† (D) digital recorder or numerical readout;†† (E) electronic particle counter, pulse amplifier (g), threshold control (t), and aperture current (ApC) control unit (a);‡ (F) X-Y plotter calibration control unit;‡ (G) preset count control unit;‡‡ (H) pulse height calibration control unit;° and (I) store pulse scaler unit.°°

*Model 34-12, Radiation Instrument Development Laboratory, Inc., Melrose Park, Illinois.

**Model 2, F. L. Moseley Company, Pasadena, California.

†Model A, Coulter Electronics, Miami, Florida.

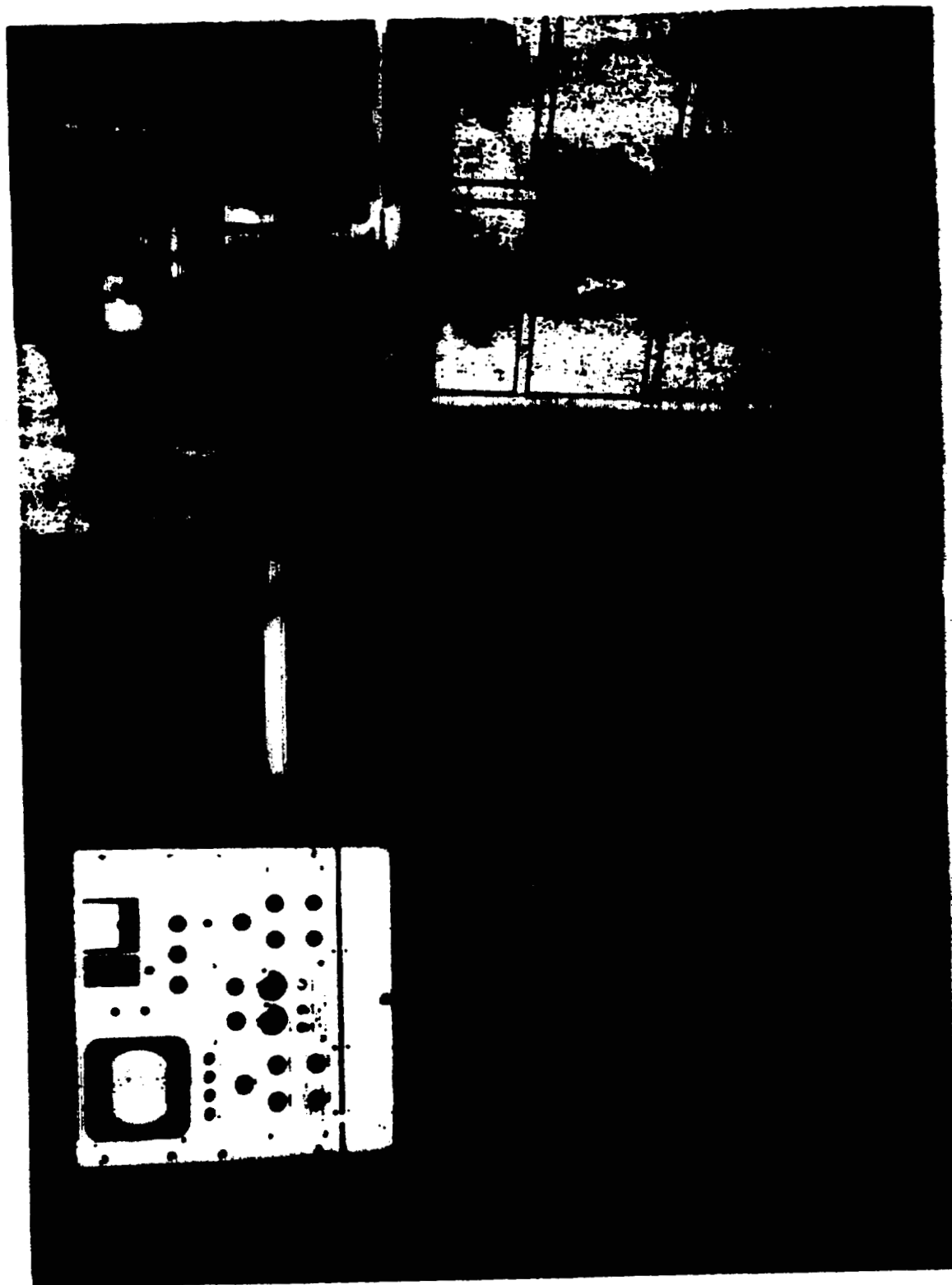
††Model 562-A Hewlett Packard Company, Palo Alto, California.

‡Model 34, Drawing 4Y-40796, Los Alamos Scientific Laboratory.

‡‡Model 7, Drawing 4Y-40806, Los Alamos Scientific Laboratory.

°Model 1560, Drawing 4Y-26828, Los Alamos Scientific Laboratory.

°°Model 750-A, Drawing 4Y-26065, Los Alamos Scientific Laboratory.



1055712

from any number preset on the preset count control unit (G) so that the number of analyses to be made for a given sample can be predetermined and controlled. For mathematical convenience, as well as for good statistics, the preset count in these determinations is kept at 100,000. RBC concentration in the solution being analyzed is kept at about 50,000/ml so that dead time loss is less than 10 per cent. Coincidence errors are not appreciable at this RBC concentration, and about 1 minute is required for each analysis. On completion of the analytical run, the data stored in the 100-channel analyzer memory are plotted out on the X-Y plotter (B) and printed out on tape by the digital recorder (D) on demand. The other 2 units shown in the apparatus (Fig. 1) are the plotter control unit (F), which determines that the X-Y axes of the graphic plotter correspond accurately with the analyzer, and a pulser (H), which enables control of the stability of the analyzer by direct measurement of pulse height voltage being stored in any particular channel from day to day.

In addition to the equipment shown in Fig. 1, 6 different aperture tubes with diameters (ApD) of 30, 50, 70, 100, 140, and 200 microns were used in this study. Another tube with an ApD of 10 microns was not used because it clogged too frequently and generated electronic noise with even low aperture currents.

CALIBRATION PROCEDURES

This pulse height analyzer system sorts PHv varying in height from 0.67 volt in channel 1 to 67 volts in channel 100, instead of 1 to 100 volts as in the previous analyzer (1), thus necessitating determination of a new scaling factor (F_1) for conversion of PHv to cellular volume (CV).

Red Blood Cell (RBC) Method

Red blood cells with different mean corpuscular volumes (MCV) were used as previously described (1,4), and an additional calibration was done with bacterial-sized latex particles.* The resulting line (Fig. 2) drawn by statistical analysis through the points correlating MCV with mean channel (MCh)** revealed that PHv from RBC $28.5 \mu^3$ in volume were being stored in channel 10 at ApD 100, ApC V, g 4. The number 2.85 is, then, the scaling factor (F_1) which enables conversion of any analyzer channel number into μ^3 at these electronic settings and physico-chemical conditions of the suspending solution (3,5-7).

*Dow Chemical Company.

**Mean channel (MCh) corresponds semantically with mean threshold (MT) in terminology of the Coulter counter.

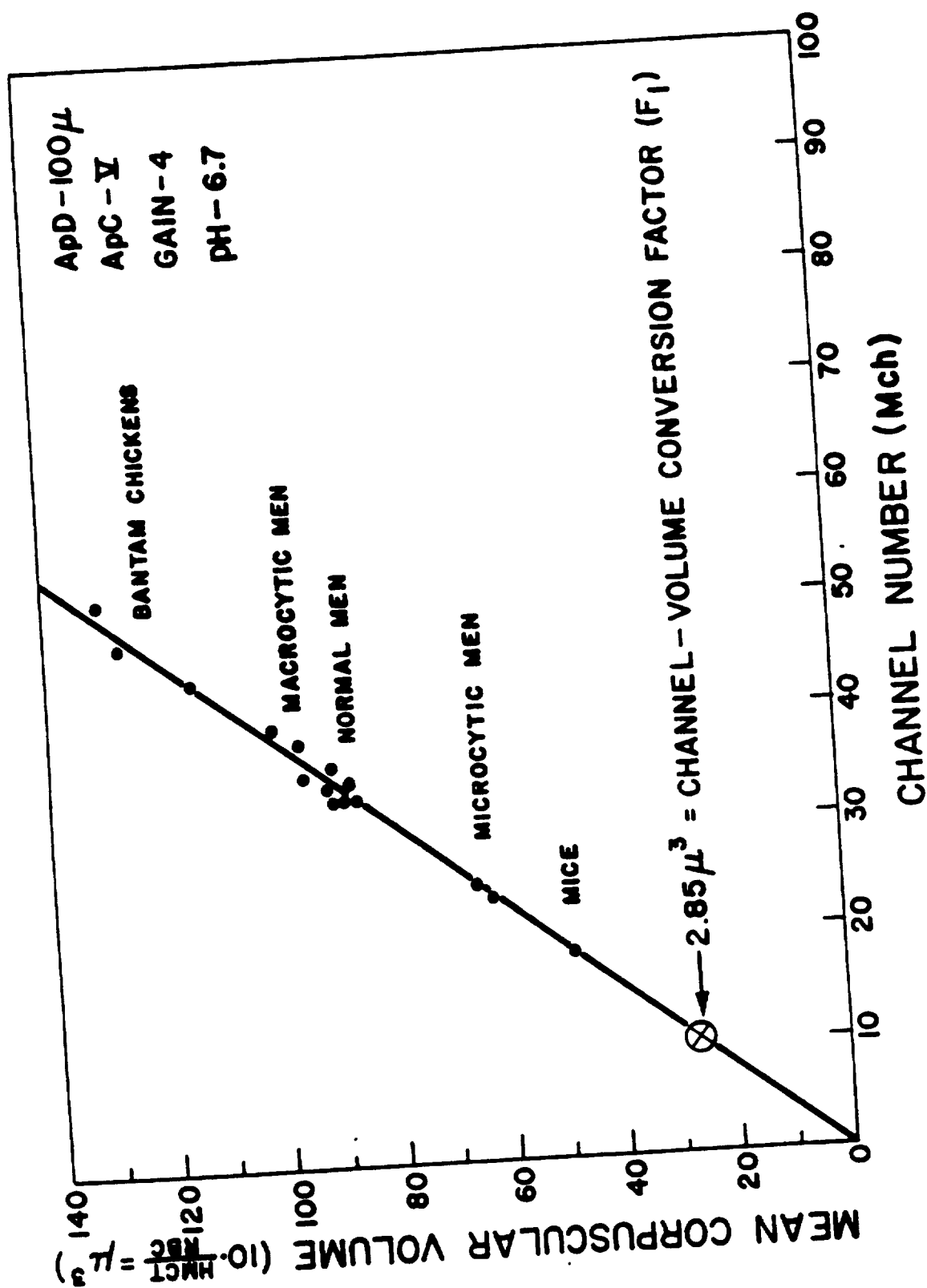


Fig. 2. The calibration line obtained for converting channel number (Ch) or μ^3 pulse height volts (PHV) to cellular volume (CV) in cubic microns (μ^3) using RBC as "standard" particles.

Latex Particle Method

It is not necessary, however, to use RBC for determination of F_1 if other particles are available whose mean volume can be measured directly by some other means. Suspensions of latex particles of different mean diameters have recently been standardized and have become available commercially. The modal volumes of these particles are computed from their known mean diameter. Using three suspensions of latex particles of differing mean volume, frequency distribution profiles of their volumes were determined with appropriate ApD, ApC, and g settings. The best fit lines for these data were determined as shown in Fig. 3 (8). The volume of channel 10 is determined from these lines, and channel volume conversion factors (F_1) are then derived for the various ApD, ApC, and g. These values are tabulated in Table 1, along with F_1 for animal RBC.

Correction Factors

Only one F_1 needs to be determined directly with RBC or latex particles, since it is possible to determine further the correction factors which will compensate for use of other ApD, ApC, and g settings than those used in determining F_1 . The definitions and purposes of these correction factors are outlined in Table 2. With these numerical factors, a

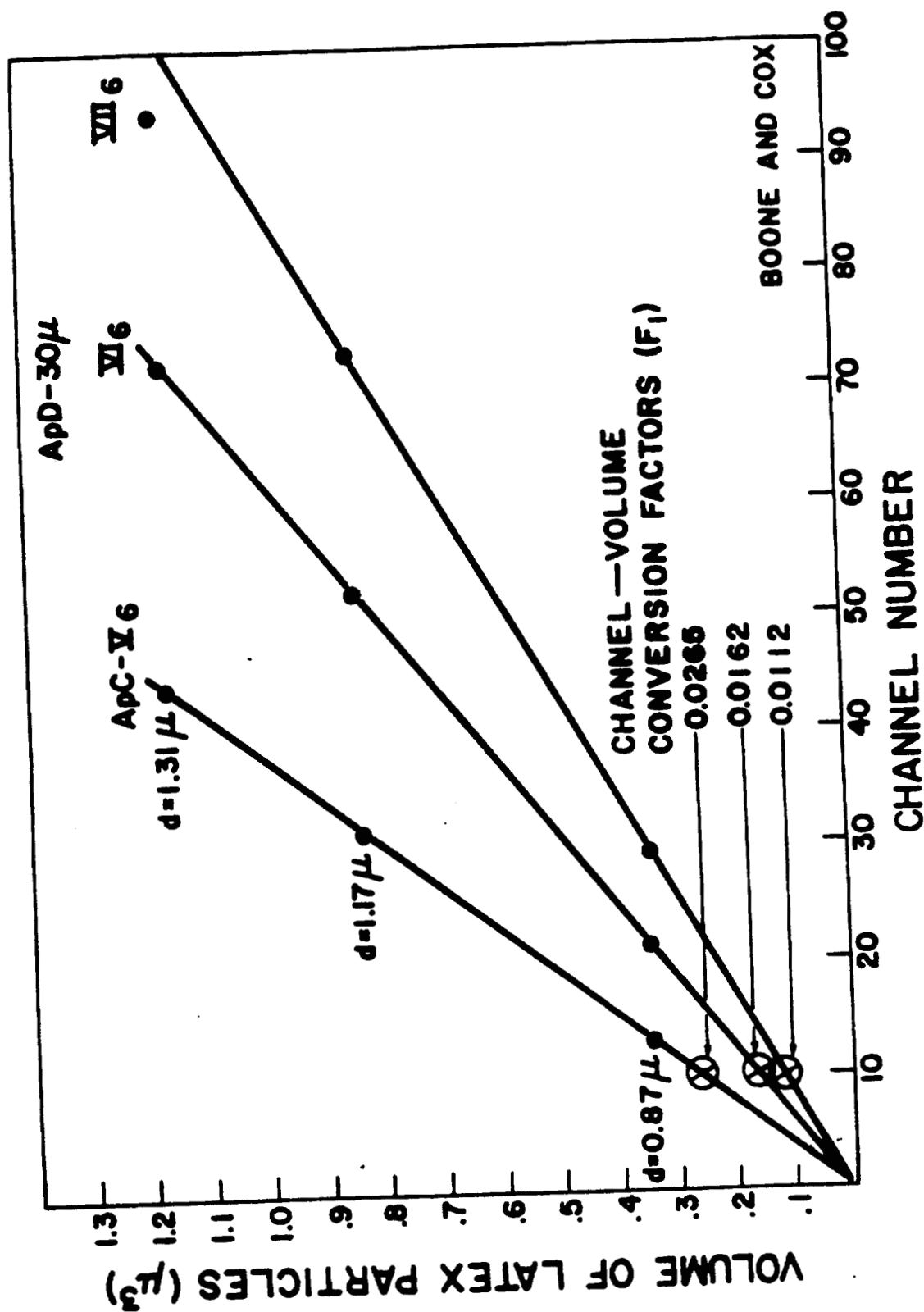


Fig. 3. Graph showing how 3 suspensions of latex particles of known mean diameter can be used to determine F_1 for a smaller ApD than that used with RBC.

TABLE 1. SCALING FACTORS (F_1) FOR CONVERTING CHANNEL NUMBER
TO VOLUME

Latex Particles (5)

ApD = 30 μ , pH uncontrolled, 0.9 per cent saline

ApC V, g 6 = 0.0265 μ^3/Ch

ApC VI, g 6 = 0.0162 μ^3/Ch

ApC VII, g 6 = 0.0112 μ^3/Ch

Animal RBC

ApD = 100 μ , pH 6.7, 0.9 per cent saline

ApC I, g 1 = 111.6 μ^3/Ch^*

ApC V, g 4 = 2.85 μ^3/Ch

ApC VII, g 1 = 3.04 μ^3/Ch^*

*By extrapolation using corrections $F_3 \times F_4$ for changes in ApC and g.

TABLE 2. PARTICLE VOLUME SCALING AND CORRECTION FACTORS

Factor	Converting	To
F_1	Analyzer channel number (pulse height)	Cubic microns (μ^3)
F_2	Aperture diameter of F_1	Any aperture diameter used
F_3	Aperture current of F_1	Any aperture current used
F_4	Amplifier gain of F_1	Any gain setting used
F_5	Physico-chemical conditions of F_1	Any pH, temperature, or osmolarity of suspending solution

pulse produced by a particle of unknown size can be corrected mathematically to standard conditions from those under which the pulse was produced.

PROCEDURE FOR DETERMINATION OF CORRECTION FACTORS

These correction factors (Table 2) were determined by measuring the shift in the channel number modes of populations of RBC caused by changing one variable while all other variables remained fixed. No attempt was made to measure the actual size of the cells or to determine mathematically their mean cell size or size of the cells at the mode. The assumption was made, based on the previously reported studies (1,2), that the cell size at the mode of frequency distribution curve of any one blood sample was constant. In the cases of pH (5) and osmolarity (6), the shift in modal peak is due to actual changes in CV because of the expansible RBC membrane.

As shown in Fig. 4, RBC from a patient were sized at pH 6.7, 0.9 per cent saline, 74° F, with ApD 140 microns and ApC VIII, while the amplifier gain settings were changed. Ratios were then made of the channel numbers of the modes at consecutive changes in one condition while other conditions were held constant, as shown in Table 3. The mean ratio for gain changes (g) determined in this manner was 0.707,

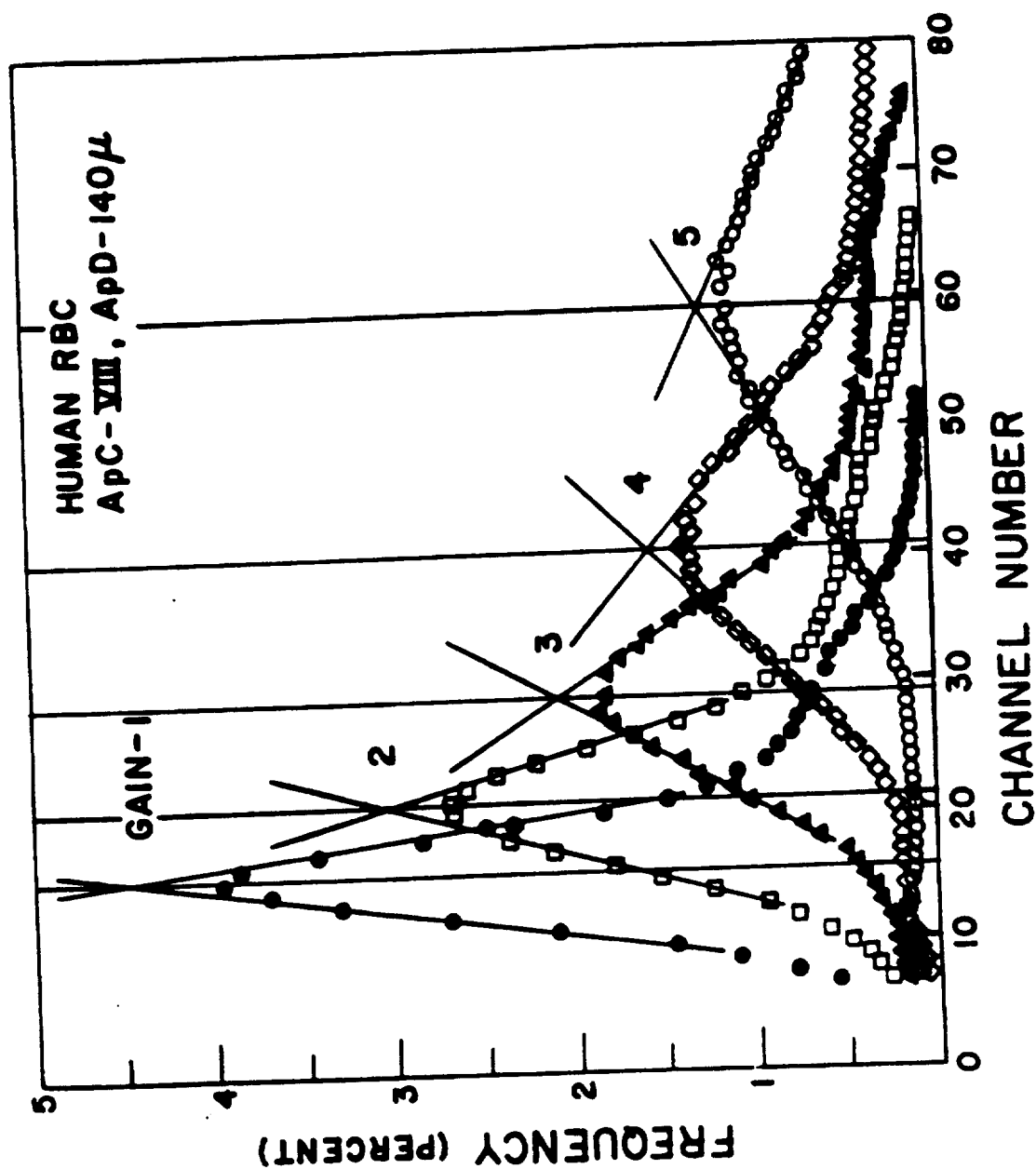


Fig. 4. Graph illustrating the "spectral peak" method of determining the effect of alterations in some condition of measurement upon the apparent mean diameter of erythrocytes.

TABLE 3. COMPARISON OF THE APPARENT VOLUME OF CHANNEL 10
AS MEASURED WITH MONODISPERSED LATEX PARTICLES (8)
AND BY EXTRAPOLATION FROM ERYTHROCYTE CALIBRATION
CURVES (2)

ApC	Gain	Channel 10 Volume (μ^3)		
		Latex Method*	RBC Method**	RBC/Latex
V	6	0.265	0.296	1.12
VI	6	0.16	0.17	1.02
VII	6	0.12	0.12	1.00

*At ApD 30.

**At ApD 100, ApC V, g 4, pH 6.7.

or $\sqrt{\frac{1}{2}}$. The ratios for ApD and ApC changes were not linear, and mean ratios could not be derived. Using these ratios, it is possible to derive the correction factors by which the experimentally determined conversion factor F_1 can be converted into scales for the other settings.

Use of Correction Factors

The accuracy of these correction factors was tested by using them to extrapolate from the F_1 determined with RBC at ApD 100, ApC V, g 4 (pH 6.7), to the F_1 values determined with latex particles at ApD 30, ApC V, VI, and VII, at g 6. The results of this test (shown in Table 3 and Fig. 5) confirm the validity of this method of calibration and correction. Figure 5 also shows the range of particle sizes that can be measured in channel 10 by appropriate changes in the three variables ApD, ApC, and g.

CONCLUSION

The inherent variability of electronic apparatus requires a means of standardizing their measurements along with a method for compensating for changes in the conditions under which the measurements are made. RBC or latex particles can be used, as described here, as a nonelectronic means of such standardization that is facile and reliable.

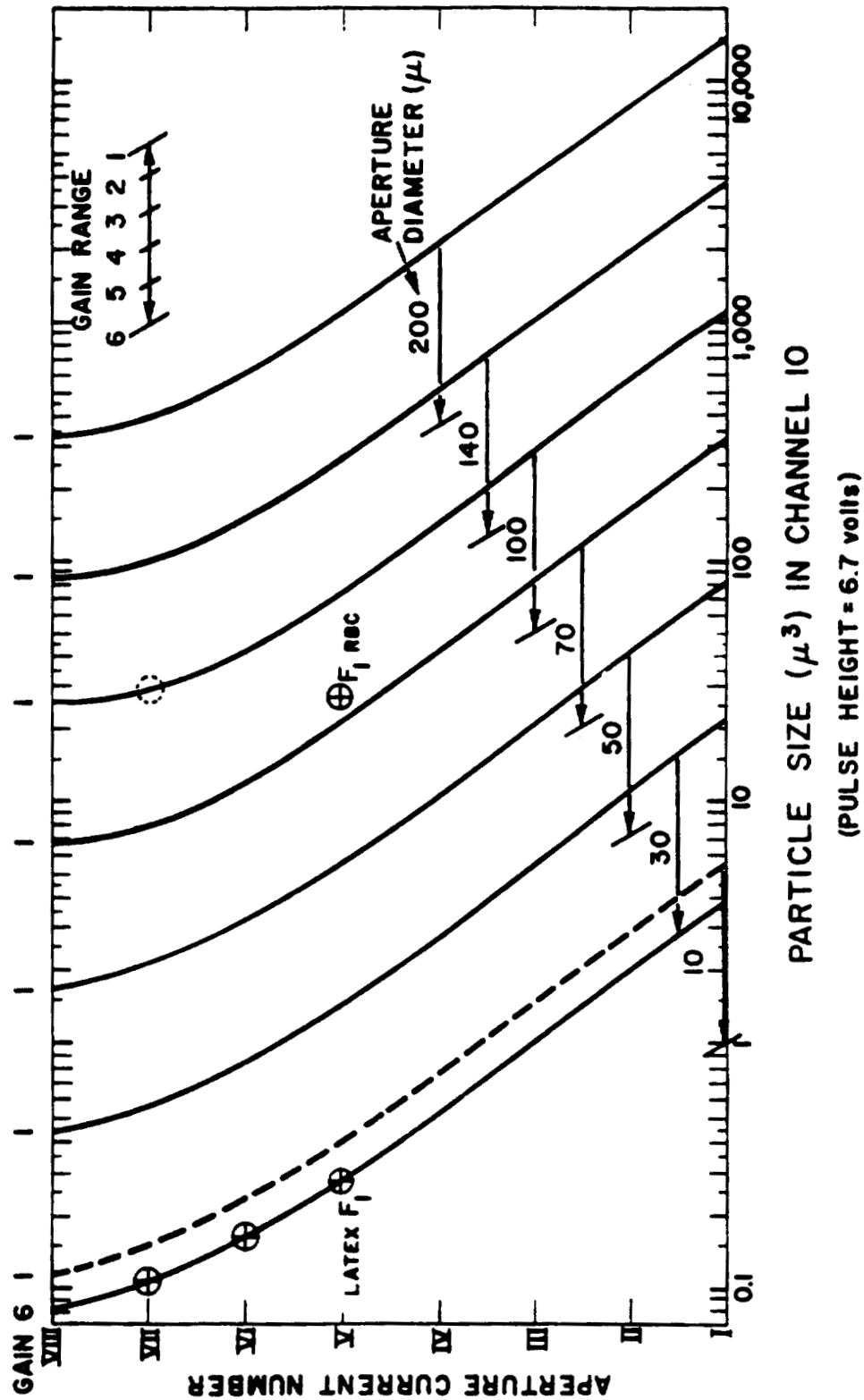


Fig. 5. Graph of the ranges of particle volumes that can be measured by various changes in aperture current, amplifier gain, and aperture diameter. The location of the latex and RBC conversion factors (F_1) that were determined experimentally are shown.

REFERENCES

- (1) C. C. Lushbaugh, J. A. Maddy, and N. J. Basmann, *Blood* 20, 233 (1962).
- (2) C. C. Lushbaugh, N. J. Basmann, and B. Glascock, *Blood* 20, 241 (1962).
- (3) G. Brecher, E. F. Jakobeic, M. A. Schneiderman, G. Z. Williams, and P. J. Schmidt, *Ann. N. Y. Acad. Sci.* 99, 242 (1962).
- (4) A. C. Peacock, G. Z. Williams, and H. F. Mengoli, *J. Nat. Cancer Inst.* 25, 63 (1960).
- (5) C. C. Lushbaugh, E. C. Anderson, H. I. Israel, D. B. Hale, and N. J. Basmann, *Change in Red Blood Cells Resulting from Non-Physiologic pH. V. This report.*
- (6) D. B. Nevius, *Am. J. Clin. Path.* 39, 38 (1963).
- (7) W. H. Coulter, presented at the National Electronics Conference, Chicago, Illinois (October 1956).
- (8) I. U. Boone and S. H. Cox, personal communication, Los Scientific Laboratory (1962).

Electronic Measurement of Cellular Volumes. V. Change in
Red Blood Cells Resulting from Non-Physiologic pH (C. C.
Lushbaugh, E. C. Anderson, H. I. Israel, D. B. Hale, and
N. J. Basmann)

INTRODUCTION

Brecher et al. (1) have shown recently using the Coulter counter that 0.9 per cent saline causes an apparent increase in red cell volume when compared with measurements made in plasma or Eagle's solution. The unavailability of large inexpensive quantities of specific plasma and the difficulties involved in making solutions routinely with as many different salts as contained in Eagle's formula led us to look for a cause for this volume increase which might be controlled when using physiologic saline so that the "true size" of RBC could be calculated from electronic determinations of RBC volume distribution profiles (1,2). Since 1867, when Schmidt (3) and later Nasse (4) described increase in RBC volume in serum under increased CO₂ tension, a relationship between RBC size and pH of the suspending medium has been known to exist (5). Although no recent studies have been made of this phenomenon, it is generally accepted that RBC swelling can result from changes in osmotic pressure resulting from pH changes exterior to the cation impermeable membrane of the cell (6,7).

METHODS AND RESULTS

Commercially available saline is unbuffered and quite variable in pH, ranging usually from 5.8 to 6.0. Prolonged storage produces a pH as low as 4.0. Saline, however, can be buffered to a desired pH without changing its isotonicity or conductivity by appropriate amounts of phosphate buffer. A study of the effect of pH on RBC volumes measured electronically was made using this buffering system and commercially available saline. In this study, individual blood samples from 20 mice and 20 men were counted and sized electronically in 0.9 per cent saline solutions at 6.0, 6.5, 7.0, and 7.5 pH. The mean cell volume (MCV) at these pH's was determined as the mean analyzer channel (Mch) by integrating the volume distribution profiles of RBC volumes measured electronically (2). In order to determine whether aperture current (ApC) settings and amplification (g) of the pulses modify change in apparent volume, the mice were measured electronically at ApC VIII, g 2, and the men at both ApC VII, g 1, and ApC V, g 4. The resulting data are shown in Table 1. Figure 1 shows the best fit line for these points plotted as the logarithm of the mean channel number of the mean RBC volume versus the pH of the saline used in the determinations. The data show that, over the pH range investigated, change in RBC volume occurs as an exponential function of

TABLE 1. EFFECT OF pH OF PHOSPHATE-BUFFERED SALINE ON HUMAN AND MOUSE ERYTHROCYTE VOLUMES (SHOWN AS CHANGES IN MEAN PULSE HEIGHT ANALYZER CHANNEL NUMBER OF RBC FREQUENCY DISTRIBUTION PROFILES OF VOLUMES)

Blood Sample Source	Electronic Counter Settings	Mean Channel Number at pH										MCV (μ)
		6.0	6.3	6.45-6.5	6.65	6.70	7.0	7.45	7.5			
Mice (20)	ApC VIII, § 2	30.2	28.56	--	27.85	--	26.44	--	24.92			49.7
Men (12)	ApC VII, § 1	--	--	29.16	--	28.31	27.74	--	26.99			87.5
Men (8)	ApC V, § 4	--	30.71	--	29.76	--	28.01	26.55	--			86.0

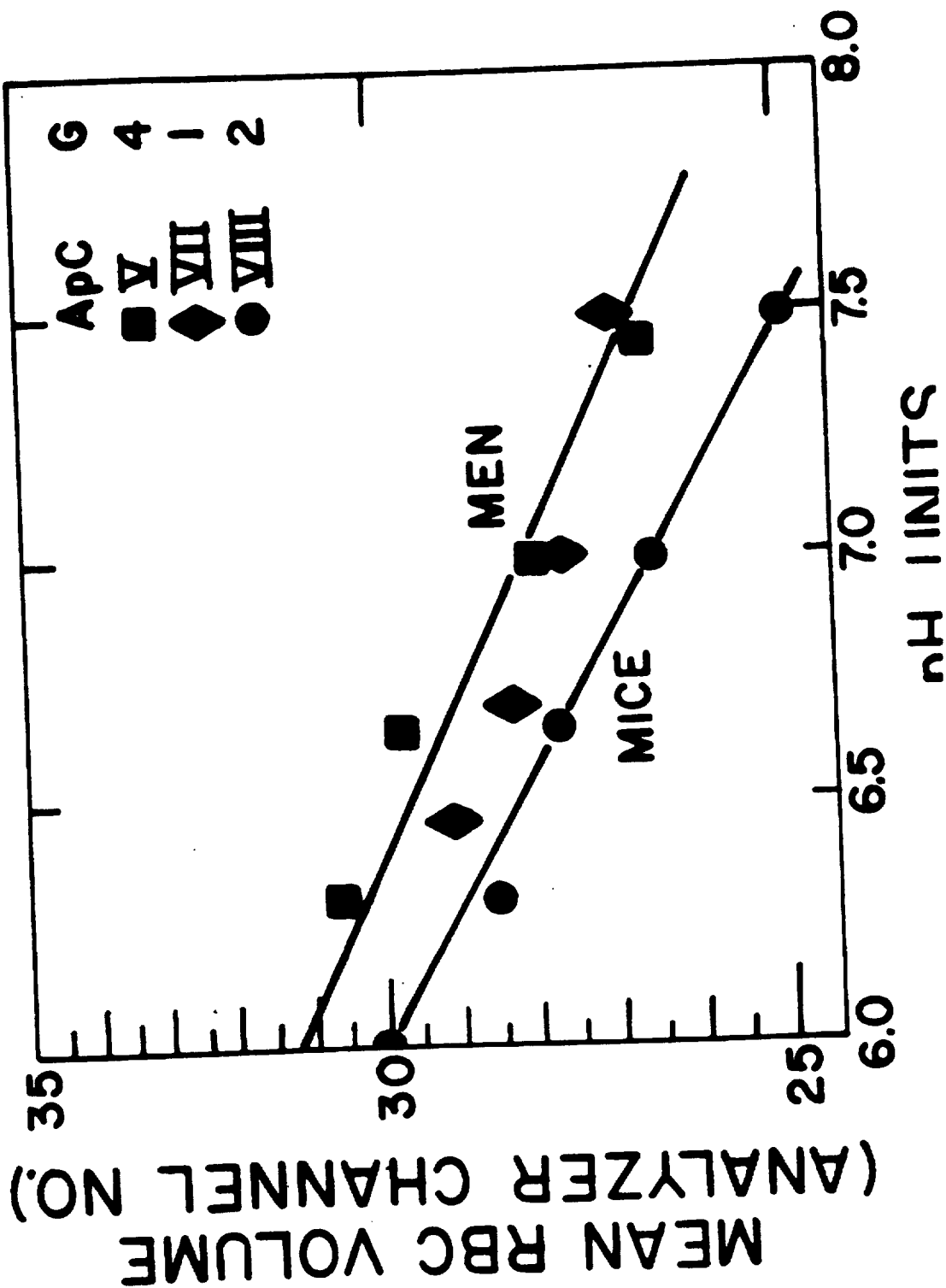


Fig. 1. Semilogarithmic plot of relationship of RBC volume to pH of the saline-phosphate buffer medium used in electronic sizing.

change in pH of the saline solution suspending them. This relationship between RBC and pH of the suspending medium implies that there is no single "true" size of RBC; human RBC in acidosis (<7.35 pH) are larger than the same RBC in normal arterial blood (7.4 pH), and measurements of RBC volume must be referred to some standard set of conditions. The actual measurement, however, could be made under some condition of pH other than the "standard" if the appropriate mathematical correction for pH was known. Also, such a correction factor for counting solutions adequately buffered at the pH of human venous blood are needed, because blood samples open to the air change pH at the rate of 0.2 pH or more per hour and are, therefore, not measured in vitro at their in vivo pH. The figure shows that the fractional change in volume of RBC, as indicated by the channel number (Ch), is proportional to the change in pH; that is,

$$\frac{\Delta Ch}{Ch} = k \cdot \Delta pH.$$

(On a logarithmic scale, a constant fractional decrement, $\Delta Ch/Ch$, appears as a constant absolute change.) The constant (k) can be evaluated by substituting numerical values for the other parameters in this equation. [Note, however, that the equation is really only the differential form of the exact exponential function and can be used as an

approximation only when the fractional volume change is small (i.e., over the range to which $1 - x$ is a good approximation for e^{-x}). For the total range shown in Fig. 1, the volume change is 25/31 or 0.81, and the approximation is good to 2.5 per cent.]

The line of best fit drawn through the 5 mouse points shows volumes corresponding to Ch 30.0 at pH 6.0 and 26.5 at pH 7.0, giving a slope $k = 0.124$. A computer calculated least squares exponential fit to the same data gave $k = 0.125$. For man, the latter gave $k = 0.106$. This slope, indicating about a 10 per cent change in RBC volume per change in 1.0 pH, corresponds well with the fractional change observed by Warburg (6) with horse blood under different CO_2 tensions. This slope (k) can be used as a volume correction factor in the following way:

$$\text{True Size} = [1 + (k \cdot \Delta pH)] \cdot \text{Size Observed},$$

or for the electronic particle size analyzer:

$$Mch_{(true)} = [1 + (0.106 \cdot \Delta pH)] \cdot Mch_{(found)}.$$

Where scaling factors (F) have been determined for converting analyzer channel number to cubic microns (μ^3) at a certain ApC setting, amplification gain, and aperture diameter (ApD), it can be used in this formula to obtain true volume in cubic microns, as

$$V = F [1 + 0.106 (\Delta pH)] \cdot Ch No.,$$

where ΔpH is the difference between the pH used in the determination of the scaling factor and 7.4. Similarly, a scaling factor (F) determined at some pH can be corrected in this manner to that for any other pH.

Since it is still true, as Ponder (5) pointed out in 1948, that "no one knows what ought to be taken as the isoelectric point of the mixture of substances which enter into the architecture of the erythrocyte, nor is enough known about the swelling of anisotropic and elastic materials in the neighborhood of their isoelectric points," the choice of pH of the saline solution used in sizing RBC would seem to depend on the preferences and biases of the investigator. The factor for change in RBC volume due to pH, as determined here, would allow interconversion of the data of others to a standard or any other pH.

SUMMARY

The reported increased size of erythrocytes suspended in saline is due to an effect of the low pH of unbuffered saline solutions commonly used in electronic particle counters. This increase in size was found to occur exponentially with decrease in pH and to be 10.6 and 12.5 per cent per pH unit below 7.4 for man and mouse, respectively.

REFERENCES

- (1) G. Brecher, E. F. Jakobiec, M. A. Schneiderman, G. Z. Williams, and P. J. Schmidt, Ann. N. Y. Acad. Sci. 99, 242 (1962).
- (2) C. C. Lushbaugh, J. A. Maddy, and N. J. Basmann, Blood 20, 233 (1962).
- (3) A. Schmidt, Ber. k. Sachs. Ges. Wiss. Math.-physikal. Cl. I. 19, 30 (1867).
- (4) H. Nasse, Pfluger's Arch. 16, 604 (1878).
- (5) E. Ponder, Hemolysis and Related Phenomena, Grune and Stratton, New York (1948), p. 112.
- (6) E. J. Warburg, Biochem. J. 16, 153 (1922).
- (7) A. C. Hampson and M. Maizels, Proceedings of the Physiological Society (October 16, 1926), 16P. In: J. Physiol. 62, xvi (1926).

Electronic Measurement of Cellular Volumes. VI. Electronic Improvement of Coulter Counter Resolution (C. C. Lushbaugh, N. J. Basmann, and D. B. Hale)

INTRODUCTION

Resolution of energy spectra depends upon accurate measurement of pulse height voltage. As first pointed out by Kubitschek (1), resolution by the Coulter counter is not maximum since the circuitry and apparatus were designed primarily for rapid enumeration of pulses rather than voltage measurement. In order to minimize coincidence loss due to 2 or more particles occupying the sizing aperture simultaneously, the pore in the hollow glass sensing probe of the Coulter counter was made relatively shallow (e.g., the aperture of 100 μ in diameter is only 75 μ in depth). The length of time a particle remains in the electrical field of the aperture is shortened further by the rapidity with which the suspending solution is drawn through it. The rise time of pulses generated by particles is comparatively slow in relation to their velocity through the pore. Lengthening the gating interval of the pulse height analyzer does not correct the tendency for this system to report lower than actual height of the pulses, since the particle often passes through the sensitive volume of solution in the aperture before the pulse has time to reach its full height. To

complicate the analysis further, all particles do not pass through the aperture at the same velocity since, as is well known, fluid moves more slowly at the periphery of a stream than in its center. As a result of this phenomenon, the pulses of the slower moving particles are sized more accurately than those from the ones with greater velocity in the central core.

Improvement in resolution might be expected with this apparatus, therefore, by any mechanism that prolongs the sizing interval. Such prolongation could be accomplished by (a) slowing down the flow rate of the suspending solution; (b) increasing the sensing volume by physical elongation of the aperture; (c) forcing all particles into the slower moving peripheral areas by obstructing the central portion of the passage; or (d) increasing the critical volume of the electrical field around the aperture openings by the use of greater aperture currents than usually used.

Of these 4 possible means of improving resolution, the use of increased aperture currents (ApC) is technically the simplest and most easily varied. Some foundation for this approach to the problem is to be found in the recently reported work of Brecher et al. (2) that shows that frequency distribution curves of RBC volumes in a single blood sample show one mode at low ApC and two modes at high ones. Brecher

concluded that the appearance of the second modal frequency peak was due to a change in RBC size caused by the higher electrical currents.

Another interpretation of this finding may be that the higher currents enable better resolution of pulse heights so that large RBC are measured more accurately and resolved from the more numerous smaller RBC. The presence of such a large but unresolved subpopulation of large RBC in the size distribution curves of human RBC was suggested by Lushbaugh et al. (3) from a mathematical analysis of the curves based on the presence of 2 easily resolved subpopulations in the blood of birds. Since then, biological evidence for the presence of a volumetrically defined subpopulation of young RBC in mammals, as well as in birds, amphibia, reptiles, and fish, has been obtained (4,5), which makes improvement of the resolution of the Coulter counter pulses with human blood quite desirable.

METHODS AND RESULTS

Erroneous Sizing Caused by Coincidence

In the first series of experiments, the possibility was investigated that the second or larger volumed population ("B") of RBC was fictitious and due to doubling by coincidence. This possibility gained support from the fact that the mode

of the "B" population of birds was almost exactly twice that of population "A," although only 1.7 times as large in man. Figure 1 shows the result obtained when the blood of small birds was measured at the same electronic settings that failed to resolve two modal peaks in the blood of man. Although the concentration of RBC in both cases was the same, the two populations were easily defined in the bird at ApC V, g 4, ApD 100, pH 8.7 (the common settings) but not in man. Obviously, if the larger modal peak was due to coincidence, it should have been found with both blood samples. Figure 2 shows in a suspension of latex particles, which are known to consist almost entirely of monodispersed particles but also containing doublets, triplets, etc., due to agglutination, that appropriate ApC can resolve peaks with doubling modalities. This figure also shows how their apparent frequency can be increased by changing the readout scale of the pulse height analyzer memory bank. Attempts to change the frequency distribution curves of RBC by coincidence of particles by increasing the RBC/ml were unsuccessful because of the apparent inability of the Coulter counter amplifier circuitry to feed proper sized pulses to the analyzer at the counting rates used.

In the second series of experiments, RBC of different modal volumes obtained from different patients were used. In each experiment, the blood of two persons was sized separately

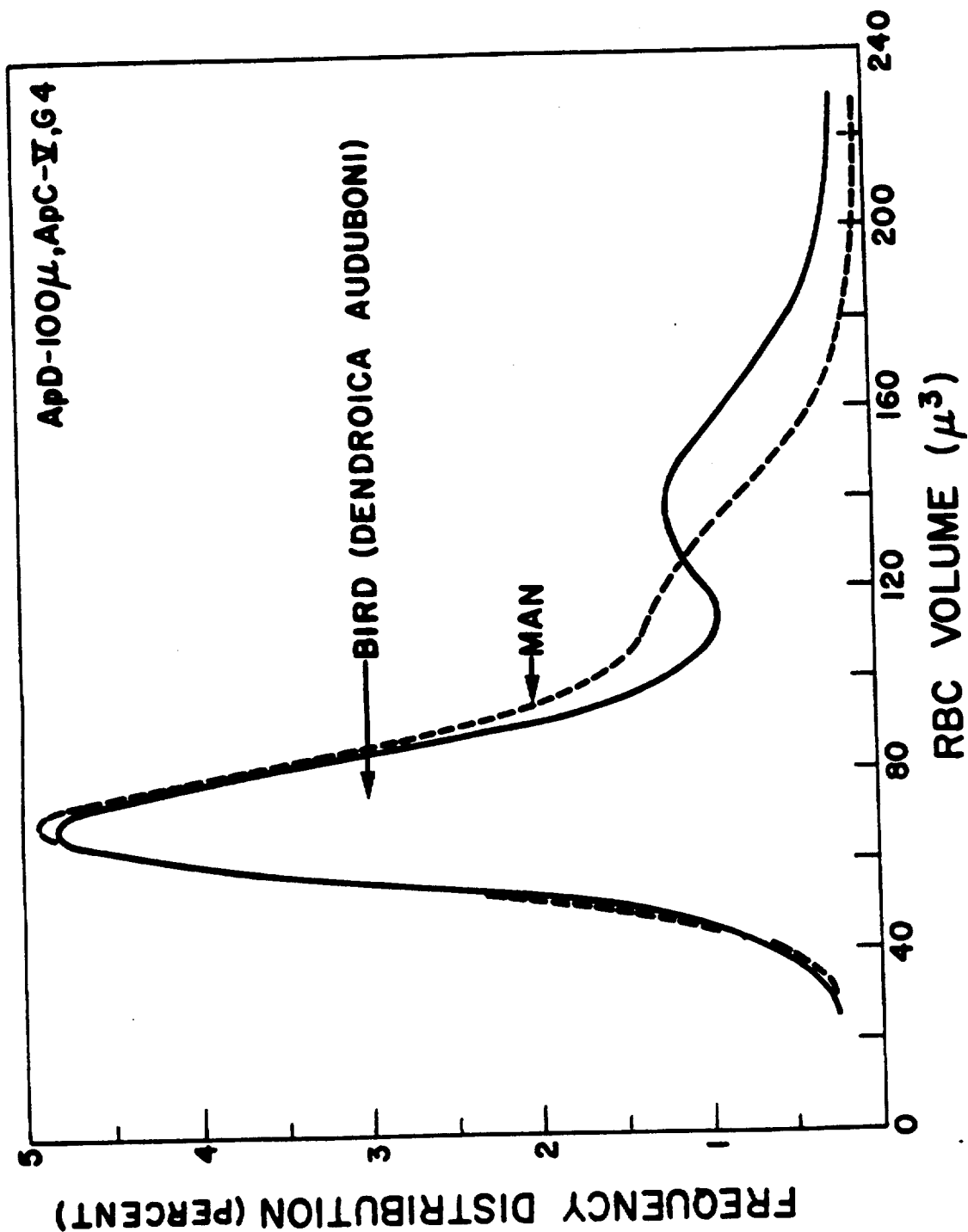


Fig. 1. Frequency distribution curves of RBC volumes of a bird and man determined under the same electronic and physical conditions, showing the resolution of two modes in the bird and only the suggestion of a second one in man.

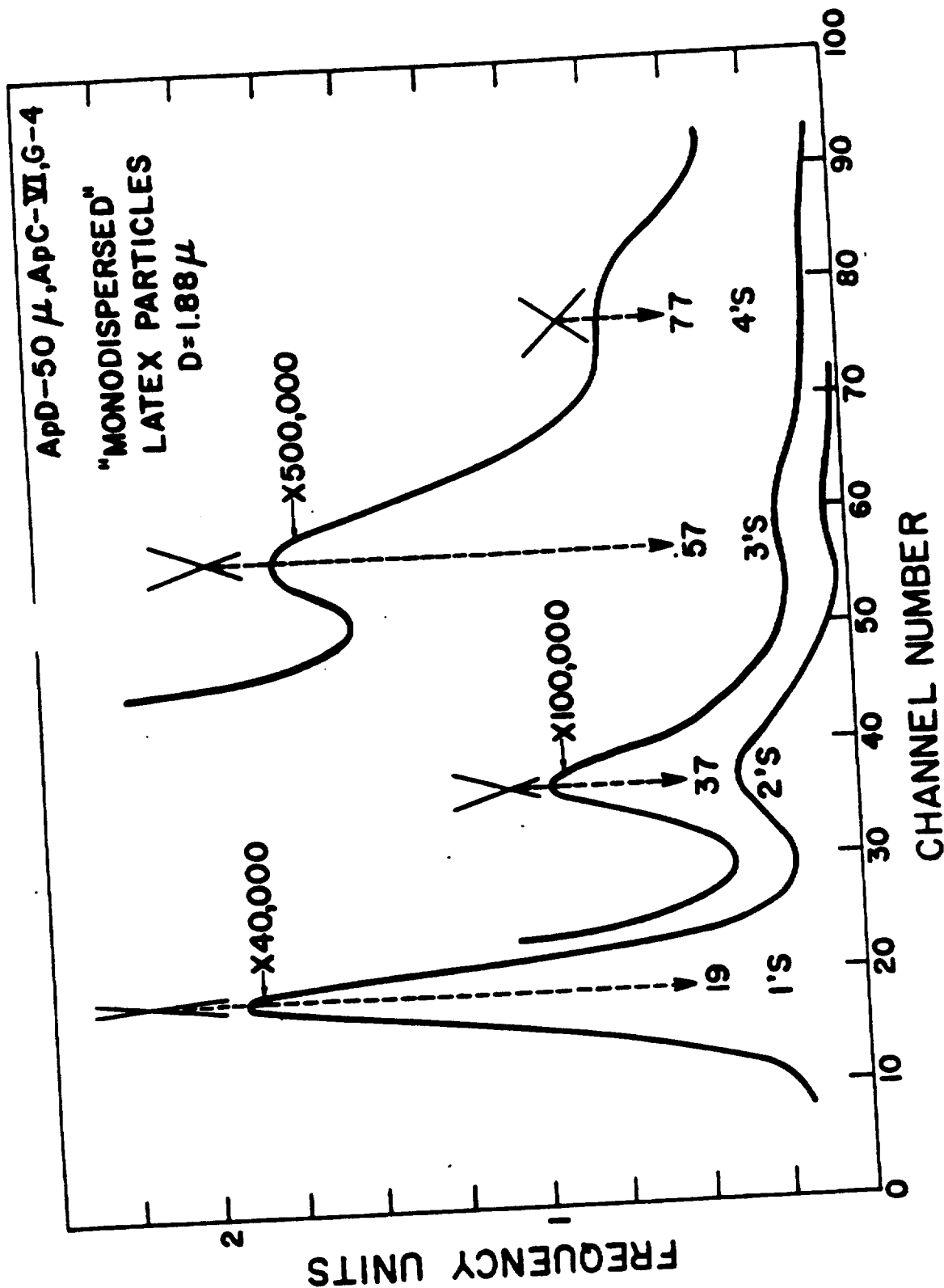


Fig. 2. Frequency distribution curves of monodispersed latex particles showing the coexistence of doublets, triplets, and quadruplets. The curves marked X 100,000 and X 500,000 are electronic magnifications of the X 40,000 curve.

at the "recommended" low ApC and g (2) and again at the highest ApC and g that seemed to resolve two subpopulations in human blood. The two frequency distribution curves that resulted were then summated, as with the shaded curves of Fig. 3. The summated curve was then transposed to another sheet of graph paper on the X-Y plotter, where it was designated the "predicted curve." An equal number of RBC from the blood of each person was then combined in vitro and suspended in the saline solution and analyzed. The resulting distribution of RBC volumes was then printed out mechanically upon the graph. The small open circles on the right-hand graphs in Fig. 3 show the excellent correspondence of the predicted and experimentally obtained curves. Comparison of the curves obtained with the different electronic settings shows quite well the better resolution of the modal peaks obtained with the higher ApC.

DISCUSSION AND CONCLUSIONS

These results seem to show that resolution of pulses from RBC passing through the sensing aperture of the Coulter counter is improved by increasing the ApC appropriately. They indicate that the appearance of double RBC populations does not result from enlargement of RBC due to excessive electrical current nor coincident pile-up. The conclusion would seem warranted that the presence of a second subpopulation

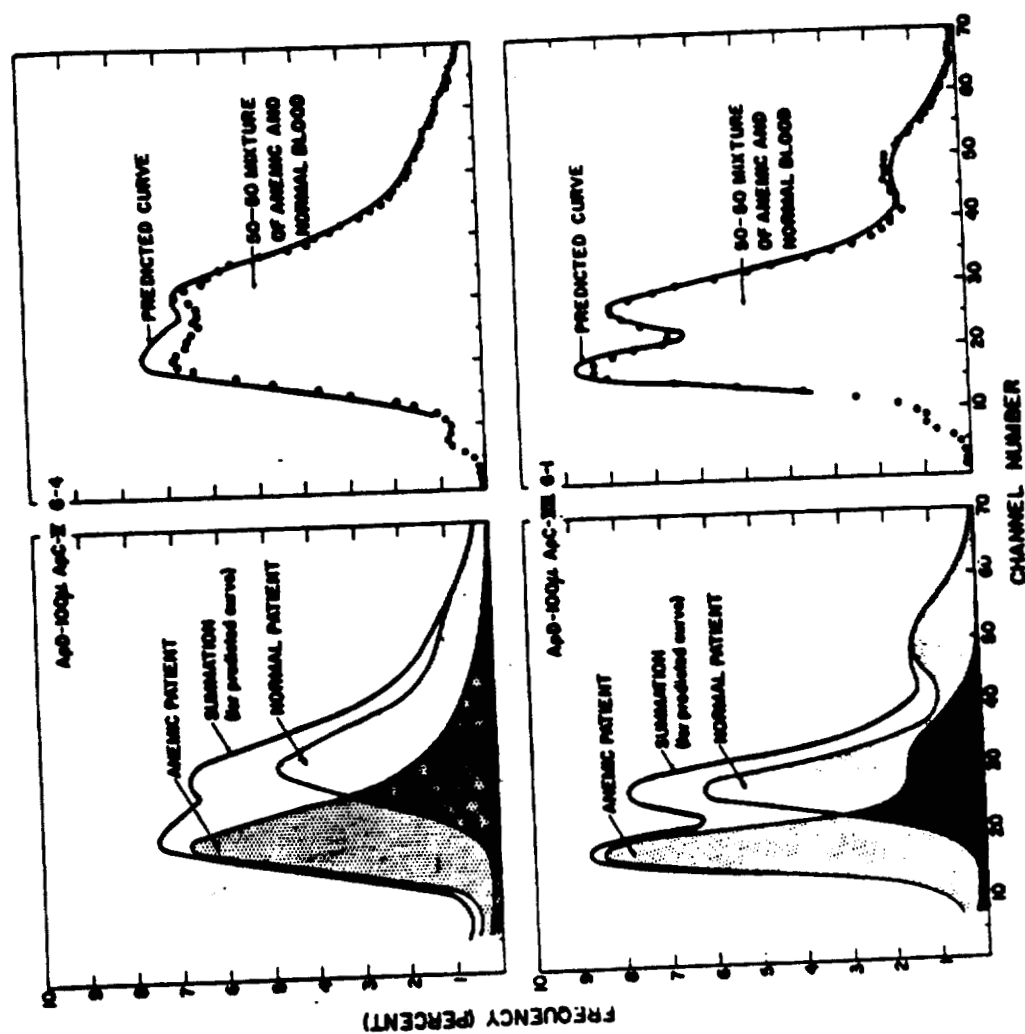


Fig. 3. Graphs showing improved resolution of the modal frequencies of distribution curves of RBC volumes by high ApC. Graphs on the left are superimposed curves of 2 blood samples analyzed separately; on the right, the curves of dots were obtained from analysis of a 50-50 mixture of the 2 blood samples.

of RBC, resolvable from another population of smaller modal size but more numerous individuals, is not due to an artifact of the techniques of measurement. This conclusion receives further support in the following study, which characterizes the "B" population as new and young RBC.

The increased resolution obtained here with increased aperture current would seem to encourage a search for other means of improving pulse generation so that RBC volume and pulse height have a more reliable constant relationship.

REFERENCES

- (1) H. E. Kubitschek, Research (London) 13, 128 (1960).
- (2) G. Brecher, E. F. Jakobieci, M. A. Schneiderman, G. Z. Williams, and P. J. Schmidt, Ann. N. Y. Acad. Sci. 99, 242 (1962).
- (3) C. C. Lushbaugh, N. J. Basmann, and B. Glascock, Blood 20, 241 (1962).
- (4) C. C. Lushbaugh and D. B. Hale, this report, p. 270.
- (5) C. C. Lushbaugh and E. S. Russell, this report, p. 279.

Electronic Measurement of Cellular Volumes. VII. Biologic Evidence for Two Volumetrically Distinct Subpopulations of Red Blood Cells (C. C. Lushbaugh and D. B. Hale)

INTRODUCTION

Some biologic support was reported previously (1) showing that it was possible to destroy red blood cells around the mode of population "A" and to leave a subpopulation of saponin-resistant red blood cells around the locus of the mathematically predicted mode of population "B." These results were obtained in the blood of man, as well as in birds where the "B" population does not require mathematical differentiation at aperture current V and gain setting 4.

The present study reports the refinement of these observations by the better resolution obtained by ApC VII, g 1 (2) and by the use of $\text{Fe}^{59}\text{SO}_4$ as a hemoglobin label in newly produced RBC.

METHODS

As in the previous study, increments of a 1:100 saponin solution were added to suspensions of human and rabbit RBC that were then sized electronically. In order to identify newly formed RBC, the rabbits were labeled with Fe^{59} ($10.3 \mu\text{C Fe}^{59}/\mu\text{g Fe}$) as FeSO_4 intravenously 3 days previously. The resulting changes in the distribution of cellular volumes were

then related graphically to saponin concentration so that the effect on 0.1 ml of blood of 1.0, 1.2, 1.4, 1.6, 1.8, and 2.0 ml of 1:100 saponin made up to 4.9 ml with saline could be determined. The hemolytic destruction was stopped after 1-1/2 minutes by (a) dilution of 0.05 ml aliquot to 100 ml for volumetric analysis, and (b) 3-minute centrifugation of the remainder. One-ml aliquots of the supernatant solution after centrifugation were then analyzed spectrophotometrically for hemoglobin content using cyanomethemoglobin, and another 1-ml aliquot was analyzed in a NaI (Tl) crystal-wall photo-spectrometer for Fe^{59} content.

RESULTS

The results of these experiments are shown graphically in Figs. 1, 2, 3, and 4. Figures 1 and 2 demonstrate that the hemolytic effect of saponin is dependent upon the saponin concentration and time of reaction. They also show that the volume distribution curves are shifted progressively to the right (large volumed RBC) as increasingly larger RBC are destroyed successively. As the result, the cells of population "A" are destroyed first and then those of population "B" are progressively hemolyzed. In Figs. 3 and 4, the frequency distribution curve of rabbit RBC has been related to the saponin concentration that was required to destroy all rabbit

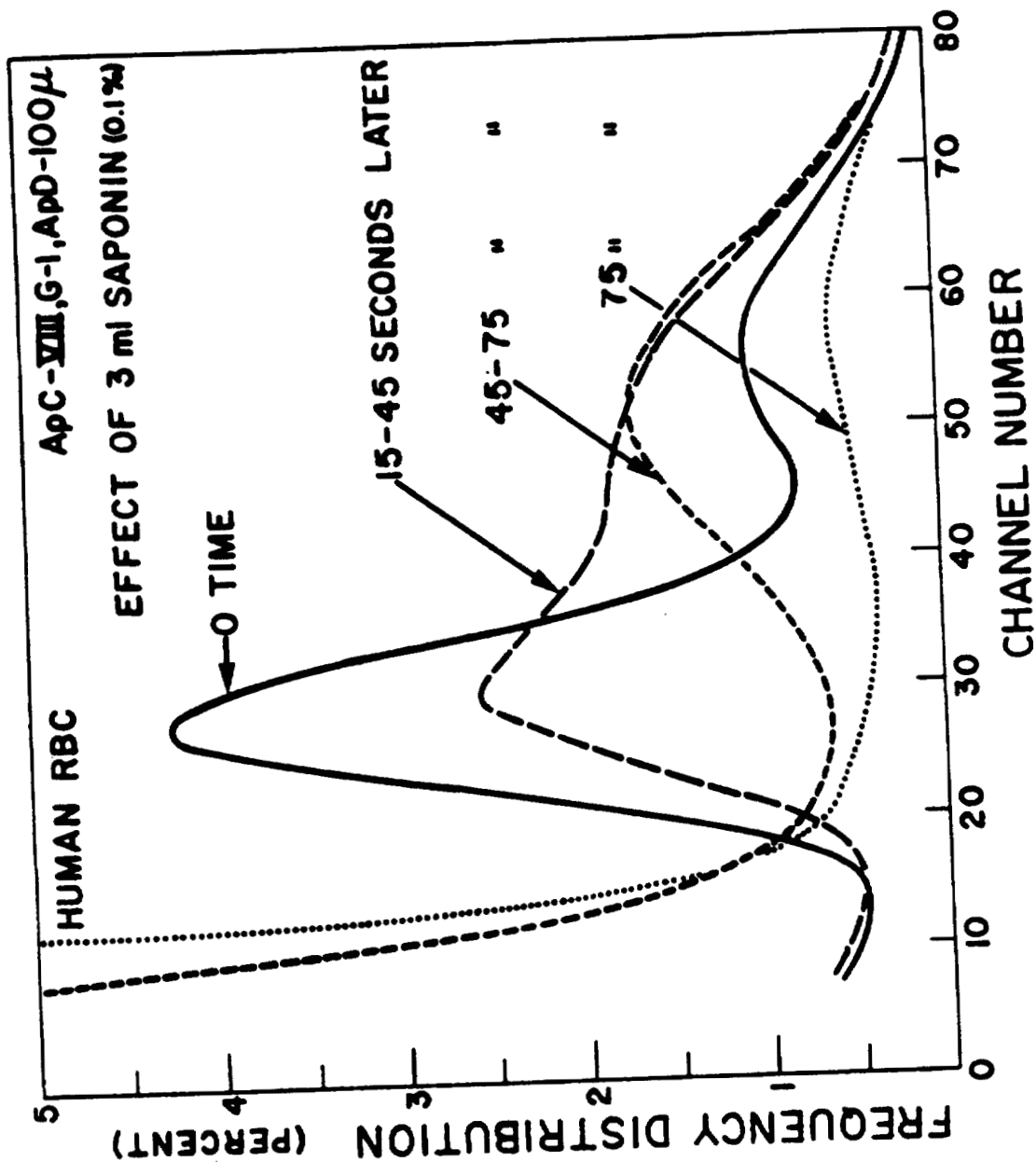


Fig. 1. Effect of saponin upon the frequency distribution of RBC volumes as a function of time after its addition.

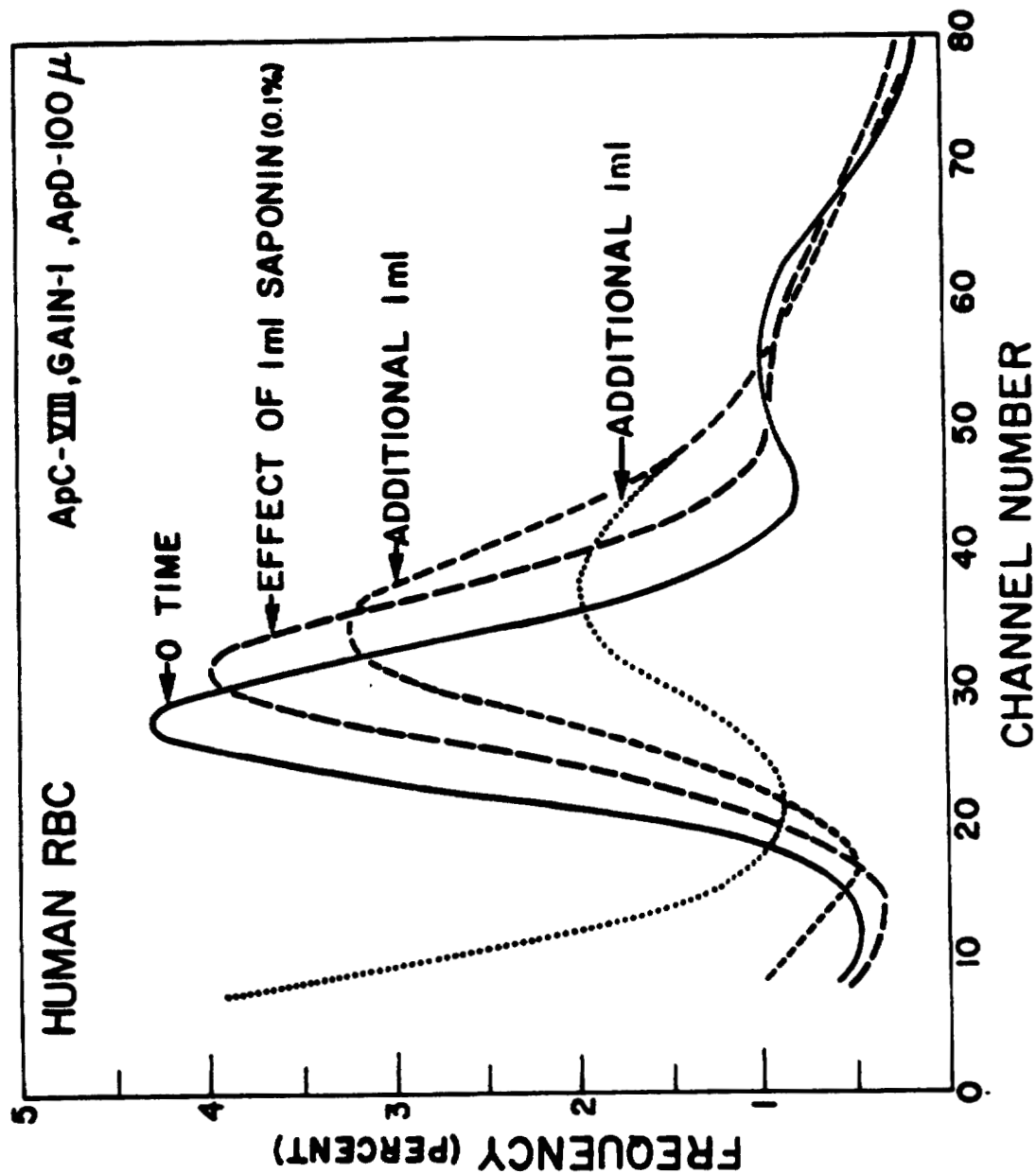


Fig. 2. Effect of increasing amounts of saponin upon the frequency distribution curves of RBC.

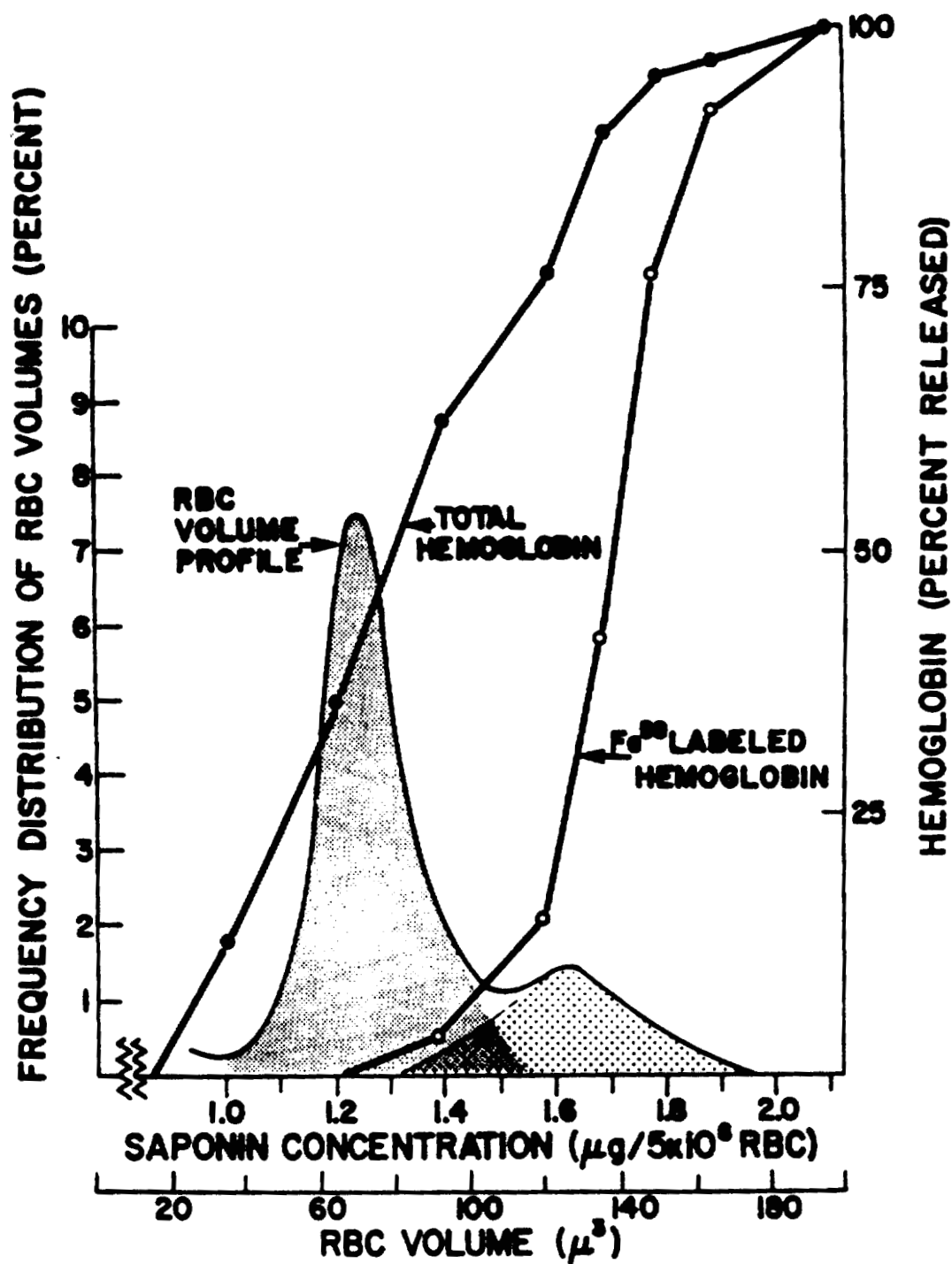


Fig. 3. Integrated curves of hemoglobin and Fe^{59} -labeled hemoglobin liberation by increasing saponin concentration shown in relation to the RBC volume frequency distribution curve of rabbits.

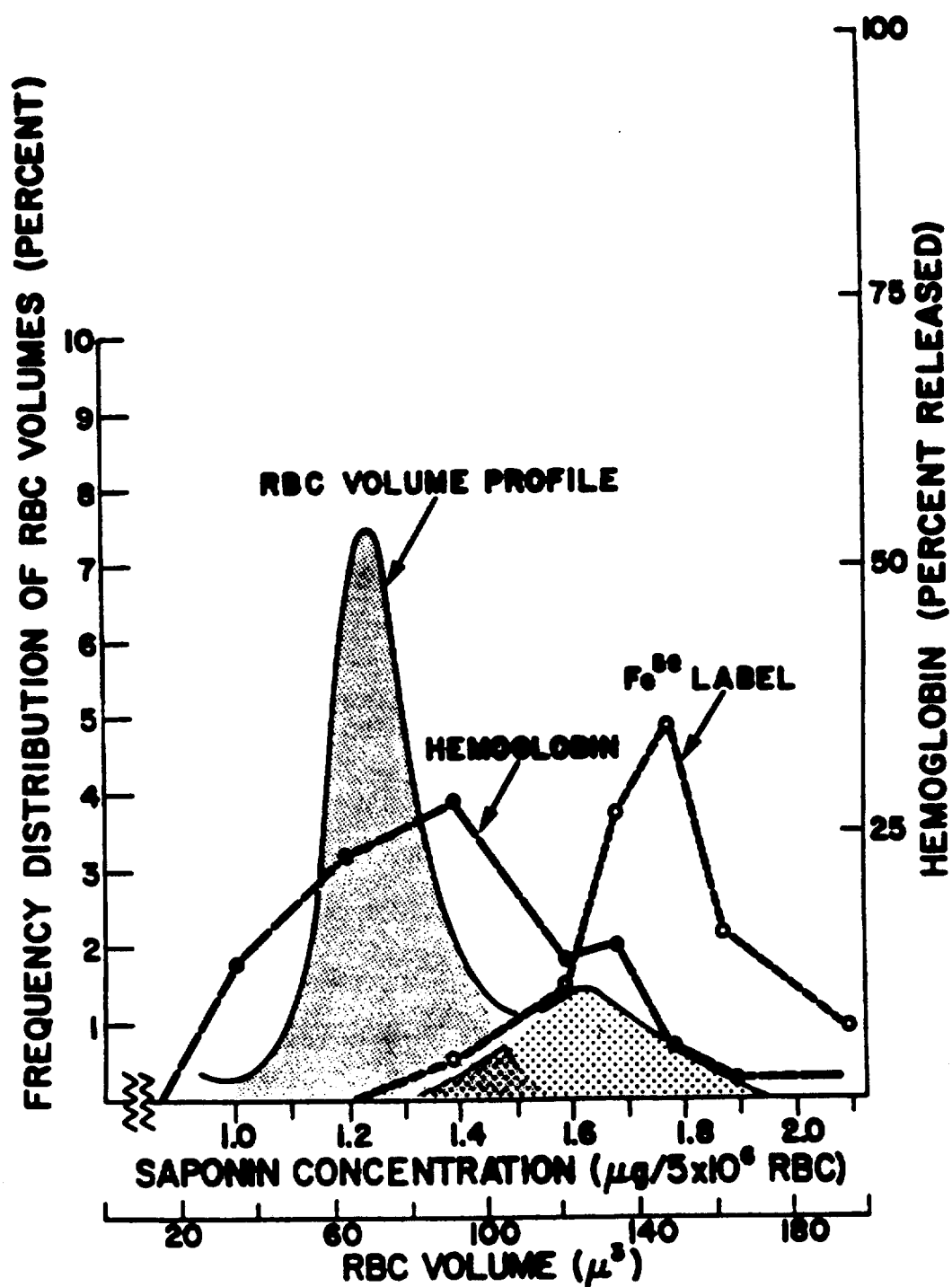


Fig. 4. Differentiated amounts of hemoglobin and Fe^{59} -labeled hemoglobin liberated by increasing saponin concentration in relation to the RBC volume frequency distribution curve of rabbits.

RBC smaller than that size. In Fig. 3, the total amounts of hemoglobin and Fe^{59} liberated by the destruction caused by the increments of saponin are shown. The same data are shown in Fig. 4 but are shown as the differential amount of hemoglobin and Fe^{59} liberated. The hemoglobin and Fe^{59} curves are dissimilar and disassociated; the largest amount of hemoglobin was unlabeled and released by destruction of population "A," and the largest amount of Fe^{59} labeled hemoglobin was obtained by destruction of the cells from the larger side of population "B."

DISCUSSION

These experiments demonstrate that the small RBC of population "A" are more sensitive to hemolysis by saponin than the large ones of population "B" and that the population of large RBC is composed of the youngest cells, since only this group of cells contained Fe^{59} -labeled hemoglobin 3 days after parenteral administration of radioactive iron. These conclusions would seem to justify alteration of the names of the bimodal peaks of RBC frequency distribution curves from "A" and "B" to "mature" and "immature," respectively. Although the names "old" and "young" might seem sufficiently descriptive and more adaptable to everyday usage, these terms do not embody the concept that RBC undergo maturation as they

age and decrease in size. Furthermore, the existence of two distinct modal frequencies in the distribution of the mature and immature RBC would seem to indicate that the process of RBC maturation is significantly shorter in duration than the mature life of the RBC. Experiments in progress with phenylhydrazine poisoned rabbits appear to show that the time involved in this volumetric change to mature size is about half of the rabbit RBC life span.

SUMMARY AND CONCLUSIONS

Taking advantage of the well-known facts that RBC sensitivity to hemolysis by saponin increases with RBC aging and that parenterally administered Fe^{59} labels RBC only as they are produced, experiments were done which showed that hemoglobin released by saponin destruction of the two subpopulations of RBC was unlabeled when only the smaller volumed RBC of population "A" were lysed. The Fe^{59} label was found in the larger volumed RBC of population "B." These findings are considered biologic evidence for the existence of two distinct subpopulations of RBC and for the belief that the bimodal frequency distribution curve of RBC volumes obtained with the LASL cell volume analyzer system is not artifactual. It is suggested, therefore, that these subpopulations be renamed as "mature" and "immature" RBC, rather than "A" and "B."

REFERENCES

- (1) C. C. Lushbaugh, N. J. Basmann, and H. Israel, Los Alamos Scientific Laboratory Report LAMS-2780 (1962), pp. 198-202.
- (2) C. C. Lushbaugh, N. J. Basmann, and D. B. Hale, this report, p. 261.

Electronic Measurement of Cellular Volumes. VIII. Volumetric Change of Circulating Erythrocytes in WW^V Genetically Anemic Mice Implanted with $w+w+$ Fetal Liver (C. C. Lushbaugh and E. S. Russell*)

INTRODUCTION

The genetically determined macrocytic anemia of WW^V mice can be "cured" by a single intraperitoneal injection of normal hematopoietic tissue contained in hepatic brei from 15-day $w+w+$ fetuses (1,2). As the number of red blood cells increases, the mean cell volume decreases to normal values, and the electrophoretically diffuse hemoglobin pattern changes to the "single" type of normal mice. Thus, the cure of the anemia appears to result from the actual replacement of the anemic cells by the implanted normal cells rather than from a change in the macrocytic cells of the host.

METHODS

In order to obtain additional support for this conclusion and to determine whether macrocytic WW^V RBC continue to be produced in chimeric implanted $W++/WW^V$ mice, the distribution of RBC volumes was studied in the anemic, donor, and chimeric animals using the cell volume analyzer system devised for the Coulter counter in Los Alamos (3). First, the blood

*From the Roscoe B. Jackson Memorial Laboratory, Bar Harbor, Maine.

of implanted WV^V mice known by their electrophoretic hemoglobin patterns to be "failures" or "cures" was studied. When the feasibility of the method was thereby established, the blood of the implanted mice was analyzed at 3-week intervals following implantation in order to determine the time required for the implant to succeed or to fail. The mice were bled from the orbital plexus by capillary pipette. The blood was diluted to 1:1,000,000 and suspended in 0.9 per cent saline buffered at pH 6.0. The Coulter counter (Model A) settings were ApC VIII, g 2, for which the scaling factor for conversion of analyzer channel to cubic microns was 1.60 (3).

RESULTS

The results of these studies (Fig. 1) showed that the blood from both the anemic and normal mice had a bimodal curve of RBC volumes as previously described (4). The macrocytosis, as might be expected, was seen by this method as a displacement of the two populations to the right or large volume. In those mice in which the hemoglobin pattern had indicated implant failure, the RBC volumes did not decrease (Fig. 1c), while the volumes were almost identical with the normal volume distribution when the implant was successful (Fig. 1d).

The results of the second experiment (Fig. 2) showed

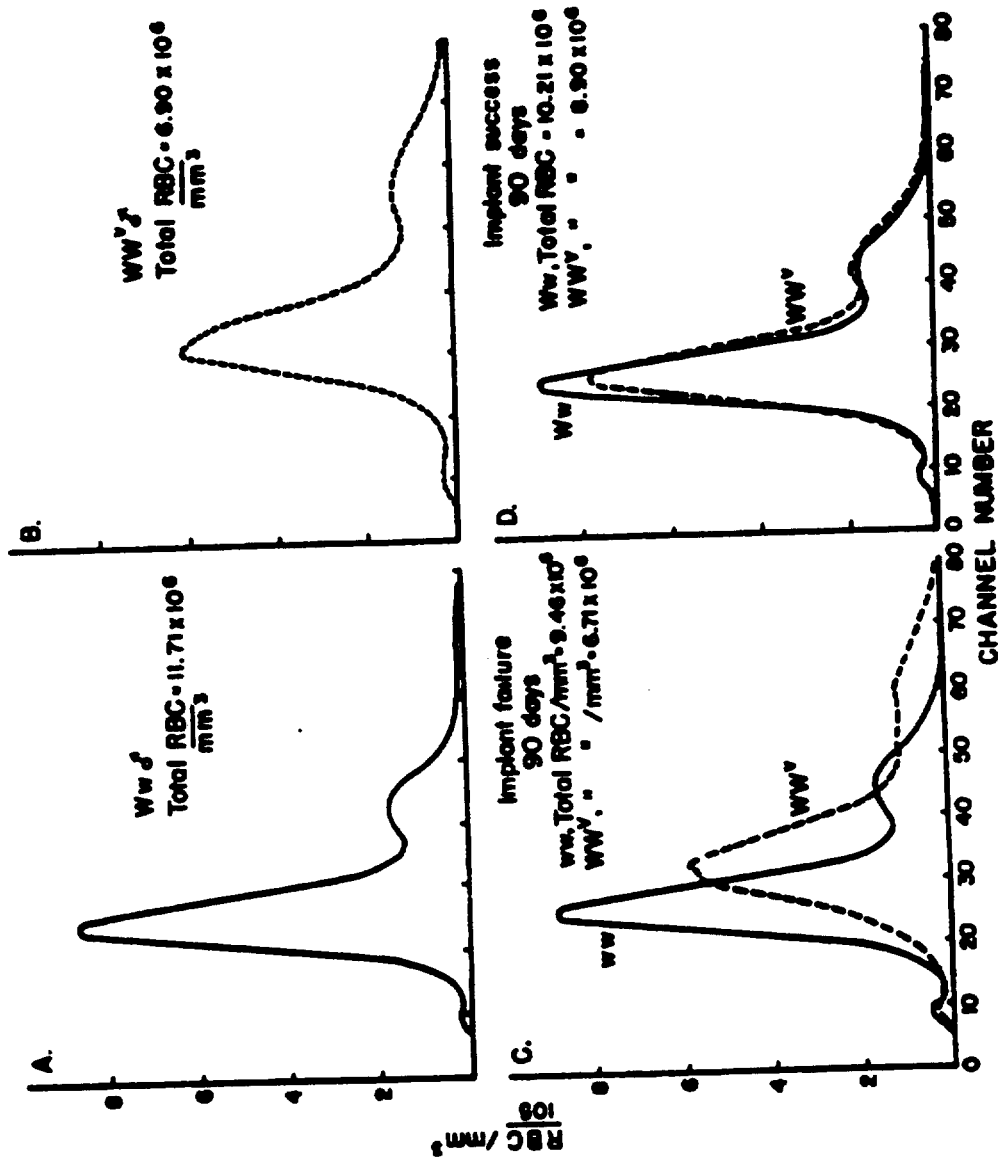


Fig. 1. Frequency RBC volume distribution profiles of (a) normal Ww mouse; (b) macrocytic anemic Ww mouse; (c) normal Ww mouse compared to a Ww mouse (dotted line) in which the w+w+ implant failed; and (d) normal Ww mouse compared to a Ww mouse (dotted line) in which the implant success is indicated by the shift of volumes to normal.

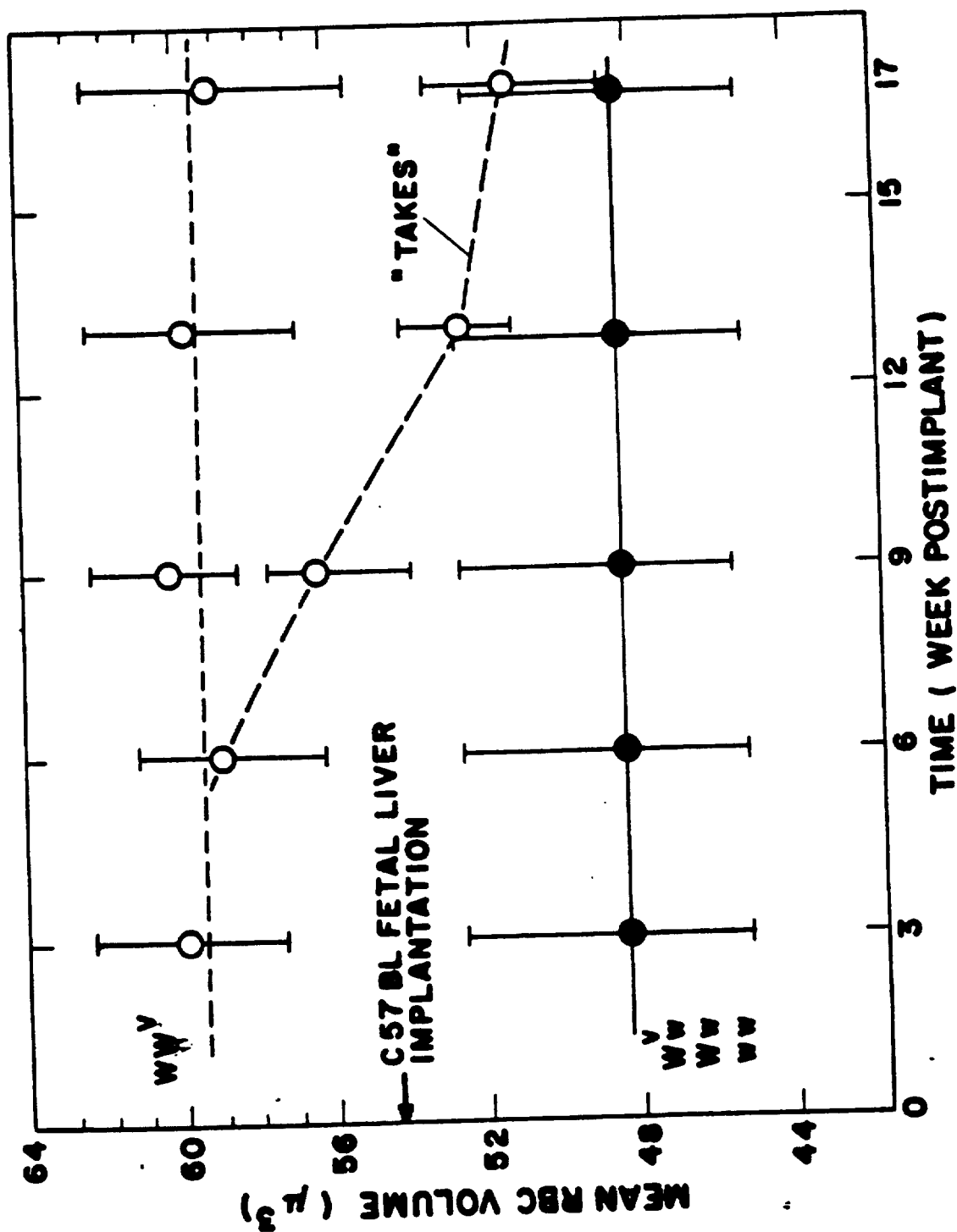


Fig. 2. Change in mean RBC volumes determined electronically in w^v anemic mice as a function of time after implantation with $w+w+$ hematopoietic tissue.

that RBC volumes commence decreasing measurably about 6 weeks after implantation and by 17 weeks are almost identical with those of normal mice (Table 1). The distribution profiles during this period of change first showed a decrease in the mode of the subpopulation of young RBC ("B"). This shift was followed by a shift in the mode of the old population ("A") until the profiles coincided as in Fig. 1d. Whether the resolution of the apparatus is not sufficiently precise, the variance of sizes too large, or the change in RBC size with age too rapid, the presence of two competing bone marrows (WW^V and $w+w+$) was not demonstrable by sizing their production of RBC using peripheral blood. The orderly change in frequency of the RBC and the volumes of the two subpopulations, however, confirmed morphologically the conclusion based previously on hemoglobin types that the $w+w+$ marrow supplanted the WW^V anemic marrow. An explanation of the failure to see two separate young populations at the stage when theoretically the normal (normocytic) and the abnormal (macrocytic) marrows are competing side by side may be that the presence of $w+w+$ hemopoietic cells suppresses the less vigorous WW^V marrow before the new smaller volumed RBC are delivered into the peripheral blood in sufficient numbers to be seen by this electronic method of measurement.

TABLE 1. COMPARISON OF SOME PARAMETERS OF THE DISTRIBUTION PROFILES OF THE RBC
VOLUMES OF NORMAL AND "CURED" ANEMIC MICE

	Modal Frequency (per cent)		Mode (μ^3)		Variation ($\bar{V} - 1/2 H$) (μ^3)	
	1*	2**	1*	2**	1*	2**
Population "A"	6.0	5.7	44.4	46.7	18.1	18.9
MCV			48.3	51.0		
Population "B"	1.8	1.7	79.0	81.0	23.5	25.3

* w^v , Ww , $W^v w$ mice.

** $w^v w^v/w+w+$ mice 17 weeks after implantation.

CONCLUSIONS

These findings imply that after successful implantation, the chimeric blood is derived entirely from the implant even though nothing was done experimentally to destroy the genetically determined macrocytic marrow of the host.

REFERENCES

- (1) S. E. Bernstein and E. S. Russell, Proc. Soc. Exptl. Biol. Med. 101, 769 (1959).
- (2) E. S. Russell, Fed. Proc. 19, 573 (1960).
- (3) C. C. Lushbaugh, D. B. Hale, and N. J. Basmann, this report, p. 235.
- (4) C. C. Lushbaugh, N. J. Basmann, and B. Glascock, Blood 20, 241 (1962).

CLINICAL INVESTIGATIONS SECTION

PUBLICATIONS

(1) C. C. Lushbaugh, J. A. Maddy, and N. J. Basmann, Electronic Measurement of Cellular Volumes. I. Calibration of the Apparatus, Blood XX(2), 233 (1962).

(2) C. C. Lushbaugh, N. J. Basmann, and B. Glascock, Electronic Measurement of Cellular Volumes. II. Frequency Distribution of Erythrocyte Volumes, Blood XX(2), 241 (1962).

(3) C. C. Lushbaugh, A Fatal Hyperplastic Inflammatory Lesion of the Stomach of Mice Exposed to Neutrons from an Atomic Bomb, Arch. Path. 74, 297 (1962).

(4) C. C. Lushbaugh and J. Langham, A Dermal Lesion from Implanted Plutonium, Arch. Dermatol. 86, 461 (1962).

(5) C. C. Lushbaugh, A Universally Applicable Method for Assaying Thyroid Function in Vertebrates, Nature 198(4883), 862 (1963).

(6) C. C. Lushbaugh and R. L. Schuch, Clinical Use of the Arm Counter in Blood Clearance Studies, In: Advances in Tracer Methodology, Vol. 1, Proceedings of the Fifth Annual Symposium on Tracer Methodology, held on October 20, 1961, Washington, D. C. (S. Rothchild, ed.), Plenum Press, New York (1963), pp. 314-325.

MANUSCRIPTS SUBMITTED

(1) G. L. Humason and P. C. Sanders, Cultivation and Slide Preparation of Mammalian Peripheral Blood Leukocytes, submitted to Stain Technology.

(2) C. C. Lushbaugh and D. B. Hale, Determination of Absorbability of Oral Radioiron in Health and Disease in Man by Whole-Body Scintillometry, to be published in the Proceedings of the Second Symposium on Radioactivity in Man, Northwestern University Medical School, Chicago, Illinois (September 5-7, 1962).

CHAPTER 6

CELLULAR RADIOBIOLOGY SECTION

Preparation of Bacterial Deoxyribonucleic Acids (I. U. Boone and E. Campbell)

INTRODUCTION

A number of investigations are in progress in this Laboratory which require the use of homogeneous high molecular weight deoxyribonucleic acid (DNA). One investigation involves an attempt to characterize resins by their ability to differentiate DNA not only on the basis of molecular weight but also on the basis of base composition of the DNA. Therefore, in addition to attempting to obtain DNA of high molecular weight, a number of different bacterial DNA's are being prepared that have a wide difference in base composition ratios.

METHODS AND DISCUSSION

A list of the bacteria from which DNA is being obtained

and characterized by guanine-cytosine ratios is given in Table 1. To date, approximately 100 mg of DNA has been obtained from *Micrococcus lysodeikticus* and *Serratia marcescens*. The *M. lysodeikticus* was grown in a tryptone-yeast extract, and *S. marcescens* was grown in nutrient broth. Both organisms were grown and aerated at room temperature. The cells were lysed in both instances by sodium lauryl sulfate and the DNA extracted by using a chloroform-alcohol procedure similar to that described by Marmur (2). Cell lysis of *Staphylococcus aureus* has been a much more difficult problem. The enzyme lysozyme has been used at pH 8 to 10. Yields have been low and, at present, other methods of cell lysis are under investigation.

Hemophilus influenzae DNA (streptomycin-resistant) has been obtained routinely in small quantities by the alcohol precipitation method for genetic transformation studies. The cells are grown in a mixture of Levinthal and Eugon broth. The cells are lysed with 10 per cent sodium deoxycholate. Sufficient quantities of DNA have been obtained from *M. lysodeikticus*, *S. marcescens*, and *H. influenzae* for molecular weight determinations. Molecular weights determined from sedimentation data in the Spinco Model E centrifuge at $\eta = 0.5$ was 1.69×10^7 for *H. influenzae*, 1.3×10^7 for *S. marcescens*, and 1.7×10^7 for *M. lysodeikticus*.

TABLE 1. REPORTED GUANINE-CYTOSINE RATIOS OF CERTAIN BACTERIAL DNA'S (1)

Microorganism	Guanine-Cytosine Content (mole fraction)
<i>Micrococcus lysodeikticus</i> ATCC* 4698	0.72
<i>Sarcina lutea</i> ATCC 9341	0.64-0.74
<i>Serratia marcescens</i> ATCC 264	0.58
<i>Staphylococcus aureus</i> ATCC 10831	0.31-0.38
<i>Hemophilus influenzae</i> Rd	0.38
<i>Escherichia coli</i> B	0.51

*ATCC - American Type Culture Collection, Washington, D. C.

DNA from *Escherichia coli* B has been obtained comparing two methods of cell lysis for quantitative yield and molecular weight. The organisms were grown in nutrient broth at 37° C for 18 hours. The bacteria were centrifuged, washed, and resuspended in a solution of 0.15 M NaCl, 0.015 M trisodium citrate, plus 0.1 M ethylenediaminetetraacetate (EDTA) at pH 8. The cell suspension was divided into approximately equal aliquots. One aliquot of cell suspension was lysed with 10 per cent sodium deoxycholate at pH 10 and the other with lysozyme also at pH 10. After lysis, the pH was rapidly adjusted to neutral. The DNA from each suspension of lysed cells was extracted and treated identically by the chloroform-alcohol method as previously described (2). The yield of DNA per gram of wet weight of cells based on DNA phosphorus determinations and the molecular weight results obtained by the sedimentation method are shown in Table 2. Not only was the yield of DNA lower from the cells which had been lysed with lysozyme, but the molecular weight was only half that of the DNA from cells lysed with 10 per cent deoxycholate.

The lower yield obtained in the lysozyme system could be partially explained on the basis of incomplete cell lysis, but the lower molecular weight obtained with the lysozyme can most likely be explained on the basis of DNase activity.

**TABLE 2. COMPARISON OF YIELD AND MOLECULAR WEIGHT OF DNA
OBTAINED FROM ESCHERICHIA COLI B BY VARYING THE
METHOD OF CELL LYSIS**

Method of Cell Lysis	DNA Yield (mg/gm wet weight of cells)	Molecular Weight (h = 0.5, Time in Sec, 720 - 960)
10 Per cent Deoxycholate	0.375	2.09×10^7
Lysozyme	0.259	1.15×10^7

Although EDTA and/or high pH both inhibit DNase activity, it appears that the inhibition was not sufficient or as effective in the lysozyme system. Perhaps the addition of a detergent such as sodium lauryl sulfate during lysozyme cell lysis, rather than after cell lysis as suggested by Marmur (2), would act as an additional DNase inhibitor. The present results tend to indicate that cell lysis by lysozyme should be avoided when possible if high molecular weight DNA is desired.

A preliminary attempt to isolate high molecular weight DNA from *E. coli* B by a modified phenol method (3) has been unsuccessful. Nine grams of *E. coli* B were lysed with 10 per cent deoxycholate in a citrate-saline and EDTA solution at pH 10. Sodium perchlorate was added to a final concentration of 1.0 M to help dissociate protein from nucleic acid. The whole mixture was treated once with chloroform-isoamyl alcohol, and the separated aqueous phase was precipitated with ethyl alcohol (2). The precipitated DNA was dissolved in a dilute citrate-saline and the mixture shaken for 25 minutes with an equal volume of phenol as described by Mandell et al. (3). The two phases were separated, and the aqueous DNA-containing phase was treated with ribonuclease. This was followed by an additional phenol extraction. The resulting DNA solution was dialyzed

against citrate-saline for 4 days to remove traces of phenol. Determinations by the Lowry method (4) were negative for the presence of protein and phenol.

Although a spectrophotometric and DNA-phosphorus analysis indicated the presence of from 100 to 150 mg of DNA/ml, a molecular weight of the preparation could not be obtained as the DNA did not clear in the ultracentrifuge. Either the molecular weight of the DNA was low due to shearing or denaturation effects of the procedure and/or some undetected interfering substance (protein, phenol, etc.) was present in the preparation to prevent the clearing of the DNA. Further attempts to obtain high molecular weight bacterial DNA are in progress.

ACKNOWLEDGMENT

The authors are indebted to Dr. George R. Shepherd and Mrs. Billie J. Noland of the Molecular Radiobiology Section for the molecular weight determinations.

REFERENCES

- (1) A. N. Belozersky and A. S. Spirin, Chemistry of Nucleic Acids of Microorganisms, Chapter 32, In: The Nucleic Acid (E. Chargaff and J. N. Davidson, eds.), Academic Press, New York (1960), pp. 147-185.
- (2) J. Marmur, J. Mol. Biol. 3, 208 (1961).
- (3) J. D. Mandell and A. D. Hershey, Anal. Biochem. 1, 66 (1960).
- (4) O. H. Lowry, N. J. Rosebrough, A. L. Farr, and R. J. Randall, J. Biol. Chem. 193, 265 (1951).

Purification and Concentration of T-4 Bacteriophage on DEAE-Cellulose Columns for DNA Isolation (I. U. Boone and E. Campbell)

INTRODUCTION

Many of the earlier methods for isolation and purification of T-phages required the use of differential centrifugation and acid precipitation techniques (1). Creaser and Taussig (2) recently described a method for purification of T-1 and T-2 phages using the cellulose anion-exchange adsorbent ECTEOLA. To facilitate the method and to increase the yields for isolation of phage deoxyribonucleic acid (DNA), a method has been developed for purification and concentration of T-4 phage on DEAE-cellulose adsorbent columns. Phenol-extracted T-4 phage DNA has been prepared from phage obtained by this method.

METHODS AND RESULTS

Preparation of Lysates

Escherichia coli B was grown in a 37° C shaking water bath on Fraser and Jerrel's glycerol-casein-hydrolysate medium (3) to 3.8×10^8 cells/ml. The bacteria were infected with T-4 phage to a concentration of 2.5×10^8 phage particles/ml. L-Tryptophane (10 µg/ml) was added as a co-factor with the infecting phage. One gram $MgSO_4$ /liter was

added as recommended by Fraser and Jerrel. Spontaneous lysis was allowed to occur for 9 hours. Lysates contained approximately 2×10^{11} plaque-forming units/ml and were stored at 4° C until purified.

Purification

Two and one-half grams of hyflow filter-cell (Celite) were added per liter of lysate and the suspension filtered on a Buchner funnel with a 3- to 5-mm pad of hyflow filter-cell covering a No. 3 Whatman filter paper (1). The filtered lysate was centrifuged at 6000 RPM in a Servall SS-3 centrifuge for 30 minutes. The supernatant contained 1.5×10^{11} plaque-forming units/ml. The bacteriophages were assayed by the standard methods (4). Estimates of the phage concentrations in the different lysate fractions could be made also by optical density measurements of the virus turbidity at $E = 400 \text{ m}\mu$, as suggested by Herriott et al. (1). A typical turbidity versus virus titer curve is shown in Fig. 1.

Concentration of Phage on DEAE-Cellulose Column

The adsorbing column was prepared by mixing 250 ml glycerol-casein-hydrolysate medium with 10 g of DEAE-cellulose (Cellex D, anion-exchange cellulose, Bio-Rad Laboratories) with an exchange capacity of 0.94 milliequivalents per g and

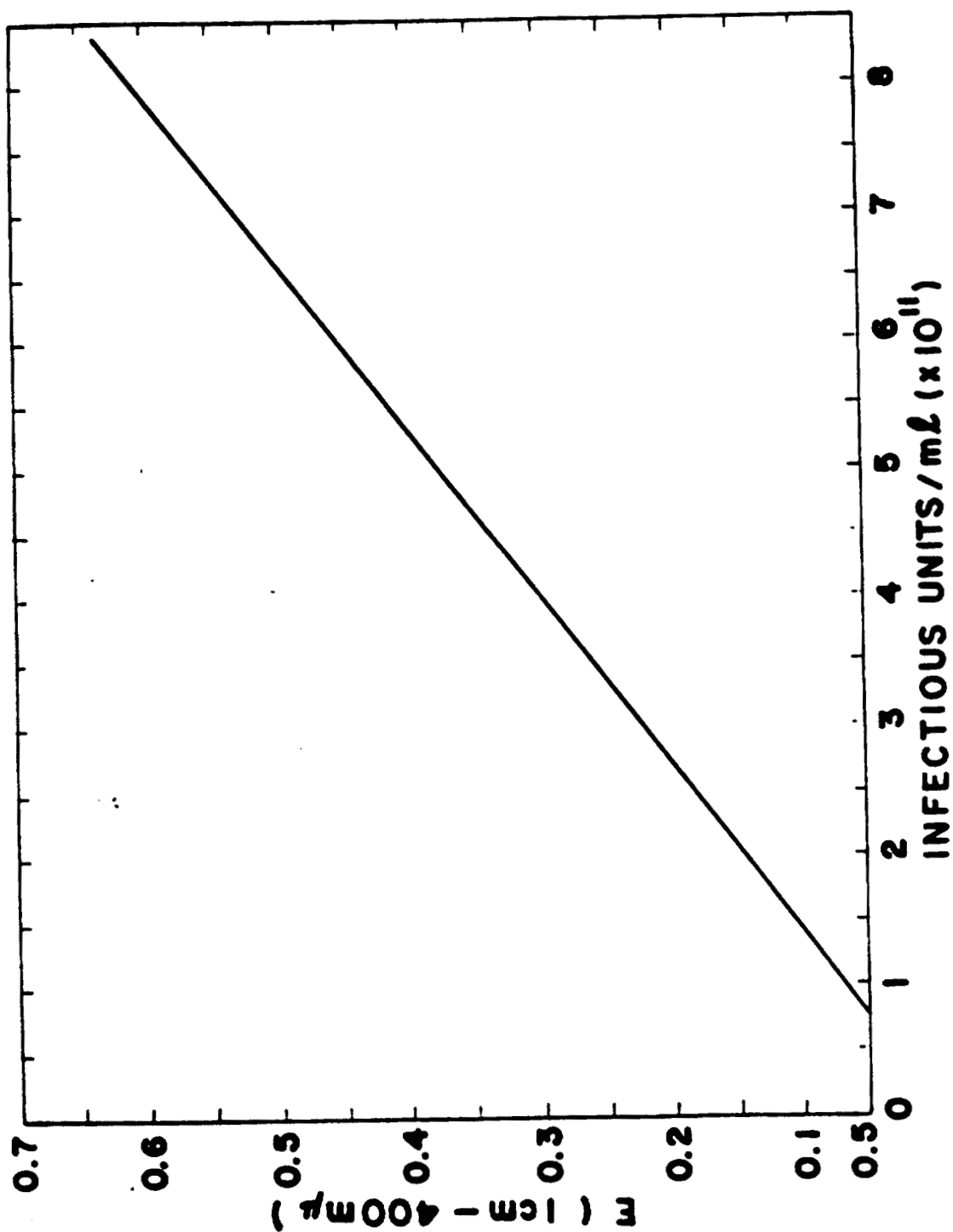


Fig. 1. Turbidity versus virus titer. The straight line was calculated from the average of a number of points of purified virus. Optical density was read at 400 m μ on a Bausch and Lomb Spectronic 20.

let stand for 15 minutes. The supernatant was decanted and the washing repeated with 400 ml of medium. A 20-mm I. D. x 400-mm L.GT column was filled with the washed DEAE. A column of this size permitted the adsorption of virus from 250 ml of lysate with a virus concentration of $\approx 2 \times 10^{11}$ particles/ml. A larger column (40-mm I. D. x 600-mm L.GT) could be prepared with 50 g of medium-washed DEAE-cellulose. Virus from 700 ml of lysate could be adsorbed on this column.

Elution of the virus from the column was attempted at salt concentrations ranging from 0.1 to 0.7 M NaCl in 0.01 M phosphate buffer. Each column containing adsorbed virus from 250 ml was eluted with 100 ml of NaCl solution of the designated salt concentration and the eluate collected in 4 separate fractions. The optical density was measured for each fraction and, wherever indicated, plaque counts were performed. A summary of the data is shown in Table 1. For salt concentrations ranging from 0.1 to 0.6 M, the average optical density and number of infective units/ml are given for each fraction. At the concentration of 0.7 M NaCl, the optical density and plaque count/ml are given for each fraction. By combining fractions 2 and 3, 250 ml of virus lysate may be concentrated into 50 ml of virus with a yield of 66 per cent of the virus in this portion. By reducing the eluting volume of 0.7 M NaCl, it is possible to collect

TABLE 1. DESORPTION OF T-4 BACTERIOPHAGE FROM DEAE-CELLULOSE ION EXCHANGE ADSORBENT

Fractions Eluted from DEAE at NaCl (concentration)	Optical Density	Plaque Count (number of infective centers/ml)
0.1 M	0.08	$> 5 \times 10^{10}$
0.2 M	0.12	1×10^{11}
0.3 M	0.03	$> 5 \times 10^{10}$
0.4 M	0.04	$> 5 \times 10^{10}$
0.5 M	0.013	$> 5 \times 10^{10}$
0.6 M	0.01	$> 5 \times 10^{10}$
0.7 M Fraction 1 (25 ml)	0.120	1×10^{11}
Fraction 2 (25 ml)	0.255	4×10^{11}
Fraction 3 (25 ml)	0.445	5×10^{11}
Fraction 4 (25 ml)	0.08	3×10^{10}

~70 per cent of the virus in a volume of 15 ml with a virus concentration of $\sim 2 \times 10^{12}$ particles/ml. In contrast, the yields obtained by using differential centrifugation methods vary over a wide range, and the procedure is time-consuming.

Isolation of DNA

The concentration of phage as eluted from the DEAE-cellulose columns was $\sim 2 \times 10^{12}$ particles/ml in 0.7 M NaCl plus 0.01 M phosphate buffer. Although the virus concentration was that desired for DNA extraction, the salt concentration was in excess of that recommended by the phenol extraction method of Mandel and Hershey (5). Therefore, the small volumes (15 to 50 ml) of concentrated phage were centrifuged for 1 hour at 20,000 x g in a Spinco Model L centrifuge and the virus pellet resuspended in 0.1 M NaCl plus 0.1 M phosphate buffer at a phage concentration of 2×10^{12} phage particles/ml. The DNA was then extracted by the phenol method (5), except that the dissolved phenol in the aqueous was removed by dialysis instead of by shaking with ether. The dialysis was carried out against the phosphate-buffered saline for 4 days. For phosphorus and molecular weight determinations of the DNA, the phosphorus was removed by dialysis against distilled water for 4 to 5 days.

A phosphorus analysis of the T-4 phage DNA revealed

that a concentration of 2×10^{12} phage particles/ml yielded 0.5 mg/ml of DNA, and a spectrophotometric analysis and a Dische diphenylamine determination agreed with the phosphorus analysis data.

Molecular weight determined from sedimentation data in the Spinco Model E centrifuge was 2.1×10^7 at $h = 0.5$. This agreed with data of DNA obtained from T-4 phage prepared by differential centrifugation. The relatively low molecular weight values are most likely the result of shearing effects during the phenol shaking-extraction procedure. A modification of this method is in progress.

REFERENCES

- (1) R. M. Herriott and J. L. Barlow, J. Gen. Physiol. 36, 17 (1952).
- (2) E. H. Creaser and A. Taussig, Virology 4, 300 (1957).
- (3) D. Fraser and E. A. Jerrel, J. Biol. Chem. 205, 291 (1953).
- (4) M. H. Adams, Bacteriophages, Interscience, New York (1959).
- (5) J. D. Mandel and A. D. Hershey, Anal. Biochem. 1, 66 (1960).

Chromosome Observations in Nonirradiated Progeny from
Several Lines of Irradiated RF Males (I. U. Boone, P. M.
LaBauve, and J. F. Spalding)

INTRODUCTION

The genetic consequence of X irradiation to progeny of 10, 15, and 20 generations of irradiated male mice is being studied extensively in this Laboratory by one of the authors (Spalding). His results have indicated that the main difference between the progeny of irradiated and nonirradiated mice has been a decreased sensitivity to chronic X-ray exposure by the progeny of the irradiated mice. Since studies in relation to other genetic consequences are being continued in the offspring of several generations of irradiated predecessors, it was felt that the chromosomes of these mice should be investigated to determine if any permanent changes could have occurred in morphology, modal number, or karyotype.

METHODS AND RESULTS

The modal patterns and other chromosomal changes resulting from irradiation spread over several generations are being studied in RF mice. The following groups of approximately 50 mice each are under investigation: (a) grandoffspring (F_{22}) of sires which had been irradiated for 20 generations

with 200 rads of a single dose of whole-body X irradiation at the time of weaning; (b) a twenty-second generation subline of mice where only the first 10 generations of sires were irradiated as under (a); and (c) control line of mice of the F₂₂ generation.

Bone marrow cells were obtained immediately after sacrifice from female mice ranging in age from 3 to 5 months. In vivo Colcemid or Vincalukoblastine was administered intraperitoneally 4 to 6 hours before sacrifice to increase the number of cells in metaphase. The chromosomes were prepared by the standard treatment with hypotonic solution, fixation, and spreading methods, and were stained with crystal violet. The chromosomes were counted visually. Only chromosomes from well spread, apparently complete, and easily countable cells were included in the study. The slides were picked at random from each group and so marked that the observer was not aware of the group until all slides were counted.

A summary of the results of the modal chromosome number for each group is given in Table 1. For convenience, the average results of all cells counted from all animals in each group are reported. Results include only data from animals from which 20 or more cells were counted. One mouse in the control group is reported separately, as it appears to have a mosaic pattern.

TABLE 1. CHROMOSOME COUNTS IN THE BONE MARROW OF MICE WHICH ARE PROGENY FROM
SEVERAL LINES OF IRRADIATED RF MICE

Number of Animals	Number of Cells Counted	Cells Containing Indicated Chromosome Count (Number)							Tetra- Abnormal or ploid Polyploid	
		38	39	40	41	42	43			
<u>Control Line (F₂₂)</u>										
21	1194	89	121	850	48	25	3	34	24	
1*	94	8	44	31				10	1	
<u>F₂₂ Subline (first 10 generations irradiated)</u>										
19	685	61	59	484	33	10	3	18	17	
<u>F₂₂ Subline (first 20 generations irradiated)</u>										
22	1008	71	94	695	66	26	13	16	27	

*Appears to have mosaic pattern.

No striking differences in the modal number have been noted among the groups of mice. Gross structural abnormalities have been rare. More subtle differences in over-all length, etc., are under study with karyotype analysis of chromosomes from individual cells. A more detailed report is planned to cover the individual differences among the animals within the various groups.

Chromosomes in Transplanted Leukemia of AKR Mice (I. U. Boone
and P. M. LaBauve)

INTRODUCTION

The observations that a number of mammalian tumors consist of a cell population with aneuploid chromosome number have frequently been interpreted as support for the theory that somatic chromosomal mutations are involved in the carcinogenic process (1,2). However, the many demonstrations that neoplastic cells can have a normal diploid chromosomal complement without detectable abnormalities (2,3) suggest that the varied abnormal chromosome patterns which generally occur in vivo in well advanced tumors and in in vitro cultured cells are of secondary importance in the acquirement of malignant properties and are probably a separate event. Chromosomal alterations in mice have been studied in spontaneous and radiation-induced leukemia by Ford et al. (1), Bayreuther (2), and Wakonig and Stich (3) with varying results. In this Laboratory, a transplantable leukemia has been carried and studied in AKR mice for several years. Since future in vitro tissue culture studies are planned using normal and leukemic cells from AKR mice, an in vivo analysis of the chromosomes of bone marrow cells was performed to establish a base line criterion for this transplantable leukemia.

METHODS AND RESULTS

An AKR transplantable leukemia which has been transferred approximately every 10 to 12 days for the past year was investigated. The leukemia was transplanted by intraperitoneal injection of 5×10^6 cells/ml of homogenized leukemic spleen. Leukemic and normal mice were injected intraperitoneally with 1 mg Vincalukoblastine (VLB) per kg body weight (4) 9 to 12 days after the leukemic transplant. VLB and Colcemid were compared and, in our limited experiments, the VLB gave the more pronounced effect of mitotic arrest. For both drugs, the strathmokinetic effect appeared to be dependent upon the freshness of the solution used for injection.

The VLB was administered 5 to 6 hours before sacrifice of the animals. Longer periods of time between giving the VLB and sacrifice resulted in overcontraction of the chromosomes for the purposes of modal counting, morphology study, and karyotype analysis.

The bone marrow was obtained from the femurs and tibias immediately after sacrifice and was suspended in normal saline. The chromosomes were prepared using a modification of the method described by Fox and Ziess (5). The dried slide preparations were stained by immersion in 1 per cent aqueous crystal violet.

The chromosome counts of cells from the bone marrow of normal and leukemic mice of both sexes are given in Table 1. Since the chromosome complement may differ greatly from animal to animal and between leukemic transplants, the results from 8 leukemic mice are presented separately. Although there was a greater heterogeneity in the distribution of chromosome number in the leukemic mice, the modal value remained that of the normal mouse. These results are in agreement with Wakonig and Stich (3), who reported that in cells from the spleen and thymus of AKR mice most of the 17 primary leukemias and 10 transplantable leukemias and tumors had a modal chromosome diploid number of 40. The occurrence of higher percentage of aneuploid (particularly with chromosome numbers over 40) and tetraploid cells was more common in the leukemic cells. Marker chromosomes similar to those described by others (1,3) were seen occasionally in one leukemic mouse.

These results show that transplantable neoplastic cells can have a diploid chromosome complement and remain diploid over a long series of transfers. In vitro experiments are in progress to determine if a diploid complement of chromosomes can be maintained in tissue culture.

TABLE 1. CHROMOSOME COUNTS IN THE BONE MARROW OF NORMAL AND LEUKEMIC MICE OF THE AKR STRAIN

	Cells Containing Indicated Chromosome Count										Total Cells
	Tetraploid Cells	36	37	38	39	40	41	42	43	44	
<u>Normal Mice</u>											
Female (3)					4	22					26
Male (5)					1	37					38
<u>Leukemic Mice</u>											
Female (1-8)					3	68					71
Female (1-8)	2				2	50	1				55
Female (9-6)				1	3	45	1				50
Female (9-6)	1				4	42	4				51
Female (9-6)						50	1				51
Male (11-28)				2	5	95	4	2			109
Male (11-28)	1				2	11	86				100
Male (11-28)	1										
Male (12-14)	2				1	3	37	1			44

REFERENCES

- (1) C. E. Ford, J. L. Hamerton, and R. H. Mole, J. Cell. Comp. Physiol. 52, Suppl. 1, 235 (1958).
- (2) K. Bayreuther, Nature 186, 6 (1960).
- (3) R. Wakonig and H. F. Stich, J. Natl. Cancer Inst. 25, 295 (1960).
- (4) G. Cardinali, G. Cardinali, and J. Blair, Cancer Res. 21, 542 (1961).
- (5) M. Fox and I. M. Ziess, Nature 192, 213 (1961).

CELLULAR RADIOBIOLOGY SECTION

PUBLICATIONS

(1) D. F. Petersen, The Growth of Monodisperse Populations of Mammalian Cells Exposed to Internal Beta Irradiation, In: Proceedings of the American Mathematical Society Symposium on Mathematical Problems in the Biological Sciences, Vol. 14 (1962), pp. 233-239.

(2) D. F. Petersen, Neutron Dose Estimates in the SL-1 Accident, Health Phys. 9, 231 (1963).

CHAPTER 7

MOLECULAR RADIOBIOLOGY SECTION

Nucleic Acids: A Technique for Automated Base Analysis **(G. R. Shepherd, D. G. Ott, and P. A. Hopkins)**

INTRODUCTION

A technique for automatic base analysis of hydrolyzed nucleic acids and synthetic polynucleotides would be of value to several molecular biology projects currently underway in this Laboratory. Such a technique would allow the application of corrective factors to phosphorus determinations to yield exact nucleic acid concentrations. It would provide a sensitive technique for the detection of anomalous bases present in nucleic acids and permit the rapid determination of composition of polynucleotides synthesized by chemical or enzymatic methods. Accordingly, the chromatographic procedure of Crampton et al. (1) was investigated for its suitability for automated flow analysis.

METHODS

A base standard containing 500 $\mu\text{g/ml}$ each of adenine, guanine, cytosine, and thymine was prepared in 0.01 N HCl. Jacketed columns (0.9 x 30 cm) were prepared using analytical grade minus 400 mesh Dowex 50X-4 ion exchange resin. Columns were equilibrated at the operating temperature (40° C) with 0.2 N ammonium formate buffer at pH 4.0 and were eluted with several types of concentration gradients of formate buffer. Column effluents were monitored in a 1-cm quartz flow cell using a 254- μ germicidal lamp source and a photovolt cell and densitometer. The present monitor does not strictly follow theory ($\log T_0/T = ecl$). The Corning glass filter system allows passage of a certain amount of light of longer wavelengths which is not absorbed by the solution. Over a certain range, however, the response is usefully proportional to concentration. Elution profiles were recorded on a Brown potentiometric recorder, as illustrated in Fig. 1.

Optimum resolution was obtained with a flow rate of 14 ml/hr and an exponential gradient following the expression:

$$C = C_2 - (C_2 - C_1) (1 - v)^{A_2/A_1},$$

where C is the mixing chamber effluent concentration at $v = n$ ml; C_1 is the concentration in the mixing chamber at $v = 0$ ml; C_2 is the concentration in the reservoir at $v = 0$ ml;

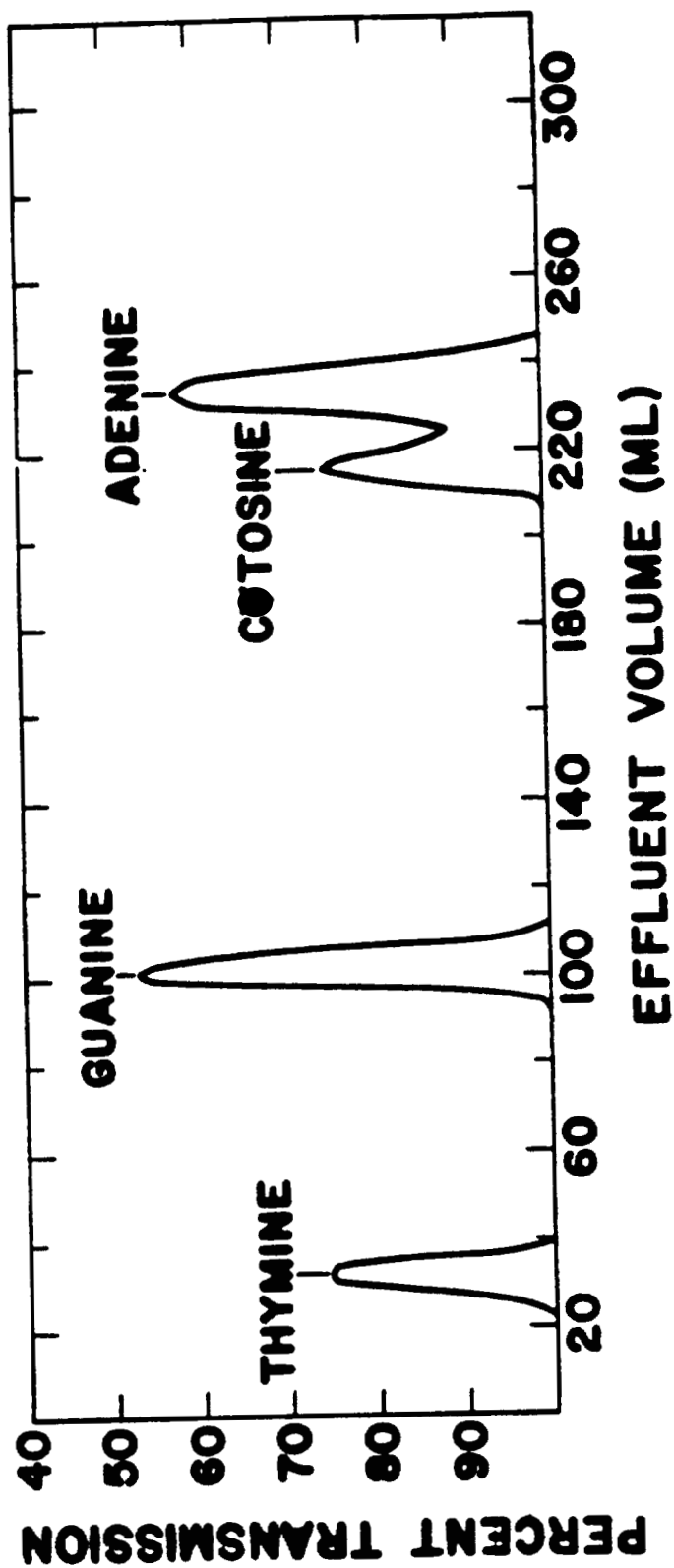


Fig. 1. Base elution profile.

v is the volume of effluent passed; A_1 is the cross sectional area of the mixing chamber; and A_2 is the cross sectional area of the reservoir. Mixing and reservoir chambers must be equi-level and siphon-connected.

RESULTS

Optimum resolution was achieved with 250 ml of 0.2 N formate buffer in the mixing chamber and 500 ml of 1.0 N formate buffer in the reservoir and when $A_2 = 1.54 A_1$. Gravity flow was used with a head of approximately 20 cm. Considerable difficulty was experienced with peak distortion due to the formation of air bubbles within the resin bed. This was eliminated by (a) maintaining the reservoir and mixing chambers at 42° C, and (b) inserting a specially designed bubble trap between the mixing chamber and column.

Recording per cent transmission yields a linear record of an exponential function; such a record would not be proportional to concentration over the range of 0 to 100 per cent T but would be reasonably proportional over the range of 35 to 100 per cent T . Quantities of bases applied to the column were regulated to remain within this range, approximately 100- μ g quantities of each base giving a suitable response. Peak areas were integrated using the half-height method and were correlated with base quantity as a constant k ,

$$k = \frac{\text{quantity of base } (\mu\text{g})}{\text{area of peak } (\text{cm}^2)} .$$

The data resulting from two duplicate runs are presented in Table 1. In view of these encouraging results, further improvements in the system will be pursued. Stable flow rates, a monochromatic light source, and a mechanically rigid light source-flow cell-photocell assembly may be expected to improve resolution and quantitation. A timer solenoid assembly will permit automatic column elution, regeneration, and re-equilibration. Resins of varying compositions and degrees of cross linking will be investigated for improved resolution. Further investigation of recorder function will be pursued, recording as a log function and using log 1/N paper, in an attempt to extend and to improve quantitation from recorder tracings.

REFERENCE

- (1) C. F. Crampton, F. R. Frankel, A. M. Benson, and A. Wade, Anal. Biochem. 1, 249 (1960).

TABLE 1. A COMPARISON OF DUPLICATE DETERMINATIONS CALCULATED BY THE PEAK AREA

METHOD						Calculated	Relative
	Quantity	Minimum	Peak Area	k	kAVG	Quantity	Error
Base	($\mu\text{g}/\text{ml}$)	(per cent T)	(cm^2)			($\mu\text{g}/\text{ml}$)	(per cent)
Thymine	110.0	85	9.20	11.96	12.23	112.5	± 2.2
			8.80	12.50		107.6	
Guanine	99.0	55	16.68	5.94	5.83	97.2	± 1.8
			17.30	5.70		100.8	
Cytosine	100.0	75	14.72	6.79	6.78	99.8	± 0.3
			14.80	6.76		100.3	
Adenine	104.0	60	24.48	4.25	4.05	99.1	± 4.7
			27.10	3.84		109.8	

Application of Automatic Computational Techniques to the
Analysis of Ultracentrifugal Sedimentation-Velocity Molecular
Weight Data for Deoxyribonucleic Acid (G. R. Shepherd, P. N.
Dean, and B. J. Noland)

INTRODUCTION

Calculation of ultracentrifugal molecular weights and sedimentation coefficient distributions for DNA is a lengthy process involving a large number of iterative computations. Such calculations require a considerable investment in skilled operator time and are highly susceptible to human error. Accordingly, a computer program was designed to perform these calculations accurately and reliably. The program was written in FORTRAN II for the IBM 704/7090 computer (Monitor System) and was designed to eliminate, insofar as possible, pre-computer calculations on the part of the operator. Provision was made for the direct entry of data in the same form in which it was obtained experimentally. Routine use of this program at the Los Alamos Scientific Laboratory has resulted in an increase in the reliability of calculated data and has encouraged the design of experiments which can effectively utilize the increased quantity of data now available..

MATHEMATICAL BASIS

Detailed mechanical and mathematical descriptions of

ultracentrifugal boundary migration are readily available (1, 2). Especially valuable in this regard is the description by Schumaker and Schachman of the use of ultraviolet absorption techniques in the ultracentrifugal analysis of dilute solutions (3). Briefly, the technique involves the clearing of a solution of macromolecules by means of a high centrifugal field. The clearing process creates a boundary, the region between solvent and solution, which moves in the direction of applied force. Since DNA macromolecules absorb ultraviolet light in the region of 260 $m\mu$, the boundary migration may be recorded on ultraviolet-sensitive film and translated to two-dimensional graphic form with an automatic scanning and recording photodensitometer.

Our work was performed with a Beckman/Spinco Model E analytical ultracentrifuge equipped with an ultraviolet absorption system using DNA solutions with 5 to 40 μg DNA/ml. An An-E rotor and 30 mm 4° sector cell were used throughout. All measurements, including those of viscosity, density, and sedimentation, were made at $25.0 \pm 0.01^\circ$ C. Care was taken to accelerate the rotor in the same manner for each run, giving times which were reproducible within ± 0.3 per cent for each run. Films were developed according to the techniques of Thomas and Berns (4), and the resulting films were traced using the Beckman/Spinco Analytrol photodensitometer with film-scanning accessory.

Figure 1 represents the theoretical time-sequential boundaries observed at t_1 , t_2 , t_3 , and t_4 of the same solute at 4 different concentrations. The migration of a boundary is expressed as the change in the log of the distance of point h on the boundary during the period t_1 to t_2 from the center of rotation. This value may be incorporated into the following equation:

$$S_{OBS} = \frac{2.303 d \log x/dt}{\left[\frac{2\pi \text{ RPM}}{60} \right]^2} \times 10^{13}.$$

S_{OBS} is the observed sedimentation value in Svedberg units and may be corrected for solution density and viscosity to a standard set of conditions:

$$S_{20,w} = S_{OBS} \left(\frac{\eta_{H_2O, t^\circ C}}{\eta_{H_2O, 20^\circ C}} \right) \left(\frac{\eta_{SOLV, t^\circ C}}{\eta_{H_2O, t^\circ C}} \right) \left(\frac{1 - \bar{V} \cdot d_{H_2O, 20^\circ C}}{1 - \bar{V} \cdot d_{SOLV, t^\circ C}} \right)$$

$S_{20,w}$ values are the values obtained had the solute been dissolved in a solvent with the density and viscosity of water at 20° C. The viscosity ratios used in the correction may either be calculated from handbook values, in the case of water at $t^\circ C$ and 20° C, or obtained directly from (time x density) ratios performed in a low shear gradient capillary

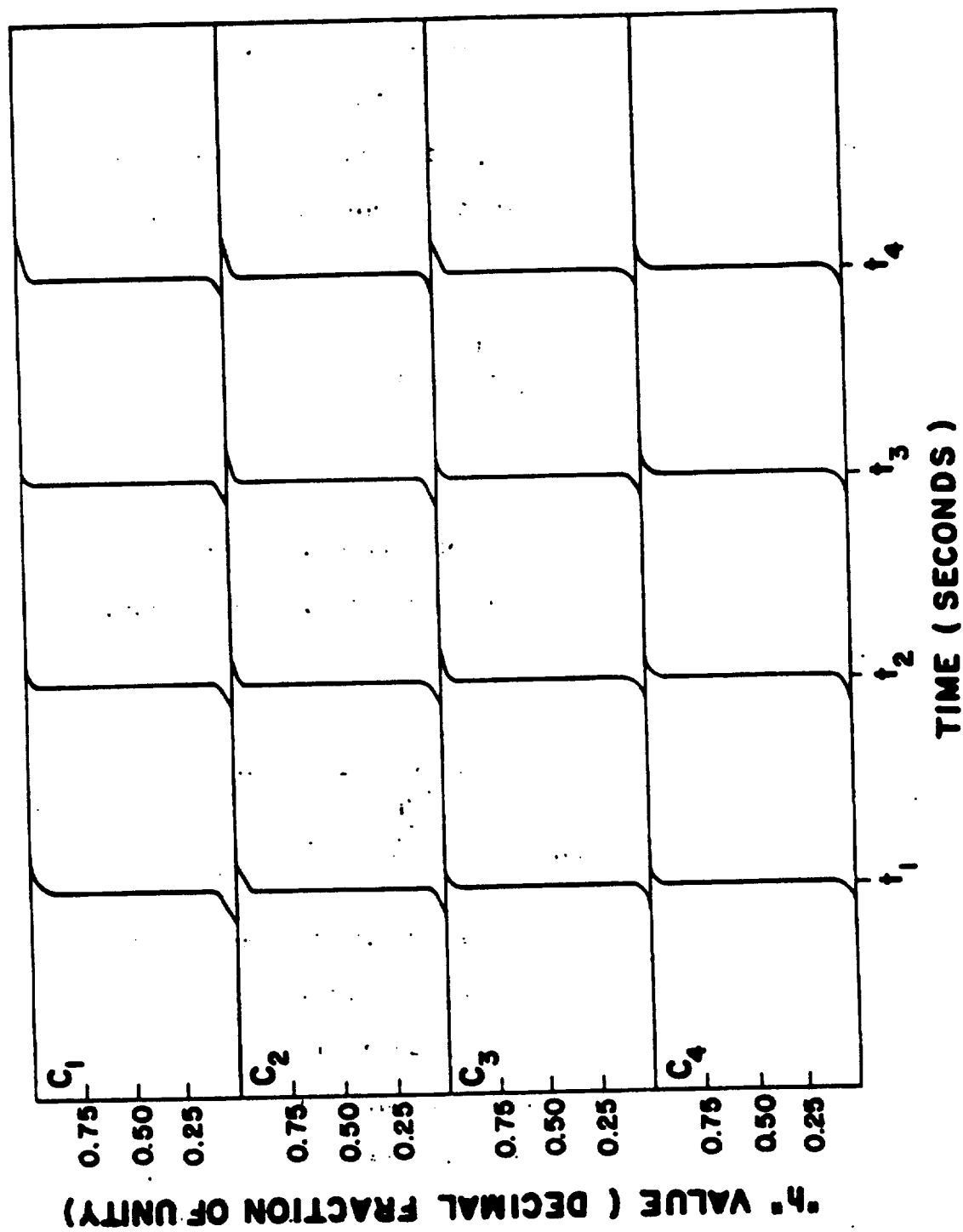


Fig. 1. Graphic representation of the relationship between parameters t , c , and h during boundary migration.

viscometer of the Ubbelohde type at $t^\circ \text{C}$. The value 0.55 for the partial specific volume (\bar{V}) was obtained from the work of Tennent and Vilbrant (5). Intrinsic viscosity $[\eta]$ may be obtained by the linear extrapolation of the ratio of specific viscosity to concentration to infinite dilution. η_{sp} Values are derived from solution and solvent flow time-density products obtained in a capillary viscometer.

Molecular weights are obtained by substitution of the proper values in the following empirical equation (6):

$$\text{M. Wt.} = 4.269 + 1.33 \log (S_0 [\eta])^{1/3},$$

where S_0 is obtained by the extrapolation of $S_{20,w}$ values, or their reciprocals, to infinite dilution.

Finally, apparent diffusion coefficients may be obtained from the slope of a plot of the squares of the differences between the x values of a boundary at $h = 0.25$ and $h = 0.75$ against time. The slope of the resulting line, divided by the constant 3.64, is the apparent diffusion coefficient in cm^2/sec .

It may be seen that, with the exception of a perfectly stable vertical boundary, each value of h will yield a different set of values for S_{OBS} , $S_{20,w}$, S_0 , and M. Wt. Information on the distribution of these values within a given sample is frequently of interest to the investigator in that

it may offer information as to the size, homogeneity, and purity of a DNA preparation. The computer program was, therefore, designed to yield the following data:

(a) One apparent diffusion coefficient for each concentration value.

(b) Intrinsic viscosity derived directly from capillary flow times and solvent and solution densities.

(c) One value of S_{OBS} for each boundary h value for each time interval for each concentration.

(d) One value of $S_{20,w}$ for each boundary h value for each time interval for each concentration.

(e) One value of S_0 for each boundary h value for each time interval.

(f) One value of M. Wt. for each boundary h value for each time interval.

Figures obtained in this manner agree closely with those obtained by simultaneous hand calculation procedures. It may be seen that the application of automatic computational techniques to the analysis of ultracentrifugal molecular weights effects a great saving of time, an increased accuracy and reliability of results, and enables the experimenter to design experiments which can utilize these data to the fullest.

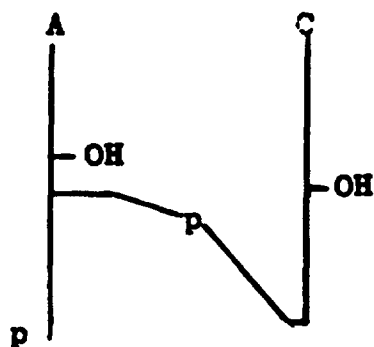
REFERENCES

- (1) H. K. Schachman, Methods in Enzymology, Vol. IV, Academic Press, New York (1957), pp. 32-103.
- (2) H. K. Schachman, Ultracentrifugation in Biochemistry, Academic Press, New York (1959).
- (3) V. N. Schumaker and H. K. Schachman, *Biochim. Biophys. Acta* 23, 628 (1957).
- (4) C. A. Thomas and K. I. Berns, *J. Mol. Biol.* 3, 277 (1961).
- (5) H. G. Tennent and G. F. Vilbrant, *J. Am. Chem. Soc.* 65, 424 (1943).
- (6) J. Eigner, C. Schilkraut, and P. Doty, *Biochim. Biophys. Acta* 55, 13 (1962).

The Representation of Oligonucleotides: A Sub-Nomenclature Problem (F. N. Hayes and D. G. Ott)

INTRODUCTION

Formal nomenclature in the oligonucleotide field is so complex that much effort has been put into devising simpler descriptive systems. In the literature and every day in the laboratory, chemical structures must be represented simply and clearly on paper and blackboard. There are two standard systems: a two-dimensional nucleoside stick structure (I) which is used whenever all the reactive functions must be shown, and a linear structure (II) when only the 3'- and 5'-linkages are represented.



I

pApdC

II

Structures I and II represent the same mixed ribo- and deoxy-ribodinucleotide. The stick sugar numbering runs from 1' at the top to 5' at the bottom. The linear linkage numbering

imitates the direction in multistick structures: each p has 3' on its left plus 5' on its right.

Both systems use the letters A, C, G, U, and T, where in the stick version the bases adenine, cytosine, guanine, uracil, and thymine are meant but where in the linear version the nucleosides adenosine, cytidine, guanosine, uridine, and thymidine are meant. Thymidine is a deoxynucleoside; whereas the other four are ribosides. The linear version also needs dA, dC, and dG to represent deoxyadenosine, deoxycytidine, and deoxyguanosine. The discovery of a ribothymidine in S-RNA has led to use of rT for it, but recently there has been agitation to redefine T as ribothymidine and to introduce dT as thymidine.

The use of p to represent phosphate ester in both the stick and linear forms is traditionally replaced by designations such as GMP, dCDP, and ATP for 5'-guanylic acid, 2'-deoxycytidine-5'-diphosphate, and adenosine 5'-triphosphate.

NEW PROPOSALS (LOCAL SYSTEM)

We entered the field of oligonucleotide synthesis with no emotional or traditional ties to the generally used nucleotide sub-nomenclature. The existing system was found to be unsystematic and troublesome enough that we wished for something better and, therefore, more useful in our work.

Almost effortlessly, the following system evolved and has been successfully used for more than a year.

Bases are represented by Ad, Cy, Gu, Th, and Ur for adenine, cytosine, guanine, thymine, and uracil. These notations appear only on the stick structures. Nucleosides in the ribose series are A, C, G, T, and U, and in the deoxyribose series are a, c, g, t, and u. Phosphate esters are represented only by the normal linear use of p.

Structure I is altered only to have A replaced by Ad and C by Cy. The linear structure II is now pApc. Likewise, GMP becomes pG, dCDP becomes p₂c, and ATP becomes p₃A.

In the following sections on oligonucleotide synthesis, the local nomenclature abbreviation system will be used.

Oligonucleotide Synthesis (D. G. Ott, D. L. Williams, V. N. Kerr, G. T. Fritz, E. Hansbury, R. E. Hine, and F. N. Hayes)

INTRODUCTION

The program of the Molecular Radiobiology Section includes a study of oligodeoxyribonucleotides: their preparation, chemical properties, and biological significance. These small units of DNA can serve as standards with catalogued properties for comparison with DNA cleavage products in sequence studies, as models in radiation experiments and for chemical and enzymic degradation, and as active participants in cell-free polymerase systems. To embark properly on our ambitious study program, a selected and considerable number of oligodeoxyribonucleotides must be prepared by whatever means seem most appropriate.

Polymerization produces large molecules with a monotonously repetitive sequence or with an unknown sequence if a mixture of monomers is used. Stepwise molecular buildup offers great sequential variety of known order, but progress toward large molecules is exceedingly slow. DNA subjected to the action of phosphodiesterase enzymes is a potential source of all conceivable oligonucleotides. How promising this approach may be depends on the technical mastery of fractionation procedures which must, at the same time, be

ultrasensitive to structural differences and handle large quantities of oligonucleotide mixtures.

GENERAL DISCUSSION

Thus far in the synthesis program, work has been limited to compounds containing the pyrimidine bases: cytosine and thymine. Polymerization of 5'-thymidylic acid has been accomplished both with dicyclohexylcarbodiimide (DCC) (1) and with ethyl polyphosphate (2) to give the well known series $(pt)_n$ with a maximum n of approximately 12 at the termination of our separation procedure. Our ethyl polyphosphate was clearly not functioning in the way it has been reported [namely, to give poly-5'-thymidylic acid of average molecular weight = 18,000 (2)]. With the recent visit of one of the authors of Ref. 2, Dr. Wolfgang Pollmann, to our Laboratory, we can now make an ethyl polyphosphate which converts 5'-thymidylic acid in low yield to polymer of considerably higher molecular weight than obtainable with DCC as the polymerization agent, but we are quite expectedly still troubled with excess phosphorus in the product.

Stepwise synthesis has been directed at the 4 possible pyrimidine dinucleotides in various stages of phosphorylation which are illustrated with thymidine as the nucleoside: tpt, ptpt, tptp, ptptp, -ptpt-, p_2tpt , and p_3tpt . The required

quantities of each product differ according to use intended. Some are starting materials for synthesis of higher oligomers, and others are end products only to be characterized. Also, to aid in biochemical studies, radioactive labeling of certain of these is being carried out.

The approach to oligodeoxyribonucleotides by enzymolysis of DNA is still in the planning stage.

INTRODUCTORY EXPERIMENTAL

Most of the syntheses are by known procedures or by minor modification of standard methods (3-5). Nucleoside and nucleotide intermediates with blocking groups situated to inhibit interfering reaction sites and chosen for selective removability from the condensation products are first prepared. These are illustrated in Fig. 1. The only difference between the thymine and cytosine representatives is that the latter require an anisoyl block on the 4-amino nitrogen.

By one-step condensation reactions, fully blocked dimers are formed according to the following representations: $I + II \rightarrow \text{tpt}$, $I + V \rightarrow \text{tpc}$, $IV + II \rightarrow \text{cpt}$, and $IV + V \rightarrow \text{cpc}$. The trityl group is acid-labile, and the acyl groups are base-labile, permitting selective removal of either the 3'- or 5'-block in a dimer followed by phosphorylation of the free hydroxyl group. In this way, 3'- and

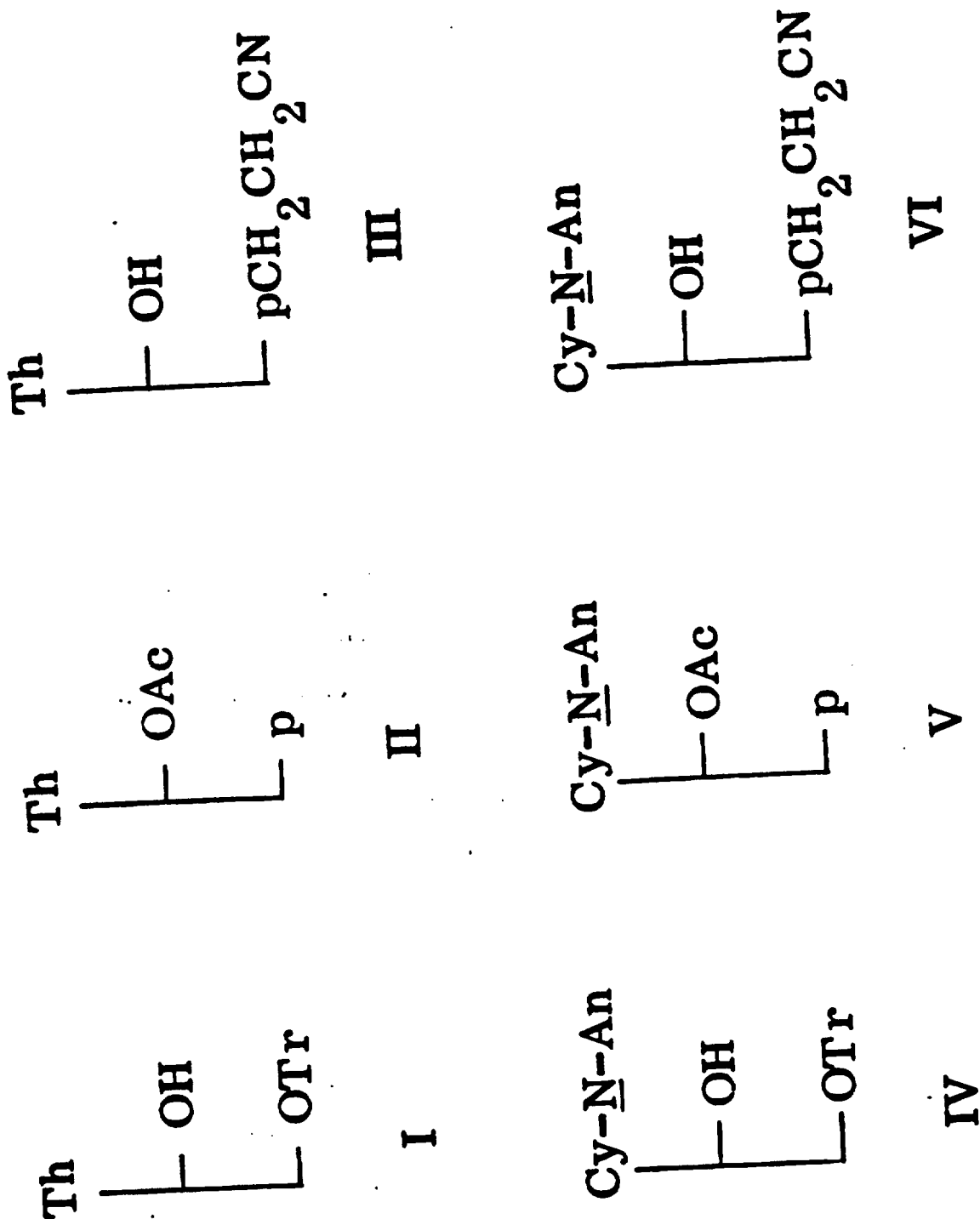


Fig. 1. Blocked intermediates for pyrimidine oligodeoxyribonucleotide synthesis
(Tr = triphenylmethyl or any of its various p-methoxy derivatives, Ac =
acetyl, and An = anisoyl).

1055805

5'-phosphates and the 3',5'-diphosphate of each dinucleotide are being prepared. A cyclic dimer results from intramolecular condensation at high dilution of either the 3'- or 5'-phosphate.

The special 2-cyanoethyl-blocked nucleotides, III and VI, are used for rapid access to the 5'-phosphorylated dimers: $\text{III} + \text{II} \longrightarrow \text{ptpt}$, $\text{III} + \text{V} \longrightarrow \text{ptpc}$, $\text{VI} + \text{II} \longrightarrow \text{pcpt}$, and $\text{VI} + \text{V} \longrightarrow \text{pcpc}$. This scheme is readily amenable to use of labeled nucleotides.

A method has been worked out for converting a dimer 5'-phosphate to its 5'-triphosphate. Thus, we will have dinucleotides at the supposedly proper chemical state for incorporation studies with polymerase systems.

Specific progress in synthesis is reported in the following section.

EXPERIMENTAL PROGRESS

Much time has been spent in mastering reaction techniques applicable to oligonucleotide synthesis. Progress in polymerization and stepwise synthesis is reported here, but product characterization information is lacking. Thus far, considerable paper and column chromatographic data have been amassed, as is necessary for identification and separation procedures used in working up reactions. Elemental microanalyses, ultraviolet and infrared spectroscopic data, and

chromatographic behavior of pure products will be presented in later reports.

5'-O-Tritylthymidine Derivatives (I). Chlorotriphenylmethane, a specific reagent for primary hydroxyl groups, reacts very slowly with thymidine at room temperature (60 per cent, 1 week) and affords 70 to 80 per cent yields of 5'-O-tritylthymidine (I) in hot pyridine during about 30 minutes. Substitution of the trityl chloride reagent with p-methoxyl groups (6) increases the reactivity of the reagent as the number of such groups is increased. With a 10 per cent molar excess of the reagents, quantitative conversions of thymidine were effected in 40 hours for one p-methoxyl, 13.5 hours for two, and 4 hours for three on a 1 to 10 mmole scale. Repeated recrystallizations from dichloromethane and cyclohexane mixtures gave yields of purified products ranging from 95 to 99 per cent. Since the monomethoxy-, dimethoxy-, and trimethoxytrityl radicals are, in that order, increasingly more sensitive to acidic hydrolysis and are much more readily removed than trityl, they offer a good means of protecting the 5'-hydroxyl function of deoxycytidine and the purine nucleosides and nucleotides with their much more acid-labile N-glycoside bonds.

2-Cyanoethyl 5'-Thymidylate (III). 2-Cyanoethyl 5'-thymidylate (III) is isolated in almost quantitative yield

as its calcium salt following the reaction of commercially available 5'-thymidylic acid (pt) (as the pyridinium salt) with dicyclohexylcarbodiimide (DCC) and a large excess of hydracrylonitrile. The diester was also formed in excellent yield using p-toluenesulfonyl chloride as the condensing agent.

N-Anisoyl-2'-deoxycytidine (IX). Compound IX has been prepared by both of the reaction sequences illustrated in Fig. 2. Tetrahydropyranylation of 2'-deoxycytidine (c) hydrochloride goes extremely slowly without added catalyst. On 0.1- to 4-mmole scale with a large excess (55 fold) of dihydropyran (DHP) in dimethylformamide solution, the addition of 1.1 equivalents (per mole) of dry HCl in dioxane catalyzed the reaction to completion in 23 hours at room temperature. A compound of intermediate R_f first formed, presumably the 5'-O-(2-tetrahydropyranyl)- derivative, which disappeared completely as the bis- derivative of higher R_f was formed. The product, 3',5'-O-bis-(2-tetrahydropyranyl)-2'-deoxycytidine (VII), was isolated as a colorless semi-solid material which has not, as yet, been crystallized. Reaction of VII with anisoyl chloride in dry pyridine gave the N-anisoyl derivative (VIII). The latter product has been extremely hard to purify because of colored by-products arising from the dihydropyran reaction. A colorless product has

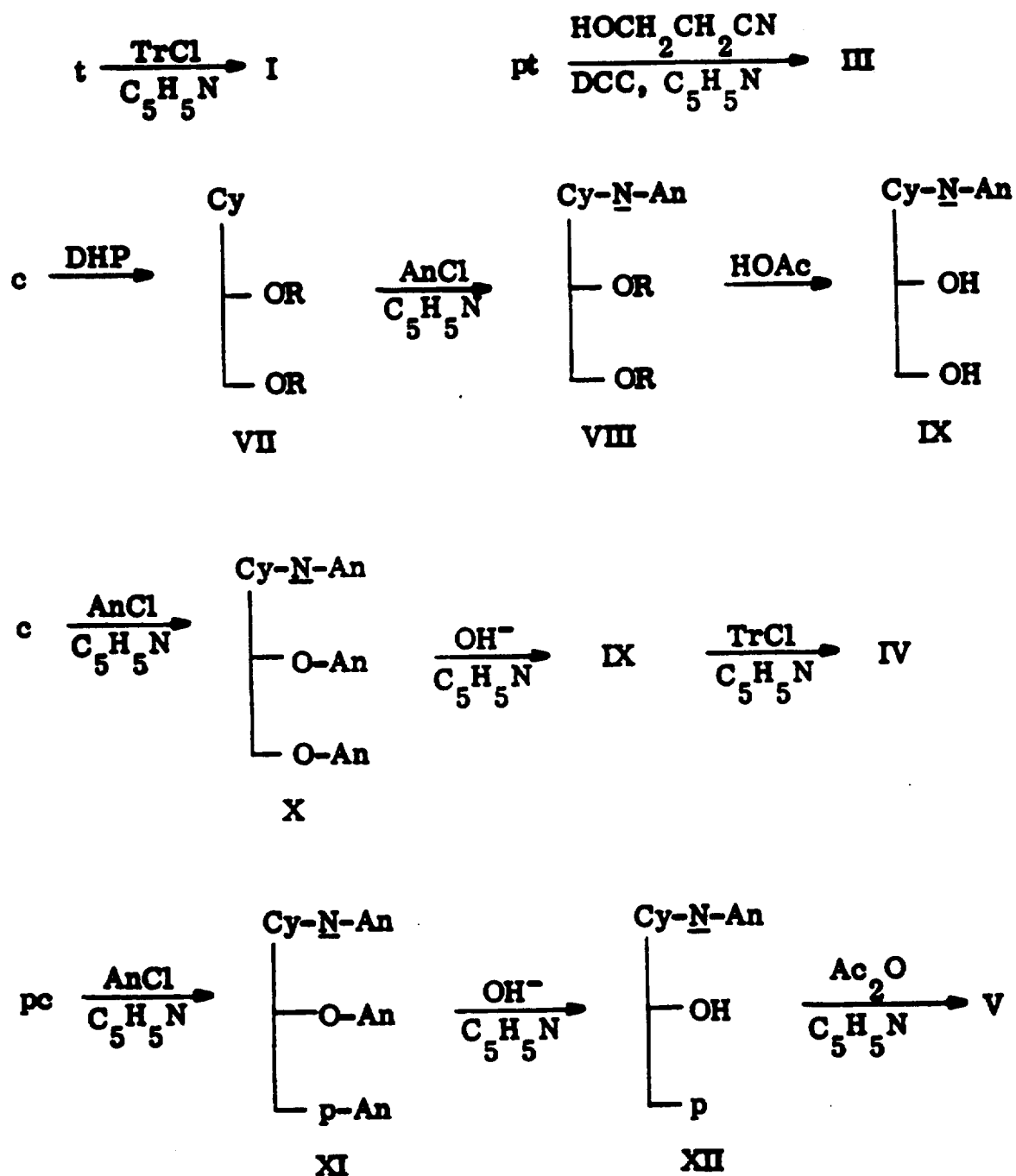


Fig. 2. Synthesis of protected intermediates (R = 2-tetrahydropyranyl).

been obtained in about 35 per cent yield by the slow crystallization of VIII from a mixture of ether and ethyl acetate. Removal of the 2-tetrahydropyranyl groups with 80 per cent acetic acid at 25° was quite slow, and a mixture of products was obtained. It appears that removal of a 3'-O-(2-tetrahydropyranyl) group in aqueous acetic acid, from deoxycytidine derivatives, is greatly facilitated by the presence of neighboring phosphate group (7).

The preferred method of preparing compound IX is via the completely anisoylated derivative, 3',5'-O-N-trianisoyl-2'-deoxycytidine (X). On the 1- to 4-mmole scale, the yield of nearly pure colorless product is essentially quantitative; upon recrystallization from ethanol, the recovery of pure material is 69 to 75 per cent and more is obtained from mother liquors. Controlled hydrolysis of X, with dilute sodium hydroxide in pyridine at 30° for 35 minutes to remove the 3'-O- and 5'-O-anisoyl groups, gives nearly a quantitative yield of N-anisoyl-2'-deoxycytidine (IX) with just a trace of 2'-deoxycytidine. Sodium ions are removed with IR-120 (pyridinium) resin, and it is important that the product be thoroughly washed from the resin with 15 to 25 per cent pyridine solution. The removal of anisic acid is effected by treating the solution briefly with an 8 fold theoretical excess of IRA-400 (OH⁻) resin. It is very important that a large excess of

pyridine be present to prevent adsorption of the product and coincident hydrolysis of the N-anisoyl group. With thorough washing of the resin with 25 per cent pyridine, the recovery of the product is quantitative. Compound IX crystallizes well from methanol.

N-Anisoyl-5'-O-(dimethoxytrityl)-2'-deoxycytidine (IV).

On a 1- to 2-mmole scale, reaction of IX with chloro-(p-methoxyphenyl)diphenylmethane, in 10 per cent excess, gives quantitative conversion to IV in 48 hours. In a similar reaction of IX with chlorobis-(p-methoxyphenyl)phenylmethane, the conversion is quantitative in <18 hours. After hydrolysis of excess reagent and neutralization of hydrochloric acid with ammonium hydroxide, the product is extracted into chloroform and thoroughly washed with water. These products crystallized from dichloromethane and cyclohexane or dichloromethane and butyl chloride.

3'-O-Acetyl-N-anisoyl-2'-deoxy-5'-cytidylic Acid (V).

Compound V was prepared from 2'-deoxy-5'-cytidylic acid (pc) according to the reaction sequence shown in Fig. 2. Complete anisoylation of pc was accomplished after 2 hours in pyridine at 25°.

The use of 2 N sodium hydroxide (7) to split the anisic phosphoric anhydride linkage selectively in XI was not feasible, since the 3'-O-acyl group was removed at about the same

rate. Hence, the anhydride and 3'-O-acyl groups were completely hydrolyzed with dilute NaOH in pyridine at 25° for 30 minutes, giving N-anisoyl-2'-deoxy-5'-cytidylic acid XII, which was then acetylated to obtain V in 71 per cent yield based on pc and isolated as the calcium salt.

5'-O-Dimethoxytritylthymidylyl-(3':5')-3'-O-acetyl-N-anisoyl-2'-deoxycytidine (XIII). The reaction of the protected nucleotide (V, 0.43 mmole) with 5'-O-dimethoxytritylthymidine (I, 0.5 mmole, 16 per cent molar excess), as illustrated in Fig. 3, afforded an 85 per cent yield of the completely protected dinucleoside (XIII). The reaction mixture was chromatographed on a DEAE-cellulose anion exchange column in the carbonate form and eluted with a linear gradient (0.005 to 0.6 M) of triethylammonium bicarbonate at pH 7.5. Many peaks were obtained: the first of these contained pyridine nucleotide, the second contained mesitylene-sulfonic acid, and the third contained unreacted V and its pyrophosphate. The fourth peak, dimethoxytritylthymidine, eluted from the column slowly, since it is water insoluble. It was spread over about 110 tubes. The fully protected product (XIII) also was eluted very slowly; it first appeared in fraction 249 (10-ml fractions) and was collected in a total of 14 liters of solvent. Since the concentration of product in the eluate was practically constant, 4 liters of

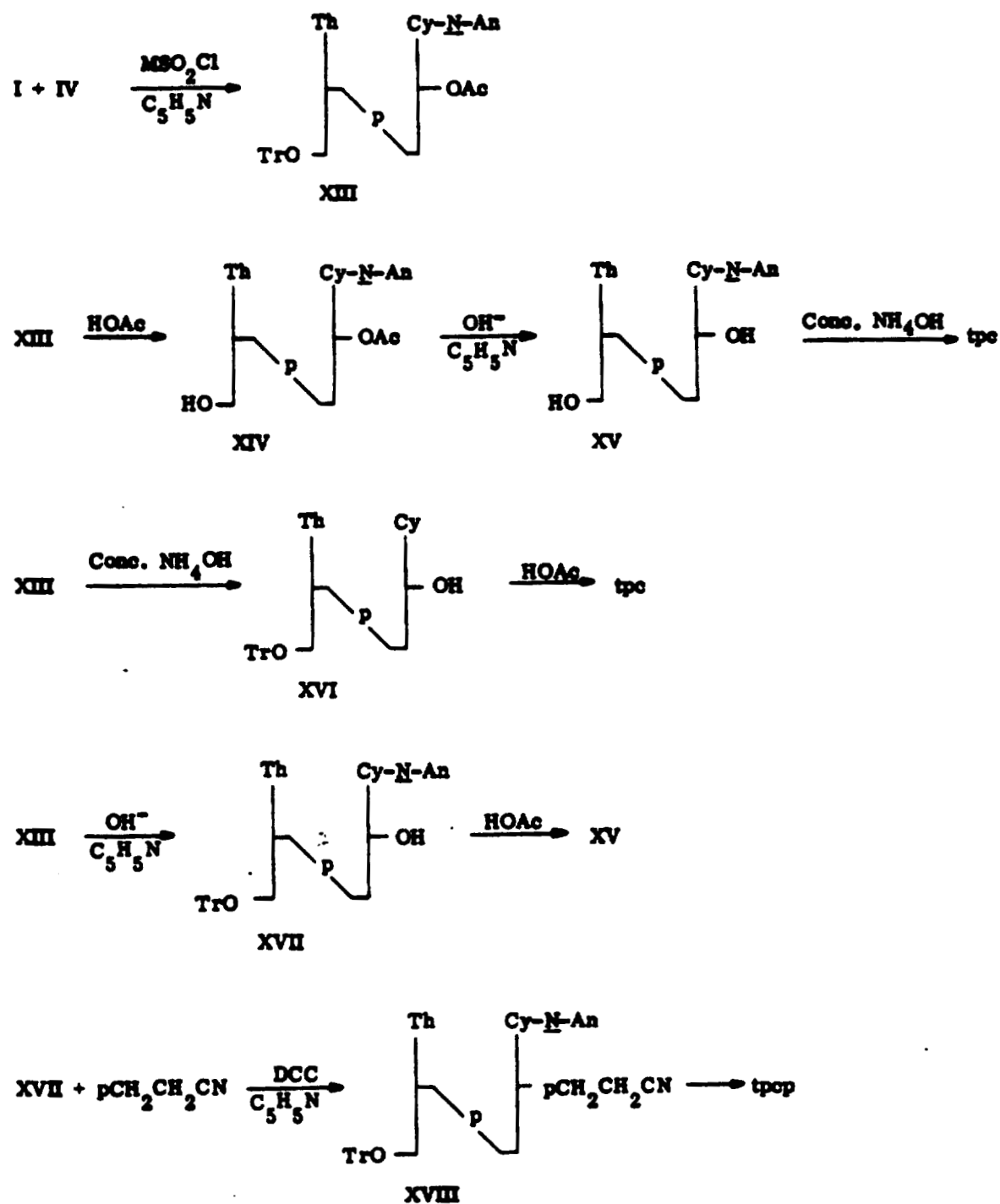


Fig. 3. Derivatives of tpc.

5 per cent ethanol in 0.6 M triethylammonium bicarbonate solution was used toward the end of the run to hasten its removal. The product was isolated from the large volume of solvent by repeated extraction with chloroform in which it is quite soluble.

A small peak which was superimposed on the product peak (tubes 586 to 600, as demonstrated by paper chromatography) was shown by hydrolysis reactions and paper chromatography to be compound XVII, which resulted from loss of the 3'-O-acetyl group from XIII during the work-up.

The major product was partially characterized by means of the reactions shown in Fig. 3, leading to the products XIV, XV, XVI, and XVII derived from XIII in various stages of its being stripped of its blocking groups to give finally, tpc.

5'-O'-Dimethoxytritylthymidylyl-(3':5')-N-anisoyl-2'-deoxycytidine (XVII). The majority of the product (XIII) was subjected to controlled basic hydrolysis with dilute sodium hydroxide in ca. 50 per cent aqueous pyridine to obtain XVII. Removal of sodium ions was effected by treating the solution with IR-120 cation resin (pyridinium form). The solution was evaporated to dryness with the pH maintained > 7 by occasional additions of pyridine.

Thymidylyl-(3':5')-2'-deoxy-3'-cytidylic Acid (tpcp).

The partially protected dinucleoside phosphate XVII, which has an available 3'-hydroxyl group, was phosphorylated with 2-cyanoethyl phosphate (6) and DCC in pyridine, as illustrated in Fig. 3. After addition of water, removal of dicyclohexylurea, and hydrolysis of protective groups from XVIII, the products were subjected to chromatography on a DEAE-cellulose column (carbonate form) and eluted with a linear gradient (0.005 to 0.3 M) of triethylammonium bicarbonate at pH 7.5. Of the 6100 optical density units applied to the column, 20 per cent was non-nucleotide colored material that was removed by a preliminary washing with water adjusted to pH 8 with triethylamine. The gradient elution pattern of nucleotidic products is shown in Fig. 4. The main product, peak 3, which is presumably tpcp as indicated by paper chromatography of the hydrolysis products and the position of the peak relative to the gradient, amounted to 52 per cent of the nucleotide material.

The small peak, shown as a part of peak 3, is now believed to be an artifact produced in loading the column. Peak 3 was rechromatographed on the same column, using a shallower gradient of triethylammonium bicarbonate; a single smooth peak was obtained.

Thymidylyl-(3':5')-deoxycytidine (tpc). Peak 1, the

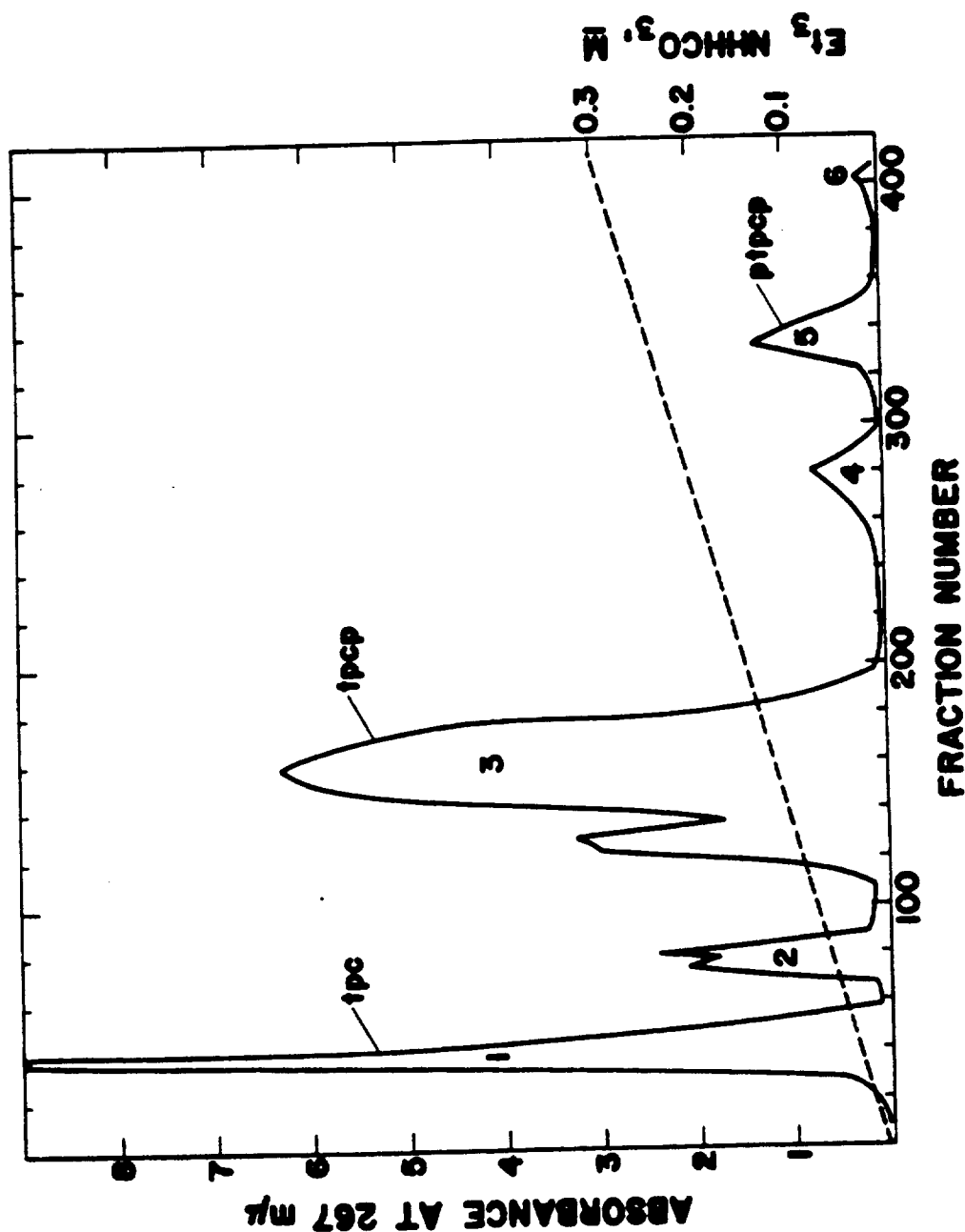


Fig. 4. Chromatography of a phosphorylation reaction mixture on a 2.5 x 30-cm column of DEAE-cellulose (carbonate form) with a linear gradient of triethylammonium bicarbonate (dashed line, right-hand ordinate). Fractions of 9.4 ml at a flow rate of 1 ml/min were collected in an automatic apparatus equipped with an ultraviolet monitor.

second largest, is believed to be tpc and amounted to 32 per cent of the material eluted. This product arises from incomplete removal of the 3'-O-acetyl group during the controlled basic hydrolysis of XIII. A more careful check of the degree of hydrolysis by chromatographing larger aliquots of the sample is in order when carrying out this hydrolysis. Using the same conditions on the micromole scale, all of the 3'-O-acetyl block was removed and in addition a small amount of the N-anisoyl block. The latter factor is unimportant in phosphorylations with 2-cyanoethyl phosphate, since the reagent is in excess and the resulting phosphoamide is easily hydrolyzed in a basic medium.

Of course, tpc would be directly obtained in the desired quantity by the hydrolysis of compound XIII, as shown in Fig. 3.

5'-Phosphorothymidylyl-(3':5')-2'-deoxy-3'-cytidylic Acid (ptpcp). Although care was taken to preserve the 5'-O-dimethoxytrityl group on XVII after removal of the 3'-O-acetyl block, a small amount of thymidylyl-(3:5)-N-anisoyl-2'-deoxycytidine (XV) was present in the phosphorylation reaction mixture. The resulting completely phosphorylated dimer, ptpcp, is believed to comprise peak 5 of the elution pattern in Fig. 4 and amounted to 5 per cent of the eluted material.

Thymidylyl-(5':3')-5'-thymidylic Acid (ptpt). The reaction of II with III in pyridine with the aid of p-toluenesulfonyl chloride (TsCl) gave XIX, as shown in Fig. 5. Following removal of the base-labile acetyl and 2-cyanoethyl protective groups, the resulting ptpt was purified by column chromatography on DEAE-cellulose (bicarbonate form, linear triethylammonium bicarbonate gradient) and crystallization of the calcium salt.

Polyphosphates

Although many effective methods have recently been developed (8) for the synthesis of nucleotide diphosphates and triphosphates, the preparation of oligonucleotides bearing these terminal groups has not been reported. The reactions shown in Fig. 5 for this purpose were developed and are quite satisfactory. Similar reactions, employing phosphorimidazolides, have been used (9) for preparing organic polyphosphates, including adenosine triphosphate. The method appears to be simpler and the yields equivalent to the more commonly employed procedure which involves phosphoromorpholidates.

5'-Thymidylic acid (pt as the pyridinium salt) is converted to the imidazolid XX by reaction with commercially available carbonyldiimidazole in dimethylformamide solution

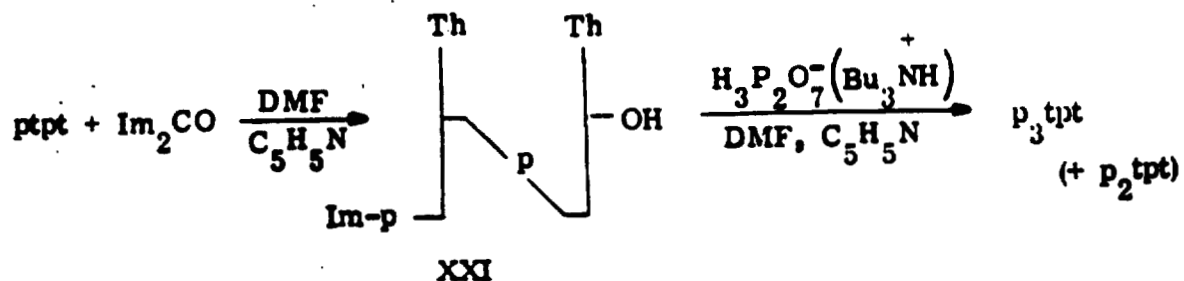
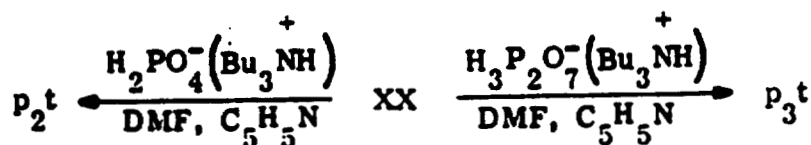
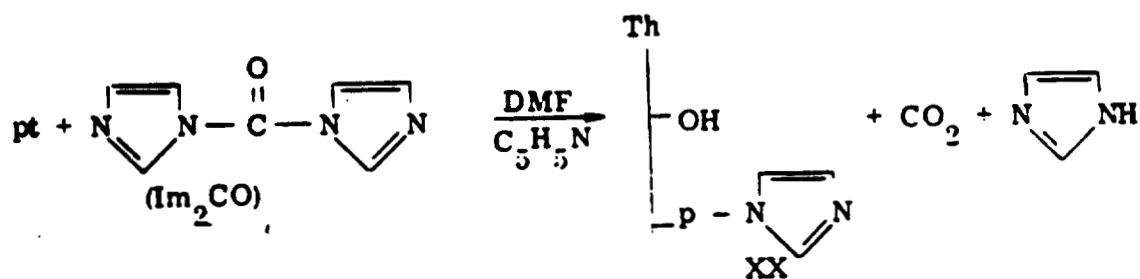
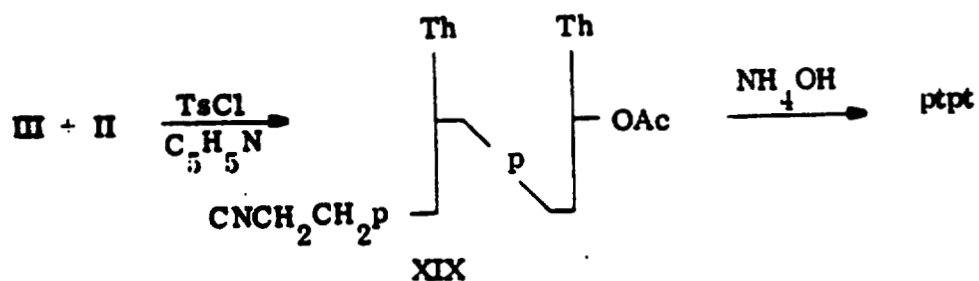


Fig. 5. Reactions involving 5'-phosphates.

at room temperature overnight. Treatment of the resulting solution of XX (without further purification) with anhydrous monotributylammonium orthophosphate gave p_2t . Similarly, treatment of XX with monotributylammonium pyrophosphate produced p_3t . In the latter reaction, it was found that imidazolium pyrophosphate was insoluble in dimethylformamide (and all other common organic solvents); consequently, excess pyrophosphate, corresponding to the amount of imidazole present after the preparation of XX, was used.

Application of the triphosphate reaction to the dinucleotide $ptpt$ gave analogous results. The products were purified by column chromatography on DEAE-cellulose (bicarbonate form) using a linear gradient of triethylammonium bicarbonate at pH 7.5. The products came off the column at approximately the same gradient concentration as do oligonucleotides having the same total number of negative charges; thus, the nucleotide polyphosphates were quite well resolved. However, contamination with inorganic polyphosphate was found (by phosphorus analysis and by paper chromatography), and other means of purification (e.g., adsorption and desorption from charcoal) are required to eliminate these by-products.

Since nucleoside polyphosphates have been observed (9) to disproportionate in such anhydrous reaction solutions, the effect of time of reaction on yield was studied. After a

reaction period of 1 day, the yield following column chromatography of p_2 tpt was 18 per cent, p_3 tpt was 48 per cent, p_4 tpt was 1.2 per cent, and starting material (ptpt, etc.) was 18 per cent. For a 6-hour reaction period, the yields were: p_2 tpt, 7 per cent; p_3 tpt, 48 per cent; p_4 tpt, 0.5 per cent; and ptpt, 25 per cent. Thus, the yield of the desired product was the same in both cases, although the proportions of the by-products varied. Although the yield is satisfactory and as expected for this type of reaction, attempts will be made to optimize it, particularly with respect to formation of inorganic polyphosphates.

REFERENCES

- (1) H. G. Khorana and J. P. Vizsolyi, J. Am. Chem. Soc. 83, 675 (1961).
- (2) G. Schramm, H. Grötsch, and W. Pollmann, Angew. Chem. 74, 53 (1962).
- (3) H. Schaller, G. Weimann, and H. G. Khorana, J. Am. Chem. Soc. 85, 355 (1963), and references cited therein.
- (4) H. G. Khorana, Some Recent Developments in the Chemistry of Phosphate Esters of Biological Interest, John Wiley and Sons, New York (1961).
- (5) F. Cramer, Angew. Chem. 73, 49 (1961).
- (6) M. Smith, D. H. Rammner, I. H. Goldberg, and H. G. Khorana, J. Am. Chem. Soc. 84, 430 (1962).

- (7) H. G. Khorana, A. F. Turner, and J. P. Vizsolyi, J. Am. Chem. Soc. 83, 686 (1961).
- (8) A. M. Michelson, The Chemistry of Nucleosides and Nucleotides, Academic Press, New York (1963).
- (9) F. Cramer and H. Neunhoeffer, Ber. 95, 1664 (1962).

Chromatography of Nucleic Acids (A. Murray, D. F. Petersen,
T. T. Trujillo, and V. E. Mitchell)

INTRODUCTION

Previous reports (1-4) have been concerned with the synthesis and equilibrium behavior of a large number of amine-substituted cellulose anion exchange resins. These studies suggested that precise control of flow and anion concentration at extremely slow rates would be necessary for optimum performance of the resins, and the theory and design of a device capable of providing adequate control of resin environment during column operation were investigated (5). This report summarizes preliminary data on the performance of the apparatus with a series of selected resin columns. In addition, screening data are presented on the behavior of these resins during equilibrium desorption of denatured and degraded salmon sperm DNA. Finally, several resins selected on the basis of exchange capacity were adapted for application to thin-layer chromatography and tested for ability to separate phosphorylated compounds of adenosine.

METHODS AND RESULTS

Equilibrium Desorption of Nucleic Acids

The continued screening of resins for polynucleotide

desorption properties was carried out under equilibrium conditions by batch elution as previously described (4).

(a) Salmon sperm DNA (Calbiochem.) was heat-denatured at 91.5° for 6 minutes, then rapidly chilled by external ice bath and internal application of frozen buffer salt solution, so that the temperature dropped to 50° in 15 seconds and 10° by 90 seconds. Table 1 presents elution profiles for this denatured DNA with 26 resins arranged in decreasing order of the desorption activity index previously found for the undenatured samples (4); average recovery was 99 per cent despite a few cases of extreme spread. All samples were completely absorbed, except for trace amounts in two related resins of rather high binding site density. The number of recovered fractions varied from 4 to the maximum possible 8. In 18 cases permitting correlation of the relative desorption activity index (average 322) with that for the undenatured sample (average 447), 13 showed a marked decrease, indicating a profile shift to tighter binding, while 5 released denatured material at lower ionic strength.

(b) The ability of resins to chaperone heat-denatured salmon sperm DNA was investigated by mixing hot solution with a heated resin slurry and allowing the mixture to cool after 30 minutes. Table 2 presents elution profiles with 7 resins, accompanied by the corresponding data for heat-denatured and

TABLE 1. PROPERTIES OF SYNTHETIC ANION EXCHANGERS FOR DESORBING HEAT DENATURED SALMON SPERM DNA UNDER EQUILIBRIUM CONDITIONS (12.9 μ eq P applied/g resin)

TABLE 1. PROPERTIES OF EQUILIBRIUM CONDITIONS (12.9 μ eq P applied/g resin)

Resin	Desorption Activity Index	DNA Recovered from Each Step Eluant (per cent)										Binding Site Density		Desorption Activity Index	
		NaCl + M/100 TRIS Buffer					NH ₄ OH + 2M NaCl					μeq exch Cl ⁻			
		15M/100 M/10 M/4		M/2 1M		2M		M/10 1M		M/2		μeq P			
		0	35	3	2	0	19	3	26	88					
ECMOB-SF1	1004	0	0	35	3	2	0	19	3	26	88	85		362	
ECPIB-SF1	655	0	5	21	1	1	0	4	3	92	127	9		308	
ECMAFDOL-SF1	646	0	3	15	7	1	0	3	2	49	80	8		238	
ECMATPOL-SF1	622	0	12	33	1	1	0	12	3	100	162	9		455	
ECMOA-SF2	531	0	0	8	22	1	0	9	2	13	55	12		237	
ECANFDOL-SF1	524	0	7	18	12	3	0	30	6	17	93	12		388	
ECMTA-SF1	524	0	8	17	2	2	0	30	4	17	80	6		320	
ECDEA-SF2	491	0	4	15	26	5	1	9	2	63	125	20		416	
CATO-2	431	0	2	33	1	1	1	10	1	4	49	13		294	
ECTOLA-EX	427	0	1	4	11	1	0	63	3	2	85	16		304	
ECDETA-SF1	411	0	0	3	11	11	1	10	9	23	68	8		217	
ECMOA-W1	401	0	11	20	16	1	0	8	3	29	86	11		382	
ECPEA-SF1	358	0	11	9	6	2	0	15	3	25	71	7		273	
ECMPIZ-SF1	258	0	0	1	16	43	1	20	4	46	131	23		436	
DEAE-EX	225	0	1	1	10	33	1	36	1	15	98	63		369	
ECTPA-SF2	197	5	1	1	0	0	11	81	2	9	110	90		315	
ACETOTPA-SF2	189	2	0	0	0	0	8	1	50	5	20	24		224	
AE-SO-W ⁺⁺	149	0	0	0	0	1	2	14	40	11	50	126		264	

TABLE 1 (continued)

TABLE 1 (continued)															
Resin	Desorption Activity Index	DNA Recovered from Each Step Eluant (per cent)										Binding Site Density		Desorption Activity Index	
		NaCl + M/100 TRIS Buffer					NH ₄ OH + 2M NaCl					NaOH			µeq exch Cl ⁻
		15M/100 M/10 M/4		M/2 1M 2M		M/10 1M		M/2		Total					
		undensaturated ^a									µeq P				
ECADPA-SF1	---	0	0	0	0	0	1	52	5	32	90	33	202		
ECTMBOLA-SF1	---	0	3	16	35	2	0	11	2	61	130	11	454		
ECGD-W1	---	0	10	3	35	7	1	7	2	46	111	19	421		
ECTAPOL-SF1	---	0	14	16	15	1	0	5	2	29	82	12	367		
ECDEANOL-W1	---	0	10	43	1	1	0	9	2	92	158	12	515		
ECAMFOL-SF1	---	0	6	13	17	4	0	34	6	9	89	15	384		
ECAPHOR-SF1	---	0	8	13	12	2	0	1	3	38	77	14	284		
ECPIZ-SF1	---	0	0	11	17	4	0	5	4	74	115	12	296		

^a11.6 µeq P applied/g resin.^b6.5 µeq P applied/g resin.

d - dissolution.

TABLE 2. PROPERTIES OF SOME SYNTHETIC ANION EXCHANGERS FOR CHAPERONING DURING DESORPTION OF HEAT
DENATURED SALMON SPERM DNA APPLIED AT 90° (12.9 µeq P applied/g resin)

Resin	State of DNA at Application	DNA Recovered from Each Step Eluant (per cent)										Binding Site Density		Description Activity Index
		NaCl + M/100 TRIS Buffer					NH ₄ OH + 2M NaCl					µeq exch Cl ⁻	µeq P	
		M/2					M/10							
		15M/100	M/10	M/4	M/2	1M	2M	M/10	1M	M/2	Total			
ECTOLA-EX	C ^a	0	1	5	13	1	1	54	2	0	77	16	295	
	D ^b	0	1	4	11	1	0	63	3	2	85	16	304	
	U ^c	0	4	38	12	0	0	16	1	6	77	18	427	
ECTEPA-SF2	C	2	1	1	0	2	30	30	5	17	88	87	262	
	D	5	1	1	0	0	11	81	2	9	110	90	326	
	U	0	0	0	0	0	22	28	12	65	127	95	197	
AE-50-W	C	4	1	1	2	3	17	38	10	50	126	132	294	
	D	0	0	0	1	2	14	40	11	49	117	127	263	
	U	7	0	0	0	2	8	21	19	40	97	76	149	
ACETOTEPA-SF2	C	0	0	0	0	24	3	25	3	21	76	23	234	
	D	2	0	0	0	8	1	50	5	20	86	24	208	
	U	0	0	0	0	11	2	24	26	21	84	26	189	
ECMP1Z-SF1	C	0	0	0	6	32	2	34	2	31	107	23	341	
	D	0	0	1	16	43	1	20	4	47	132	23	437	
	U	1	0	0	5	23	2	27	11	43	112	26	258	
ECQADPA-SF1	C	3	0	1	0	0	2	39	5	42	92	33	184	
	D	0	0	0	0	0	1	52	5	32	90	33	202	
	U	0	0	0	0	0	0	0	0	0	0	19	264	
ECGD-W1	C	0	0	1	13	8	1	34	4	25	86	19	421	
	D	0	10	3	35	7	1	7	2	46	111	19		

^aChaperone.

^bDenatured.

^cUndenatured.

undenatured samples. A comparison of desorption activity indices indicates that these resins vary widely in ability to prevent renaturation of DNA.

(c) The ability of resins to detect degraded DNA was investigated by comparison of elution profiles with those of undegraded samples. Aliquots of salmon sperm DNA were degraded by vigorous mechanical shaking for 24 hours, by rapid passage 3 times through a 27-gauge hypodermic needle, by stirring with a Virtis mixer 24 hours at 3° with minimum cavitation, by sonication 10 minutes at 10 KC in a water-cooled polyethylene bottle, or by exposure of both denatured and undenatured samples to 25,000 r of X rays.

Table 3 presents elution profiles of 2 resins with 4 samples of DNA subjected to ordered scission and 2 with random scission. In the former classification, shear with the needle appeared to be least damaging.

(d) The effect of aging upon DNA solutions stored at refrigerator temperature was studied by determining the change in elution profiles. Table 4 presents the profiles of 4 resins and evidence that homogeneously decreased resin capacity and binding site density shift the profile of fresh DNA to lower ionic strengths, and extended storage of DNA solutions at refrigerator temperature results in marked shifts to higher ionic strengths and anomalously high recoveries by alkali.

TABLE 3. PROPERTIES OF SEVERAL SYNTHETIC ANION EXCHANGERS FOR DESORBING DEGRADED SALMON SPERM DNA UNDER EQUILIBRIUM CONDITIONS (12.9 μ eq P applied/g resin)

Resin	Mode of Scission	DNA Recovered from Each Step Eluant (per cent)										Binding Site Density		Desorption Activity Index
		NaCl + M/100 TRIS Buffer					NH ₄ OH + 2M NaCl		NaOH		Total	μ eq exch Cl ⁻		
		15M/100 M/10		M/4	M/2	1M	2M	M/10	1M	M/2				
		M/10	M/10	M/4	M/2	1M	2M	M/10	1M	M/2				
ECDEA-SF2	Shake	0	0	7	45	6	0	3	1	40	102	20	400	
	Needle	0	0	9	38	6	0	3	0	48	104	20	378	
	Stir	0	0	6	52	6	0	3	1	44	113	18*	439	
	Sonication	0	0	8	50	6	1	2	0	60	112	20	460	
	X-ray	0	0	5	54	6	1	6	2	55	129	20	470	
	None	0	0	12	57	5	1	11	2	0	88	22**	492	
ECMATPOL-SF1	X-ray, denatured	0	0	4	32	6	1	11	1	61	116	20	350	
	None, denatured	0	4	15	26	5	1	9	2	63	125	20	416	
	Shake	0	0	62	1	1	0	2	2	74	142	9	535	
	Needle	0	2	46	1	1	0	2	1	68	121	9	409	
	Stir	0	1	65	1	1	0	2	2	84	135	18*	540	
	Sonication	0	0	57	2	1	0	2	1	80	153	9	514	
	X-ray	0	0	71	1	1	0	4	2	101	180	9	625	
	None	1	3	79	4	0	0	3	0	34	124	10**	611	
	X-ray, denatured	0	1	43	1	1	0	14	3	100	163	9	468	
	None, denatured	0	12	33	1	1	0	12	3	100	162	9	480	

*14.2 μ eq P.

**11.6 μ eq P, another DNA solution.

TABLE 4. PROPERTIES OF SYNTHETIC ANION EXCHANGERS FOR DESORBING FRESH AND STORED SALMON SPERM DMA UNDER EQUILIBRIUM CONDITIONS

EQUILIBRIUM CONDITIONS

Resin		Binding Site		DMA Recovered from Each Step Eluant (per cent)												
Designation	Capacity meq exch Cl ⁻ gram	Mode of Dilution	meq exch Cl ⁻ meq P	Age	Applied		NaCl + M/100 TRIS Buffer								NH ₄ OH + 2M NaCl NaOH	
					x g Resin	meq P	15M/100 M/10 M/4 M/2 1M 2M M/10 1M M/2	Total								
ECTOLA-SF2	0.36	Chemical	31	Fresh	11.6 meq 1.0 g		0	0	0	25	9	2	35	3	0	74
ECTOLA-EK	0.21	Chemical	18	Fresh	11.6 meq 1.0 g		0	4	38	12	0	0	16	1	6	73
ECTOLA-SF2	0.36	Chemical	31	4-1/2 Mo. refrig.	11.6 meq 1.0 g		0	0	0	15	21	4	48	4	(7)	(99)
ECTOLA-SF2	0.18	Physical	31	4-1/2 Mo. refrig.	5.8 meq 0.5 g + 0.5 g cell.		0	0	0	14	10	3	77	5	(60)	(169)
ECDEA-SF2	0.26	Chemical	22	Fresh	11.6 meq 1.0 g		0	0	12	57	5	1	11	2	0	88
ECDEA-SF1	0.07	Chemical	6	Fresh	11.6 meq 1.0 g		0	90	0	0	0	0	0	0	25	115
ECDEA-SF2	0.09	Physical	22	4-1/2 Mo. refrig.	5.8 meq 0.5 g + 1.0 g cell.		0	0	2	28	4	3	80	6	(150)	(273)
ECMATPOL-SF1	0.12	Chemical	10	Fresh	11.6 meq 1.0 g		1	3	80	4	0	0	3	0	35	126
ECMATPOL-SF1	0.04	Physical	10	4-1/2 Mo. refrig.	5.8 meq 0.5 g + 1.0 g cell.		0	0	48	7	6	1	44	21	(170)	(297)
ECTETA-SF1	0.04	Chemical	11	Fresh	11.6 meq 1.0 g		70	13	18	9	1	0	1	0	30	142
ECTETA-SF1	0.04	Chemical	15	4-1/2 Mo. refrig.	2.6 meq 1.0 g		0	0	0	17	11	1	32	30	(91)	(182)

The A_{260} of neutral buffered stock solution of salmon sperm DNA under storage at 3° gradually increased (4 per cent at 1 week, 5 per cent in 3 weeks). At room temperature, however, the change amounted to 21 per cent in 1 week and may account for high recoveries observed with certain resins, especially since the equilibrium studies involved several months at the higher temperature. This increase is halved by resorting to a base line determination between 310 and 230 m μ , as employed above.

(e) The properties of 50 resins for desorbing mammalian liver-soluble RNA are being screened under equilibrium conditions at 3°.

Column Desorption of DNA

(a) Positive-Displacement Gradient-Elution Device. The art of chromatography does not yet allow one to predict the exact shape and composition of an elution gradient for best separating a complex mixture; therefore, in practice, one requires a near linear gradient that is reproducible and subject to independent manipulation of local portions. There has been completed and put into operation a "synchrovarigrad" (Fig. 1) capable of providing parallel, continuously-variable gradient-elution of 16 columns under identical conditions of constant predetermined flow rate. A mixer, built of

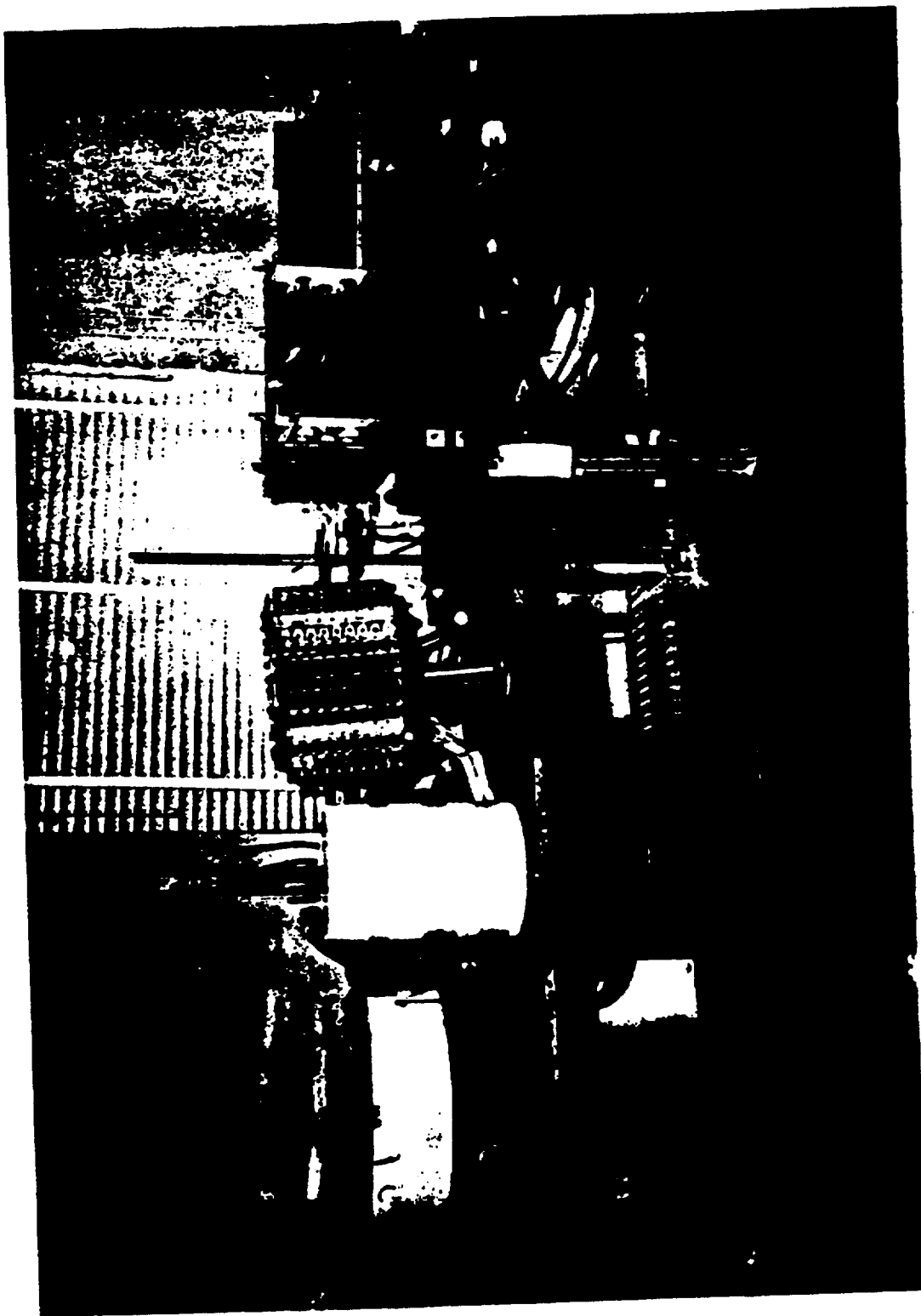


Fig. 1. The "synchrovarigrad."

9 identical stacked Lucite chambers, is fed by a positive-displacement pump of precision glass tubing. The 16 mixers are mounted in a cage which is suspended in gimbals and tilted eccentrically, thereby rolling a glass marble in each chamber to afford continuous mixing. The chambers are loaded successively from the bottom upward by means of a tube penetrating a central loading port, which then self-seals by the automatic seating of a floating polyethylene ball. Small apertures connect adjoining chambers 180° apart to circumvent laminar flow. The pump input feeds the bottom chamber, and the output to the column issues from the top. Pump plungers of special design are sealed with 4 silicone rubber O-rings lubricated with silicone grease (Apiezon N for NaOH solutions), and all connections are made by polyethylene tubing threaded through silicone rubber stoppers. All pumps are actuated by a single 1 RPM synchronous motor driving a converted lathe mechanism through an appropriate gear box, chain, and sprocket. The columns are packed at 2° under 5 psi, then clipped to a metal screen immersed in a stirred water bath automatically maintained at 2° by an electrical refrigeration coil.

Calibration of this device revealed that each mixer contained an average volume of 964.4 ± 0.6 ml, and each of 8 pumps delivered 64 measured fractions at an average rate of 16.3 ± 0.0 ml/150 minutes. The gradient developed is determined

by the initial concentrations charged into each chamber of the mixer and pump. Figure 2 presents the 9 simplest gradients obtained by loading the indicated number of upper chambers with water, and the remainder and pump with 2 M NaCl; the curves describe the theoretical gradients obtained from the computer program (5), while the points were determined by titration. A truly linear gradient may be obtained by loading the chambers with 8/9, 7/9, 6/9 1/9 of the limiting concentration contained in the pump. At any time, a second gradient may be superposed on the initial one by recharging the pump with a different solution. The device appears to provide the precise control of column environment required for meaningful evaluation of a large number of amine-substituted anion exchange resins.

(b) Choice of a Bacteriostatic Agent Compatible with Materials in the Gradient Mixer. The bacterial growth control properties of trichloroethanol, chlorethane (concentrations of 0.25, 0.5, and 1.0 per cent), and of chloroform (saturation) were determined by incubating 10^6 spores of bacillus subtilis in 25 ml of thioglycollate broth for 7 days at 37°. Complete growth inhibition was found with all agents at the highest concentration; chlorethane was effective for 6 days at 0.5 per cent, but ineffective at 0.25 per cent; trichloroethanol was effective for 2 days at 0.5 per cent,

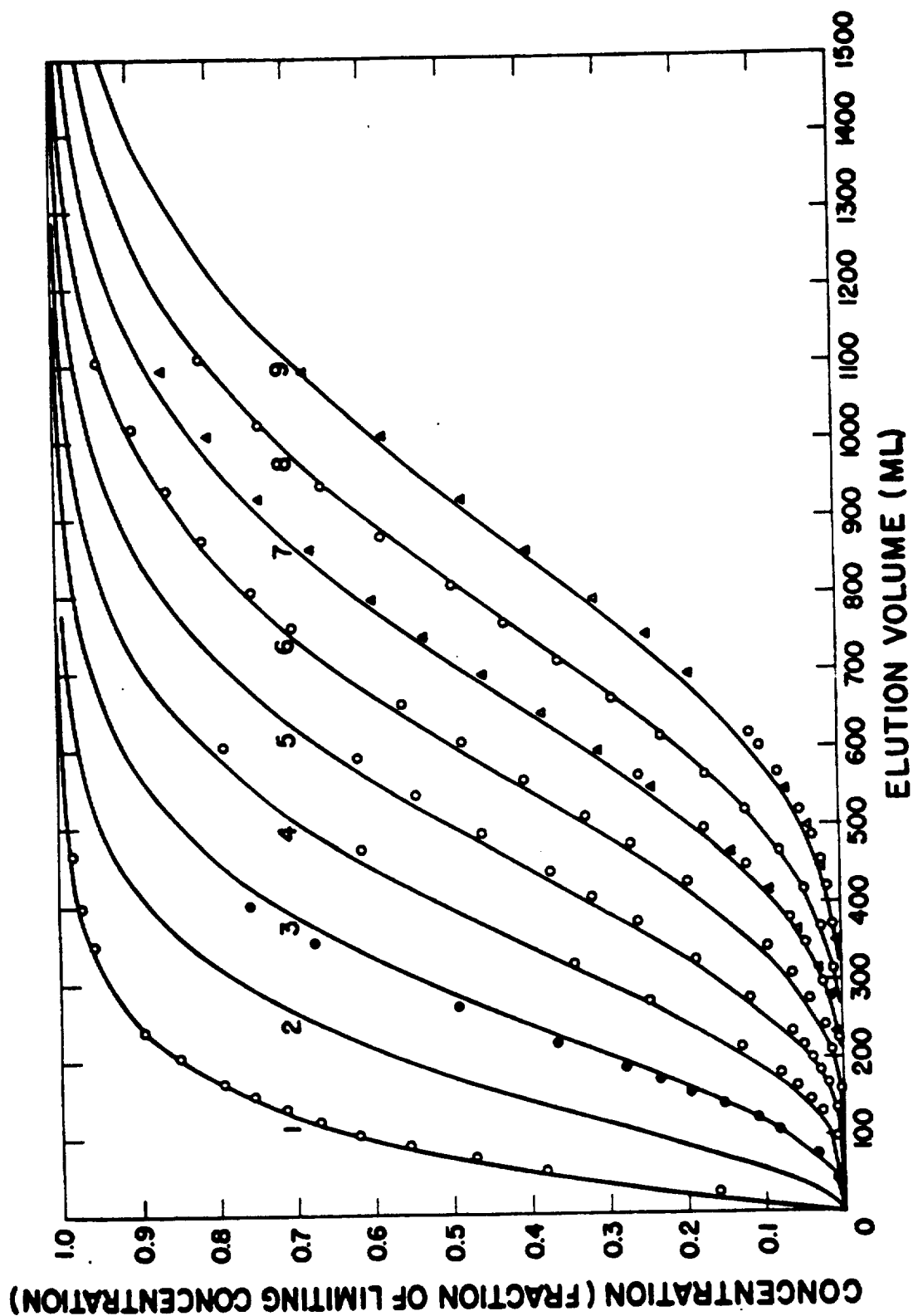


Fig. 2. Simple elution gradients developed by a 9-chambered mixer.

1055835

but ineffective at 0.25 per cent. Inoculation of fresh broth with 0.5-ml aliquots from completely inhibited cultures showed the mechanism to be bacteriostatic rather than bactericidal.

Loss of these reagents from solution through scavenging was assessed by shaking with granulated Lucite in polyethylene bottles for 4 days, followed by re-assay for halogenated compound by the Fujiwara reaction (chloroform 99 per cent, trichloroethanol 20 per cent, and chlorethane relatively little loss).

On the basis of these findings and spectrophotometry in the region of 315 to 240 $m\mu$, chlorethane appeared the agent of choice.

(c) Synchronous Column Elution. Figure 3 is a stylized graphical presentation of 32 comparative elution profiles obtained at 2° with 16 resins (1 g each) and fresh salmon sperm DNA under controlled conditions of flow rate, salt gradient, and resin/DNA binding density. Profiles were determined spectrophotometrically (A_{260} to A_{310}), and each contained single smooth peaks eluted by salt and by alkali, but in varying proportions. The ordinate expresses the molarity of sodium chloride at threshold, peak, and tail of the salt peak. The resins are arranged in ascending order of per cent elution by salt, and the designation is preceded by the capacity

BINDING SITE DENSITY (μ eq exch $\text{cl}^- + \mu$ eq P)
 16 6 16 8 16 6 20 19 16 20 16 13 48 81 16 13 17 12 16 10 16 8 16 9 16 9 16 13 16 5 16 6
 PROFILE DISTRIBUTION INDEX (% RECOVERY NaOH + % RECOVERY NaCl)
 > 3.2 > 3.0 10 0.4 39 32 43 30 44 29 44 24 40 27 2.8 14 27 15 29 23 24 15 24 15 2.9 12 12 0.7 15 0.7
 PERCENT SLIP
 2 49 2 47 1 14 22 20 1 3 3 11 0 2 1 9 11 50 1 21 1 4 1 3 1 3 1 4 3 32 4 50
 PERCENT RECOVERY BY NaCl
 0 15 0 20 15 61 17 19 18 24 19 22 19 30 21 24 26 20 28 30 29 29 32 37 32 38 36 43 45 40 46 30

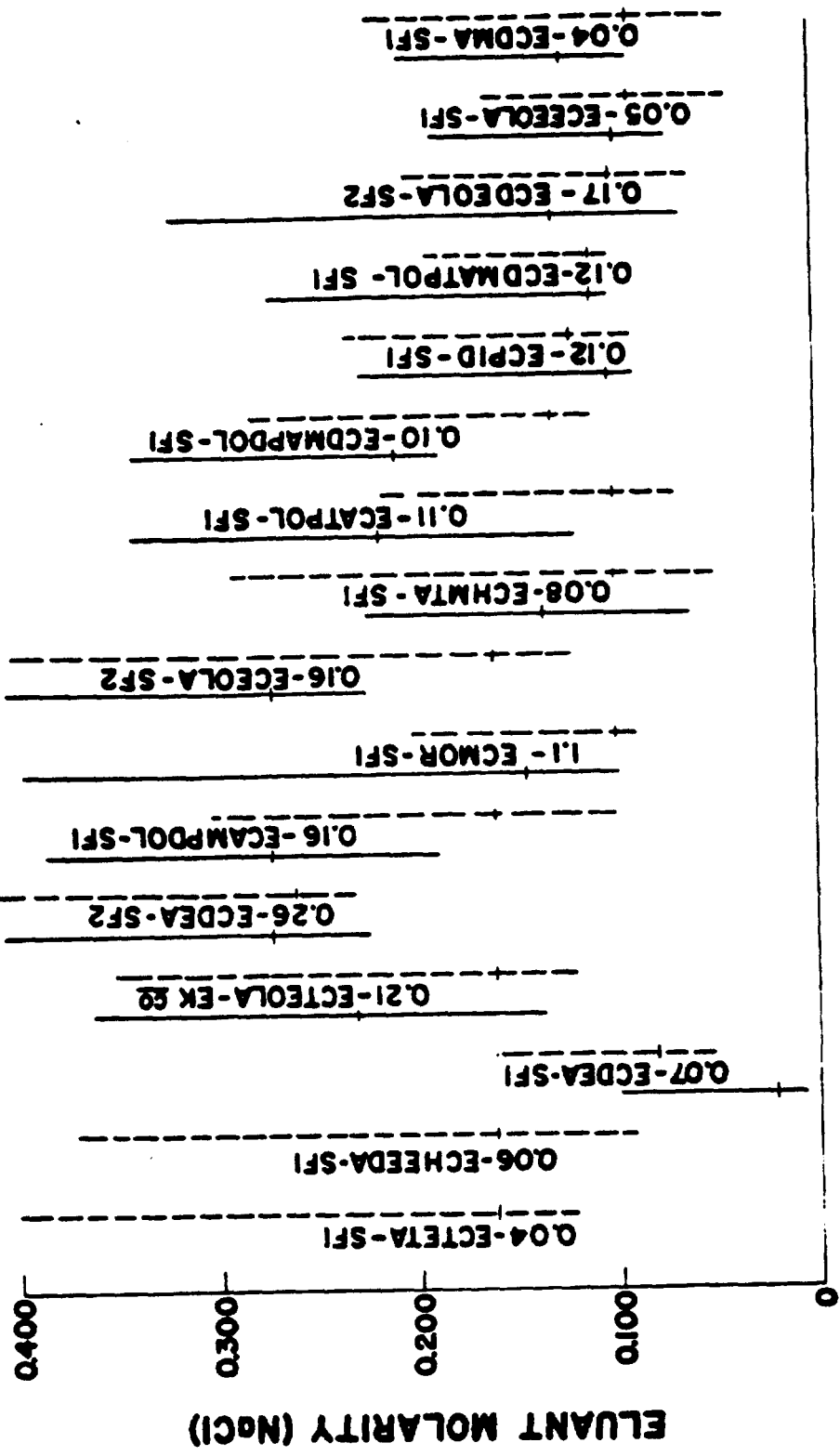


Fig. 3. Chromatographic profile of salmon sperm DNA.

in meq exch Cl^-/g . The appropriate binding site density, per cent non-bound DNA, and profile distribution index (per cent recovery by alkali divided by per cent recovery by salt) are indicated for each resin.

Dotted lines represent a run at constant DNA loading/g resin (variable binding site density), chloroform bacteriostat, and collection rate 10 ml/400 minutes; mean recovery was 100 per cent. Alkaline elution was achieved with 2 M NaCl, 0.5 M NaOH.

Solid lines represent a run at constant binding site density (variable DNA loading/g resin), chlorethane bacteriostat, and collection rate 10 ml/125 minutes; mean recovery was 110 per cent. A flatter salt gradient was used (Fig. 2, No. 9, C_0 0.015 M NaCl, 0.01 M TRIS buffer, C_L 0.85 M NaCl, 0.01 M TRIS). Only ECTEOLA and ECHMTA exhibited appreciable slip, despite larger binding site densities. The general increase in profile distribution index at the 2.8 X faster flow rate is noteworthy and indicative of pronounced shift to higher ionic strength with departure from equilibrium. The location of peaks in the ordinate expresses the relation between rise and degree of tailing.

Table 5 presents mean S_{obs} values of significant peak fractions from the slower run, arranged in order of increasing non-bound DNA. It is apparent that these resins vary

TABLE 5. MEAN S_{obs} VALUES OF SIGNIFICANT PEAK FRACTIONS

Resin	Non-bound DNA (per cent)	Binding Site Density	Mean S_{obs} Values of Fractions		
			Non-bound Fraction	NaCl Peak	NaOH Peak
ECMOR-SF1	2	81	--	6	27
ECDMATPOL-SF1	3	9	--	7	22
ECPID-SF1	3	9	--	8	18
ECDEA-SF2	3	20	--		9
ECDEOLA-SF2	4	13	--	7	16
ECDMAPDOL-SF1	5	8	--		11
ECEOLA-SF2	9	13			18
ECAMPDOL-SF1	11	13			10
ECDEA-SF1	14	6	3		18
ECTEOLA-EK	20	19			8
ECATPOL-SF1	21	10		11	8
ECEBOLA-SF1	32	5	15	5	7
ECHEEDA-SF1	47	8			8
ECTETA-SF1	49	6	11		11
ECHMTA-SF1	50	12	3	5	10
ECDMA-SF1	50	6	13	6	7

widely in the degree to which they fractionate a slip fraction.

Spectrophotometric determination of base ratios (6) in various fractions of all 32 profiles failed to reveal any significant variations.

Thin-Layer Chromatography

Thin-layer chromatographic techniques afford considerable economy of material in working out optimum conditions for desorption, as well as providing a convenient procedure for systematic investigation of the effects of binding site density and binding intensity on the mobility of hydrophylic anions. Resins of low, intermediate, and high capacity were tested for ability to separate phosphorylated adenosine compounds as a function of ionic strength. Resins were ground in a mortar and suspended in a Virtis homogenizer at maximum speed for 10 minutes to obtain an appropriate particle size of approximately 10 μ judged by uniformity of the layers. Plates 2 x 20 cm were prepared by masking the edges with electrical tape and applying 1 cc of a slurry containing 150 mg of resin. Uniform spreads were obtained by gently tilting the plates, which were then air-dried and the tape removed. Commercial TLC DEAE-cellulose (Bio-Rad), polyethyleneimine (PEI) cellulose, and unmodified TLC cellulose

were also used as test media. In all cases except unmodified cellulose, minimal background ultraviolet absorbance permitted intermittent monitoring of nucleotide migration on the plates during development in open dishes. Plates were developed ascending for times ranging from 45 minutes to 1-1/2 hours. For comparison in these experiments, 0.5 micro-mole each of AMP, ADP, and ATP were spotted on chromatoplates and developed with dilute HCl, NaCl, or NH_4HCO_3 . Useful separations were obtained with all 3 solvents, but the best resolution was obtained using either ECPEDA-SF2 or ECAHMPDOL-SF1 with 0.3 to 0.5 M HCl. In the case of DEAE, ECPEDA-SF2, and ECAHMPDOL-SF1, R_f values were proportional to HCl concentration in the region from 0.02 to 0.05 M. PEI-cellulose, on the other hand, yielded excellent separations with both 0.05 M ammonium bicarbonate and 0.05 M NaCl.

DISCUSSION

Systematic screening of a large number of substituted cellulose ion exchangers has resulted in the recognition of several features of exchange chromatography amenable to improvement in column performance. In the course of the present studies (5), it was recognized that changes in flow rate caused by resin swelling altered elution profiles, and that intentional interruption of flow rate invariably results

in the generation of artifact peaks. Under conditions of precise control, however, each emerging peak exhibited only 2 slopes and the ionic strength required for desorption became more nearly dependent upon the equilibrium constant for a particular resin. The device described in this report adequately controls column environment. These studies suggest that the binding of small molecules cannot be compared directly with that of macromolecules. ECTEOLA was anomalous from the standpoint of macromolecular slip, thus demonstrating several factors influencing binding. Steric relationships which prevent all exchange sites from reacting, such as hindrance between polycation and polyanion groups and the interspacing of polycation groups on the matrix, could account for differences in binding of small and large molecules. The alternate modes by which polyfunctional amines may react with epichlorohydrin leads to a second order of chemical heterogeneity difficult to control in resin preparations. While variability in synthesis is recognized (e.g., ECTEOLA), discussion of the use of simple symmetrical groups to attain more chemically uniform binding sites is perhaps premature.

Studies involving the use of unmodified cellulose to disperse reactive resin particles (heterogeneous dilution) and controlled chemical synthesis (homogeneous dilution) may

shed light on the relative inter- and intra-cellulose particle contribution to binding and the elution profile.

The choice of salmon sperm DNA as a common test material has both advantages and disadvantages; spectrophotometric indications of resolution of this grossly heterogeneous material are usefully apparent, but satisfactory characterization by ultracentrifugal techniques is difficult. The majority, but not all, of the resins release native material more readily than denatured. Experiments with degraded DNA were inconclusive and will require the greater resolution of column chromatography and a less heterogeneous starting DNA. Some materials appear to be more effective chaperones than others. In this regard, it will be of interest to determine the effect of resin absorption upon storage life of nucleic acids.

Continued investigation of resin properties will involve studies on performance reproducibility, as well as more precise characterization of the polynucleotide. At present, it is not known whether any of the resins can detect differences in polynucleotide base composition. DNA fragments from *E. coli*, *Serratia marcescens*, and *Micrococcus lysodeikticus* will be fractionated, with definitive chemical analysis replacing current optical techniques for base evaluation. Defined molecular weights which can be assigned to

DNA and fragments derived from T-4 phage should disclose the capacity of these resins to fractionate on the basis of molecular weight. Further screening of the equilibrium behavior of soluble RNA and other polynucleotides of intermediate molecular weight on these resins is in progress.

Evaluation of the exchangers synthesized in this Laboratory suggests that their greatest applicability may lie in the separation of oligonucleotides too large for satisfactory separation by existing resins, and smaller than the highly polymeric DNA where they lack the specificity of columns employing specific polynucleotides as fractionating media. Some promising preparations appear to be ECDEA, ECMOR, and ECHMTA; these may also conveniently provide rapid separation of mononucleotides and small oligonucleotides by thin-layer chromatography as evidenced by the preliminary studies on phosphorylated derivatives of adenosine.

It is anticipated that meaningful evaluation and some design requirements for specific substituted cellulose exchangers can be readily attained from the simultaneous operation of 16 columns under conditions which allow the resin, gradient, flow rate, or polynucleotide to be the experimental variable. The feasibility of continuous automatic spectrophotometric monitoring of the effluent from 16 columns is being investigated.

ACKNOWLEDGMENT

The authors gratefully acknowledge the assistance of Dr. I. U. Boone and Mr. and Mrs. E. Campbell in establishing the efficacy of the bacteriostatic agents, of Dr. G. R. Shepherd in performing the ultracentrifugal analysis of isolated fractions, and of Dr. W. Goad in performing the computer analysis of the theoretical gradient elution curves.

REFERENCES

- (1) A. Murray, Los Alamos Scientific Laboratory Report LAMS-2455 (1960), p. 138.
- (2) A. Murray, E. H. Lilly, and L. B. Cole, Los Alamos Scientific Laboratory Report LAMS-2526 (1960), p. 245.
- (3) A. Murray, V. E. Mitchell, and D. F. Petersen, Los Alamos Scientific Laboratory Report LAMS-2627 (1961), p. 33.
- (4) A. Murray, E. H. Lilly, V. E. Mitchell, and D. F. Petersen, Los Alamos Scientific Laboratory Report LAMS-2780 (1962), p. 248.
- (5) D. F. Petersen, A. Murray III, W. Goad, Jr., and J. H. Larkins, Los Alamos Scientific Laboratory Report LAMS-2780 (1962), p. 259.
- (6) E. Fredericq, A. Oth, and F. Fontaine, J. Mol. Biol. 3, 11 (1961).

MOLECULAR RADIOBIOLOGY SECTION

PUBLICATIONS

- (1) E. Hansbury, J. D. Perrings, and D. G. Ott, Thin-Layer Chromatography Apparatus, J. Chem. Educ. 40, 31 (1963).
- (2) E. Hansbury, J. Langham, and D. G. Ott, A Photographic Method for Recording Chromatograms, J. Chromat. 9, 393 (1962).
- (3) G. R. Shepherd and P. C. Sanders, The Complementary Effects of 2-Mercaptoethanol and Trypsin in the Lysis of HeLa Cells, J. Cell Biol. 14, 346 (1962).
- (4) G. R. Shepherd and D. F. Petersen, Separation of Phenol and Deoxyribonucleic Acid by Sephadex Gel Filtration, J. Chromatog. 9, 445 (1962).
- (5) G. R. Shepherd and P. A. Hopkins, The Distributions of Certain Proteins, Polypeptides and Polyamines in an Aqueous-Phenol System, Biochem. Biophys. Res. Comm. 10, 103 (1963).
- (6) D. L. Williams, Synthesis of Carbon-14 Labeled Deoxyribonucleosides, Canad. J. Chem. 40, 1742 (1962).

MANUSCRIPTS SUBMITTED

(1) D. G. Ott, Oligonucleotides. I. Acetyl and Tetrahydropyranyl Derivatives of 3'-uridylic Acid, submitted for publication as a Los Alamos Scientific Laboratory report.

(2) G. R. Shepherd and P. A. Hopkins, Determination of Protein Contamination of Deoxyribonucleic Acid by the Folin-Lowry Method, submitted to Anal. Chem.